Power Counting in the Standard Model Effective Field Theory

with Applications to $gg \to t\bar{t}$ and $h \to gg$

Christoph Müller-Salditt

München 2023

Power Counting in the Standard Model Effective Field Theory

with Applications to $gg \to t\bar{t}$ and $h \to gg$

Christoph Müller-Salditt

Dissertation
an der Fakultät für Physik
der Ludwig-Maximilians-Universität
München

vorgelegt von
Christoph Müller-Salditt
aus Buchloe

München, den 14.06.2023

Erstgutacher: Prof. Dr. Gerhard Buchalla
Zweitgutachter: Prof. Dr. Stefan Hofmann
Tag der mündlichen Prüfung: 28.07.2023

Contents

Zusammenfassung

Eine konsistente Vorschrift zum Ordnen der Operatorstrukturen in der Standard Model Effective Field Theory (Standardmodell der Teilchenphysik als Effektive Feldtheorie) erfordert mehr als die kanonische Dimension der Operatoren, da diese keine Informationen über die perturbative Expansion der zugrunde liegenden Quantenfeldtheorie bei hohen Energien enthalten. Obwohl dies in der Literatur seit vielen Jahren bekannt ist, steht hierzu ein konsistenter quantitativer Ansatz noch aus. In dieser Arbeit präsentieren wir eine Lösung für Operatoren der kanonischen Dimension sechs, die auf dem Konzept der chiralen Dimension basiert. Unsere Ergebnisse werden durch explizite analytische Berechnungen für zwei wichtige Beispiele an Hadronenbeschleunigern veranschaulicht, nämlich die Fusion von zwei Gluonen, die mit der Produktion eines Top-Quark-Paares einhergeht, und den Zerfall eines Higgs-Bosons in zwei Gluonen oder Photonen. Wir präsentieren kurze numerische Studien für beide Prozesse, um hypothetische Abweichungen vom Standardmodell abzuschätzen.

Abstract

A consistent power-counting prescription for the Standard Model Effective Field Theory requires more than the canonical dimension of operators, as they contain no information about the perturbative expansion of the underlying Quantum Field Theory at high energies. Although this has been noted in the literature for many years, a consistent quantitative approach remains to be completed. In this work, we present a solution for operators of canonical dimension six based on the notion of chiral dimensions. Our results are illustrated by explicit analytic calculations for two major examples at hadron colliders. These are the fusion of two gluons associated with the production of a top-quark pair, and the decay of a Higgs boson into two gluons or photons. We provide numerical studies for both processes to estimate hypothetical deviations from the Standard Model.

1. Introduction

The combination of Special Relativity and Quantum Mechanics, the cornerstones of modern physics, leads inevitably to the formalism of Quantum Field Theory (QFT), which is until today the only physical framework that can unite concepts like causality or the equivalence of mass and energy and the quantum world, i.e. wave-particle duality or the uncertainty relations, in a superordinate theory [1–4]. It predicts the existence of antimatter, particle creation and annihilation and explains mysteries like the connection between spin and quantum statistics that remain unresolved otherwise [5–8].
According to QFT, matter represents itself as various *fields*, that is entities that depend on the spacetime they "live on". Neighboring field points - so to speak - are held together like two point masses connected by a spring - only that they are actually infinitely close together. Embedded into a fully-fledged quantum theory, the notion of elementary *particles* arises when interpreted as the fundamental excitations of the corresponding quantum oscillators. They propagate through space like waves within a chain of coupled springs. Particle *interactions* are caused by deviations from the superposition principle of the harmonic limit. The familiar *forces* (gravity, electromagnetism) are nothing else than the long-range manifestations of some of these interactions. The Standard Model (SM) ultimately unifies all known particles and interactions in the QFT framework. It includes the quantum theories for electromagnetism known as Quantum Electrodynamics (QED) [9–11], the strong interaction referred to as Quantum Chromodynamics (QCD) [12–14], as well as the weak interaction [15–17] and even gravity to some extent [18–20].
The QFTs relevant to particle physics are usually defined in terms of a function, the *Lagrange density* or *Lagrangian*, which encodes all the information about the interactions of the involved particles. Its often relatively simple form is dictated by the *symmetries* of the physics under consideration. The Lagrangian is linked to the quantum mechanical transition amplitudes for particular particle processes by virtue of the *path integral*. Unfortunately, the path integral can only be solved directly in the rarest cases, so approximation methods must be used to make the necessary predictions for experiments from QFT. The most common method is *perturbation theory*. Here, the transition amplitudes are expanded in terms of perturbative series around the aforementioned harmonic limit of the oscillators. They are organized in such a way that only the first terms are relevant. In practice, the perturbative series is a power series in a small parameter, such as the electromagnetic fine structure constant $\alpha \approx 1/137$ in QED, which indicates the strength of the electromagnetic interaction. In this case, the individual terms of the perturbative series can be represented graphically by *Feynman diagrams*. In QED, the terms with the lowest power of α are denoted as *tree diagrams* and usually form the contributions of classical physics within the formalism of QFT. They are generally easy to compute and already provide accurate predictions for experimentally measurable quantities. From a phenomenological, as well as theoretical point of view, the higher order terms in α become particularly interesting. These are called *loop diagrams* and form the quantum

corrections to the classical result of the tree diagrams[1]. Many of these diagrams are not directly computable in the sense that the associated terms of the perturbative series diverge - often in the form of complicated integrals leading to undefined masses, field (wavefunction) normalizations, and other Lagrangian parameters. At first glance, this means the demise of the perturbative series. It took decades for physicists to solve the problem of divergent loop diagrams. The strategy commonly used today involves first parameterizing the divergences, which is known as *regularization*. By introducing appropriate *counterterms* in the Lagrangian, the divergences can be eliminated, which is known as *renormalization*. As a positive side effect, this gives the actual definitions of the parameters of the Lagrangian as experimentally measurable quantities. Theories in which a finite number of counterterms is sufficient to handle the divergences of all loop diagrams to all orders are called *renormalizable*. The most prominent example QFTs, that is QED and QCD, are renormalizable. In fact, the entire SM (excluding gravity) is renormalizable.

For a long time, it was believed that only such renormalizable theories could be considered for a general understanding of nature. This idea is certainly correct when it comes to establishing a *theory of everything* that includes the SM as a certain limit. In practice, however, questions often arise that are very difficult to answer within the framework of a renormalizable theory, for instance when perturbation theory fails or in the context of higher-spin particles like the graviton. A classic article by Steven Weinberg [23] in 1979 finally presented the proposal to give physical sense also to *non-renormalizable* QFTs - under certain conditions. Here, a finite number of counterterms is not sufficient to absorb all divergences of the loop diagrams. In such theories, therefore, an infinite counterterm extension of the Lagrangian necessarily results, and hence also an infinite tower of further interactions, which is why they do not seem very attractive at first sight. Examples of non-renormalizable theories are the Fermi theory of the weak interaction [24, 25], Chiral Perturbation Theory for the low-energy spectrum of the strong interaction [26, 27], and also general relativity as a theory of gravity [28, 29]. Their respective phenomenal success teaches us that even non-renormalizable theories must have their right to exist.

The key to the success of a non-renormalizable theory lies in the organization of the de facto infinite number of terms in the Lagrangian into relevant and less relevant terms for the physical problem - the *power counting*. Non-renormalizable QFTs in which some form of power-counting is applied are called Effective Field Theories (EFTs). Also the SM is nowadays considered as an EFT, which can be extended by non-renormalizable terms to include physics beyond the SM. It eventually has to be abandoned in favor of a more complete theory for higher energies whose precise form is one of the main subjects in current research.

From a physical point of view, an EFT is nothing else than a calculational framework for which the correct degrees of freedom for the problems at hand have been chosen. In particle physics, this mainly concerns the energy range at which experiments are done. For instance, below the energy threshold for the production of a certain heavy particle,

[1] This is - strictly speaking - not true, see e.g. [21, 22].

the latter is not part of the physical particle spectrum and does therefore not appear as a propagating degree of freedom in a low-energy EFT. Were it not for the inherent quantum nature of our universe, this could be trivial in the sense that low-energy physics remains unaffected by the heavier states. In reality, however, quantum mechanical uncertainty essentially allows the heavy particle to ”smear” into the low-energy regime, thus influencing physical predictions. For example, the (light) muon ”knows” about the existence of heavy quarks via their effects on its anomalous magnetic moment.

In the context of the SM at the electroweak scale, these potential heavy states are unknown to date. Without an explicit model theory, the EFT has to be constructed from first principles. Different scenarios are possible. For instance, assuming a mass gap between the SM fields and weakly coupling new heavy states results in a framework commonly referred to as Standard Model Effective Field Theory (SMEFT) [30–35]. As another example, allowing arbitrary new-physics effects in the Higgs sector of the SM leads to the formalism named Electroweak Chiral Lagrangian[2] (EWChL) [36–47]. Further EFTs with different assumptions can be constructed. All theories have in common the need for extraordinarily high precision in quantitative analyses, both theoretically and experimentally. Indeed, the impact of new physics below its threshold decreases dramatically for lower energies making deviations from the SM background hard to detect.

In this work, we explore the role of power-counting for high-precision calculations in the context of SMEFT. Based on simple examples and specific models, we derive a general power-counting formula providing estimates for the Wilson coefficients of the SMEFT operators depending on their particle content. Our results are underpinned by in-depth calculations and phenomenological studies for two prominent particle reactions at the Large Hadron Collider (LHC), namely the fusion of two gluons associated with the production of a top-anti-top-quark pair ($gg \to t\bar{t}$), and the decay of a Higgs boson into two gluons ($h \to gg$).

The organization is as follows. Section 2 contains a brief heuristic as well as a quantitative summary of our general setup and the conventions we use by reviewing the basic properties of the SM. The main conceptional results regarding the application of chiral dimensions to SMEFT are presented in Section 3. Our major examples, that is $gg \to t\bar{t}$ at leading order (LO) in QCD and $h \to gg$ at next-to-leading order (NLO) in QCD can be found in Section 4 and Section 5, respectively. We conclude in Section 6. While lengthy calculational details are collected in small appendices that are integrated within the main text, the major appendices starting from Appendix A feature additional information such as input parameters and Feynman rules, but also further examples.

[2] This theory is sometimes also referred to as the Higgs Effective Field Theory (HEFT).

2. The Standard Model of particle physics

This section serves as a summary of the basic concepts and the formalism behind the SM. Physicists should skip the first subsection without further ado as it merely contains a heuristic popular scientific review of the "periodic table" of elementary particles. Readers who are already familiar with the SM on a quantitative level might also want to omit the second subsection and turn to SMEFT right away in order to catch up with the conventions used in this work. Finally, working particle physicists may immediately jump to Section 3 concerning non-trivial loop counting and chiral dimensions in SMEFT.

2.1. Informal invitation

Particle physics is the science of the basic building blocks of matter and the fundamental forces - or, in modern language, of particles and their interactions. Its central goal is to explore and explain what elementary particles and interactions were present in the early universe - or equivalently, are still present today at the smallest scales - and how they connect to our measurements at the world's largest machines, i.e. particle accelerators. In doing so, we realize that on a microscopic scale, our world is mathematically much simpler than superficial observations at larger scales - say the size of a human - would suggest. In fact, the interactions of the elementary particles are, mathematically speaking, dictated by some of the least complex *symmetries* of nature. In the following lines, the basic ideas of the SM will be explained in an intuitive and qualitative way. Good heuristic as well as quantitative reviews and introductory texts can be found in [48–51]. Let aside to precisely define the notion of a particle, we assume that, at first sight in a model universe, there are four different species of particles, known as the fundamental *fermions*. They are called up-quark (u), down-quark (d), electron (e) and neutrino (ν) and we take them as massless and electrically neutral[3]. Furthermore, these particles feature some kind of internal angular momentum, the spin, which selects one particular direction in space for a given particle[4]. The same (massless) particle moves through space in a certain direction (with the speed of light), which distinguishes a second direction. If one projects the spin axis onto the motion axis, two possibilities arise: The spin can be oriented *in* the direction of motion or *against* the direction of motion. We speak of right or left *handedness* or *helicity* of the particle and introduce subscripts, i.e. e_L or e_R, etc., to distinguish the respective cases[5]. So far, a left-handed electron will forever

[3] The attempt to consider mass and electrical charge from the beginning turns out to be problematic. It is more clever to implement these concepts later by a suitable mechanism.

[4] As a first approximation, we can imagine the fundamental fermions as little spinning tops, all rotating with the same speed, whose rotation axes point in different directions. However, this view is strictly speaking wrong. Spin is a genuine quantum effect with no classical analog and requires the notion of complex numbers for a consistent mathematical treatment [52].

[5] Important here is the assumption of vanishing masses and hence light speed; otherwise a reference frame could be chosen, in which the handedness would be reversed by boosting to a reference frame with higher velocity than the particle (but still below the speed of light). Based on the transformation properties of spinors under the Lorentz group, it is, however, possible to introduce the concept of *chirality* that makes a frame independent distinction of e_L and e_R, etc. possible even for massive particles.

stay a left-handed electron, etc., and it seems reasonable, that none of the possibilities (left- or right-handed) should be treated differently when we turn on interactions in this model universe.

It is, however, more than astonishing that nature chooses to distinguish on a fundamental level between left- and right-handed particles. To be precise, a mechanism exists that can convert a left-handed up-quark u_L into a left-handed down-quark d_L and an electron e_L into a neutrino ν_L (and vice versa). In contrast, all right-handed particles are unaffected by this mechanism. So to speak, they remain unseen by it. It is called the *chiral interaction*. For the sake of book-keeping, we collect the particles that can be converted into each other in a lepton doublet l_L and a quark doublet q_L as

$$l_L = \begin{pmatrix} \nu_L \\ e_L \end{pmatrix} \text{ and } q_L = \begin{pmatrix} u_L \\ d_L \end{pmatrix} \tag{2.1}$$

A transformation of the particles inside a doublet into each other by the chiral interaction is now caused by a rotation in the internal space of the doublets whose precise interpretation is dictated by the probabilistic laws of quantum mechanics. It is mathematically sufficient to describe the rotational behavior under very small, infinitesimal rotations, which are completely characterized by three *generators*[6]. These correspond to the massless *gauge bosons* W^1 , W^2 and W^3. A left-handed electron, for example, could thus turn into a left-handed neutrino by emitting or absorbing a certain combination of W-bosons. Right-handed particles, on the other hand, are introduced as chiral singlets e_R , u_R and d_R which cannot rotate into each other and hence do not interact with the W-bosons. The right-handed neutrino does not appear in the SM, because it is an uncharged and color-neutral (see below) particle and cannot interact with the other constituents of the SM by the other interactions. In the SM, there are three copies of each of these chiral doublets and singlets, which are called the three particle *generations*. Communication between the generations is possible by virtue of the Cabibbo-Kobayashi-Maskawa matrix (CKM matrix) for quarks and the Pontecorvo-Maki-Nakagawa-Sakata matrix (PMNS matrix) for leptons, which we neglect here for simplicity.

Besides the chiral interaction, nature knows the *strong interaction* for which, slightly abusing our notation, we introduce the quark triplets

$$u = \begin{pmatrix} u_r \\ u_g \\ u_b \end{pmatrix} \text{ and } d = \begin{pmatrix} d_r \\ d_g \\ d_b \end{pmatrix} \tag{2.2}$$

where the chirality indices L or R have been suppressed. In contrast to the chiral interaction, the strong interaction does not distinguish between left- and right-handed particles, but between leptons and quarks. Leptons do not feel the strong interaction, so to speak. The individual components of the quark triplets differ in their *color* or *color charge*. They are usually referred to as red, green, and blue (r, g and b). The strong interaction now leads to transformations of the quarks within a triplet. As before, these

[6] The number three results from the fact that, mathematically, the Lie algebra of the doublet rotation group $SU(2)$ is three-dimensional.

transformations are caused by the generators of the infinitesimal rotations in the internal space of the triplets. In the case of the strong interaction, eight gauge bosons result[7], which are called *gluons*. For example, a red up quark can transform into a green one by emitting a suitable gluon.

Let us turn back to the chiral interaction. Since we have neglected masses and charges so far, there is no way to distinguish, within the chiral interaction, between a left-handed neutrino and a left-handed electron. The world would be symmetric with respect to the chiral interaction. In reality, the components of the chiral doublets as well as the W-bosons have non-vanishing and - crucially - different masses and charges (with a corresponding gauge boson, the *photon*), so that the chiral symmetry in the real world must be broken - or rather hidden. On the other hand, it is clear that the chiral symmetry must have been present in some form, otherwise the elementary particles would not interact with the W-bosons of the real world in the observed way, which resembles the chiral interaction in some sense[8].

The SM solves the symmetry problem of the chiral interaction by linking the origins of mass and electric charge to the properties of the physical vacuum. Electric charge and the massless photon are replaced by the *hypercharge* and a gauge boson B. They preserve the chiral symmetry like W^1 , W^2 and W^3 and distinguish only between left- and right-handed particles. In other words, the components of the chiral doublets are each assigned the same hypercharge, whereas the corresponding chiral singlets pick up different hypercharge values. Introduced in this way, the latter is now able to explain both masses and the electric charge. This is done via a so-called *electroweak symmetry breaking* mechanism, which states that the symmetries of the physical vacuum and the symmetries of the fundamental interactions differ. It can be achieved by the presence of a condensate[9] with non-vanishing hypercharge. The most prominent example of a realization of electroweak symmetry breaking is the *Higgs mechanism*. In this case, a chiral doublet is introduced giving rise to a new particle - the *Higgs particle* - which prefers a non-vanishing vacuum expectation value everywhere in space. It "breaks" the chiral symmetry by interacting with the other elementary particles to generate their distinct masses and charges. Hypercharge and chiral interaction are thereby converted into electric charge and weak interaction as we know them today. Thereby, the gauge bosons W^1, W^2, W^3 and B transform into the gauge bosons of the real world, namely W^+, W^-, Z^0 and the photon γ. The masses of W^+, W^- and Z^0 are generated in the correct ratio, while γ remains massless as it should.

Because of its enormous predictive power, which has withstood any experimental test up to the present day, the SM belongs to the canon of "confirmed" theories in physics. Thus, every form of physics beyond the SM must be able to reproduce the SM as a limit. Electroweak symmetry breaking, i.e. the transition of a physical vacuum which respects

[7] Again, the number eight relates to the fact that the Lie algebra of the triplet rotation group $SU(3)$ is eight-dimensional.

[8] This is the *weak interaction*. Such a dilemma, however, does not occur in the strong interaction, because the masses and charges of the quarks are independent of their colour. The world is therefore symmetric with respect to the strong interaction.

[9] This is in essence some background to which everything has to couple in one or the other way.

the symmetries of the fundamental interactions, into another vacuum breaking these symmetries by the Higgs condensate, should have taken place in the early universe when the average available energy (i.e. temperature) was much larger than it is today. Particle accelerators that mimic these extreme situations by high-energy particle collisions may therefore be viewed as time machines enabling us to probe matter under the conditions of the very early universe. The discovery of the Higgs particle in 2012 at the LHC at CERN (Conseil Européen pour la Recherche Nucléaire) [53] is regarded as one of the greatest moments in the history of particle physics and is the prime example of the predictive power of theoretical physics, which had already postulated it in 1964 [54–59]. To this day, the Higgs particle and hence the nature of electroweak symmetry breaking is at the center of research in particle physics.

2.2. Standard Model Lagrangian

The previous section comprises a heuristic summary of the renormalizable part of the SM[10]. We can construct a Lagrangian for the SM by writing down all renormalizable terms that respect the symmetries. These are Lorentz invariance on one hand, and the internal gauge symmetries left-handed isospin $SU(2)_L$, hypercharge $U(1)_Y$ and colour $SU(3)_c$ on the other hand. The matter content consists of the quarks and leptons (up-quark u, down quark d and neutrino ν, electron e, respectively), all coming in three copies, and a complex scalar field φ, referred to as the Higgs field. Their $SU(2)_L$ representation as well as hypercharge assignments Y are given by

$$\text{Left-handed lepton doublet } l_L = \begin{pmatrix} \nu_L \\ e_L \end{pmatrix} \text{ with } Y = -\frac{1}{2} \tag{2.3}$$

$$\text{Right-handed lepton singlet } e_R \text{ with } Y = -1 \tag{2.4}$$

$$\text{Left-handed quark doublet } q_L = \begin{pmatrix} u_L \\ d_L \end{pmatrix} \text{ with } Y = \frac{1}{6} \tag{2.5}$$

$$\text{Right-handed up-quark singlet } u_R \text{ with } Y = \frac{2}{3} \tag{2.6}$$

$$\text{Right-handed down-quark singlet } d_R \text{ with } Y = -\frac{1}{3} \tag{2.7}$$

$$\text{Higgs doublet } \varphi = \begin{pmatrix} \varphi^+ \\ \varphi^0 \end{pmatrix} \text{ with } Y = \frac{1}{2} \tag{2.8}$$

We have suppressed the fermion generation[11], as well as quark colour indices like in (2.1). Note that a right-handed neutrino is absent. Furthermore, we work in the flavour

[10] We reserve the acronym SM exclusively for the renormalizable part - the non-renormalizable part will be denoted by SMEFT, see below.

[11] In a suboptimal notation, these would be given by

$$\nu \longrightarrow (\nu_e, \nu_\mu, \nu_\tau); \quad e \longrightarrow (e, \mu, \tau); \quad u \longrightarrow (u, c, t); \quad d \longrightarrow (d, s, b) \tag{2.9}$$

for all chiralities. Numbered indices like u^1, u^2 or u^3 for u, c and t, etc. are also common. It should be clear from the context what is meant.

basis rather than the mass basis. A conversion can be done by the CKM matrix for the quarks (or PMNS matrix for the leptons if a right-handed neutrino is considered). This is, however, unimportant for our purposes. The covariant derivative featuring the $SU(2)_L$, $U(1)_Y$ and $SU(3)_c$ gauge bosons W^α_μ, B_μ and G^A_μ with couplings g, g' and g_s, respectively, is defined by

$$D_\mu = \partial_\mu + igW^\alpha_\mu \tau^\alpha + ig'YB_\mu + ig_s G^A_\mu T^A \tag{2.10}$$

depending on the field they act on, i.e. the $SU(2)_L$-part is absent for right-handed fields and the $SU(3)_c$-part concerns only quarks, irrespective of their handedness. To avoid writing too many Kronecker deltas, fundamental indices are not displayed. Do not confuse Lorentz indices with adjoint $SU(2)_L$ indices as both are denoted by Greek letters. The generators for the non-Abelian gauge groups are normalized as $[\tau^\alpha, \tau^\beta] = i\epsilon^{\alpha\beta\gamma}\tau^\gamma$ and $[T^A, T^B] = if^{ABC}T^C$, where ϵ and f denote the Levi-Civita symbol and the structure constants of $SU(3)$, respectively[12]. Note that only the gluon field G^A_μ is physical - the isospin and hypercharge gauge bosons are mere linear combinations of physical fields.

The most general Lagrangian should include kinetic terms for the fermions, the Higgs field and the gauge bosons, as well as all allowed interaction terms, i.e. a φ^4-interaction as well as Yukawa interactions. Mass terms for the gauge bosons as well as for the fermions are forbidden by the underlying symmetries. However, a Higgs mass term $\sim \varphi^2$ is not excluded by the symmetries. Also, there is no mechanism to determine the sign of this term. Compared to the canonical choice of sign for mass terms, that is $\mathcal{L} \sim -m^2\varphi^2$, the SM realizes such a term with a flipped sign, namely $\mathcal{L} \sim +m^2\varphi^2$. It is this tiny detail that is responsible for a broad variety of phenomenological observations, not least for the fermion- and gauge-boson masses. The list of allowed terms is exhausted by the SM Lagrangian[13]

$$\begin{aligned}
\mathcal{L}_{SM} = & -\frac{1}{4}B_{\mu\nu}B^{\mu\nu} - \frac{1}{2}\langle W_{\mu\nu}W^{\mu\nu}\rangle - \frac{1}{2}Tr\left(G_{\mu\nu}G^{\mu\nu}\right) + \\
& + i\bar{l}_L \not{D} l_L + i\bar{e}_R \not{D} e_R + i\bar{q}_L \not{D} q_L + i\bar{u}_R \not{D} u_R + i\bar{d}_R \not{D} d_R + \\
& + \left(D_\mu\varphi\right)^\dagger D^\mu\varphi + m^2\varphi^\dagger\varphi - \frac{1}{2}\lambda(\varphi^\dagger\varphi)^2 + \\
& - \left(\bar{l}_L\Gamma_e e_R\varphi + \bar{q}_L\Gamma_d d_R\varphi + \bar{q}_L\Gamma_u u_R\tilde{\varphi} + h.c.\right)
\end{aligned} \tag{2.11}$$

where $h.c.$ denotes the hermitian conjugate of the last line. Our conventions are as follows. We constructed the field strength tensors from the gauge fields via $B_{\mu\nu} = \partial_\mu B_\nu - \partial_\nu B_\mu$, $W^\alpha_{\mu\nu} = \partial_\mu W^\alpha_\nu - \partial_\nu W^\alpha_\mu - g\epsilon^{\alpha\beta\gamma}W^\beta_\mu W^\gamma_\nu$ and $G^A_{\mu\nu} = \partial_\mu G^A_\nu - \partial_\nu G^A_\mu - g_s f^{ABC} G^B_\mu G^C_\nu$ with $W_{\mu\nu} = W^\alpha_{\mu\nu}\tau^\alpha$ and $G_{\mu\nu} = G^A_{\mu\nu}T^A$. The abbreviations $\langle ...\rangle$ and $Tr(...)$ denote traces over fundamental isospin and colour indices, respectively. For later use, we define the dual gauge boson tensors via $\tilde{B}_{\mu\nu} = \epsilon_{\mu\nu\alpha\beta}B^{\alpha\beta}/2$, etc. with $\epsilon_{0123} = 1$. The isospin

[12] We can thus write $\tau^\alpha = \sigma^\alpha/2$ and $T^A = \lambda^A/2$, where σ^α and λ^A for $\alpha = 1, 2, 3$ and $A = 1, ..., 8$ are the Pauli- and Gell-Mann matrices, respectively.

[13] We neglect topological terms and related issues like the strong CP-problem.

components of the dual Higgs field $\tilde{\varphi}$ with $Y = -1/2$ are given by $\tilde{\varphi}_i = \epsilon_{ij}\varphi_j^*$ with $\epsilon_{12} = 1$ and the star refers to complex conjugation. We have denoted the Yukawa couplings by Γ_e, etc. They are matrices in generation space; as stated above, diagonalizing the fermion mass terms after electroweak symmetry breaking changes their couplings to the gauge fields. The resulting CKM matrix mainly affects the W-boson interactions and is, as stated above, not taken into account here.
The Higgs potential $V(\varphi^\dagger\varphi) = \lambda(\varphi^\dagger\varphi)^2/2 - m^2\varphi^\dagger\varphi$ has a minimum for $\varphi^\dagger\varphi = v^2/2$ where $v = \sqrt{2m^2/\lambda}$ is the Higgs vacuum expectation value and the original $SU(2)_L$ symmetry is broken when expanding around this minimum. Fluctuations around the vacuum expectation value are then interpreted as the physical fields. Without loss of generality, we can choose the coordinate system in isospin space such that the vacuum expectation value is entirely shifted to the lower component φ^0, i.e. we write

$$\varphi = \begin{pmatrix} \varphi^+ \\ \frac{1}{\sqrt{2}}\,(v + h + i\eta) \end{pmatrix} \tag{2.12}$$

where $1/\sqrt{2}$ is just a normalization convention. The emergence of a dimensionful constant v enables the generation of gauge boson masses via the Higgs kinetic term, as well as fermion masses via the Yukawa interactions. The upper component φ^+ along with the field η remain massless and can be interpreted as the Goldstone bosons for the symmetry breaking-pattern at hand. In unitary gauge, they can be absorbed as the respective third degrees of freedom for the now massive gauge bosons. The residual field h is massive and comprises the only surviving physical object from the Higgs field φ. This is the Higgs boson. It couples to all massive particles in the SM.
The renormalizable part of the SM is hereby complete. To sum up, it consists of all operators up to canonical dimension four that are allowed by symmetry. Interpreted as an EFT, its only ordering mechanism in perturbation theory is the loop order of Feynman diagrams. A given process usually has an infinite number of contributions associated with an ever increasing loop-order, each contributing a loop suppression factor of $1/(16\pi^2)$ and additional powers of weak couplings, i.e. parameters $\lesssim 4\pi$, assuring the non-divergence[14] of the series[15]. Renormalizability keeps the number of input parameters constant to arbitrary precision, that is to all orders. Although the theoretical validity of the SM may be extended to arbitrary high energies, it should be noted that its particle content is restricted to masses $\lesssim v$, as they are all generated via the same mechanism. A naïve extrapolation into the deep UV[16] in terms of the SM therefore seems unnatural as there might indeed exist (much) heavier particles with no relation to v. The precise dynamics of such particles might not be straightforwardly embeddable into the SM framework.

[14] To be precise, the series expansion is in fact only *asymptotic* and hence eventually divergent. Such issues, however, do not touch the low-loop considerations presented in this work.

[15] If additional loops are associated with two powers of weak couplings κ, it is advantageous to work with finestructure constants $\alpha_\kappa \equiv \kappa^2/(4\pi)$, so that the expansion parameter is $\alpha_\kappa/(4\pi)$.

[16] In particle physics, the abbreviation UV (ultraviolet) is taken over from the classification of the visible light spectrum and generally refers to small scales (wavelengths) and hence high energies. The opposite, IR (infrared), is associated with large scales or low energies.

2.3. Standard Model Effective Field Theory

The more compelling part starts when we add higher dimensional operators, i.e. of canonical dimension $d_c > 4$, to the SM Lagrangian, resulting in SMEFT. To compensate for the dimensional discrepancy in four-dimensional spacetime, such operators come with an extra energy scale Λ that divides out the excess. The SM Lagrangian then gets enlarged to

$$\mathcal{L}_{SMEFT} = \mathcal{L}_{SM} + \sum_i \frac{C_i}{\Lambda} Q_{5,i} + \sum_i \frac{C_i}{\Lambda^2} Q_{6,i} + ... \tag{2.13}$$

with dimensionless Wilson coefficients C_i and generic d_c-dimensional operators $Q_{d_c,i}$. The index i labels the operators with fixed d_c. As this list with increasing d_c would continue until infinity, we need a power-counting assumption on the Lagrangian level to guarantee the non-collapse of the theory. This can be achieved by choosing Λ to be large compared to the SM energy scales[17]. The resulting Lagrangian is then renormalizable *order-by-order* in the following sense. Despite featuring an infinite number of parameters, only a finite number is usually relevant for a given process with fixed precision. All higher-order effects in Λ (an infinite number of effects) would then contribute below this precision benchmark point and can therefore consistently be neglected. From a phenomenological point of view, the higher dimensional local operators are in fact the manifestation of heavy non-SM particles at the SM energy scales $\lesssim v$. Indeed, all theories with weakly coupling heavy particles of mass $M \gg v$ reduce to SMEFT with $\Lambda \approx M$ when the non-SM fields are integrated out. Obtaining non-vanishing experimental constraints on the SMEFT Wilson coefficients[18] would therefore be a good hint towards physics beyond the SM, e.g. heavy SUSY particles or dark-matter candidates.

Let us now turn to the explicit construction of the higher-dimensional operators. In order to obtain a complete and non-redundant set of operators for a given d_c, several manipulations have to be made. This includes the application of Fierz identities, as well as field redefinitions. The latter are equivalent to using the equations of motion on the Lagrangian level [6]. There exists only a single dimension-five (lepton number violating) operator [60]

$$Q_{\nu\nu} = (\tilde{\varphi}^\dagger l_L)^T C (\tilde{\varphi}^\dagger l_L) \tag{2.14}$$

where open generation indices have been suppressed on both sides of the equation and the transposition refers to the spinor space. In constructing this operator, it is advantageous to convert the right-handed fields into their left-handed charge conjugates by virtue of the matrix $C = i\gamma^2\gamma^0$. Making isospin indices explicit, the hypercharge of two Higgs doublets $\varphi_j\varphi_m$ is $Y = 1$, so only two fermions $l_{Li}^T C l_{Ln}$ (this is Lorentz invariant) with combined $Y = -1$ are possible for a combination. The isospin indices then have to be contracted

[17]In addition, the Wilson-coefficients must not grow arbitrarily for higher canonical dimension. The suppression mechanism is thus entirely accounted for by Λ.

[18]Note that it is actually only the ratio C_i/Λ^{d_c-4} that enters the experimental observables. It is therefore common to actually *identify* $\Lambda \equiv M$ and absorb everything else, that is weak couplings and dimensionless numerical numbers, into C_i.

with $\epsilon_{ij}\epsilon_{nm}$ in order to achieve a non-vanishing result. After electroweak symmetry breaking, this operator gives rise to (Majorana) neutrino masses. However, due to astonishing experimental constraints [61–64], the Wilson coefficient of this operator has to be quite small, so we can neglect this operator as a first approximation [65].
Next up are the dimension-six operators [30, 31, 66]. A full basis has first been written down in its modern form in [31] and is commonly referred to as the *Warsaw basis*. Imposing baryon number conservation, it consists of 59 independent operators for one particle generation. Defining

$$\varphi^\dagger \overleftrightarrow{D}_\mu \varphi \equiv \varphi^\dagger D_\mu \varphi - (D_\mu \varphi)^\dagger \varphi \tag{2.15}$$

and

$$\varphi^\dagger \overleftrightarrow{D}^\alpha_\mu \varphi \equiv \varphi^\dagger \tau^\alpha D_\mu \varphi - (D_\mu \varphi)^\dagger \tau^\alpha \varphi \tag{2.16}$$

the full set of pure bosonic (left column) and mixed fermionic-bosonic (right column) operators is given by the following list.

$$\begin{aligned}
&Q_G = f^{ABC} G_\mu^{A\nu} G_\nu^{B\lambda} G_\lambda^{C\mu} &\qquad& Q_{e\varphi} = (\varphi^\dagger\varphi)(\bar{l}_L e_R \varphi) &(2.17)\\
&Q_{\tilde{G}} = f^{ABC} \tilde{G}_\mu^{A\nu} G_\nu^{B\lambda} G_\lambda^{C\mu} && Q_{u\varphi} = (\varphi^\dagger\varphi)(\bar{q}_L u_R \tilde{\varphi}) &(2.18)\\
&Q_W = \epsilon^{\alpha\beta\gamma} W_\mu^{\alpha\nu} W_\nu^{\beta\lambda} W_\lambda^{\gamma\mu} && Q_{d\varphi} = (\varphi^\dagger\varphi)(\bar{q}_L d_R \varphi) &(2.19)\\
&Q_{\tilde{W}} = \epsilon^{\alpha\beta\gamma} \tilde{W}_\mu^{\alpha\nu} W_\nu^{\beta\lambda} W_\lambda^{\gamma\mu} && Q_{eW} = (\bar{l}_L \sigma_{\mu\nu} e_R)\tau^\alpha \varphi W^\alpha_{\mu\nu} &(2.20)\\
&Q_\varphi = (\varphi^\dagger\varphi)^3 && Q_{eB} = (\bar{l}_L \sigma_{\mu\nu} e_R)\varphi B_{\mu\nu} &(2.21)\\
&Q_{\varphi\Box} = (\varphi^\dagger\varphi)\Box(\varphi^\dagger\varphi) && Q_{uG} = (\bar{q}_L \sigma_{\mu\nu} T^A u_R)\tilde{\varphi} G^A_{\mu\nu} &(2.22)\\
&Q_{\varphi D} = (\varphi^\dagger D^\mu \varphi)^*(\varphi^\dagger D_\mu \varphi) && Q_{uW} = (\bar{q}_L \sigma_{\mu\nu} u_R)\tau^\alpha \tilde{\varphi} W^\alpha_{\mu\nu} &(2.23)\\
&Q_{\varphi G} = \varphi^\dagger \varphi G^A_{\mu\nu} G^{A\mu\nu} && Q_{uB} = (\bar{q}_L \sigma_{\mu\nu} u_R)\tilde{\varphi} B_{\mu\nu} &(2.24)\\
&Q_{\varphi W} = \varphi^\dagger \varphi W^\alpha_{\mu\nu} W^{\alpha\mu\nu} && Q_{dG} = (\bar{q}_L \sigma_{\mu\nu} T^A d_R)\varphi G^A_{\mu\nu} &(2.25)\\
&Q_{\varphi B} = \varphi^\dagger \varphi B_{\mu\nu} B^{\mu\nu} && Q_{dW} = (\bar{q}_L \sigma_{\mu\nu} d_R)\tau^\alpha \varphi W^\alpha_{\mu\nu} &(2.26)\\
&Q_{\varphi WB} = \varphi^\dagger \tau^\alpha \varphi W^\alpha_{\mu\nu} B^{\mu\nu} && Q_{dB} = (\bar{q}_L \sigma_{\mu\nu} d_R)\varphi B_{\mu\nu} &(2.27)\\
&Q_{\varphi \tilde{G}} = \varphi^\dagger \varphi \tilde{G}^A_{\mu\nu} G^{A\mu\nu} && Q^{(1)}_{\varphi l} = (\varphi^\dagger i \overleftrightarrow{D}_\mu \varphi)(\bar{l}_L \gamma^\mu l_L) &(2.28)\\
&Q_{\varphi \tilde{W}} = \varphi^\dagger \varphi \tilde{W}^\alpha_{\mu\nu} W^{\alpha\mu\nu} && Q^{(3)}_{\varphi l} = (\varphi^\dagger i \overleftrightarrow{D}^\alpha_\mu \varphi)(\bar{l}_L \gamma^\mu \tau^\alpha l_L) &(2.29)\\
&Q_{\varphi \tilde{B}} = \varphi^\dagger \varphi \tilde{B}_{\mu\nu} B^{\mu\nu} && Q_{\varphi e} = (\varphi^\dagger i \overleftrightarrow{D}_\mu \varphi)(\bar{e}_R \gamma^\mu e_R) &(2.30)\\
&Q_{\varphi \tilde{W}B} = \varphi^\dagger \tau^\alpha \varphi \tilde{W}^\alpha_{\mu\nu} B^{\mu\nu} && Q^{(1)}_{\varphi q} = (\varphi^\dagger i \overleftrightarrow{D}_\mu \varphi)(\bar{q}_L \gamma^\mu q_L) &(2.31)\\
& && Q^{(3)}_{\varphi q} = (\varphi^\dagger i \overleftrightarrow{D}^\alpha_\mu \varphi)(\bar{q}_L \gamma^\mu \tau^\alpha q_L) &(2.32)\\
& && Q_{\varphi u} = (\varphi^\dagger i \overleftrightarrow{D}_\mu \varphi)(\bar{u}_R \gamma^\mu u_R) &(2.33)\\
& && Q_{\varphi d} = (\varphi^\dagger i \overleftrightarrow{D}_\mu \varphi)(\bar{d}_R \gamma^\mu d_R) &(2.34)\\
& && Q_{\varphi ud} = (\varphi^\dagger i \overleftrightarrow{D}_\mu \varphi)(\bar{u}_R \gamma^\mu d_R) &(2.35)
\end{aligned}$$

It is sometimes convenient to eliminate $Q_{\varphi D}$ from this basis by writing

$$Q_{\varphi D} = -\frac{1}{4}\left(Q_{\varphi\Box} + (\varphi^\dagger \overleftrightarrow{D}_\mu \varphi)(\varphi^\dagger \overleftrightarrow{D}^\mu \varphi)\right) \tag{2.36}$$

which can be derived upon integration by parts. The baryon number conserving pure fermionic operators are given by

$$Q_{ll} = (\bar{l}_L\gamma^\mu l_L)(\bar{l}_L\gamma_\mu l_L) \qquad Q_{le} = (\bar{l}_L\gamma^\mu l_L)(\bar{e}_R\gamma_\mu e_R) \tag{2.37}$$

$$Q_{qq}^{(1)} = (\bar{q}_L\gamma^\mu q_L)(\bar{q}_L\gamma_\mu q_L) \qquad Q_{lu} = (\bar{l}_L\gamma^\mu l_L)(\bar{u}_R\gamma_\mu u_R) \tag{2.38}$$

$$Q_{qq}^{(1)} = (\bar{q}_L\gamma^\mu \tau^\alpha q_L)(\bar{q}_L\gamma_\mu \tau^\alpha q_L) \qquad Q_{ld} = (\bar{l}_L\gamma^\mu l_L)(\bar{d}_R\gamma_\mu d_R) \tag{2.39}$$

$$Q_{lq}^{(1)} = (\bar{l}_L\gamma^\mu l_L)(\bar{q}_L\gamma_\mu q_L) \qquad Q_{qe} = (\bar{q}_L\gamma^\mu q_L)(\bar{e}_R\gamma_\mu e_R) \tag{2.40}$$

$$Q_{lq}^{(1)} = (\bar{l}_L\gamma^\mu \tau^\alpha l_L)(\bar{q}_L\gamma_\mu \tau^\alpha q_L) \qquad Q_{qu}^{(1)} = (\bar{q}_L\gamma^\mu q_L)(\bar{u}_R\gamma_\mu u_R) \tag{2.41}$$

$$Q_{ee} = (\bar{e}_R\gamma^\mu e_R)(\bar{e}_R\gamma_\mu e_R) \qquad Q_{qu}^{(8)} = (\bar{q}_L\gamma^\mu T^A q_L)(\bar{u}_R\gamma_\mu T^A u_R) \tag{2.42}$$

$$Q_{uu} = (\bar{u}_R\gamma^\mu u_R)(\bar{u}_R\gamma_\mu u_R) \qquad Q_{qd}^{(1)} = (\bar{q}_L\gamma^\mu q_L)(\bar{d}_R\gamma_\mu d_R) \tag{2.43}$$

$$Q_{dd} = (\bar{d}_R\gamma^\mu d_R)(\bar{d}_R\gamma_\mu d_R) \qquad Q_{qd}^{(8)} = (\bar{q}_L\gamma^\mu T^A q_L)(\bar{d}_R\gamma_\mu T^A d_R) \tag{2.44}$$

$$Q_{eu} = (\bar{e}_R\gamma^\mu e_R)(\bar{u}_R\gamma_\mu u_R) \qquad Q_{ledq} = (\bar{l}_{Li} e_R)\delta_{ij}(\bar{d}_R q_{Lj}) \tag{2.45}$$

$$Q_{ed} = (\bar{e}_R\gamma^\mu e_R)(\bar{d}_R\gamma_\mu d_R) \qquad Q_{quqd}^{(1)} = (\bar{q}_{Li} u_R)\epsilon_{ij}(\bar{q}_{Lj} d_R) \tag{2.46}$$

$$Q_{ud}^{(1)} = (\bar{u}_R\gamma^\mu u_R)(\bar{d}_R\gamma_\mu d_R) \qquad Q_{quqd}^{(8)} = (\bar{q}_{Li} T^A u_R)\epsilon_{ij}(\bar{q}_{Lj} T^A d_R) \tag{2.47}$$

$$Q_{ud}^{(8)} = (\bar{u}_R\gamma^\mu T^A u_R)(\bar{d}_R\gamma_\mu T^A d_R) \qquad Q_{lequ}^{(1)} = (\bar{l}_{Li} e_R)\epsilon_{ij}(\bar{q}_{Lj} u_R) \tag{2.48}$$

$$Q_{lequ}^{(3)} = (\bar{l}_{Li}\sigma_{\mu\nu} e_R)\epsilon_{ij}(\bar{q}_{Lj}\sigma^{\mu\nu} u_R) \tag{2.49}$$

Again, the fermion generation indices have been left open. As an example, they may be restored like $Q_{eu}^{1231} = (\bar{e}_R^1\gamma^\mu e_R^2)(\bar{u}_R^3\gamma_\mu u_R^1) \to (\bar{e}_R\gamma^\mu \mu_R)(\bar{t}_R\gamma_\mu u_R)$, etc. The Warsaw-basis operators are sometimes collected into the self-explaining schematic classes $X_{\mu\nu}^3$, φ^6, $\partial^2\varphi^4$, $\varphi^3\psi^2$, $\partial\varphi^2\psi^2$, $\varphi^2 X_{\mu\nu}^2$, $\varphi\psi^2 X_{\mu\nu}$ and ψ^4 where $X_{\mu\nu}$, φ, ψ and ∂ are general abbreviations for SM field strength tensors, scalars, fermions and (covariant) derivatives.
It is conceptually self-explanatory, but cumbersome, to construct SMEFT bases for even higher dimensions [67–73]. However, such higher-dimension operators are even more suppressed with respect to the heavy new-physics scale Λ. Let aside the dimension-five operator (2.14), the dimension-six operators (2.17)-(2.49) thus represent the leading and therefore most promising new-physics effects. Having still to be discovered, it is these leading-order effects that reasonable phenomenological studies should be primarily concentrated on.
Introduced in this way, it seems that the loop expansion inherited from the SM completely decouples from the $1/\Lambda$-expansion in SMEFT. After all, when looking at the world through "EFT glasses", the latter is nothing more than an additional power-counting scheme on top of the usual counting of loops. The operators are simply constructed from the ground up without referring to potential new-physics models. At first glance, being maximally agnostic towards high-energy theories, this seems to be the procedure

of choice. This view, however, lacks a reference to what is really happening at high energies, namely the generation of these operators from first principles in the realm of the real-world new-physics scenario. It is therefore more advantageous to look through ”new-physics glasses” in the sense that one should ask the question of whether there are certain hierarchies between Warsaw-basis operators over the course of their creation *in general*. In the next section, we will argue that this is indeed the case.

3. Loop counting in SMEFT

The phenomenology of the six-dimensional Warsaw-basis operators has been studied extensively in the literature. A naïve application of (2.17)-(2.49), however, not only has the major disadvantage of introducing a maximal set of new coefficients to be accounted for, but is also inconsistent with a broad class of possible high-energy scenarios. In this section, we advertise a consistent approach based on an additional power-counting prescription for loops, the chiral dimension, that interferes with the $1/\Lambda$-expansion handled by canonical dimensions in a non-trivial manner. As a positive side effect, this may also reduce the number of relevant parameters for a given process drastically. This section is partly based on [74].

3.1. Toy model analysis

Before diving into SMEFT at canonical dimension six, let us consider a toy model, namely QED - symbolically standing for the SM - with a light electron ψ of negligible mass and a top-quark t of mass m, supplemented by a heavy scalar S of mass M, representing the beyond-the-SM physics. A more realistic scenario with relevance for the SM is given in Appendix G, where we consider the Two-Higgs-Doublet Model (2HDM). The Lagrangian for the toy model is given by [74, 75]

$$\begin{aligned}\mathcal{L} = &-\frac{1}{4}F_{\mu\nu}F^{\mu\nu} + \bar{\psi}i\not{D}\psi + \bar{t}(i\not{D} - m)t + \\ &+ \frac{1}{2}\partial_\mu S\partial^\mu S - \frac{1}{2}M^2S^2 - \frac{b}{6}S^3 - \frac{\lambda}{24}S^4 - g\bar{t}tS\end{aligned} \tag{3.1}$$

where the covariant derivatives are defined as

$$D_\mu\psi = \partial_\mu\psi - ieA_\mu\psi \tag{3.2}$$

and

$$D_\mu t = \partial_\mu t + i\frac{2e}{3}A_\mu t \tag{3.3}$$

and $F_{\mu\nu} = \partial_\mu A_\nu - \partial_\nu A_\mu$ is the photon field strength tensor. Taking the dimensionless couplings g and λ as $\mathcal{O}(1)$ numbers and the super-renormalizable coupling $b \sim M$ to allow the generation of an unsuppressed four-point interaction via connecting two three-point vertices by a heavy propagator, this theory naturally possesses two scales, m and M. It may serve as a prototype for a weakly coupled, fully renormalizable (in the traditional sense) UV theory.

We are now interested in how the scalar S modifies the dynamics of the electron and the top-quark at low energies for the case $m \ll M$. As an example, we consider electron-positron annihilation associated with top-anti-top pair production ($e^+e^- \to \bar{t}t$). The incoming electron and positron momenta are denoted by k_1 and k_2 and the outgoing top and anti-top momenta by p_1 and p_2, respectively, with $k_1^2 = k_2^2 = 0$ and $p_1^2 = p_2^2 = m^2$.

Furthermore, we define $q \equiv k_1 + k_2 = p_1 + p_2$. At LO in QED, there is only one diagram with an amplitude of

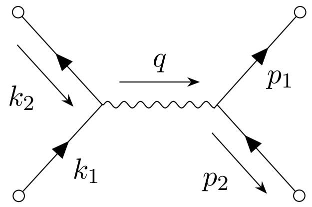

$$\equiv -\frac{2e^2}{3q^2}\,\bar{v}(k_2)\gamma_\mu u(k_1)\,\bar{u}(p_1)\gamma^\mu v(p_2) \tag{3.4}$$

with a self-explaining notation for the spinors. As the heavy scalar S only couples to the top-quark, we expect its effects to only modify the photon-top-anti-top vertex. At NLO, we therefore replace

$$\bar{u}(p_1)\gamma^\mu v(p_2) \longrightarrow \bar{u}(p_1)\Gamma^\mu v(p_2) \tag{3.5}$$

where $\Gamma^\mu \equiv \gamma^\mu + \delta\Gamma^\mu$. The correction $\delta\Gamma^\mu$ is then given by the triangle diagram

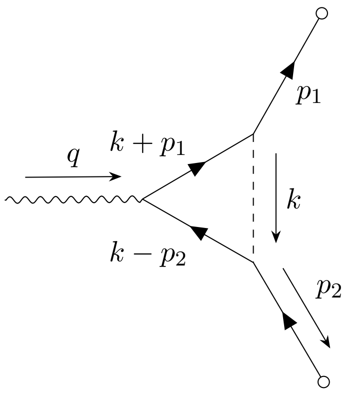

$$= -i\frac{2e}{3}\bar{u}(p_1)\delta\Gamma^\mu v(p_2) \tag{3.6}$$

where

$$\begin{aligned}
&\bar{u}(p_1)\delta\Gamma^\mu v(p_2) = \\
&\quad = ig^2\mu^{2\epsilon}\int \frac{d^dk}{(2\pi)^d}\frac{\bar{u}(p_1)(\not{k} + \not{p}_1 + m)\gamma^\mu(\not{k} - \not{p}_2 + m)v(p_2)}{\big(k^2 - M^2 + i\eta\big)\big((k+p_1)^2 - m^2 + i\eta\big)\big((k-p_2)^2 - m^2 + i\eta\big)}
\end{aligned} \tag{3.7}$$

in dimensional regularization with $d = 4 - 2\epsilon$ and $0 < \eta \ll 1$. In the appendix to this section, we show three different ways how to calculate the loop integral to LO in $1/M^2$. Employing the OS (on-shell) renormalization scheme, the final result is given by

$$\begin{aligned}
\delta\Gamma^\mu = -\frac{g^2}{16\pi^2}\frac{1}{M^2}\Bigg(&\left(\frac{\ln r}{3} + \frac{4}{9} + h_1(z)\right)q^2\gamma^\mu + \\
&+\left(\ln r + \frac{7}{6} + h_2(z)\right)i\sigma^{\mu\nu}q_\nu m\Bigg) + \mathcal{O}\left(\frac{1}{M^4}\right)
\end{aligned} \tag{3.8}$$

where the definitions

$$\sigma^{\mu\nu} \equiv \frac{i}{2}[\gamma^\mu, \gamma^\nu]\,, \qquad r \equiv \frac{m^2}{M^2}\,, \qquad z \equiv \frac{q^2}{4m^2} \tag{3.9}$$

and

$$h_1(z) \equiv \int_0^1 dx\, 2x(1-x)\, \ln\big(1 - 4x(1-x)z - i\eta\big) = \left(\frac{1}{3} + \frac{1}{6z}\right) h_2(z) + \frac{1}{9} \tag{3.10}$$

$$h_2(z) \equiv \int_0^1 dx\, \ln\big(1 - 4x(1-x)z - i\eta\big) = \sqrt{1 - \frac{1}{z}}\, \ln\left(\frac{\sqrt{1-\frac{1}{z}}+1}{\sqrt{1-\frac{1}{z}}-1}\right) - 2 \tag{3.11}$$

have been used.

The compact expression (3.8) contains the full information on the heavy scalar's impact on low energy scales, where terms of higher order in $1/M^2$ can be neglected. At these scales, however, the scalar is not part of the physical particle spectrum, so here the dynamics is best described by an EFT with the scalar integrated out. The parameters (Wilson coefficients) of the EFT are then completely determined by either matching the EFT to the full theory (top-down approach) or by fixing their values via experimental input (bottom-up approach). Let us focus on the top-down approach first before commenting on the bottom-up approach.

Because the LO vertex-correction given by (3.6) is a one-loop diagram, we have to go at least to the one-loop order in the matching procedure to fully capture all effects. As a first step, we integrate out S at tree-level, i.e. solve its classical equation of motion. The latter is given by

$$\Box S + M^2 S + \frac{b}{2} S^2 + \frac{\lambda}{6} S^3 + g\bar{t}t = 0 \tag{3.12}$$

with the formal solution

$$S = -\frac{1}{\Box + M^2 + \frac{b}{2}S + \frac{\lambda}{6}S^2} g\bar{t}t = -\frac{g}{M^2}\bar{t}t + \mathcal{O}\left(\frac{1}{M^4}\right) \tag{3.13}$$

Reinserted into (3.1) yields

$$\mathcal{L}_{eff} \supset \frac{g^2}{2M^2}\bar{t}t\bar{t}t \equiv \frac{C_1}{M^2}Q_1 \tag{3.14}$$

with $C_1 = g^2/2$ and $Q_1 = \bar{t}t\bar{t}t$. For the one-loop operators, we have to refer to the local operators generated in (3.8). These are given by

$$\mathcal{L}_{eff} \supset \frac{C_2}{M^2}Q_2 + \frac{C_3}{M^2}Q_3 \tag{3.15}$$

with

$$Q_2 = \partial_\mu F^{\mu\nu}\, \bar{t}\gamma_\nu t \tag{3.16}$$

and

$$Q_3 = m\bar{t}\sigma_{\mu\nu}t\, F^{\mu\nu} \tag{3.17}$$

Their coefficients C_2 and C_3 can be determined by carrying out the full one-loop matching. Schematically, suppressing the prefactors present in (3.6), we have

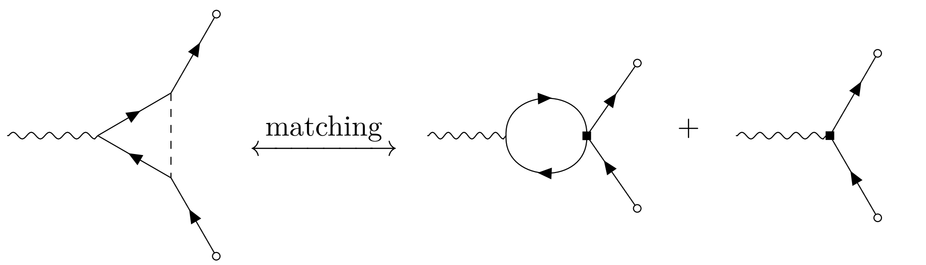

$$\delta\Gamma^\mu \quad = \quad \delta\Gamma^\mu_{Q_1} \quad + \quad \delta\Gamma^\mu_{Q_2} + \delta\Gamma^\mu_{Q_3} \tag{3.18}$$

with the full theory result on the left-hand side given by (3.8) and EFT vertices represented by black squares on the right-hand side. Here, the tree level local contributions are given by[19]

$$\delta\Gamma^\mu_{Q_2} = \frac{3C_2}{2eM^2} q^2\gamma^\mu \tag{3.21}$$

and

$$\delta\Gamma^\mu_{Q_3} = -\frac{3C_3}{eM^2} m i\sigma^{\mu\nu} q_\nu \tag{3.22}$$

whereas the non-local loop diagram reads

$$\delta\Gamma^\mu_{Q_1} = i\frac{2C_1}{M^2}\mu^{2\epsilon}\int \frac{d^dk}{(2\pi)^d}\frac{\bar{u}(p_1)(\not{k}+m)\gamma^\mu(\not{k}-\not{q}+m)v(p_2)}{\big(k^2-m^2\big)\big((k-q)^2-m^2\big)} \tag{3.23}$$

The factor 2 stems from two possible contractions of the four-top operator (3.14) and the closed fermion loop induces an extra factor of (-1). This integral is calculated using the strategy of regions for the full theory contribution in (3.99) in the appendix

[19] As the photon eventually contracts with the electron current, we can use the Dirac equation $\bar{v}(k_2)\not{q}u(k_1) = 0$ implicitly to drop terms $\sim q^\mu$. As a consequence, the term $\sim \partial_\mu A^\mu$ in Q_2 does not contribute. Note that upon using the equation of motion for the photon field, i.e.

$$\partial_\mu F^{\mu\nu} = -e\bar{\psi}\gamma^\nu\psi + \frac{2e}{3}\bar{t}\gamma^\nu t \tag{3.19}$$

we can get rid of the second derivative obtaining the operator

$$Q_2' = -e\bar{\psi}\gamma^\nu\psi\bar{t}\gamma_\nu t + \frac{2e}{3}\bar{t}\gamma^\nu t\bar{t}\gamma_\nu t \tag{3.20}$$

instead of Q_2. The first term in (3.20) gives the same contribution to the process considered above by virtue of a plain four-fermion vertex.

to this section. When the $\overline{\text{MS}}$ (modified minimal subtraction) renormalization scheme[20] is employed, we are left with

$$\delta\Gamma^{\mu}_{Q_1} = -\frac{C_1}{8\pi^2 M^2}\left(\left(\frac{1}{3}\ln\frac{m^2}{\mu^2} + h_1(z)\right) q^2\gamma^{\mu} + \left(\ln\frac{m^2}{\mu^2} + h_2(z)\right) mi\sigma^{\mu\nu}q_{\nu}\right) \tag{3.24}$$

Matching the EFT to the full theory then leads to

$$C_2 = -\frac{eg^2}{24\pi^2}\left(\frac{1}{3}\ln\frac{\mu^2}{M^2} + \frac{4}{9}\right) \tag{3.25}$$

and

$$C_3 = \frac{eg^2}{24\pi^2}\left(\frac{1}{2}\ln\frac{\mu^2}{M^2} + \frac{7}{12}\right) \tag{3.26}$$

together with $C_1 = g^2/2$ as stated above[21].
As we can clearly see, the Wilson coefficients C_i/M^2 with $i = 1, 2, 3$ contain all the information associated with the high energy scale M, whereas the low energy dynamics solely results from the non-local loop contribution as given by logarithms and the loop functions $h_1(z)$ and $h_2(z)$. It is not possible to capture the full theory result (3.8) with local operators alone. At this point, this observation might seem rather trivial, as the full theory is a genuine one-loop effect, so a tree-level EFT treatment should have been doomed to fail from the beginning. Of course, it was easy in this case, since the UV theory, the scalar S, is known to us. In the context of the SM, however, this is no longer the case. "Knowing" only about the right-hand side of (3.18) makes it clear that a proper loop-counting rule is unavoidable even for simple cases like this toy model[22]. In fact, an ordering prescription based on a topological counting of loops alone - that is, considering only $\delta\Gamma^{\mu}_{Q_2}$ and $\delta\Gamma^{\mu}_{Q_3}$ as they are of tree-level topology - would lead to wrong conclusions and predictions for experimental setups. One might argue that such an order-by-order matching (of loops) between the full theory and the EFT would still be enough to take these observations into account. After all, in this model, we are talking about a one-loop effect within the full theory, so we should trivially not expect to capture it by the EFT when using tree-level topologies only. The latter may serve as a leading order approximation only - though a quite inaccurate one due to the properties of this specific model. When the UV theory is generally unknown, fixing the loop order in EFT calculations would then ensure to never miss any UV effect up to this order (in the full theory). This, of course, comes with the disadvantage of featuring a maximal

[20] The $1/\epsilon$-poles in (3.99) have exactly the form of Q_2 and Q_3, which is why they serve as counterterms.

[21] It is now straight forward to compute the beta-functions $\beta_i \equiv 16\pi^2\mu\, dC_i/d\mu$ for $i = 2, 3$. They are given by

$$\beta_2 = -\frac{8e}{9}C_1 \quad \text{and} \quad \beta_3 = \frac{4e}{3}C_1 \tag{3.27}$$

[22] The crucial criteria of this toy model are its renormalizability to all orders, and its weak couplings to the low energy spectrum.

and potentially redundant number of Wilson coefficients to be fitted to the experimental data.
To make this more clear, we now turn to the bottom-up approach for the toy model. Pretending to not know about the heavy scalar S and its mass M, we are supposed to work with the first line of (3.1) supplemented by all possible higher dimensional operators built from the electron, the top-quark and the photon. When CP conservation is assumed to hold, there are 22 dimension-six operators in total, most of them four-fermion ones. They are all suppressed by a factor of $1/M^2$, where M now denotes the (unknown) scale of new physics (see also footnote 18). A complete (hermitian) basis is given by the following table (we have introduced a small electron mass m_e to catch up with ordinary QED results at one-loop):

four-electron	four-top	mixed electron-top	field strength
$\bar{\psi}\psi\bar{\psi}\psi$	$\bar{t}t\bar{t}t \leftarrow$	$\bar{\psi}\psi\bar{t}t$	$m\bar{t}\sigma^{\mu\nu}tF_{\mu\nu} \leftarrow$
$i\bar{\psi}\psi\bar{\psi}\gamma_5\psi$	$i\bar{t}t\bar{t}\gamma_5 t$	$i\bar{\psi}\psi\bar{t}\gamma_5 t$	$m_e\bar{\psi}\sigma^{\mu\nu}\psi F_{\mu\nu}$
$\bar{\psi}\gamma_5\psi\bar{\psi}\gamma_5\psi$	$\bar{t}\gamma_5 t\bar{t}\gamma_5 t$	$i\bar{\psi}\gamma_5\psi\bar{t}t$	$\partial_\mu F^{\mu\nu}\,\bar{t}\gamma_\nu t \leftarrow$
$\bar{\psi}\gamma_\mu\psi\bar{\psi}\gamma^\mu\psi$	$\bar{t}\gamma_\mu t\bar{t}\gamma^\mu t$	$\bar{\psi}\gamma_5\psi\bar{t}\gamma_5 t$	
$\bar{\psi}\gamma_\mu\psi\bar{\psi}\gamma^\mu\gamma_5\psi$	$\bar{t}\gamma_\mu t\bar{t}\gamma^\mu\gamma_5 t$	$\bar{\psi}\gamma_\mu\psi\bar{t}\gamma^\mu\gamma_5 t$	
		$\bar{\psi}\gamma_\mu\gamma_5\psi\bar{t}\gamma^\mu t$	
		$\bar{\psi}\gamma_\mu\gamma_5\psi\bar{t}\gamma^\mu\gamma_5 t$	
		$\bar{\psi}\sigma_{\mu\nu}\psi\bar{t}\sigma^{\mu\nu}t$	
		$i\bar{\psi}\sigma_{\mu\nu}\gamma_5\psi\bar{t}\sigma^{\mu\nu}t$	

We have used Fierz identities and the equations of motion to eliminate redundant operators[23]. The ones that are generated by the scalar S - i.e. Q_1, Q_2 and Q_3 - are marked with an arrow.
Let us now - once more - summarize the two possible procedures mentioned above to parameterize the new-physics impact on $e^+e^- \to \bar{t}t$:

- If we rely on canonical dimensions only, there is no reason why we should not take all Wilson coefficients as $\mathcal{O}(1)$-numbers[24]. As a first approximation, we would

[23] It is common to remove second-derivative operators by virtue of their equations of motion. Therefore, we could have replaced $\partial_\mu F^{\mu\nu}\,\bar{t}\gamma_\nu t$ in favour of $\bar{\psi}\gamma_\mu\psi\bar{t}\gamma^\mu t$ (see also footnote 19 above). We chose not to in order to keep the relation to the toy model more transparent

[24] If completely arbitrary values were allowed, the effects of even higher dimensional operators, e.g. of canonical dimension eight, could outperform lower dimensional ones and the whole operator series

therefore take all tree-level diagrams with single dimension-six insertions, as they collectively scale as $\sim 1/M^2$ compared to the leading-order non-new-physics result given in (3.4). These include plain $\bar{\psi}\psi\bar{t}t$-vertices as well as photon exchange diagrams with local operator insertions featuring the photon, i.e. field strength tensors. Some of them read

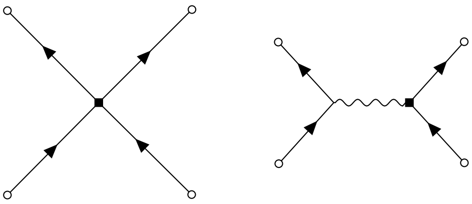

(first approximation) (3.28)

It is only until the precision of the calculation needs to be improved, that one-loop contributions are considered. Here, we have closed fermion bubble-like loops attached to the virtual photon, but also triangle graphs with modified local vertices. They all scale as $\sim 1/(16\pi^2 M^2)$ compared to (3.4) and are hence loop-suppressed with respect to the first-approximation graphs (3.28). Examples are given by

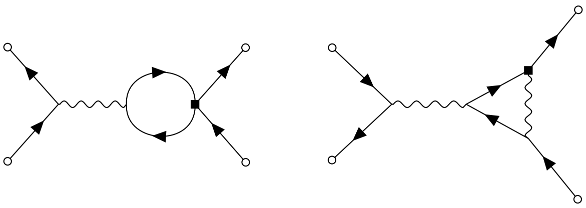

(subleading contributions)

(3.29)

Such a power-counting scheme will, however, never be able to capture the physics of the toy model correctly. Indeed, the first-approximation graphs (3.28) fail to reproduce the non-local contributions given by $h_1(z)$ and $h_2(z)$, whereas the subleading contributions given by (3.29) would introduce a much higher level of complexity than needed. In fact, the photon-exchange triangle graph needs to be supplemented by a two-loop diagram with a four-fermion insertion in order to be compatible with the toy model and its renormalization group equations (3.27). This is clearly beyond the scope of this exercise. We can thus never end up with a consistent EFT description when focusing on the canonical dimension of operators alone.

- We can cure this improper power-counting setup by allowing for another ordering parameter *in addition* to the canonical dimension, the implicit loop order. It can be captured in a quantitative way by the notion of chiral dimensions (and we will do so below), but for now, we simply state that all operators involving field strength tensors are generated one loop order higher than others. In this case, our first approximation ($\sim 1/M^2$ with respect to (3.4)) would solely be the four-fermion-

would break down. Indeed, for the operator series not to break down as a whole, the suppression mechanism of operators of canonical dimension d_c with Wilson coefficient C_i to scale like $C_i/M^{d_c-4} \sim 1/M^{d_c-4}$ has to be functional in general, see also footnote 17.

vertex diagram

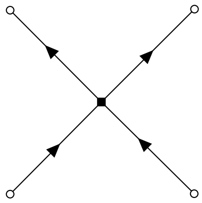

(first approximation) (3.30)

For the toy model, it turns out that this equals zero, i.e. all mixed electron-top Wilson coefficients vanish. Beyond a first approximation, we have the diagrams

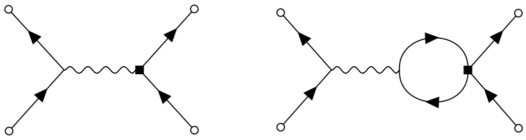

(subleading contributions) (3.31)

scaling like $\sim (1/16\pi^2 M^2)$, whereas the triangle graph in (3.29) appears to be even more suppressed, namely $\sim 1/\big((16\pi^2)^2 M^2\big)$. This is exactly the right pattern for the toy model.

Instead of arguing solely based on the explicit topological loop order of diagrams, we emphasize the existence of an implicit loop order incorporated in the Wilson coefficients C_2 and C_3, which needs to be equally accounted for. According to this view, there simply *is* no tree-level result in the EFT, as all operators are genuine one-loop effects: Q_1 via its one-loop topology, Q_2 and Q_3 via an implicit loop factor hidden in their Wilson coefficients. In contrast to the order-by-order treatment mentioned above, this will not only lead to the correct pattern of low-energy operators in the toy model, but also reduce the number of parameters drastically for more general scenarios. In essence, *if* the UV theory fulfills the aforementioned quite general properties, counting loop orders already on the operator level is crucial for making sensible and experimentally accessible predictions. Doing otherwise would then correspond to the opposite assumption, namely that the UV theory does *not* possess these properties. Either case corresponds to further assumptions about the UV sector besides its mass gap to the SM. An entirely model-independent notion of the EFT is therefore not possible in general.

It is a matter of definition whether one should use the word "inconsistent" for the pattern highlighted in (3.28) and (3.29) as we have done before. In fact, there are actually no *mathematical* inconsistencies associated with such an approach within the pure EFT as a theory on its own. However, one should always keep in mind that without the possibility of referring to a UV theory the EFT eventually matches to, such studies would remain purely academic and doomed to irrelevance by construction. They are - in some sense - inconsistent with reality.

Having explored the non-trivial matching properties of the fairly generic toy model provides enough motivation to consider broader scenarios like SMEFT, where the only sensible approaches close to reality are - if at all - bottom-up.

3.2. Canonical and chiral dimensions

Any EFT, renormalizable or non-renormalizable, must be based on some *power-counting* prescription which can provide a hierarchy pattern between the operators [76–78]. The latter are built out of quantum fields representing the *degrees of freedom* of a given theory and must respect its *symmetries*, which are usually postulated. For example, the renormalizable part of the SM consists of all dimension-four operators built from SM fields that are invariant under $SU(3)_c \times SU(2)_L \times U(1)_Y$ and is expanded in terms of loops. SMEFT is obtained when the restriction of renormalizability is abandoned. We then gain a second possibility on top of the loop expansion, the expansion in terms of canonical dimensions. The latter are a quantitative tool for counting the order at which hypothetical beyond-the-SM effects enter on the level of the Lagrangian. Let us now see how a similar tool emerges for keeping track of loop orders.
Generally speaking, the LO SM consists of a Higgs doublet φ, fermions ψ and (non-Abelian) gauge fields X. Fermionic interactions are either gauge- or Yukawa-like and are associated with one weak coupling κ. For consistency reasons, the quartic Higgs self-interaction comes with two weak couplings, i.e. κ^2 (imagine constructing it from two triple-vertices, each proportional to $\mu\kappa$, where μ is an energy scale, connected by a propagator coming with $1/\mu^2$, thus canceling the μ-dependence), and the gauge bosons are collectively described by the field strength, which we symbolically write as $X_{\mu\nu} \sim \partial X + \kappa X^2$. Schematically, we have the following list of operator structures[25]:

$$X_{\mu\nu}X^{\mu\nu}, \quad \kappa^2\phi^4, \quad \bar{\psi}\not{D}\psi, \quad \kappa\bar{\psi}\psi\varphi \tag{3.32}$$

All structures must scale homogeneously under some quantitative power-counting measure, otherwise they could barely be viewed as the LO content of an EFT. Let us therefore introduce a *dimension* d to count the building blocks of operators with varying weights. A given operator with N_φ bosons (scalars or vectors), $N_{\bar{\psi}\psi}$ fermion bilinears, N_∂ derivatives and N_κ weak couplings is then associated with a dimension

$$d = W_\varphi N_\varphi + W_{\bar{\psi}\psi} N_{\bar{\psi}\psi} + W_\partial N_\partial + W_\kappa N_\kappa \tag{3.33}$$

where W_i are the respective weights of the building blocks. For the LO operators in (3.32) to scale homogeneously ($d = const$ for all operators), we find the following set of equations

$$\begin{aligned} d = 2W_\varphi + 2W_\partial = 3W_\varphi + W_\partial + W_\kappa = 4W_\varphi + 2W_\kappa = \\ = W_{\bar{\psi}\psi} + W_\partial = W_{\bar{\psi}\psi} + W_\varphi + W_\kappa \end{aligned} \tag{3.34}$$

leading to

$$W_\partial = W_\kappa + W_\varphi \tag{3.35}$$

$$\frac{d}{2} = W_\kappa + 2W_\varphi \tag{3.36}$$

[25] The Higgs mass term will be discussed below.

$$W_{\bar{\psi}\psi} = W_\kappa + 3W_\varphi \tag{3.37}$$

For this system of equations to be uniquely determined, we need to specify two weights, e.g. W_φ and W_κ. The rows of the following table provide the independent resulting patterns of weights for different choices:

W_φ	W_κ	W_∂	$W_{\bar{\psi}\psi}$	d	
0	0	0	0	0	
1	0	1	3	4	d_c
0	1	1	1	2	d_χ

Choosing $W_\varphi = W_\kappa = 0$ yields a trivial assignment to the other weights and is therefore not relevant. The other independent cases are exhausted by allowing either W_φ or W_κ to be non-zero. Interestingly, this leads unambiguously to the notion of canonical dimensions $d = d_c = 4$ for the case $W_\varphi = 1$ and $W_\kappa = 0$. However, setting $W_\varphi = 0$ together with $W_\kappa = 1$ leads to a second possibility, this time with $d = 2$. An assignment based on $W_\varphi = 0$ is called *chiral dimension* (abbreviated as d_χ) and is as suited as the canonical dimension as a power-counting tool for EFTs. It is associated with the loop expansion as we will see below. Taking $W_\varphi = 1$ and $W_\kappa = 1$ at the same time corresponds to a mere linear combination of d_c and d_χ and contains no additional information.
The LO SM terms in (3.32) thus allow for two independent counting mechanisms[26], the canonical dimension

$$d_c = N_\varphi + 3N_{\bar{\psi}\psi} + N_\partial \tag{3.40}$$

and the chiral dimension

$$d_\chi = N_{\bar{\psi}\psi} + N_\partial + N_\kappa \tag{3.41}$$

The LO SM operators have $d_c = 4$ and $d_\chi = 2$, respectively. We will now explore the roles of d_c and d_χ in SMEFT. In particular, we will derive a general power-counting formula estimating the natural values of the dimensionless Wilson coefficients for a given operator structure.

[26] The choice of taking W_φ and W_κ as the parameters the other weights depend on is pragmatic and arbitrary: φ and κ are the only entities for which a classical non-relativistic limit exists. This does not mean that non-trivial solutions with zero-weights other than W_φ and W_κ cannot be found. In fact, they read

$$d = 2, \quad W_\varphi = -1, \quad W_{\bar{\psi}\psi} = 0, \quad W_\partial = 2, \quad W_\kappa = 3 \tag{3.38}$$

and

$$d = 2, \quad W_\varphi = 1, \quad W_{\bar{\psi}\psi} = 2, \quad W_\partial = 0, \quad W_\kappa = -1 \tag{3.39}$$

However, negative weights are not suited as a consistent power-counting prescription. Such solutions are therefore not relevant.

3.3. Power-counting formula for SMEFT

Let us consider a completely generic weakly coupling renormalizable (gauge) theory featuring the following particle content:

heavy scalar S
heavy vector V
heavy fermion F
light scalar s
light vector v
light fermion f

We combine them into sets $B = \{S, V\}$ and $b = \{s, v\}$ collecting heavy and light bosons, and $\beta = \{B, b\}$ and $\psi = \{F, f\}$ denoting bosons and fermions, respectively. Our goal is to find a general power-counting formula for the Wilson coefficients of operators built from light fields when the heavy fields representing new physics are integrated out. For this, we need to specify all interactions between the various interactions and count their associated weak couplings κ. Denoting the respective interaction classes by $\bar{\psi}\psi'\beta$, $\beta\beta'\beta''$, $\beta\beta'\beta''\beta'''$ and $\beta\beta'\partial\beta''$, all allowed interaction vertices are schematically given by the following table:

$\bar{\psi}\psi'\beta$	$\beta\beta'\beta''$	$\beta\beta'\beta''\beta'''$	$\beta\beta'\partial\beta''$
$\bar{f}fb$	$bb'b''$	$bb'b''b'''$	$bb'\partial b''$
$\bar{f}fB$	$bb'B$	$bb'b''B$	$bB\partial b'$
$\bar{f}Fb$	bBB'	$bb'BB'$	$bB\partial B'$
$\bar{f}FB$	$BB'B''$	$bBB'B''$	$BB'\partial B''$
$\bar{F}fb$		$BB'B''B'''$	
$\bar{F}fB$			
$\bar{F}Fb$			
$\bar{F}FB$			
κ	$\mu\kappa$	κ^2	$p\kappa$

The corresponding number of weak couplings is displayed at the bottom. As stated above, quadruple-boson vertices possess two weak couplings. In addition, we have made an energy scale associated with triple-boson vertices as well as the momentum from the derivative interaction explicit. A term $bb'\partial B$ can be eliminated in favor of the ones shown upon partial integration. Primes denote different members of the same set, but the indistinguishability of particles has not been implemented. This is, however, enough for our purpose.

Consider now a general $\tilde{N}_L$-loop diagram $\mathcal{D}$ with only light external legs. Denote by N_i the number of vertices of type i (this notation will be self-explaining), $\mathcal{N}_i$ the number of propagators of type i and $\tilde{N}_i$ exterior numbers of type i (such as external light fields, number of loop-factors, etc.). Such a diagram would scale like

$$\mathcal{D} \sim \left(\frac{1}{16\pi^2}\right)^{\tilde{N}_L} \left(\bar{f}f\right)^{\tilde{N}_f} h^{\tilde{N}_h} v_{\mu\nu}^{\tilde{N}_v} \kappa^{\tilde{N}_\kappa} p^{\tilde{N}_p} \mu^{\sum N_{\beta\beta'\beta''}} \tag{3.42}$$

Here we have enforced Lorentz invariance by allowing fermion-bilinears only. Furthermore, the field strength tensor $v_{\mu\nu}$ of the light vector v (in an abstract index notation) ensures gauge invariance. Covariant derivatives are represented as momenta on the amplitude level. The object $\sum N_{\beta\beta'\beta''}$ represents the total number of non-derivative triple-boson vertices. Sums are generally taken over open index sets, that is β, β' and β'' in this case, but overcounting should be avoided. We can relate $\tilde{N}_\kappa$ and $\tilde{N}_p$ to the vertices and propagators by counting their respective contributions displayed in the table above. This leads to

$$\tilde{N}_\kappa = \sum N_{\bar{\psi}\psi'\beta} + \sum N_{\beta\beta'\beta''} + 2\sum N_{\beta\beta'\beta''\beta'''} + \sum N_{\beta\beta'\partial\beta''} \tag{3.43}$$

and

$$\tilde{N}_p = 4\tilde{N}_L - \tilde{N}_v + \sum N_{\beta\beta'\partial\beta''} - 2\sum \mathcal{N}_\beta - \sum \mathcal{N}_\psi \tag{3.44}$$

For the latter (which can get negative), we have made use of the fact that every loop introduces an integration over unconstrained momenta and that fermion and boson propagators scale like $1/p$ and $1/p^2$, respectively. Since the (Abelian) field strength tensor $v_{\mu\nu}$ contains a factor of momentum, we have to shift $\tilde{N}_p$ by $-\tilde{N}_v$ to account for the right energy dimensions. We can obtain an expression for the total number of loops $\tilde{N}_L$ by counting the numbers of propagators and vertices, as the former introduce unconstrained momenta and hence an integration, whereas the latter enforce momentum conservation and therefore reduce the number of unconstrained momenta. Keeping a global Dirac-delta for momentum conservation of external particles in mind, we obtain

$$\tilde{N}_L = 1 + \sum \mathcal{N}_\beta + \sum \mathcal{N}_\psi - \sum N_{\bar{\psi}\psi'\beta} - \sum N_{\beta\beta'\beta''} - \sum N_{\beta\beta'\beta''\beta'''} - \sum N_{\beta\beta'\partial\beta''} \tag{3.45}$$

Let us now eliminate the number of propagators $\mathcal{N}_i$ from our formulas. For this, we write $4\tilde{N}_L = 2\tilde{N}_L + 2 + 2\tilde{N}_L - 2$ in (3.44) and plug in (3.45) for one of the terms. We then obtain

$$\tilde{N}_p = 2\tilde{N}_L + 2 - \tilde{N}_v + \sum \mathcal{N}_\psi - 2\sum N_{\bar{\psi}\psi'\beta} - 2\sum N_{\beta\beta'\beta''} - 2\sum N_{\beta\beta'\beta''\beta'''} - \sum N_{\beta\beta'\partial\beta''} \tag{3.46}$$

The remaining fermionic propagator terms can be eliminated upon noting that every external fermion is connected to a vertex and that every propagator connects two vertices. Having distinguished fermions and anti-fermions in our notation, this translates to

$$\tilde{N}_f + \mathcal{N}_f = \sum N_{\bar{f}\psi\beta} = \sum N_{\bar{\psi}f\beta} \tag{3.47}$$

and, using that the number of external heavy fermion lines is zero

$$\mathcal{N}_F = \sum N_{\bar{F}\psi\beta} = \sum N_{\bar{\psi}F\beta} \tag{3.48}$$

Combining both equations in (3.46) exactly cancels the fermionic vertex terms leading to

$$\tilde{N}_p = 2\tilde{N}_L + 2 - \tilde{N}_v - \tilde{N}_f - \tilde{N}_\kappa - \sum N_{\beta\beta'\beta''} \tag{3.49}$$

We thus arrive at

$$\mathcal{D} \sim \left(\frac{1}{16\pi^2}\right)^{\tilde{N}_L} \left(\bar{f}f\right)^{\tilde{N}_f} h^{\tilde{N}_h} v_{\mu\nu}^{\tilde{N}_v} \kappa^{\tilde{N}_\kappa} p^{2\tilde{N}_L+2-\tilde{N}_v-\tilde{N}_f-\tilde{N}_\kappa} \left(\frac{p}{\mu}\right)^{-\sum N_{\beta\beta'\beta''}} \tag{3.50}$$

As a special case, we switch off the super-renormalizable interaction by setting $N_{\beta\beta'\beta''} = 0$ for all combinations. The impact of heavy fields then manifests itself as higher dimensional operators suppressed by the heavy scale. Denote it by Λ and consider operators of canonical dimension d_c. To compensate for a change of energy dimension of the object $\mathcal{D}$, the momentum has to be shifted, as it is the only liable source of new physics. In other words, a suppression in terms of Λ has to emerge from heavy propagators (or loop functions) being expanded in terms of the inverse heavy mass. We can therefore write

$$\mathcal{D} \sim \left(\frac{1}{16\pi^2}\right)^{\tilde{N}_L} \frac{1}{\Lambda^{d_c-4}} \left(\bar{f}f\right)^{\tilde{N}_f} h^{\tilde{N}_h} v_{\mu\nu}^{\tilde{N}_v} \kappa^{\tilde{N}_\kappa} p^{\tilde{d}+d_c-4} \tag{3.51}$$

where

$$\tilde{d} \equiv 2\tilde{N}_L + 2 - \tilde{N}_v - \tilde{N}_f - \tilde{N}_\kappa \tag{3.52}$$

On one hand, for the corresponding local operator to be of canonical dimension d_c, this formula is subject to the constraint

$$d_c = 3\tilde{N}_f + \tilde{N}_h + 2\tilde{N}_v + \tilde{d} + d_c - 4 \tag{3.53}$$

On the other hand, the chiral dimension d_χ is given by

$$d_\chi = \tilde{N}_f + \tilde{N}_v + \tilde{N}_\kappa + \tilde{d} + d_c - 4 \tag{3.54}$$

Eliminating $\tilde{d}$ yields an expression for the $\tilde{N}_L$, namely

$$\tilde{N}_L = 1 + \frac{d_\chi - d_c}{2} \tag{3.55}$$

The power-counting formula for a Wilson coefficient C_i of a generic SMEFT operator therefore depends on an interplay between d_c and d_χ. The former solely determines the suppression with respect to the high energy scale Λ, whereas both are needed for the power of the loop factor $1/(16\pi^2)$.
It is straightforward to generalize our formulas even if $N_{\beta\beta'\beta''} \neq 0$. One then has to distinguish between two cases: The scale μ might be light or heavy. In the former case, according to the homogeneity in d_χ of the LO terms in perturbation theory, the scale has to be counted as $\mu \sim \kappa$ and our former analysis can be taken over without modifications[27]. For large scales $\mu \sim \Lambda$, however, there would be no additional weak coupling. In addition to the heavy propagators, there is now another possible source for producing the factor $1/\Lambda^{d_c-4}$ in (3.51). For a fixed canonical dimension, the constrained interplay between heavy propagators and large-scale super-renormalizable interactions can be implemented by an auxiliary excess quantity δ. It can be introduced by modifying the p-dependence in (3.51) to

$$p^{\tilde{d}+d_c-4} \longrightarrow p^{\tilde{d}+d_c-4+\delta-\sum N_{\beta\beta'\beta''}} \mu^{\sum N_{\beta\beta'\beta''}-\delta} \tag{3.56}$$

We now split the sum of super-renormalizable terms into vertices associated with heavy scales and light scales, denoted by $N^h_{\beta\beta'\beta''}$ and $N^l_{\beta\beta'\beta''}$, respectively[28]. We have to require $\delta = \sum N^h_{\beta\beta'\beta''}$ to ensure the correct power of Λ in the final expression. We then end up with

$$p^{\tilde{d}+d_c-4-\sum N^l_{\beta\beta'\beta''}} \mu^{\sum N^l_{\beta\beta'\beta''}} \tag{3.57}$$

Counting $\mu \sim \kappa$ for light scales reveals that the number of light-scale super-renormalizable interaction vertices drops out in (3.54), so (3.55) stays intact.
As a bookkeeping device, we introduce the quantity

$$f \equiv \frac{\Lambda}{4\pi} \tag{3.58}$$

which kind of determines a reasonable energy scale at which SMEFT is an appropriate description of nature: For scales much smaller than f, effects of higher dimensional operators are heavily suppressed; for scales much larger than f, the perturbative series might get in trouble as an infinite tower of higher dimensional operators gets important. However, in contrast to strongly coupled scenarios, such as Chiral Perturbation Theory, being a mere definition, f has no dynamical interpretation.
The power-counting formula is then given by

$$C_i = \frac{f^{4-d_c}}{(4\pi)^{d_\chi-2}} \tag{3.59}$$

[27]This is in fact generic: Small mass parameters have to be counted as weak couplings, so that no peculiarities arise. In the SM, for instance, this is obvious because all SM masses are associated with (weak) Yukawa couplings.

[28]Note that $N_{bb'b''}$ is necessarily associated with a weak scale, otherwise it cannot be part of a LO EFT Lagrangian since it would violate the scale separation assumption between the light and heavy degrees of freedom. In contrast, the vertices with at least one (suppressed) heavy boson might be linked to the large scale Λ.

which estimates the expected size of a Wilson coefficient in terms of d_c and d_χ. The object $L \equiv (d_\chi - 2)/2$ is often referred to as the "loop-order" - a relic from Chiral Perturbation Theory. It puts the loop expansion on the same footing as the $1/\Lambda$-expansion and should not be confused with the "loop-factor" $1/(16\pi^2)$, which is counted by $\tilde{N}_L$. For instance, a ten-dimensional operator with two-loop suppression ($d_c = 10$ and $\tilde{N}_L = 2$) would have $L = 5$, as it is suppressed with respect to the SM with 5 factors of $1/\Lambda^2$ or $1/(16\pi^2)$. For the $d_c = 6$-operators of the toy model in Section 3.1, we find

$$d_\chi\left(C_1\mathcal{O}_1\right) = 4, \qquad d_\chi\left(C_2\mathcal{O}_2\right) = 6, \qquad d_\chi\left(C_3\mathcal{O}_3\right) = 6 \tag{3.60}$$

indicating the relative suppression between the Wilson coefficients of $\mathcal{O}_1$ and $\mathcal{O}_{2,3}$. It is compensated by the topological loop of $\mathcal{O}_1$, which is, of course, not part of the power-counting formula.

3.4. Weak-coupling assignments for the Warsaw basis

For the practical application, (3.59) has a big disadvantage: It needs the number of weak couplings as an input parameter via d_χ. In reality, this can be achieved by explicitly matching SMEFT to specific model scenarios. To avoid this, one can, however, give a general estimate for a minimal number of associated weak couplings for a given operator by counting the number of possible interactions of the external fields. This depends, of course, on some minimal assumptions on the underlying dynamics and varies for different values of d_c. We will now explore the implications on Warsaw-basis operators when all interactions are assumed to be weak and renormalizable. As the weak-coupling assignment for a given operator is in fact the crucial point for its expected impact, we present two contrasting approaches; the first one catches up with our topological considerations of the last subsection, the second one makes use of the dimensional distinction between masses and weak couplings.

Topological reasoning
In the case of the leading new-physics effects, we can use our topological formula (3.51) with $d_c = 6$. Furthermore, the equations of motion can be employed to eliminate redundant operator structures to match with the Warsaw basis, which does not contain second-derivative operators[29]. We can therefore set

$$\tilde{d} + 2 \leq 1 \tag{3.61}$$

Focusing first on the case, $\tilde{d} + 2 = 0$, we obtain

$$d_\chi = \tilde{N}_f + \tilde{N}_v + \tilde{N}_\kappa = 2\tilde{N}_L + 4 \tag{3.62}$$

and find the following cases for the numbers of external fields

$$\tilde{N}_v = 3 \Longrightarrow \tilde{N}_f = 0,\ \tilde{N}_h = 0,\ d_\chi = 3 + \tilde{N}_\kappa \tag{3.63}$$

[29]The Higgs operators with second derivatives do not matter here as we are primarily interested in operators with field strength tensors. We comment on them below.

$$\tilde{N}_v = 2 \Longrightarrow \tilde{N}_f = 0,\ \tilde{N}_h = 2,\ d_\chi = 2 + \tilde{N}_\kappa \tag{3.64}$$

$$\tilde{N}_v = 1 \Longrightarrow \tilde{N}_f = 1,\ \tilde{N}_h = 1,\ d_\chi = 2 + \tilde{N}_\kappa \tag{3.65}$$

$$\tilde{N}_f = 0,\ \tilde{N}_h = 4,\ d_\chi = 1 + \tilde{N}_\kappa \tag{3.66}$$

$$\tilde{N}_v = 0 \Longrightarrow \tilde{N}_f = 2,\ \tilde{N}_h = 0,\ d_\chi = 2 + \tilde{N}_\kappa \tag{3.67}$$

$$\tilde{N}_f = 1,\ \tilde{N}_h = 3,\ d_\chi = 1 + \tilde{N}_\kappa \tag{3.68}$$

$$\tilde{N}_f = 0,\ \tilde{N}_h = 6,\ d_\chi = \tilde{N}_\kappa \tag{3.69}$$

The minimal number of weak couplings can now be estimated by inspecting the allowed interactions. For instance, we have to exclude vertices involving a light gauge boson v and two different bosons/fermions, i.e. bBv or $\bar{f}Fv$, etc. since the kinetic terms - they involve the gauge boson v via the covariant derivative - of scalars and fermions can always be chosen diagonal, independent of their mass terms. Furthermore, a plain $v^2\beta\beta'$-vertex has to be excluded by gauge invariance as we want to end up with an external field strength $v_{\mu\nu}$. This leads us to the observation that the $\tilde{N}_v = 3$-case (3.63) needs at least three weak couplings - one for each field strength separately, rendering $d_\chi = 6$ and thus $\tilde{N}_L = 1$. Similarly, two external v-fields together with two light bosons h in (3.64) require at least $\tilde{N}_\kappa = 4$, since we have excluded the plain vertex, and thus $d_\chi = 6$. Things get more interesting when we come to the case $\tilde{N}_v = 1$. Lorentz-invariance forces us to contract the (antisymmetric) field strength indices with $\sigma^{\mu\nu}$ in the case of $\tilde{N}_f = 1$. However, $\bar{f}\sigma^{\mu\nu}f$ is a non-renormalizable interaction that has to emerge from an off-shell particle exchange giving rise to at least two couplings. Together with an extra coupling from each $v_{\mu\nu}$ and h, we again end up with $d_\chi = 6$. The case $\tilde{N}_v = 1$ with $\tilde{N}_h = 4$ is forbidden by Lorentz-invariance. Finally, we have the operators with $\tilde{N}_v = 0$. The first class, the ones with $\tilde{N}_f = 2$, can be generated with a total of two weak couplings - one for each fermion bilinear - leading to $d_\chi = 4$, i.e. tree-level. Likewise, the $\tilde{N}_f = 1$ together with $\tilde{N}_h = 3$-case requires one coupling for the fermion bilinear and at least two couplings for the h^3-part, either by combining all three bosons in a quadruple-boson vertex counting as κ^2 or by splitting them apart into two groups with triple-boson vertices counting as one κ each. The result is again $d_\chi = 4$. Finally, we have the h^6-operator. Here, we need at least three couplings to attach the external fields to the diagram, three pairs of two fields with one κ each (triple-vertices) or two pairs of three fields with κ^2 each (quadruple-vertices), but at least another coupling for the diagram to be connected. Again, we end up with $d_\chi = 4$, i.e. $\tilde{N}_L = 0$.
The second case, $\tilde{d}+2 = 1$, features only $\tilde{N}_v = 0$-operators due to the hidden derivative in $v_{\mu\nu}$. We would otherwise end up with higher-derivative operators that can be eliminated by the equations of motion. We now have

$$d_\chi = \tilde{N}_f + \tilde{N}_v + \tilde{N}_\kappa + 1 = 2\tilde{N}_L + 4 \tag{3.70}$$

and find the following two cases

$$\tilde{N}_f = 1,\ \tilde{N}_h = 2,\ d_\chi = 2 + \tilde{N}_\kappa \tag{3.71}$$

$$\tilde{N}_f = 0,\ \tilde{N}_h = 5,\ d_\chi = 1 + \tilde{N}_\kappa \tag{3.72}$$

$$(3.73)$$

The first case ($\tilde{N}_f = 1$) is straightforward: We need two couplings, one for the fermion bilinear and one for the two bosons. The result is $d_\chi = 4$. The second case does not exist due to Lorentz invariance.
The last class of operators contained in the Warsaw basis features four light bosons and two derivatives. The bosons require two couplings and, together with the derivatives, the chiral dimension is $d_\chi = 4$.
This concludes the weak-coupling and hence the chiral-dimension assignments for all Warsaw-basis operators. Our analysis was based on topological considerations only, i.e. our line of reasoning was as general as possible. As a cross-check of our findings, we consider another general setup based on differentiating between energy scales and inverse length scales.

Dimensional reasoning
In this approach, we analyze the dimensional structure of a given operator to read off its implicit number of weak couplings. Throughout our previous analysis, we have worked in units where $\hbar = c = 1$. This implies the existence of only one dimensional scale, the energy E. Everything, i.e. masses, length scales, time, etc. can be expressed in terms of energies. Let us now restore the dependence on $\hbar$ and check whether the minimal number of weak couplings can also be derived on dimensional grounds [8, 21, 79] by superficially counting loops with factors of $\hbar$. This new system of units then includes energy E, as well as length L. The old units can be restored upon noting that the dimension of $\hbar$ is given by $[\hbar] \sim EL$ (square brackets evaluate the dimensional units of the objects inside). Employing the convention that the classical action be free of factors of $\hbar$, an n-loop diagram then scales like $\sim \hbar^{n-1}$. This can be derived from the path integral representation of amplitudes. Indeed, the generating functional is given in terms of the path integral, i.e.

$$Z \sim \int \mathcal{D}\Phi \; e^{i\frac{S[\Phi]}{\hbar}} \tag{3.74}$$

where $\mathcal{D}\Phi$ denotes the functional integral over the entire field content $\Phi = \{\phi, \psi\}$ with generic bosons ϕ and fermions ψ and $S[\Phi] = \int d^4x \; \mathcal{L}(\Phi)$, written as a functional of the fields, is the classical action. The generating functional is related to Feynman graphs via expanding the exponential function and contracting the fields inside the various factors of $\mathcal{L}(\Phi)$ appropriately (Wick's theorem). As the vertices (propagators) of Feynman diagrams are - loosely speaking - proportional (anti-proportional) to the corresponding terms in $\mathcal{L}(\Phi)$, the $\hbar$-dependence of the exponent of the generating functional provides an $\hbar$-counting for the Feynman rules. Vertices and propagators then come with factors of $1/\hbar$ and $\hbar$, respectively. Since the number of loops of a specific *connected* diagram is given by $\tilde{N}_L = 1 - N + \mathcal{N}$ (see (3.45)), where N and $\mathcal{N}$ are the total numbers of vertices and propagators, there is a one-to-one correspondence between the number of loops and

a superficial[30] power of $\hbar$.
With $\hbar \neq 1$, using $[d^4x] = L^4$ and $[\partial] = L^{-1}$, we find the following dimensional dependencies for the action S, the Lagrangian $\mathcal{L}$, masses m, weak couplings κ (excluding super-renormalizable interactions), bosonic field ϕ (including gauge fields) and fermionic fields ψ

$$\begin{aligned} &[S] = EL, \quad [\mathcal{L}] = EL^{-3}, \quad [m] = L^{-1}, \\ &[\kappa] = E^{-\frac{1}{2}}L^{-\frac{1}{2}}, \quad [\phi] = E^{\frac{1}{2}}L^{-\frac{1}{2}}, \quad [\psi] = E^{\frac{1}{2}}L^{-1} \end{aligned} \tag{3.75}$$

We will turn to the field strength $X_{\mu\nu} \sim \partial\phi + \kappa\phi^2$ below. These relations are solely derived from kinetic terms $\partial^2\phi^2$, $\partial\psi^2$, mass terms $m^2\phi^2$, $m\psi^2$ and interaction terms $\kappa\phi\psi^2$, $\kappa\partial\phi^3$, $\kappa^2\phi^4$. Instead of energy E and length L, however, we can use a system of units based on the independent entities mass m and weak coupling κ. Consider now a generic operator

$$\mathcal{Q} = c\, \partial^{\tilde{N}_\partial}\phi^{\tilde{N}_\phi}\psi^{\tilde{N}_\psi} \tag{3.76}$$

with a compensating factor c accounting for dimensional commensurability with $\mathcal{L}$. Its dimension can be determined upon noting that

$$[\partial^{\tilde{N}_\partial}\phi^{\tilde{N}_\phi}\psi^{\tilde{N}_\psi}] = L^{-\tilde{N}_\partial-\frac{1}{2}\tilde{N}_\phi-\tilde{N}_\psi}E^{\frac{1}{2}\tilde{N}} = m^{\tilde{N}_\partial+\tilde{N}_\phi+\frac{3}{2}\tilde{N}_\psi}\kappa^{-\tilde{N}} \tag{3.77}$$

where $\tilde{N} \equiv \tilde{N}_\phi + \tilde{N}_\psi$ and we have eliminated L and E in favour of m and κ in the second step. Since $[\mathcal{L}] = \kappa^{-2}m^4$, the dimension of c is given by

$$[c] = m^{4-d_c}g^{\tilde{N}-2} \tag{3.78}$$

with $d_c = \tilde{N}_\partial + \tilde{N}_\phi + 3\tilde{N}_\psi/2$ as usual. When recognizing m as the large mass scale Λ, this formula provides the number of associated weak couplings for a given operator in SMEFT for a minimum number of $\hbar$- and hence loop-factors. This number can easily be raised by multiplying with powers of $\hbar$. However, as $[\hbar] = EL$, every $\hbar$ comes with compensating factors of κ^2.
Let us work out the relevant cases for the Warsaw basis (2.17)-(2.49) with $d_c = 6$. We first consider the classes without field strength tensors, i.e. φ^6, $\partial^2\varphi^4$, $\varphi^3\psi^2$, $\partial\varphi^2\psi^2$ and ψ^4, where φ is now the Higgs field. The coefficients are given by

$$\varphi^6 \longrightarrow [c] = m^{-2}\kappa^4 \tag{3.79}$$
$$\partial^2\varphi^4 \longrightarrow [c] = m^{-2}\kappa^2 \tag{3.80}$$
$$\varphi^3\psi^2 \longrightarrow [c] = m^{-2}\kappa^3 \tag{3.81}$$
$$\partial\varphi^2\psi^2 \longrightarrow [c] = m^{-2}\kappa^2 \tag{3.82}$$
$$\psi^4 \longrightarrow [c] = m^{-2}\kappa^2 \tag{3.83}$$

[30] Cancellations of $\hbar$-factors *after* expanding or integrating the propagators due to the different units of momentum and mass may appear. They ultimately spoil our classical/quantum - tree/loop classification, but are in principle unrelated to the points we make [80, 81].

which leads to the same weak-coupling prescription we obtained previously. Concerning field-strength operators, note that both $\partial\phi$ and $\kappa\phi^2$ scale homogeneously in E and L or κ and m leading to the scaling behaviour $[X_{\mu\nu}] = m^2\kappa^{-1}$. The resulting dimensional pattern is equivalent to counting $X_{\mu\nu}$ as a boson field in (3.78). We find

$$X^3_{\mu\nu} \longrightarrow [c] = m^{-2}\kappa \tag{3.84}$$

$$\varphi^2 X^2_{\mu\nu} \longrightarrow [c] = m^{-2}\kappa^2 \tag{3.85}$$

$$\varphi\psi^2 X_{\mu\nu} \longrightarrow [c] = m^{-2}\kappa^2 \tag{3.86}$$

By construction, the results in (3.84)-(3.86) are the weak-coupling assignments at tree-level, i.e. there are no factors of $\hbar$ involved. Here, however, the displayed number of weak couplings is unrealistic. For instance, without loss of generality, the purely non-Abelian part of $X^3_{\mu\nu}$ comes already with κ^3 - an additional factor of κ^2 with respect to the tree-level result (3.84). The only available object to compensate for this dimensional excess is $\hbar$ which raises the loop order by one unit. Similarly, for the other cases, since every $X_{\mu\nu}$ adds a weak coupling κ that is necessarily associated with the gauge field alone, we need additional factors of κ to separately couple the residual fields. This adds at least another κ^2 or one loop order for both cases $\varphi^2 X^2_{\mu\nu}$ and $\varphi\psi^2 X_{\mu\nu}$.
We conclude that every Warsaw-basis operator that has at least one field strength tensor comes with at least one loop factor, whereas all operators without the former can be generated at tree level. This is a generic result that holds for a broad class of high-energy scenarios [82–85]. As a last point, one might argue that field redefinitions or the application of the equations of motion are always possible. These could transform a tree-level generated non-field-strength operator into a field-strength operator without loop suppression. However, the so-obtained operators are not part of the Warsaw basis [86]. In fact, when restricted to the latter, our findings can be applied without further limitations.
The phenomenological role of the power-counting formula (3.59) together with the weak-coupling assignments highlighted in this subsection cannot be overestimated. In fact, when confronted with the sheer number of Wilson coefficients suggested by the plain Warsaw basis, every sensible evaluation of experimental data must at some point restrict the parameter space to facilitate the eventual detection of any beyond-the-SM effects. Our analysis shows that such a truncation is not arbitrary and can indeed be done systematically. In the remaining sections, we demonstrate how this works in practice. We do this by evaluating the leading new-physics effects for two specific processes at the LHC, showing explicitly how a systematic reduction of the Warsaw-basis parameter space leads to a manageable number of coefficients that represent the unknown physics.

Appendix: Three independent calculations of the triangle diagram to $\mathcal{O}(1/M^2)$ and OS counterterm

Perturbative calculations in QFT are often cumbersome and prone to errors. It is therefore advantageous to verify and confirm final results by alternative approaches whenever possible. In fact, every loop calculation in this thesis has been approved by at least two different methods. As an example, in this appendix, we list three different ways to solve the loop integral (3.7) to $\mathcal{O}(1/M^2)$, as well as the calculation of the counterterm required to impose the OS renormalization scheme. Throughout this section, we will make use of identities like $p_1^2 = p_2^2 = m^2$ and $p_1 \cdot p_2 = \frac{1}{2}q^2 - m^2$ or the Dirac-equations $\bar{u}(p_1)\not{p}_1 = m\bar{u}(p_1)$ and $\not{p}_2 v(p_2) = -mv(p_2)$ and the Gordon identity $\bar{u}(p_1)(p_1^\mu - p_2^\mu)v(p_2) = 2m\bar{u}(p_1)\gamma^\mu v(p_2) - \bar{u}(p_1)i\sigma^{\mu\nu}q_\nu v(p_2)$ without further comments and suppress the spinors. The $i\eta$-prescription and hence the analytic structure of the loop functions in the complex plane will be restored in the end upon sending $m^2 \to m^2 - i\eta$. We will start with a straightforward evaluation of the complicated loop integral in terms of Feynman parameters. In a second approach, we split the multi-scale integral into different integration regions and sum up the respective contributions, which leads to the calculation of two easier integrals. A third possibility highlights the reduction of the tensor structure in the original expression to scalar functions by expanding the former in terms of all possible Lorentz structures. As expected, although differing in methodology, all three approaches yield the same final result, namely (3.8).

Brute force calculation
First, we perform the integral all at once in one shot. For this, we introduce Feynman parameters via the formula

$$\frac{1}{ABC} = \int_0^1 dx \int_0^1 dy \frac{2x}{\big(A + (B-A)x + (C-B)xy\big)^3} \tag{3.87}$$

and find

$$\bar{u}(p_1)\delta\Gamma^\mu v(p_2) = ig^2 \int_0^1 dx \int_0^1 dy\ \mu^{2\epsilon} \int \frac{d^dk}{(2\pi)^d} \frac{\bar{u}(p_1)N^\mu v(p_2)}{(k^2-\Delta)^3} \tag{3.88}$$

with the abbreviations

$$\Delta \equiv M^2 \left(1 - x + x^2\frac{m^2}{M^2} - x^2y(1-y)\frac{q^2}{M^2}\right) \tag{3.89}$$

$$\begin{aligned} N^\mu \equiv& 2x(2g^{\mu\alpha}\gamma^\beta - g^{\alpha\beta}\gamma^\mu)k_\alpha k_\beta + 2x(4-x^2)m^2\gamma^\mu - 2x^3y(y-1)q^2\gamma^\mu + \\ &- 4mx^2(x-2)(y-1)p_1^\mu - 4mx^2(x-2)yp_2^\mu \end{aligned} \tag{3.90}$$

Note that the denominator is symmetric with respect to the exchange $y \leftrightarrow (1-y)$. We can therefore write

$$\begin{aligned} N^\mu =& 2x(2g^{\mu\alpha}\gamma^\beta - g^{\alpha\beta}\gamma^\mu)k_\alpha k_\beta + 2x(4-4x+x^2)m^2\gamma^\mu + \\ &+ 2x^3y(1-y)q^2\gamma^\mu - 2mx^2(x-2)i\sigma^{\mu\nu}q_\nu \end{aligned} \tag{3.91}$$

Performing the momentum integral in dimensional regularization using the expressions given in Appendix D results in

$$\delta\Gamma^\mu = -\frac{g^2}{16\pi^2M^2}\left(I_1 mi\sigma^{\mu\nu}q_\nu - I_2q^2\gamma^\mu - I_3m^2\gamma^\mu - \left(\frac{1}{\epsilon} + \ln\frac{4\pi}{e^\gamma} + \ln\frac{\mu^2}{M^2} + \frac{1}{2}\right)\frac{M^2\gamma^\mu}{2}\right) \tag{3.92}$$

The form factors are given by

$$I_1 = \int_0^1 dy \int_0^1 dx \frac{y^2(y-2)}{1-y+y^2\frac{m^2}{M^2}-y^2x(1-x)\frac{q^2}{M^2}} = \frac{7}{6} + \ln\frac{m^2}{M^2} + h_2(z) + \mathcal{O}\left(\frac{1}{M^2}\right) \tag{3.93}$$

$$I_2 = \int_0^1 dy \int_0^1 dx \frac{y^3x(1-x)}{1-y+y^2\frac{m^2}{M^2}-y^2x(1-x)\frac{q^2}{M^2}} = -\frac{11}{36} - \frac{1}{6}\ln\frac{m^2}{M^2} - \frac{h_1(z)}{2} + \mathcal{O}\left(\frac{1}{M^2}\right) \tag{3.94}$$

$$\begin{aligned} I_3 = \int_0^1 dy \int_0^1 dx \Bigg(& \frac{y(4-4y+y^2)}{1-y+y^2\frac{m^2}{M^2}-y^2x(1-x)\frac{q^2}{M^2}} + \\ & - \frac{M^2}{m^2} y \ln\left(1-y+y^2\frac{m^2}{M^2}-y^2x(1-x)\frac{q^2}{M^2}\right) - \frac{3M^2}{4m^2}\Bigg) = \\ =1 - \frac{5}{36}\frac{q^2}{m^2} - \frac{1}{6}\frac{q^2}{m^2}\ln\frac{m^2}{M^2} - \frac{q^2}{2m^2}h_1(z) + \mathcal{O}\left(\frac{1}{M^2}\right) \end{aligned} \tag{3.95}$$

In evaluating the integrals, it turns out to be advantageous to view $\big(m^2-x(1-x)q^2\big)/M^2$ as a single object of small numerical absolute value and perform the y-integration at first. The so obtained expressions can be Taylor-expanded before the x-integration is tackled, which can be written in terms of $h_1(z)$ and $h_2(z)$ (see (3.10) and (3.11)). However, the complicated expressions I_1, I_2 and I_3 require disproportionately high calculational power for the problem at hand. The next technique tries to avoid this by splitting our multi-scale problem into several single-scale ones.

Strategy of regions

This method is based on dividing the original integral into several integration *regions* that are determined by the relevant scales of the problem at hand. The integrand is then expanded around the respective region which reduces the complexity of the integration by a fair amount. Adding up all contributions from all regions yields the original integral [65, 87, 88]. For our case, there are two regions of the loop momentum k to consider, namely

$$\begin{aligned} \mathbb{I}: &\quad m, p_1, p_2, k \ll M \\ \mathbb{III}: &\quad m, p_1, p_2 \ll k, M \end{aligned}$$

Let us first evaluate region $\mathbb{I}$. Expanding the integrand in the relevant limit, i.e. the propagator of the heavy particle, and introducing Feynman parameters, we find

$$\begin{aligned} \bar{u}(p_1)\delta\Gamma^\mu_{\mathbb{I}}v(p_2) \equiv & \frac{ig^2}{-M^2}\mu^{2\epsilon}\int \frac{d^dk}{(2\pi)^d}\frac{\bar{u}(p_1)(\not{k}+m)\gamma^\mu(\not{k}-\not{q}+m)v(p_2)}{\big(k^2-m^2\big)\big((k-q)^2-m^2\big)} = \\ = & \frac{ig^2}{-M^2}\int_0^1 dx\ \mu^{2\epsilon}\int\frac{d^dk}{(2\pi)^d}\frac{\bar{u}(p_1)N^\mu v(p_2)}{\big(k^2-\Delta\big)^2} \end{aligned} \tag{3.96}$$

where

$$\Delta \equiv m^2 - x(1-x)q^2 \tag{3.97}$$

$$N^\mu \equiv (2g^{\mu\alpha}\gamma^\beta - g^{\alpha\beta}\gamma^\mu)k_\alpha k_\beta + m^2\gamma^\mu + mi\sigma^{\mu\alpha}q_\alpha + x(1-x)q^2\gamma^\mu \tag{3.98}$$

and terms of $\mathcal{O}(1/M^4)$ or higher are consistently neglected. The momentum integral yields (see Appendix D for the necessary formulas)

$$\delta\Gamma^\mu_{\mathbb{I}} = \frac{g^2}{16\pi^2 M^2}\left(\left(\frac{1}{\epsilon} + \ln\frac{4\pi}{e^\gamma} + \ln\frac{\mu^2}{m^2}\right)\left(\frac{q^2\gamma^\mu}{3} + mi\sigma^{\mu\nu}q_\nu\right) + \right.$$
$$\left. - \left(h_1(z)q^2\gamma^\mu + h_2(z)mi\sigma^{\mu\nu}q_\nu\right)\right) \tag{3.99}$$

with the form factors $h_1(z)$ and $h_2(z)$ given by (3.10) and (3.11).
Moving on to region $\mathbb{III}$, we first rewrite the integrand according to

$$\bar{u}(p_1)\delta\Gamma^\mu v(p_2) = ig^2\mu^{2\epsilon}\int\frac{d^dk}{(2\pi)^d}\frac{\bar{u}(p_1)(\not{k}\gamma^\mu\not{k} + 4mk^\mu + 4m^2\gamma^\mu)v(p_2)}{(k^2-M^2)k^4\left(1+\frac{2k\cdot p_1}{k^2}\right)\left(1-\frac{2k\cdot p_2}{k^2}\right)} \tag{3.100}$$

The corresponding expression $\bar{u}(p_1)\delta\Gamma^\mu_{\mathbb{III}}v(p_2)$ is obtained by expanding the nominator and denominator in the relevant limit and keeping only even powers of k (the integration is symmetric with respect to $k \leftrightarrow -k$). Dropping terms of $\mathcal{O}(1/k^2)$ and higher, we obtain

$$\frac{\not{k}\gamma^\mu\not{k} + 4mk^\mu + 4m^2\gamma^\mu}{\left(1+\frac{2k\cdot p_1}{k^2}\right)\left(1-\frac{2k\cdot p_2}{k^2}\right)} \approx$$
$$\approx \not{k}\gamma^\mu\not{k} + 4m^2\gamma^\mu - \frac{8mk^\mu k\cdot(p_1-p_2)}{k^2} + \frac{4\not{k}\gamma^\mu\not{k}\left((k\cdot p_1)^2 + (k\cdot p_2)^2 - (k\cdot p_1)(k\cdot p_2)\right)}{k^4} \tag{3.101}$$

Within the integral, due to symmetry, this expression is equal to

$$\left(\frac{2}{d}-1\right)\gamma^\mu k^2 + \frac{2q^2\gamma^\mu}{d+2} + \frac{4(d^2-5d+4)m^2\gamma^\mu}{d(d+2)} + \frac{8(d-1)mi\sigma^{\mu\nu}q_\nu}{d(d+2)} \tag{3.102}$$

After performing the integral, we obtain

$$\delta\Gamma^\mu_{\mathbb{III}} \equiv \frac{g^2}{16\pi^2M^2}\left(\left(\frac{1}{\epsilon} + \ln\frac{4\pi}{e^\gamma} + \ln\frac{\mu^2}{M^2} + \frac{1}{2}\right)\frac{M^2\gamma^\mu}{2} - \left(\frac{1}{\epsilon} + \ln\frac{4\pi}{e^\gamma} + \ln\frac{\mu^2}{M^2} + \frac{4}{3}\right)\frac{q^2\gamma^\mu}{3} + \right.$$
$$\left. - \left(\frac{1}{\epsilon} + \ln\frac{4\pi}{e^\gamma} + \ln\frac{\mu^2}{M^2} + \frac{7}{6}\right)mi\sigma^{\mu\nu}q_\nu + m^2\gamma^\nu\right) \tag{3.103}$$

Adding both regions yields

$$\delta\Gamma^\mu = \delta\Gamma^\mu_{\mathbb{I}} + \delta\Gamma^\mu_{\mathbb{III}} = -\frac{g^2}{16\pi^2M^2}\left(\left(\ln\frac{m^2}{M^2} + \frac{7}{6} + h_2(z)\right)mi\sigma^{\mu\nu}q_\nu + \right.$$

$$+\left(\frac{1}{3}\ln\frac{m^2}{M^2}+\frac{4}{9}+h_1(z)\right)q^2\gamma^\mu-m^2\gamma^\mu-\left(\frac{1}{\epsilon}+\ln\frac{4\pi}{e^\gamma}+\ln\frac{\mu^2}{M^2}+\frac{1}{2}\right)\frac{M^2\gamma^\mu}{2}\Bigg) \tag{3.104}$$

Of course, this matches the expression above (see (3.92)).
The strategy of regions has the particular advantage of being conceptually related to the philosophy of the EFT approach to physics. Indeed, for our problem, the two regions are nothing else than the domains of validity of the respective theory. Region $\mathbb{I}$, the soft region, is equivalent to the low-energy EFT and hence the bubble-diagram contribution (3.24) featuring the non-local structure functions $h_1(z)$ and $h_2(z)$, whereas region $\mathbb{II}$, the hard region, gives rise to local operators and Wilson coefficients that are determined by the matching procedure of the EFT to the full theory. The renormalization scale μ separates the domains and is canceled when both contributions are finally combined.

Passarino-Veltman reduction
Finally, we provide an in-depth study of the tensor structure of our integral in terms of scalar functions [89–91]. Although this method is usually accompanied by lengthy calculations and a confusing number of equations to keep track of, it is actually quite reliable when it comes to complicated applications. For instance, there could be cases where the evaluation of tensor integrals as in (3.87)-(3.95) is simply not possible in a straightforward manner. Especially when making use of computer algebra systems such as FeynCalc, FormCalc or Package-X [92–94], the integral reduction method turns out to be quite fruitful, but should only be employed if unavoidable.
We rewrite the integral in terms of basic triangle integrals[31]

$$\begin{aligned}-\frac{i}{g^2}\bar{u}(p_1)\delta\Gamma^\mu v(p_2)=&\mu^{2\epsilon}\int\frac{d^dk}{(2\pi)^d}\frac{\bar{u}(p_1)(\not{k}+2m)\gamma^\mu(\not{k}+2m)v(p_2)}{(k^2-M^2)\big((k+p_1)^2-m^2\big)\big((k-p_2)^2-m^2\big)}=\\ =&\bar{u}(p_1)(\gamma^\alpha\gamma^\mu\gamma^\beta C_{\alpha\beta}+4mC^\mu+4m^2\gamma^\mu C)v(p_2)\end{aligned} \tag{3.105}$$

where

$$\begin{aligned}C\equiv&\mu^{2\epsilon}\int\frac{d^dk}{(2\pi)^d}\frac{1}{D_1D_2D_3}=\\ =&-\frac{i}{16\pi^2M^2}\int_0^1dy\int_0^1dx\frac{y}{1-y+y^2\left(1-x(1-x)\frac{q^2}{m^2}\right)\frac{m^2}{M^2}}=\\ =&\frac{i}{16\pi^2M^2}\Bigg(1+\ln\frac{m^2}{M^2}+h_2(z)+\frac{7m^2}{2M^2}\left(1-\frac{q^2}{6m^2}\right)+\frac{3m^2}{M^2}\left(1-\frac{q^2}{6m^2}\right)\ln\frac{m^2}{M^2}+\\ &+\frac{3m^2}{M^2}h_2(z)-\frac{3q^2}{2M^2}h_1(z)+\frac{m^4}{M^4}\left(1-\frac{q^2}{3m^2}+\frac{q^4}{30m^4}\right)\left(\frac{37}{3}+10\ln\frac{m^2}{M^2}\right)+\\ &+10\frac{m^4}{M^4}h_2(z)-10\frac{m^2q^2}{M^4}h_1(z)+10\frac{q^4}{M^4}h_3(z)\Bigg)+\mathcal{O}\left(\frac{1}{M^8}\right)\end{aligned} \tag{3.106}$$

[31] Do not confuse these expressions (and subsequent ones) with the abbreviations introduced in Appendix E.

$$C^\mu \equiv \mu^{2\epsilon} \int \frac{d^d k}{(2\pi)^d} \frac{k^\mu}{D_1 D_2 D_3} \tag{3.107}$$

$$C_{\alpha\beta} \equiv \mu^{2\epsilon} \int \frac{d^d k}{(2\pi)^d} \frac{k_\alpha k_\beta}{D_1 D_2 D_3} \tag{3.108}$$

with the abbreviations

$$D_1 \equiv k^2 - M^2 \Longrightarrow k^2 = D_1 + M^2 \tag{3.109}$$

$$D_2 \equiv k^2 + 2k \cdot p_1 \Longrightarrow k \cdot p_1 = \frac{1}{2}(D_2 - D_1 - M^2) \tag{3.110}$$

$$D_3 \equiv k^2 - 2k \cdot p_2 \Longrightarrow k \cdot p_2 = \frac{1}{2}(D_1 - D_3 + M^2) \tag{3.111}$$

The one parameter integral in the scalar triangle C could be done using

$$\int_0^1 dy \frac{y}{1 - y + y^2 A} = \frac{\ln(A) + \frac{\ln\left(-2A + \sqrt{1-4A} + 1\right) - \ln(2A)}{\sqrt{1-4A}}}{2A} \tag{3.112}$$

In addition to $h_1(z)$ and $h_2(z)$ in (3.10) and (3.11), we defined

$$h_3(z) \equiv \int_0^1 dx\ x^2(1-x)^2 \ln\left(1 - 4x(1-x)z\right) =$$

$$= \left(\frac{1}{30} + \frac{1}{60z} + \frac{1}{80z^2}\right) h_2(z) + \frac{1}{120z} + \frac{13}{900} \tag{3.113}$$

It is also useful to define[32]

$$B(i,j) \equiv \mu^{2\epsilon} \int \frac{d^d k}{(2\pi)^d} \frac{1}{D_i D_j} \tag{3.114}$$

$$A(i) \equiv \mu^{2\epsilon} \int \frac{d^d k}{(2\pi)^d} \frac{1}{D_i} \tag{3.115}$$

with

$$B(1,2) = B(1,3) = \frac{i}{16\pi^2} \left(\frac{1}{\epsilon} + \ln \frac{4\pi}{e^\gamma} + \int_0^1 dx \ln \frac{\mu^2}{x^2 m^2 + (1-x) M^2}\right) \tag{3.116}$$

$$B(2,3) = \frac{i}{16\pi^2} \left(\frac{1}{\epsilon} + \ln \frac{4\pi}{e^\gamma} + \int_0^1 dx \ln \frac{\mu^2}{m^2 - x(1-x) q^2}\right) \tag{3.117}$$

$$A(1) = \frac{i}{16\pi^2} M^2 \left(\frac{1}{\epsilon} + \ln \frac{4\pi}{e^\gamma} + \ln \frac{\mu^2}{M^2} + 1\right) \tag{3.118}$$

$$A(2) = A(3) = \frac{i}{16\pi^2} m^2 \left(\frac{1}{\epsilon} + \ln \frac{4\pi}{e^\gamma} + \ln \frac{\mu^2}{m^2} + 1\right) \tag{3.119}$$

[32] We generally refer to the A, B and C-functions as *tadpoles*, *bubbles* and *triangles*, irrespective of their indices. For later use, diagrams with four propagators are denoted by D and referred to as *boxes*.

and

$$B^\mu(i,j) \equiv \mu^{2\epsilon} \int \frac{d^dk}{(2\pi)^d} \frac{k^\mu}{D_i D_j} \tag{3.120}$$

For every combination of i and j in $B^\mu(i,j)$, we have to identify the available Lorentz vectors and expand the vector integral accordingly. This suggests us to write

$$B^\mu(1,2) \equiv Q p_1^\mu \tag{3.121}$$
$$B^\mu(1,3) \equiv R p_2^\mu \tag{3.122}$$
$$B^\mu(2,3) \equiv \mu^{2\epsilon} \int \frac{d^dk}{(2\pi)^d} \frac{k^\mu - p_1^\mu}{\big(k^2 - m^2\big)\big((k-q)^2 - m^2\big)} = S q^\mu - p_1^\mu B(2,3) \tag{3.123}$$

where we have shifted $k \to k - p_1$ in the last formula. We now have to determine the unknown coefficients Q, R and S. Contracting the above equations with p_1 and p_2, respectively, yields

$$p_{1\mu} B^\mu(1,2) = \mu^{2\epsilon} \int \frac{d^dk}{(2\pi)^d} \frac{k \cdot p_1}{D_1 D_2} = \frac{1}{2}\big(A(1) - A(2) - M^2 B(1,2)\big) = Q m^2 \tag{3.124}$$
$$p_{2\mu} B^\mu(1,3) = \mu^{2\epsilon} \int \frac{d^dk}{(2\pi)^d} \frac{k \cdot p_2}{D_1 D_3} = \frac{1}{2}\big(A(3) - A(1) + M^2 B(1,3)\big) = R m^2 \tag{3.125}$$
$$\begin{aligned} q_\mu B^\mu(2,3) =& \mu^{2\epsilon} \int \frac{d^dk}{(2\pi)^d} \frac{k \cdot q}{\big(k^2 - m^2\big)\big((k-q)^2 - m^2\big)} - \frac{1}{2} q^2 B(2,3) = \\ =& \frac{1}{2} q^2 B(2,3) - \frac{1}{2} q^2 B(2,3) = 0 = S q^2 - \frac{1}{2} q^2 B(2,3) \end{aligned} \tag{3.126}$$

where we have expanded $k \cdot q$ in terms of the denominator structure in the last expression and shifted the loop momentum for the resulting tadpole functions to cancel each other. We then obtain

$$Q = - R = \frac{1}{2m^2}\big(A(1) - A(2) - M^2 B(1,2)\big) \tag{3.127}$$
$$S = \frac{1}{2} B(2,3) \tag{3.128}$$

Next, for the same reasons as before, we write

$$C^\mu \equiv A p_1^\mu + B p_2^\mu \tag{3.129}$$

with unknown A and B (not to be confused with the tadpole and bubble functions above). The relevant contractions read

$$p_{1\mu} C^\mu = \mu^{2\epsilon} \int \frac{d^dk}{(2\pi)^d} \frac{k \cdot p_1}{D_1 D_2 D_3} = \frac{1}{2}\big(B(1,3) - B(2,3) - M^2 C\big) = A m^2 + B (p_1 \cdot p_2) \tag{3.130}$$

$$p_{2\mu}C^\mu = \mu^{2\epsilon}\int \frac{d^dk}{(2\pi)^d}\frac{k\cdot p_2}{D_1D_2D_3} = \frac{1}{2}\big(B(2,3)-B(1,2)+M^2C\big) = A(p_1\cdot p_2)+Bm^2 \tag{3.131}$$

From this, we obtain

$$\begin{aligned} A = -B = &-\frac{m^2}{2\big(m^4-(p_1\cdot p_2)^2\big)}\bigg(\Big(1+\frac{p_1\cdot p_2}{m^2}\Big)\big(B(2,3)+M^2C\big)+ \\ &-B(1,3)-\frac{p_1\cdot p_2}{m^2}B(1,2)\bigg) = -\frac{1}{4m^2-q^2}\big(B(2,3)-B(1,2)+M^2C\big) \end{aligned} \tag{3.132}$$

where the left-hand side of (3.116) has been used. Similarly, we have

$$C_{\alpha\beta} \equiv Xg_{\alpha\beta}+Yp_{1\alpha}p_{1\beta}+Zp_{2\alpha}p_{2\beta}+W(p_{1\alpha}p_{2\beta}+p_{2\alpha}p_{1\beta}) \tag{3.133}$$

with the four coefficients X, Y, Z and W. The contractions are given by (d is the spacetime dimension)

$$g^{\alpha\beta}C_{\alpha\beta} = \mu^{2\epsilon}\int \frac{d^dk}{(2\pi)^d}\frac{k^2}{D_1D_2D_3} = B(2,3)+M^2C = Xd+Ym^2+Zm^2+2W(p_1\cdot p_2) \tag{3.134}$$

$$\begin{aligned} p_1^\alpha p_1^\beta C_{\alpha\beta} =& \mu^{2\epsilon}\int \frac{d^dk}{(2\pi)^d}\frac{(k\cdot p_1)^2}{D_1D_2D_3} = \mu^{2\epsilon}\int \frac{d^dk}{(2\pi)^d}\frac{\frac{1}{2}(D_2-D_1-M^2)(k\cdot p_1)}{D_1D_2D_3} = \\ =&\frac{1}{2}\big(p_{1\mu}B^\mu(1,3)-p_{1\mu}B^\mu(2,3)-M^2p_{1\mu}C^\mu\big) = \\ =&Xm^2+Ym^4+Z(p_1\cdot p_2)^2+2Wm^2(p_1\cdot p_2) \end{aligned} \tag{3.135}$$

$$\begin{aligned} p_2^\alpha p_2^\beta C_{\alpha\beta} =& \mu^{2\epsilon}\int \frac{d^dk}{(2\pi)^d}\frac{(k\cdot p_2)^2}{D_1D_2D_3} = \mu^{2\epsilon}\int \frac{d^dk}{(2\pi)^d}\frac{\frac{1}{2}(D_1-D_3+M^2)(k\cdot p_2)}{D_1D_2D_3} = \\ =&\frac{1}{2}\big(p_{2\mu}B^\mu(2,3)-p_{2\mu}B^\mu(1,2)+M^2p_{2\mu}C^\mu\big) = \\ =&Xm^2+Y(p_1\cdot p_2)^2+Zm^4+2Wm^2(p_1\cdot p_2) \end{aligned} \tag{3.136}$$

$$\begin{aligned} p_1^\alpha p_2^\beta C_{\alpha\beta} =& \mu^{2\epsilon}\int \frac{d^dk}{(2\pi)^d}\frac{(k\cdot p_1)(k\cdot p_2)}{D_1D_2D_3} = \mu^{2\epsilon}\int \frac{d^dk}{(2\pi)^d}\frac{\frac{1}{2}(D_2-D_1-M^2)(k\cdot p_2)}{D_1D_2D_3} = \\ =&\frac{1}{2}\big(p_{2\mu}B^\mu(1,3)-p_{2\mu}B^\mu(2,3)-M^2p_{2\mu}C^\mu\big) = \\ =&X(p_1\cdot p_2)+Ym^2(p_1\cdot p_2)+Zm^2(p_1\cdot p_2)+W\big(m^4+(p_1\cdot p_2)^2\big) \end{aligned} \tag{3.137}$$

Let us write

$$J_1 \equiv B(2,3)+M^2C \tag{3.138}$$

$$J_2 \equiv \frac{1}{2}\big(p_{1\mu}B^\mu(1,3)-p_{1\mu}B^\mu(2,3)-M^2p_{1\mu}C^\mu\big) \tag{3.139}$$

$$J_3 \equiv \frac{1}{2}\big(p_{2\mu}B^\mu(2,3)-p_{2\mu}B^\mu(1,2)+M^2p_{2\mu}C^\mu\big) \tag{3.140}$$

$$J_4 \equiv \frac{1}{2}\big(p_{2\mu}B^\mu(1,3) - p_{2\mu}B^\mu(2,3) - M^2 p_{2\mu}C^\mu\big) \tag{3.141}$$

Note that only J_1 is written in a manifestly reduced form. The others are only implicitly reduced. The coefficients are then given by

$$X = \frac{1}{(d-2)q^2(q^2-4m^2)}\big(q^2(q^2-4m^2)J_1 + 4m^2 J_2 + 4m^2 J_3 + (8m^2-4q^2)J_4\big) \tag{3.142}$$

$$\begin{aligned} Y =& \frac{1}{(d-2)q^4(q^2-4m^2)^2}\Big(4m^2q^2(q^2-4m^2)J_1 + 16(d-1)m^4 J_2 + \\ &+ \big(16(d-1)m^4 - 16(d-2)m^2q^2 + 4(d-2)q^4\big)J_3 + \\ &+ 16(d-1)m^2(2m^2-q^2)J_4\Big) \end{aligned} \tag{3.143}$$

$$\begin{aligned} Z =& \frac{1}{(d-2)q^4(q^2-4m^2)^2}\Big(4m^2q^2(q^2-4m^2)J_1 + \\ &+ \big(16(d-1)m^4 - 16(d-2)m^2q^2 + 4(d-2)q^4\big)J_2 + \\ &+ 16(d-1)m^4 J_3 + 16(d-1)m^2(2m^2-q^2)J_4\Big) \end{aligned} \tag{3.144}$$

$$\begin{aligned} W =& -\frac{1}{(d-2)q^4(q^2-4m^2)^2}\Big((16m^4q^2 - 12m^2q^4 + 2q^6)J_1 + \\ &- 8(d-1)m^2(2m^2-q^2)J_2 - 8(d-1)m^2(2m^2-q^2)J_3 + \\ &- \big(32(d-1)m^4 - 16dm^2q^2 + 4dq^4\big)J_4\Big) \end{aligned} \tag{3.145}$$

Inserting the explicit expressions for the integrals (i.e. (3.116) and (3.117) into (3.129) with (3.132)), we find

$$\begin{aligned} C^\mu =& \frac{p_1^\mu - p_2^\mu}{q^2-4m^2}\left(\frac{i}{16\pi^2}\int_0^1 dx \ln\left(\frac{x^2 + (1-x)\frac{M^2}{m^2}}{1 - x(1-x)\frac{q^2}{m^2}}\right) + M^2 C\right) \equiv \\ \equiv& \frac{p_1^\mu - p_2^\mu}{q^2-4m^2}(F + M^2 C) \end{aligned} \tag{3.146}$$

$$\begin{aligned} p_{2\mu}B^\mu(1,2) =& -p_{1\mu}B^\mu(1,3) = \frac{q^2-2m^2}{4m^2}\big(A(1) - A(2) - M^2 B(1,2)\big) \equiv \frac{q^2-2m^2}{4}G = \\ =& \frac{q^2-2m^2}{4}\frac{i}{16\pi^2}\left(\frac{M^2}{m^2}\left(1 + \int_0^1 dx \ln\Big(1 - x + x^2\frac{m^2}{M^2}\Big)\right) + \right. \\ & \left. - \left(\frac{1}{\epsilon} + \ln\frac{4\pi}{e^\gamma} + \ln\frac{\mu^2}{m^2} + 1\right)\right) \end{aligned} \tag{3.147}$$

$$\begin{aligned} p_{2\mu}B^\mu(2,3) =& -p_{1\mu}B^\mu(2,3) = \frac{4m^2-q^2}{4}B(2,3) = \\ =& \frac{4m^2-q^2}{4}\frac{i}{16\pi^2}\left(\frac{1}{\epsilon} + \ln\frac{4\pi}{e^\gamma} + \int_0^1 dx \ln\frac{\mu^2}{m^2 - x(1-x)q^2}\right) \end{aligned} \tag{3.148}$$

$$p_{1\mu}B^\mu(1,2) = -p_{2\mu}B^\mu(1,3) = \frac{1}{2}\big(A(1) - A(2) - M^2 B(1,2)\big) = \frac{m^2}{2}G \tag{3.149}$$

where we have defined F and G on the go. Reinserted into (3.139)-(3.141) gives

$$J_2 = J_3 = -J_4 - \frac{q^2}{8}G = -\frac{q^2-2m^2}{8}G + \frac{4m^2-q^2}{8}B(2,3) + \frac{M^2}{4}(F+M^2C) \tag{3.150}$$

It is useful to separate the finite from the infinite parts by defining

$$B(2,3) \equiv I + \tilde{B}(2,3) \tag{3.151}$$

$$G \equiv -I + \tilde{G} \tag{3.152}$$

where

$$I \equiv \frac{i}{16\pi^2}\left(\frac{1}{\epsilon} + \ln\frac{4\pi}{e^\gamma} + \ln\frac{\mu^2}{m^2}\right) \tag{3.153}$$

$$\tilde{B}(2,3) \equiv -\frac{i}{16\pi^2}\int_0^1 dx \ln\left(1 - x(1-x)\frac{q^2}{m^2}\right) \tag{3.154}$$

$$\tilde{G} \equiv \frac{i}{16\pi^2}\left(-1 + \frac{M^2}{m^2} + \frac{M^2}{m^2}\int_0^1 dx \ln\left(1 - x + x^2\frac{m^2}{M^2}\right)\right) = = \frac{i}{16\pi^2}\left(\frac{M^2}{m^2} - 1\right) - \frac{M^2}{m^2}H \tag{3.155}$$

with

$$H \equiv -\frac{i}{16\pi^2}\int_0^1 dx \ln\left(1 - x + x^2\frac{m^2}{M^2}\right) \tag{3.156}$$

Also, we have

$$F = \tilde{B}(2,3) - \frac{i}{16\pi^2}\ln\frac{m^2}{M^2} + \frac{i}{16\pi^2}\int_0^1 dx \ln\left(1 - x + x^2\frac{m^2}{M^2}\right) = = \tilde{B}(2,3) + \frac{i}{16\pi^2}\left(\frac{m^2}{M^2} - \ln\frac{m^2}{M^2} - 1\right) + \frac{m^2}{M^2}\tilde{G} = \tilde{B}(2,3) - H - \frac{i}{16\pi^2}\ln\frac{m^2}{M^2} \tag{3.157}$$

where we have used (3.155) in the last step. Eliminating J_3 and J_4 via (3.150) in (3.142)-(3.145) leads to

$$X = \frac{q^2(q^2-4m^2)J_1 + 4q^2J_2 - (8m^2-4q^2)\frac{q^2}{8}G}{(d-2)q^2(q^2-4m^2)} = = \frac{1}{2(d-2)}I + \frac{1}{4}\tilde{B}(2,3) + \left(\frac{M^2}{2} - \frac{M^4}{2(4m^2-q^2)}\right)C - \frac{M^2}{2(4m^2-q^2)}F \tag{3.158}$$

$$Y = \frac{4m^2q^2(q^2-4m^2)J_1 + \left(16m^2q^2 + 4(d-2)q^4\right)J_2 - 16(d-1)(2m^4-m^2q^2)\frac{q^2}{8}G}{(d-2)q^4(q^2-4m^2)^2} = = -\frac{(d-4)m^2}{(d-2)q^2(q^2-4m^2)}I - \frac{q^2-2m^2}{2q^2(q^2-4m^2)}\tilde{B}(2,3) - \frac{q^2-2m^2}{2q^2(q^2-4m^2)}\tilde{G} +$$

$$+\frac{M^2\big(-8m^4+2m^2(M^2+q^2)+M^2q^2\big)}{q^2(q^2-4m^2)^2}C+\frac{M^2(2m^2+q^2)}{q^2(q^2-4m^2)^2}F \tag{3.159}$$

$$Z=Y \tag{3.160}$$

$$\begin{aligned}W=&-\frac{(16m^4q^2-12m^2q^4+2q^6)J_1-(16m^2q^2-4dq^4)J_2}{(d-2)q^4(q^2-4m^2)^2}+\\&-\frac{(32(d-1)m^4-16dm^2q^2+4dq^4)\frac{q^2}{8}G}{(d-2)q^4(q^2-4m^2)^2}=\\=&\frac{(d-4)(q^2-2m^2)}{2(d-2)q^2(q^2-4m^2)}I+\frac{m^2}{q^2(q^2-4m^2)}\tilde{B}(2,3)+\frac{m^2}{q^2(q^2-4m^2)}\tilde{G}+\\&-\frac{M^2\big(8m^4-2m^2(M^2+3q^2)+2M^2q^2+q^4\big)}{q^2(q^2-4m^2)^2}C-\frac{2M^2(q^2-m^2)}{q^2(q^2-4m^2)^2}F\end{aligned} \tag{3.161}$$

where J_1, J_2 and G (or rather $\tilde{G}$) were eliminated via (3.138), (3.150) and (3.155), respectively. The function H can be decomposed into F and $\tilde{B}(2,3)$ and vice versa upon using (3.157). Note that Y, Z and W are finite, since $d-4\sim\epsilon$ cancels the $1/\epsilon$-dependence in I. Catching up with (3.105), after using the Dirac equation and the Gordon identity, we arrive at

$$4mC^\mu+4m^2\gamma^\mu C=\left(\frac{8m^2}{q^2-4m^2}(F+M^2C)+4m^2C\right)\gamma^\mu-\frac{4m}{q^2-4m^2}(F+M^2C)i\sigma^{\mu\nu}q_\nu \tag{3.162}$$

$$\gamma^\alpha\gamma^\mu\gamma^\beta C_{\alpha\beta}=\big(2m^2(Y-W)-q^2W-(d-2)X\big)\gamma^\mu+2m(W-Y)i\sigma^{\mu\nu}q_\nu \tag{3.163}$$

where (3.146) and (3.133) have been used. We also have

$$\begin{aligned}W-Y=&\frac{d-4}{2(d-2)(q^2-4m^2)}I+\frac{1}{2(q^2-4m^2)}\tilde{B}(2,3)+\frac{1}{2(q^2-4m^2)}\tilde{G}+\\&-\frac{3M^2}{(q^2-4m^2)^2}F-\frac{M^2(-4m^2+3M^2+q^2)}{(q^2-4m^2)^2}C\end{aligned} \tag{3.164}$$

Where F and $\tilde{G}$ can be eliminated in favor of H by virtue of (3.157) and (3.155) as before. For very large M^2, the parameter integral (3.156) is given by

$$\begin{aligned}H=&\frac{i}{16\pi^2}\frac{4\frac{m^2}{M^2}-\left(2\frac{m^2}{M^2}-1\right)\ln\left(\frac{m^2}{M^2}\right)-\sqrt{1-4\frac{m^2}{M^2}}\ln\left(-\frac{2\frac{m^2}{M^2}+\sqrt{1-4\frac{m^2}{M^2}}-1}{2\frac{m^2}{M^2}}\right)}{2\frac{m^2}{M^2}}=\\=&\frac{i}{16\pi^2}\left(1+\frac{1}{2}\frac{m^2}{M^2}\left(2\ln\left(\frac{m^2}{M^2}\right)+1\right)+\frac{1}{3}\frac{m^4}{M^4}\left(6\ln\left(\frac{m^2}{M^2}\right)+5\right)\right)+\mathcal{O}\left(\frac{m^6}{M^6}\right)\end{aligned} \tag{3.165}$$

When the dust settles, keeping only $\mathcal{O}(1/M^2)$-effects, we end up with

$$\left(-\frac{4m}{q^2-4m^2}(F+M^2C)+2m(W-Y)\right)i\sigma^{\mu\nu}q_\nu=$$

$$= \frac{i}{16\pi^2 M^2}\left(\frac{7}{6} + \ln\frac{m^2}{M^2} + h_2(z)\right) i\sigma^{\mu\nu} q_\nu m \tag{3.166}$$

and

$$\left(\frac{8m^2}{q^2-4m^2}(F+M^2C) + 4m^2C + 2m^2(Y-W) - q^2W - (d-2)X\right)\gamma^\mu =$$
$$= \frac{i}{16\pi^2}\left(-\frac{m^2}{M^2} + \frac{q^2}{3M^2}\ln\frac{m^2}{M^2} + \frac{4q^2}{9M^2} + \frac{q^2}{M^2}h_1(z) - \frac{1}{2\epsilon} - \frac{1}{2}\ln\frac{4\pi}{e^\gamma} - \frac{1}{2}\ln\frac{\mu^2}{M^2} - \frac{1}{4}\right)\gamma^\mu \tag{3.167}$$

Reinserted into (3.105), this is the desired result and matches (3.92) and (3.104).

Counterterms
In this appendix, we have so far calculated the unrenormalized divergent amplitude. In addition to being finite, the renormalized amplitude should also fulfill the OS condition

$$\delta\Gamma^\mu = 0 \quad \text{for} \quad q = 0 \tag{3.168}$$

This guarantees a proper interpretation of e as the electric elementary charge in Coulomb's law for large distances, i.e. for $q = 0$.
To fix the counterterms on a quantitative level, we need to evaluate the following self-energy diagram

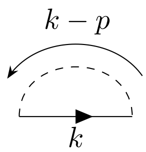

$$\equiv i\Sigma = g^2\mu^{2\epsilon}\int \frac{d^dk}{(2\pi)^d}\frac{\not{k}+m}{\left((k-p)^2-M^2\right)\left(k^2-m^2\right)} \tag{3.169}$$

Introducing Feynman parameters and performing the momentum integration as usual, we find

$$\begin{aligned} i\Sigma =& g^2\int_0^1 dx\ \mu^{2\epsilon}\int\frac{d^dk}{(2\pi)^d}\frac{x\not{p}+m}{\left(k^2 - xM^2 - (1-x)m^2 + x(1-x)p^2\right)^2} = \\ =& \frac{ig^2}{16\pi^2}\int_0^1 dx\ (x\not{p}+m)\left(\frac{1}{\epsilon} + \ln\frac{4\pi}{e^\gamma} + \ln\frac{\mu^2}{xM^2 + (1-x)m^2 - x(1-x)p^2}\right) \end{aligned} \tag{3.170}$$

We can choose the OS renormalization scheme for the top-quark's mass by imposing[33]

$$Z_2 - 1 \equiv \delta_2 = -\frac{d}{d\not{p}}\Sigma(\not{p})\Big|_{\not{p}=m} \tag{3.171}$$

where Z_2 is the wavefunction renormalization of the top-quark. We find

$$\frac{d}{d\not{p}}\Sigma(\not{p}) = \frac{ig^2}{16\pi^2}\int_0^1 dx\left(x\left(\frac{1}{\epsilon} + \ln\frac{4\pi}{e^\gamma} + \ln\frac{\mu^2}{xM^2 + (1-x)m^2 - x(1-x)\not{p}^2}\right) + \right.$$

[33]See for example equation (18.43) in [8].

$$+\frac{2\not{p}x(1-x)(x\not{p}+m)}{xM^2+(1-x)m^2-x(1-x)\not{p}^2}\Bigg) \tag{3.172}$$

which gives

$$\delta_2 = -\frac{ig^2}{16\pi^2}\left(\frac{1}{2}\left(\frac{1}{\epsilon}+\ln\frac{4\pi}{e^\gamma}+\ln\frac{\mu^2}{M^2}\right)-\int_0^1 dx\; x\ln\left(x+(1-x)^2\frac{m^2}{M^2}\right)+\right.$$
$$\left.+\frac{m^2}{M^2}\int_0^1 dx\;\frac{2(1-x)(1+x)}{1+\frac{(1-x)^2}{x}\frac{m^2}{M^2}}\right) \tag{3.173}$$

In the limit $m^2 \ll M^2$, this evaluates to

$$\delta_2 = -\frac{ig^2}{16\pi^2 M^2}\left(\left(\frac{1}{\epsilon}+\ln\frac{4\pi}{e^\gamma}+\ln\frac{\mu^2}{M^2}+\frac{1}{2}\right)\frac{M^2}{2}+m^2\right) \tag{3.174}$$

dropping higher-order terms. The Ward identity implies $Z_1 = Z_2$, where Z_1 renormalizes the top-quark-photon interaction and is hence associated with γ^μ, so using (3.92) and (3.104), the renormalized final result is given by

$$\delta\Gamma^\mu = -\frac{g^2}{16\pi^2 M^2}\left(\left(\ln\frac{m^2}{M^2}+\frac{7}{6}+h_2(z)\right)mi\sigma^{\mu\nu}q_\nu+\left(\frac{1}{3}\ln\frac{m^2}{M^2}+\frac{4}{9}+h_1(z)\right)q^2\gamma^\mu\right) \tag{3.175}$$

which matches (3.8) from the main text and fulfills (3.168). Here, we have not introduced extra indices to distinguish between renormalized and unrenormalized amplitudes, as this should be clear from the context.

4. Gluon fusion top-pair production $gg \to t\bar{t}$ in SMEFT

As a first example, we look at the leading SMEFT corrections for the partonic scattering process $gg \to t\bar{t}$ at LO in QCD. The gluon-fusion channel is dominant for top-pair production at hadron colliders where the competing quark-anti-quark fusion channel $q\bar{q} \to t\bar{t}$ becomes less and less important for increasing center-of-mass energies[34]. Our primary focus lies on the chromomagnetic operator Q_{uG} which induces a new magnetic-moment type interaction between a quark line and a gluon. Recent calculations can be found in [97, 98]. The power-counting rules argued for in this work suggest its accompaniment by four-fermion operators entering at a higher-order loop topology. This section is based on [99].

4.1. Setup and SM result

We consider the process of gluon fusion $gg \to t\bar{t}$, where two initial gluons with momenta k_1 and k_2 and colours B and C merge together to yield a top-anti-top pair with momenta p_1 and p_2 and colours c_1 and c_2, respectively:

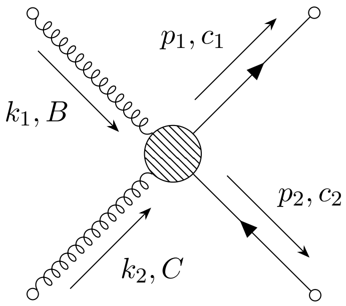

(4.1)

The differential cross-section for this process within the SM can be calculated by evaluating only three Feynman diagrams. In this case, the relevant parameters are the strong coupling constant g_s and the mass of the top-quark m_t. In SMEFT, the situation becomes more cumbersome. The first non-vanishing contributions appear at operator dimension six and the relevant parameters now also include the Wilson coefficients C_i of the new operators $Q_{6,i}$ as well as the Higgs mass m_h, its vacuum expectation value v, and the other quark masses m_b, m_c, etc., and the CKM matrix entries. However, we restrict ourselves to the third generation only and neglect the CKM matrix.
The total amplitude is given by a sum of the SM result and the leading order SMEFT correction

$$i\mathcal{M} = i\mathcal{M}_{SM} + \frac{1}{\Lambda^2} i\mathcal{M}_{SMEFT}, \tag{4.2}$$

[34] This does not only apply to proton-proton colliders like the LHC, but also to proton-anti-proton colliders (e.g. Tevatron) due to the overwhelming dominance of the gluon PDF (parton distribution function) over its quark or anti-quark counterparts [95, 96].

where Λ denotes the (potentially very high) scale of new physics as usual. The cross-section depends on $|\mathcal{M}|^2$ which to order $1/\Lambda^2$ takes the form

$$|\mathcal{M}|^2 \equiv |\mathcal{M}_{SM}|^2 + \frac{2}{\Lambda^2}\,\mathrm{Re}\,\{\mathcal{M}^*_{SM}\mathcal{M}_{SMEFT}\} \tag{4.3}$$

Before we come to dimension-six operators, let us first review the LO cross-section for $gg \to t\bar{t}$ within the SM [100]. Applying the usual notation for spinors $\bar{u}(p_1) \equiv \bar{u}$ and $v(p_2) \equiv v$, polarization vectors $\epsilon_\mu(k_1) \equiv \epsilon_\mu$ and $\epsilon_\nu(k_2) \equiv \epsilon_\nu$ (which we assume to be transversal, i.e. $k_1^\mu\epsilon_\mu = k_2^\nu\epsilon_\nu = 0$), and the Gell-Mann matrices $\lambda^A = 2T^A$, the three diagrams and their respective contributions are given by

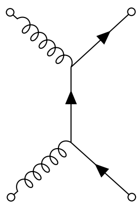

$$\equiv i\mathcal{M}^{(t)}_{SM} = -ig_s^2(T^BT^C)_{c_1c_2}\bar{u}\Big(\gamma^\mu\frac{\not{k}_2 - \not{p}_2 + m_t}{-2p_2\cdot k_2 + i\eta}\gamma^\nu\Big)v\epsilon_\mu\epsilon_\nu \tag{4.4}$$

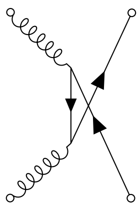

$$\equiv i\mathcal{M}^{(u)}_{SM} = -ig_s^2(T^CT^B)_{c_1c_2}\bar{u}\Big(\gamma^\nu\frac{\not{p}_1 - \not{k}_2 + m_t}{-2p_1\cdot k_2 + i\eta}\gamma^\mu\Big)v\epsilon_\mu\epsilon_\nu \tag{4.5}$$

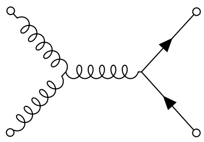

$$\equiv i\mathcal{M}^{(s)}_{SM} = -ig_s^2 if^{ABC}T^A_{c_1c_2}\big(-2g^{\sigma\mu}k_1^\nu + g^{\mu\nu}(k_1 - k_2)^\sigma + 2g^{\nu\sigma}k_2^\mu\big)\cdot$$

$$\cdot\frac{1}{q^2 + i\eta}\bar{u}\gamma_\sigma v\epsilon_\mu\epsilon_\nu \tag{4.6}$$

The Ward identity can be checked straightforwardly by sending ϵ_μ to $k_{1\mu}$, etc.
In the center-of-mass frame, the differential cross-section is given by

$$\frac{d\sigma}{d\Omega} = \frac{\overline{|\mathcal{M}|^2}}{64\pi^2 s}\frac{|\boldsymbol{p_1}|}{|\boldsymbol{k_1}|} \tag{4.7}$$

where $\overline{|\mathcal{M}|^2}$ is initial (final) spin and colour summed (averaged) amplitude squared and the Mandelstam variables read

$$\begin{aligned} s &= q^2 = E_{cm}^2 = (k_1 + k_2)^2 = (p_1 + p_2)^2 = 2k_1\cdot k_2 = 2p_1\cdot p_2 + 2m_t^2 = \\ &= 2m_t^2 - t - u \\ t &= (k_1 - p_1)^2 = (k_2 - p_2)^2 = -2k_1\cdot p_1 + m_t^2 = -2k_2\cdot p_2 + m_t^2 = \end{aligned} \tag{4.8}$$

$$= m_t^2 - \frac{s}{2}\left(1 - \sqrt{1 - \frac{4m_t^2}{s}}\cos\theta\right) \tag{4.9}$$

$$u = (k_1 - p_2)^2 = (k_2 - p_1)^2 = -2k_1 \cdot p_2 + m_t^2 = -2k_2 \cdot p_1 + m_t^2 =$$

$$= m_t^2 - \frac{s}{2}\left(1 + \sqrt{1 - \frac{4m_t^2}{s}}\cos\theta\right) \tag{4.10}$$

where we have parameterized the four vectors according to

$$k_1 = \left(\frac{E_{cm}}{2}, 0, 0, \frac{E_{cm}}{2}\right), \quad p_1 = \left(\frac{E_{cm}}{2}, \boldsymbol{p_1}\right) \tag{4.11}$$

$$k_2 = \left(\frac{E_{cm}}{2}, 0, 0, -\frac{E_{cm}}{2}\right), \quad p_2 = \left(\frac{E_{cm}}{2}, -\boldsymbol{p_1}\right) \tag{4.12}$$

with $k_1^2 = k_2^2 = 0$, $p_1^2 = p_2^2 = m_t^2$ and E_{cm} the center-of-mass energy. The angle θ is the scattering angle, i.e. the angle between the incoming gluon with four-momentum k_1 and the final-state top-quark. The spatial momenta of the quarks read $\boldsymbol{p_1} = -\boldsymbol{p_2} = |\boldsymbol{p_1}|(\sin\theta, 0, \cos\theta)$. We have

$$|\boldsymbol{p_1}| = \sqrt{\left(\frac{E_{cm}}{2}\right)^2 - m_t^2} = \frac{E_{cm}}{2}\sqrt{1 - \frac{4m_t^2}{s}} \tag{4.13}$$

$$|\boldsymbol{k_1}| = \frac{E_{cm}}{2} \tag{4.14}$$

which can be inserted in (4.7). The full amplitude is given by the sum of the three diagrams

$$i\mathcal{M}_{SM} \equiv i\mathcal{M}_{SM}^{(s)} + i\mathcal{M}_{SM}^{(t)} + i\mathcal{M}_{SM}^{(u)} \tag{4.15}$$

Summing and averaging over final and initial spins and colours results in

$$\overline{|\mathcal{M}_{SM}|^2} = \frac{1}{8^2}\frac{1}{2^2}\sum |\mathcal{M}_{SM}|^2 \tag{4.16}$$

Using $\alpha_s = g_s^2/4\pi$ and employing the usual relations for traces and hermitian conjugates of gamma matrices as well as the Dirac equation, we eventually find the result (see also [101] or the latest version [61])

$$\left(\frac{d\sigma}{d\Omega}\right)_{SM} = \frac{\alpha_s^2}{32s}\sqrt{1 - \frac{4m_t^2}{s}}\left(\frac{6(m_t^2 - t)(m_t^2 - u)}{s^2} - \frac{m_t^2(s - 4m_t^2)}{3(m_t^2 - t)(m_t^2 - u)} + \right.$$
$$+ \frac{\frac{4}{3}(m_t^2 - t)(m_t^2 - u) - \frac{8}{3}m_t^2(m_t^2 + t)}{(m_t^2 - t)^2} + \frac{\frac{4}{3}(m_t^2 - t)(m_t^2 - u) - \frac{8}{3}m_t^2(m_t^2 + u)}{(m_t^2 - u)^2} +$$
$$\left. - \frac{3(m_t^2 - t)(m_t^2 - u) + 3m_t^2(u - t)}{s(m_t^2 - t)} - \frac{3(m_t^2 - t)(m_t^2 - u) + 3m_t^2(t - u)}{s(m_t^2 - u)}\right) =$$

$$= \frac{\alpha_s^2}{32s}\sqrt{1-\frac{4m_t^2}{s}}\left(-\frac{N}{3s^2(m_t^2-t)^2(m_t^2-u)^2}\right) \tag{4.17}$$

with

$$N \equiv \Big(7m_t^4 - 7m_t^2(t+u) + 4t^2 - tu + 4u^2\Big)\cdot$$
$$\cdot\Big(6m_t^8 - m_t^4(3t^2+14tu+3u^2) + m_t^2(t+u)(t^2+6tu+u^2) - tu(t^2+u^2)\Big) \tag{4.18}$$

We now move to the SMEFT computation for this process.

4.2. SMEFT corrections

As stated above, the leading new-physics contributions to $gg \to \bar{t}t$ appear at operator dimension six. At tree-level, these include only operators featuring field strength tensors. We have shown in Section 3 that these operators are generally associated with inherent loop factors by virtue of their Wilson coefficients. Consistent power-counting rules therefore require the inclusion of topological one-loop diagrams, even for a lowest-order treatment. We can write

$$i\mathcal{M}_{SMEFT} \equiv i\mathcal{M}_{SMEFT}^{(trees)} + i\mathcal{M}_{SMEFT}^{(loops)} \tag{4.19}$$

Let us first evaluate the tree diagrams.

Trees

The tree contributions are straightforward to write down [66, 102, 103] and are given by the following list (insertions of dimension-six operators are indicated by black squares):

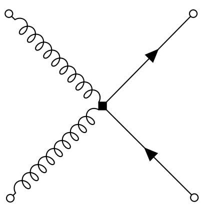

$$\equiv i\mathcal{M}_{SMEFT}^{(trees,1)} = \frac{i\sqrt{2}vg_s}{\Lambda^2} if^{ABC}T^A_{c_1c_2}\bar{u}\left(C_{uG}^* i\sigma^{\mu\nu}P_L + C_{uG} i\sigma^{\mu\nu}P_R\right)v\epsilon_\mu\epsilon_\nu \tag{4.20}$$

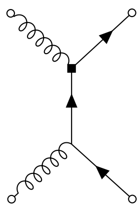

$$\equiv i\mathcal{M}_{SMEFT}^{(trees,2)} = \frac{i\sqrt{2}vg_s}{\Lambda^2}(T^BT^C)_{c_1c_2}\bar{u}\Big(\big(C_{uG}^* i\sigma^{\mu\alpha}k_{1\alpha}P_L +$$
$$+ C_{uG} i\sigma^{\mu\alpha}k_{1\alpha}P_R\big)\frac{\not{k}_2 - \not{p}_2 + m_t}{-2p_2\cdot k_2 + i\eta}\gamma^\nu\Big)v\epsilon_\mu\epsilon_\nu \tag{4.21}$$

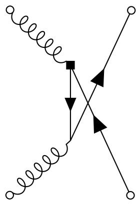

$$\equiv i\mathcal{M}^{(trees,3)}_{SMEFT} = \frac{i\sqrt{2}vg_s}{\Lambda^2}(T^C T^B)_{c_1c_2}\bar{u}\Big(\gamma^\nu \frac{\not{p}_1 - \not{k}_2 + m_t}{-2p_1\cdot k_2 + i\eta}\big(C^*_{uG} i\sigma^{\mu\alpha}k_{1\alpha}P_L + $$
$$+ C_{uG} i\sigma^{\mu\alpha}k_{1\alpha}P_R\big)\Big)v\epsilon_\mu\epsilon_\nu \tag{4.22}$$

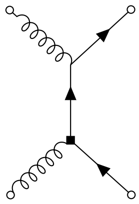

$$\equiv i\mathcal{M}^{(trees,4)}_{SMEFT} = \frac{i\sqrt{2}vg_s}{\Lambda^2}(T^B T^C)_{c_1c_2}\bar{u}\Big(\gamma^\mu \frac{\not{p}_1 - \not{k}_1 + m_t}{-2p_1\cdot k_1 + i\eta}\big(C^*_{uG} i\sigma^{\nu\alpha}k_{2\alpha}P_L + $$
$$+ C_{uG} i\sigma^{\nu\alpha}k_{2\alpha}P_R\big)\Big)v\epsilon_\mu\epsilon_\nu \tag{4.23}$$

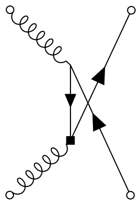

$$\equiv i\mathcal{M}^{(trees,5)}_{SMEFT} = \frac{i\sqrt{2}vg_s}{\Lambda^2}(T^C T^B)_{c_1c_2}\bar{u}\Big(\big(C^*_{uG} i\sigma^{\nu\alpha}k_{2\alpha}P_L + $$
$$+ C_{uG} i\sigma^{\nu\alpha}k_{2\alpha}P_R\big)\frac{\not{k}_1 - \not{p}_2 + m_t}{-2p_2\cdot k_1 + i\eta}\gamma^\mu\Big)v\epsilon_\mu\epsilon_\nu \tag{4.24}$$

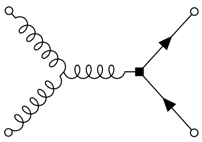

$$\equiv i\mathcal{M}^{(trees,6)}_{SMEFT} = \frac{i\sqrt{2}vg_s}{\Lambda^2} if^{ABC}T^A_{c_1c_2}\big(-2g^{\sigma\mu}k_1^\nu + g^{\mu\nu}(k_1 - k_2)^\sigma + 2g^{\nu\sigma}k_2^\mu\big)\cdot$$
$$\cdot \frac{1}{q^2 + i\eta}\bar{u}\Big(C^*_{uG} i\sigma_{\sigma\alpha}q^\alpha P_L + C_{uG} i\sigma_{\sigma\alpha}q^\alpha P_R\Big)v\epsilon_\mu\epsilon_\nu \tag{4.25}$$

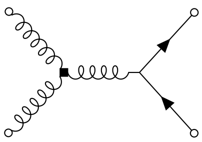

$$\equiv i\mathcal{M}^{(trees,7)}_{SMEFT} = \frac{i6C_G g_s}{\Lambda^2} if^{ABC}T^A_{c_1c_2}\big(k_1^\nu k_2^\mu - (k_1\cdot k_2)g^{\mu\nu}\big)\cdot$$
$$\cdot \frac{1}{q^2 + i\eta}\bar{u}(\not{k}_1 - \not{k}_2)v\epsilon_\mu\epsilon_\nu \tag{4.26}$$

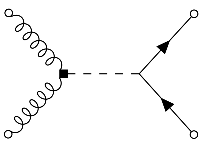

$$\equiv i\mathcal{M}^{(trees,8)}_{SMEFT} = \frac{-i4C_{\phi G}}{\Lambda^2}\delta_{BC}\delta_{c_1c_2}\frac{m_t}{m_h^2 - q^2}\big(k_1^\nu k_2^\mu - (k_1\cdot k_2)g^{\mu\nu}\big)\bar{u}v\epsilon_\mu\epsilon_\nu \tag{4.27}$$

where $P_{L/R} = (\mathbb{I} \mp \gamma_5)/2$ are the left- and right-handed projectors in spinor space. The total tree level amplitude is then given by

$$i\mathcal{M}_{SMEFT}^{(trees)} = \sum_{k=1}^{8} i\mathcal{M}_{SMEFT}^{(trees,k)} \tag{4.28}$$

Note that we have explicitly written down the crossed versions of diagrams. For instance, the four diagrams $i\mathcal{M}_{SMEFT}^{(trees,2)}$ to $i\mathcal{M}_{SMEFT}^{(trees,5)}$ should not be viewed as independent contributions as they can be converted into each other by reversing the fermion flow and/or repositioning the dimension-six insertion. In this section, however, making every crossing explicit helps with keeping track of the Ward identity when it gets less transparent (see below). For $i\mathcal{M}_{SMEFT}^{(trees)}$, the Ward identity is fulfilled, as can easily be checked.
As mentioned before, this is not the final result for the complete SMEFT amplitude at LO. For instance, being a genuine one-loop operator, the Wilson coefficient of the chromomagnetic Operator Q_{uG} depends on some renormalization scale μ (we will not distinguish the renormalization scale from the one introduced upon dimensional regularization) via its renormalization group equation [104–107]. This dependence has to be canceled by the corresponding loop amplitudes. In fact, the operator Q_{uG} provides the necessary counterterms for the divergent four-fermion loop amplitudes. Crucially, a non-trivial cancellation of infinities depends on the bottom mass m_b. We will therefore include the full bottom-mass effects to our analysis.

Loops

The loop structure for this process is quite complicated because of bubble diagrams as well as triangle diagrams featuring the Dirac matrix γ_5 in $d \neq 4$ dimensions [108]. The explicit calculations are cumbersome and lengthy; we show them in the appendix to this section together with the notational abbreviations. The result is given by[35]

$$i\mathcal{M}_{SMEFT}^{(loops)} \equiv \sum_{k=I}^{V} i\mathcal{M}_{SMEFT}^{(loops,k)} \tag{4.30}$$

[35] Similar to Section 5, the diagram (4.27) is actually accompanied with the one-loop contribution

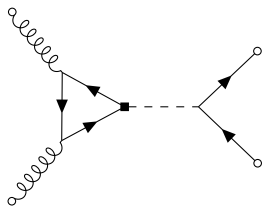

(4.29)

and its fermion-flow reversed version. These should be taken into account for fully consistent phenomenological studies. However, here we are mainly interested in the chromomagnetic operator Q_{uG} and its accompanying four-fermion operators, so we ignore the diagram (4.29) for the sake of simplicity.

The list of amplitude structures is long. It reads

$$
\begin{aligned}
i\mathcal{M}_{SMEFT}^{(loops,I)} =& \frac{ig_s^2}{16\pi^2\Lambda^2} Tr(T^B T^C)\delta_{c_1c_2}\bar{u}\Bigg(\Big(k_1^\nu k_2^\mu - (k_1\cdot k_2)g^{\mu\nu}\Big)Y_1 + i\epsilon^{\alpha\beta\mu\nu}k_{1\alpha}k_{2\beta}Y_2 + \\
&+\Big((k_1\cdot k_2)i\gamma_\lambda\epsilon^{\lambda\alpha\mu\nu}(k_2-k_1)_\alpha - (i\gamma_\lambda\epsilon^{\lambda\alpha\beta\mu}k_1^\nu - i\gamma_\lambda\epsilon^{\lambda\alpha\beta\nu}k_2^\mu)k_{1\alpha}k_{2\beta}\Big)Y_3\Bigg)v\epsilon_\mu\epsilon_\nu
\end{aligned}
\tag{4.31}
$$

with

$$
\begin{aligned}
Y_1 \equiv& \frac{4S_9^b}{m_b}\left(C_{quqd}^{(1)} + \frac{1}{12}C_{quqd}^{(8)}\right)P_R + \frac{4S_9^b}{m_b}\left(C_{quqd}^{(1)*} + \frac{1}{12}C_{quqd}^{(8)*}\right)P_L - \frac{4S_9^t}{m_t}C_{qu}^{(8)} \\
Y_2 \equiv& \frac{4S_{14}^b}{m_b}\left(C_{quqd}^{(1)} + \frac{1}{12}C_{quqd}^{(8)}\right)P_R - \frac{4S_{14}^b}{m_b}\left(C_{quqd}^{(1)*} + \frac{1}{12}C_{quqd}^{(8)*}\right)P_L + \frac{4S_{14}^t}{m_t}C_{qu}^{(8)}\gamma^5 \\
Y_3 \equiv& \Bigg(\frac{8S_{17}^b}{m_b^2}\left(2C_{qq}^{(3)} - 2C_{qq}^{(1)} + C_{qd}^{(1)} - \frac{1}{6}C_{qd}^{(8)}\right) + \\
&+\frac{8S_{17}^t}{m_t^2}\left(-2C_{qq}^{(3)} - 2C_{qq}^{(1)} + C_{qu}^{(1)} - \frac{1}{6}C_{qu}^{(8)}\right)\Bigg)P_L + \\
&+\Bigg(\frac{8S_{17}^b}{m_b^2}\left(C_{ud}^{(1)} - \frac{1}{6}C_{ud}^{(8)} - C_{qu}^{(1)} + \frac{1}{6}C_{qu}^{(8)}\right) + \frac{8S_{17}^t}{m_t^2}\left(2C_{uu} - C_{qu}^{(1)} + \frac{1}{6}C_{qu}^{(8)}\right)\Bigg)P_R
\end{aligned}
\tag{4.32}
$$

$$
\begin{aligned}
i\mathcal{M}_{SMEFT}^{(loops,II)} =& \frac{ig_s^2}{16\pi^2\Lambda^2}\{T^B, T^C\}_{c_1c_2}\bar{u}\Bigg(\Big(k_1^\nu k_2^\mu - (k_1\cdot k_2)g^{\mu\nu}\Big)Y_4 + i\epsilon^{\alpha\beta\mu\nu}k_{1\alpha}k_{2\beta}Y_5 + \\
&+\Big((k_1\cdot k_2)i\gamma_\lambda\epsilon^{\lambda\alpha\mu\nu}(k_2-k_1)_\alpha - (i\gamma_\lambda\epsilon^{\lambda\alpha\beta\mu}k_1^\nu - i\gamma_\lambda\epsilon^{\lambda\alpha\beta\nu}k_2^\mu)k_{1\alpha}k_{2\beta}\Big)Y_6\Bigg)v\epsilon_\mu\epsilon_\nu
\end{aligned}
\tag{4.33}
$$

with

$$
\begin{aligned}
Y_4 \equiv& \frac{S_9^b}{m_b}\left(C_{quqd}^{(1)} + \frac{5}{6}C_{quqd}^{(8)}\right)P_R + \frac{S_9^b}{m_b}\left(C_{quqd}^{(1)*} + \frac{5}{6}C_{quqd}^{(8)*}\right)P_L - \frac{4S_9^t}{m_t}\left(C_{qu}^{(1)} - \frac{1}{6}C_{qu}^{(8)}\right) \\
Y_5 \equiv& \frac{S_{14}^b}{m_b}\left(C_{quqd}^{(1)} + \frac{5}{6}C_{quqd}^{(8)}\right)P_R - \frac{S_{14}^b}{m_b}\left(C_{quqd}^{(1)*} + \frac{5}{6}C_{quqd}^{(8)*}\right)P_L + \\
&+ \frac{4S_{14}^t}{m_t}\left(C_{qu}^{(1)} - \frac{1}{6}C_{qu}^{(8)}\right)\gamma^5 \\
Y_6 \equiv& \Bigg(\frac{2S_{17}^b}{m_b^2}\left(-8C_{qq}^{(3)} + C_{qd}^{(8)}\right) - \frac{8S_{17}^t}{m_t^2}\left(C_{qq}^{(1)} + C_{qq}^{(3)}\right)\Bigg)P_L +
\end{aligned}
$$

$$+\left(\frac{2S_{17}^b}{m_b^2}\left(C_{ud}^{(8)}-C_{qu}^{(8)}\right)+\frac{8S_{17}^t}{m_t^2}C_{uu}\right)P_R-\frac{2S_{17}^t}{m_t^2}C_{qu}^{(8)}\gamma^5 \tag{4.34}$$

$$\begin{aligned}
i\mathcal{M}_{SMEFT}^{(loops,III)} =&\frac{ig_s^2}{16\pi^2\Lambda^2}if^{ABC}T^A_{c_1c_2}\bar{u}\Big((\not{k}_1-\not{k}_2)\Big(k_1^\nu k_2^\mu-(k_1\cdot k_2)g^{\mu\nu}\Big)Y_7+\\
&+\big(i\sigma^{\nu\alpha}k_{1\alpha}k_2^\mu-i\sigma^{\mu\alpha}k_{2\alpha}k_1^\nu+i\sigma^{\alpha\beta}k_{1\alpha}k_{2\beta}g^{\mu\nu}+(k_1\cdot k_2)i\sigma^{\mu\nu}\big)Y_8+\\
&+\big(i\sigma^{\nu\alpha}k_{2\alpha}k_2^\mu-i\sigma^{\mu\alpha}k_{1\alpha}k_1^\nu\big)Y_9\Big)v\epsilon_\mu\epsilon_\nu
\end{aligned} \tag{4.35}$$

with

$$\begin{aligned}
Y_7\equiv&\left(\frac{S_{10}^b}{m_b^2}\left(8C_{qq}^{(3)}+C_{qd}^{(8)}\right)+\frac{4S_{10}^t}{m_t^2}\left(C_{qq}^{(1)}+C_{qq}^{(3)}\right)\right)P_L+\\
&+\left(\frac{S_{10}^b}{m_b^2}\left(C_{ud}^{(8)}+C_{qu}^{(8)}\right)+\frac{4S_{10}^t}{m_t^2}C_{uu}\right)P_R+\frac{S_{10}^t}{m_t^2}C_{qu}^{(8)}\\
Y_8\equiv&\left(\frac{m_b}{k_1\cdot k_2}X_2^b+\frac{S_{14}^b}{m_b}\right)\left(\left(C_{quqd}^{(1)}-\frac{1}{6}C_{quqd}^{(8)}\right)P_R+\left(C_{quqd}^{(1)*}-\frac{1}{6}C_{quqd}^{(8)*}\right)P_L\right)+\\
&+\frac{m_t}{k_1\cdot k_2}\left(2C_{qu}^{(1)}-\frac{1}{3}C_{qu}^{(8)}\right)\\
Y_9\equiv&\frac{m_t}{k_1\cdot k_2}\left(2C_{qu}^{(1)}-\frac{1}{3}C_{qu}^{(8)}\right)
\end{aligned} \tag{4.36}$$

$$\begin{aligned}
i\mathcal{M}_{SMEFT}^{(loops,IV)} =&\frac{ig_s^2}{16\pi^2\Lambda^2}(T^BT^C)_{c_1c_2}\bar{u}\Big(m_ti\sigma^{\mu\alpha}k_{1\alpha}Y_{10}\frac{\not{k}_2-\not{p}_2+m_t}{-2p_2\cdot k_2}\gamma^\nu\Big)v\epsilon_\mu\epsilon_\nu+\\
&+\frac{ig_s^2}{16\pi^2\Lambda^2}(T^CT^B)_{c_1c_2}\bar{u}\Big(\gamma^\nu\frac{\not{p}_1-\not{k}_2+m_t}{-2p_1\cdot k_2}m_ti\sigma^{\mu\alpha}k_{1\alpha}Y_{10}\Big)v\epsilon_\mu\epsilon_\nu+\\
&+\frac{ig_s^2}{16\pi^2\Lambda^2}(T^BT^C)_{c_1c_2}\bar{u}\Big(\gamma^\mu\frac{\not{p}_1-\not{k}_1+m_t}{-2p_1\cdot k_1}m_ti\sigma^{\nu\alpha}k_{2\alpha}Y_{10}\Big)v\epsilon_\mu\epsilon_\nu+\\
&+\frac{ig_s^2}{16\pi^2\Lambda^2}(T^CT^B)_{c_1c_2}\bar{u}\Big(m_ti\sigma^{\nu\alpha}k_{2\alpha}Y_{10}\frac{\not{k}_1-\not{p}_2+m_t}{-2p_2\cdot k_1}\gamma^\mu\Big)v\epsilon_\mu\epsilon_\nu
\end{aligned} \tag{4.37}$$

with

$$Y_{10}\equiv\left(2C_{qu}^{(1)}-\frac{1}{3}C_{qu}^{(8)}\right) \tag{4.38}$$

$$\begin{aligned}
i\mathcal{M}_{SMEFT}^{(loops,V)} =&\frac{ig_s^2}{16\pi^2\Lambda^2}(T^BT^C)_{c_1c_2}\bar{u}\Big(m_bi\sigma^{\mu\alpha}k_{1\alpha}Y_{11}\frac{\not{k}_2-\not{p}_2+m_t}{-2p_2\cdot k_2}\gamma^\nu\Big)v\epsilon_\mu\epsilon_\nu+\\
&+\frac{ig_s^2}{16\pi^2\Lambda^2}(T^CT^B)_{c_1c_2}\bar{u}\Big(\gamma^\nu\frac{\not{p}_1-\not{k}_2+m_t}{-2p_1\cdot k_2}m_bi\sigma^{\mu\alpha}k_{1\alpha}Y_{11}\Big)v\epsilon_\mu\epsilon_\nu+
\end{aligned}$$

$$
\begin{aligned}
&+\frac{ig_s^2}{16\pi^2\Lambda^2}(T^BT^C)_{c_1c_2}\bar{u}\Big(\gamma^\mu\frac{\not{p}_1-\not{k}_1+m_t}{-2p_1\cdot k_1}m_b i\sigma^{\nu\alpha}k_{2\alpha}Y_{11}\Big)v\epsilon_\mu\epsilon_\nu+\\
&+\frac{ig_s^2}{16\pi^2\Lambda^2}(T^CT^B)_{c_1c_2}\bar{u}\Big(m_b i\sigma^{\nu\alpha}k_{2\alpha}Y_{11}\frac{\not{k}_1-\not{p}_2+m_t}{-2p_2\cdot k_1}\gamma^\mu\Big)v\epsilon_\mu\epsilon_\nu+\\
&+\frac{ig_s^2}{16\pi^2\Lambda^2}if^{ABC}T^A_{c_1c_2}\frac{m_b}{k_1\cdot k_2}\bar{u}\Big(i\sigma^{\nu\alpha}q_\alpha k_2^\mu-i\sigma^{\mu\alpha}q_\alpha k_1^\nu+\\
&\qquad\qquad+i\sigma^{\alpha\beta}k_{1\alpha}k_{2\beta}g^{\mu\nu}+(k_1\cdot k_2)i\sigma^{\mu\nu}\Big)Y_{11}v\epsilon_\mu\epsilon_\nu
\end{aligned}
\tag{4.39}
$$

with

$$
Y_{11}\equiv\left(\frac{1}{\epsilon}+\ln\frac{4\pi}{e^\gamma}+\ln\frac{\mu^2}{m_b^2}\right)\left(\left(C^{(1)}_{quqd}-\frac{1}{6}C^{(8)}_{quqd}\right)P_R+\left(C^{(1)*}_{quqd}-\frac{1}{6}C^{(8)*}_{quqd}\right)P_L\right)\tag{4.40}
$$

The loop functions S are defined in the appendix to this section. Note that $i\mathcal{M}^{(loops,V)}_{SMEFT}$ is the only divergent expression. This issue can be resolved by going back to the tree amplitudes, in particular to the chromomagnetic operator Q_{uG} and its hermitian conjugate. Remarkably, this effect only comes into play when the bottom mass is non-zero. The relevant part of the renormalization group equation for the chromomagnetic operator is given by [104, 106]

$$
\frac{dC_{uG}}{d\ln\mu^2}=-\frac{g_s m_b}{16\pi^2\sqrt{2}v}\left(C^{(1)}_{quqd}-\frac{1}{6}C^{(8)}_{quqd}\right)\tag{4.41}
$$

Not counting hermitian conjugates, out of the eleven four-fermion operators, only the two operators appearing in Y_{11} are divergent and hence responsible for the cancellation of the renormalization scale dependence between the different loop orders. We introduce counterterms $i\mathcal{M}^{(counter)}_{SMEFT}$ of the form of the chromomagnetic operator Q_{uG} and choose the $\overline{\text{MS}}$ scheme to cancel the divergent entity $1/\epsilon+\ln(4\pi/e^\gamma)$.
Adding all these contributions yields

$$
\begin{aligned}
i\mathcal{M}^{(loops,V)}_{SMEFT}&+\sum_{k=1}^{6}i\mathcal{M}^{(trees,k)}_{SMEFT}+i\mathcal{M}^{(counter)}_{SMEFT}=\\
&=\frac{ig_s^2}{16\pi^2\Lambda^2}(T^BT^C)_{c_1c_2}\bar{u}\Big(i\sigma^{\mu\alpha}k_{1\alpha}Y_{12}\frac{\not{k}_2-\not{p}_2+m_t}{-2p_2\cdot k_2}\gamma^\nu\Big)v\epsilon_\mu\epsilon_\nu+\\
&+\frac{ig_s^2}{16\pi^2\Lambda^2}(T^CT^B)_{c_1c_2}\bar{u}\Big(\gamma^\nu\frac{\not{p}_1-\not{k}_2+m_t}{-2p_1\cdot k_2}i\sigma^{\mu\alpha}k_{1\alpha}Y_{12}\Big)v\epsilon_\mu\epsilon_\nu+\\
&+\frac{ig_s^2}{16\pi^2\Lambda^2}(T^BT^C)_{c_1c_2}\bar{u}\Big(\gamma^\mu\frac{\not{p}_1-\not{k}_1+m_t}{-2p_1\cdot k_1}i\sigma^{\nu\alpha}k_{2\alpha}Y_{12}\Big)v\epsilon_\mu\epsilon_\nu+\\
&+\frac{ig_s^2}{16\pi^2\Lambda^2}(T^CT^B)_{c_1c_2}\bar{u}\Big(i\sigma^{\nu\alpha}k_{2\alpha}Y_{12}\frac{\not{k}_1-\not{p}_2+m_t}{-2p_2\cdot k_1}\gamma^\mu\Big)v\epsilon_\mu\epsilon_\nu+\\
&+\frac{ig_s^2}{16\pi^2\Lambda^2}if^{ABC}T^A_{c_1c_2}\frac{1}{k_1\cdot k_2}\bar{u}\Big(i\sigma^{\nu\alpha}q_\alpha k_2^\mu-i\sigma^{\mu\alpha}q_\alpha k_1^\nu+
\end{aligned}
$$

$$+ i\sigma^{\alpha\beta} k_{1\alpha} k_{2\beta} g^{\mu\nu} + (k_1 \cdot k_2) i\sigma^{\mu\nu}\Big) Y_{12} v \epsilon_\mu \epsilon_\nu \tag{4.42}$$

with

$$\begin{aligned} Y_{12} = & \left(m_b \ln \frac{\mu^2}{m_b^2} \left(C^{(1)}_{quqd} - \frac{1}{6} C^{(8)}_{quqd} \right) + \frac{\sqrt{2} v}{g_s} C_{uG} \right) P_R + \\ & + \left(m_b \ln \frac{\mu^2}{m_b^2} \left(C^{(1)*}_{quqd} - \frac{1}{6} C^{(8)*}_{quqd} \right) + \frac{\sqrt{2} v}{g_s} C^{*}_{(uG)} \right) P_L \end{aligned} \tag{4.43}$$

We have

$$\frac{dY_{12}}{d \ln \mu^2} = 0 \tag{4.44}$$

as it should. The gauge invariance of the full amplitude (4.30) can be checked straightforwardly.
The final results for the SMEFT corrections to the differential cross-section are obtained by squaring the amplitudes and using (4.7). The list is given by

$$\left(\frac{d\sigma}{d\Omega}\right)_{Q_G} = -\frac{C_G}{\Lambda^2} \frac{\alpha_s^{3/2} m_t^2 \sqrt{1 - \frac{4m_t^2}{s}}}{64\sqrt{2} s} \frac{9(t-u)^2}{(m_t^2 - t)(m_t^2 - u)} \tag{4.45}$$

$$\left(\frac{d\sigma}{d\Omega}\right)_{Q_{\varphi G}} = \frac{C_{\varphi G}}{\Lambda^2} \frac{\alpha_s m_t^2 \sqrt{1 - \frac{4m_t^2}{s}} \left(1 - \frac{4m_t^2}{s}\right)}{64\pi} \frac{s^2}{(m_t^2 - t)(m_t^2 - u)(m_h^2 - s)} \tag{4.46}$$

$$\left(\frac{d\sigma}{d\Omega}\right)_{Q_{uG}} = -\frac{\mathrm{Re}\{C_{uG}(\mu)\}}{\Lambda^2} \frac{\alpha_s^{3/2} v m_t \sqrt{1 - \frac{4m_t^2}{s}}}{24\sqrt{2\pi} s} \frac{7m_t^4 - 7m_t^2(t+u) + 4t^2 - tu + 4u^2}{(m_t^2 - t)(m_t^2 - u)} \tag{4.47}$$

$$\begin{aligned} \left(\frac{d\sigma}{d\Omega}\right)_{Q^{(1)}_{quqd}} = & -\frac{\mathrm{Re}\{C^{(1)}_{quqd}\}}{16\pi^2\Lambda^2} \frac{\alpha_s^2 m_t \sqrt{1 - \frac{4m_t^2}{s}}}{192 m_b s} \frac{1}{(m_t^2 - t)(m_t^2 - u)} \cdot \\ & \cdot \left(19 s^2 \left(2m_t^2 S_1(a_b) + m_b^2 \left(1 - \frac{4m_t^2}{s}\right) (2S_1(a_b) - 1) \right) + \right. \\ & \left. + 8m_b^2 \left(7m_t^4 - 7m_t^2(t+u) + 4t^2 - tu + 4u^2\right) \ln \frac{\mu^2}{m_b^2} \right) \end{aligned} \tag{4.48}$$

$$\begin{aligned} \left(\frac{d\sigma}{d\Omega}\right)_{Q^{(8)}_{quqd}} = & -\frac{\mathrm{Re}\{C^{(8)}_{quqd}\}}{16\pi^2\Lambda^2} \frac{\alpha_s^2 m_t \sqrt{1 - \frac{4m_t^2}{s}}}{1152 m_b s} \frac{1}{(m_t^2 - t)(m_t^2 - u)} \cdot \\ & \cdot \left(41 s^2 \left(2m_t^2 S_1(a_b) + m_b^2 \left(1 - \frac{4m_t^2}{s}\right) (2S_1(a_b) - 1) \right) + \right. \\ & \left. - 8m_b^2 \left(7m_t^4 - 7m_t^2(t+u) + 4t^2 - tu + 4u^2\right) \ln \frac{\mu^2}{m_b^2} \right) \end{aligned} \tag{4.49}$$

$$\left(\frac{d\sigma}{d\Omega}\right)_{Q_{qd}^{(1)}} = -\frac{C_{qd}^{(1)}}{16\pi^2\Lambda^2}\frac{\alpha_s^2 m_t^2 s\sqrt{1-\frac{4m_t^2}{s}}}{32}\frac{2S_1(a_b)-1}{(m_t^2-t)(m_t^2-u)} \tag{4.50}$$

$$\left(\frac{d\sigma}{d\Omega}\right)_{Q_{ud}^{(1)}} = \frac{C_{ud}^{(1)}}{16\pi^2\Lambda^2}\frac{\alpha_s^2 m_t^2 s\sqrt{1-\frac{4m_t^2}{s}}}{32}\frac{2S_1(a_b)-1}{(m_t^2-t)(m_t^2-u)} \tag{4.51}$$

$$\begin{aligned}\left(\frac{d\sigma}{d\Omega}\right)_{Q_{qd}^{(8)}} = &-\frac{C_{qd}^{(8)}}{16\pi^2\Lambda^2}\frac{\alpha_s^2 m_t^2\sqrt{1-\frac{4m_t^2}{s}}}{384s}\cdot \\ &\cdot\frac{5s^2\big(2S_1(a_b)-1\big)+3(t-u)^2\big(6S_1(a_b)-12S_2(a_b)-1\big)}{(m_t^2-t)(m_t^2-u)}\end{aligned} \tag{4.52}$$

$$\begin{aligned}\left(\frac{d\sigma}{d\Omega}\right)_{Q_{ud}^{(8)}} = &\frac{C_{ud}^{(8)}}{16\pi^2\Lambda^2}\frac{\alpha_s^2 m_t^2\sqrt{1-\frac{4m_t^2}{s}}}{384s}\cdot \\ &\cdot\frac{5s^2\big(2S_1(a_b)-1\big)-3(t-u)^2\big(6S_1(a_b)-12S_2(a_b)-1\big)}{(m_t^2-t)(m_t^2-u)}\end{aligned} \tag{4.53}$$

$$\begin{aligned}\left(\frac{d\sigma}{d\Omega}\right)_{Q_{uu}} = &\frac{C_{uu}}{16\pi^2\Lambda^2}\frac{\alpha_s^2 m_t^2\sqrt{1-\frac{4m_t^2}{s}}}{96s}\cdot \\ &\cdot\frac{13s^2\big(2S_1(a_t)-1\big)-3(t-u)^2\big(6S_1(a_t)-12S_2(a_t)-1\big)}{(m_t^2-t)(m_t^2-u)}\end{aligned} \tag{4.54}$$

$$\begin{aligned}\left(\frac{d\sigma}{d\Omega}\right)_{Q_{qq}^{(1)}} = &\frac{C_{qq}^{(1)}}{16\pi^2\Lambda^2}\frac{\alpha_s^2 m_t^2\sqrt{1-\frac{4m_t^2}{s}}}{96s}\frac{1}{(m_t^2-t)(m_t^2-u)}\Big(6s^2\big(2S_1(a_b)-1\big)+ \\ &+13s^2\big(2S_1(a_t)-1\big)-3(t-u)^2\big(6S_1(a_t)-12S_2(a_t)-1\big)\Big)\end{aligned} \tag{4.55}$$

$$\begin{aligned}\left(\frac{d\sigma}{d\Omega}\right)_{Q_{qq}^{(3)}} = &\frac{C_{qq}^{(3)}}{16\pi^2\Lambda^2}\frac{\alpha_s^2 m_t^2\sqrt{1-\frac{4m_t^2}{s}}}{96s}\frac{1}{(m_t^2-t)(m_t^2-u)}\Big(8s^2\big(2S_1(a_b)-1\big)+ \\ &+13s^2\big(2S_1(a_t)-1\big)-6(t-u)^2\big(6S_1(a_b)-12S_2(a_b)-1\big)+ \\ &-3(t-u)^2\big(6S_1(a_t)-12S_2(a_t)-1\big)\Big)\end{aligned} \tag{4.56}$$

$$\begin{aligned}\left(\frac{d\sigma}{d\Omega}\right)_{Q_{qu}^{(1)}} = &-\frac{C_{qu}^{(1)}}{16\pi^2\Lambda^2}\frac{\alpha_s^2\sqrt{1-\frac{4m_t^2}{s}}}{96s}\frac{1}{(m_t^2-t)(m_t^2-u)}\Big(3m_t^2s^2\big(2S_1(a_b)-1\big)+56m_t^6+ \\ &+4m_t^2\Big(14m_t^2s\big(2S_1(a_t)-1\big)-7s^2S_1(a_t)+8t^2-2tu+8u^2\Big)+ \\ &-8m_t^2s^2\big(2S_1(a_t)-1\big)-56m_t^4(t+u)+14s^3S_1(a_t)\Big)\end{aligned} \tag{4.57}$$

$$\left(\frac{d\sigma}{d\Omega}\right)_{Q_{qu}^{(8)}} = -\frac{C_{qu}^{(8)}}{16\pi^2\Lambda^2}\frac{\alpha_s^2\sqrt{1-\frac{4m_t^2}{s}}}{1152s}\frac{1}{(m_t^2-t)(m_t^2-u)}\Big(15m_t^2s^2\big(2S_1(a_b)-1\big)+$$

$$
\begin{aligned}
&-14m_t^2s^2\big(2S_1(a_t)-1\big)-112m_t^6+112m_t^4(t+u)+\\
&-8m_t^2\Big(-22m_t^2s\big(2S_1(a_t)-1\big)+11s^2S_1(a_t)+8t^2-2tu+8u^2\Big)+\\
&+9m_t^2(t-u)^2\big(6S_1(a_b)-12S_2(a_b)-1\big)+44s^3S_1(a_t)\Big)
\end{aligned}
\tag{4.58}
$$

where

$$
\begin{aligned}
S_1(a_i) =&\mathrm{Re}\left\{\int_0^1 dz\int_0^{1-z} dy\frac{1}{1-4yza_i-i\eta}\right\}=\\
=&\mathrm{Re}\left\{\frac{\mathrm{Li}_2\left(-\frac{2\sqrt{a_i}}{\sqrt{a_i-1}-\sqrt{a_i}}\right)+\mathrm{Li}_2\left(\frac{2\sqrt{a_i}}{\sqrt{a_i-1}+\sqrt{a_i}}\right)}{4a_i}\right\}=\\
=&\frac{-\ln^2(a_i)-4\ln(2a_i)\ln(2)+\pi^2}{8a_i}+\mathcal{O}\left(\frac{1}{a_i^2}\right)
\end{aligned}
\tag{4.59}
$$

$$
\begin{aligned}
S_2(a_i) =&\mathrm{Re}\left\{\int_0^1 dz\int_0^{1-z} dy\frac{y}{1-4yza_i-i\eta}\right\}=\\
=&\mathrm{Re}\left\{\frac{a_i-\sqrt{a_i-a_i^2}\tan^{-1}\left(\frac{\sqrt{a_i}}{\sqrt{1-a_i}}\right)}{2a_i^2}\right\}=\\
=&\frac{-\ln(4a_i)+2}{4a_i}+\mathcal{O}\left(\frac{1}{a_i^2}\right)
\end{aligned}
\tag{4.60}
$$

in the relevant energy regime and $a_i \equiv s/4m_i^2$ for $i=t,b$.

4.3. Numerical results

So far, we have evaluated the analytic differential cross-section formulas for the parton-level particle reaction $gg \to t\bar{t}$ at LO QCD. However, we expect NLO QCD corrections for processes with external gluon states to enhance the numerical values of our results by a significant amount [109, 110], see also Section 5. A cautious numerical evaluation of our formulas must therefore always be taken with a grain of salt. But since QCD corrections affect both the SM result and the SMEFT corrections on an equal footing, our formulas can still be viewed as a first approximation for the size of the expected phenomenological new-physics impact on SM observables based on this parton-level process. Absolute values should then be multiplied by the relevant K-factors for this process, which is about 1.5 [97]. Of course, such an artificial adjustment can ultimately not replace a full QCD study at NLO, see [111, 112] for different examples. We will therefore not consider any sort of extrapolation towards higher order QCD effects[36] and keep in mind that our values only represent the qualitative behavior and might quantitatively be far off from reality.

The input parameters for our formulas are shown in Appendix A. We use the $\overline{\mathrm{MS}}$ bottom

[36]This includes the running of the strong coupling constant as well as the quark masses.

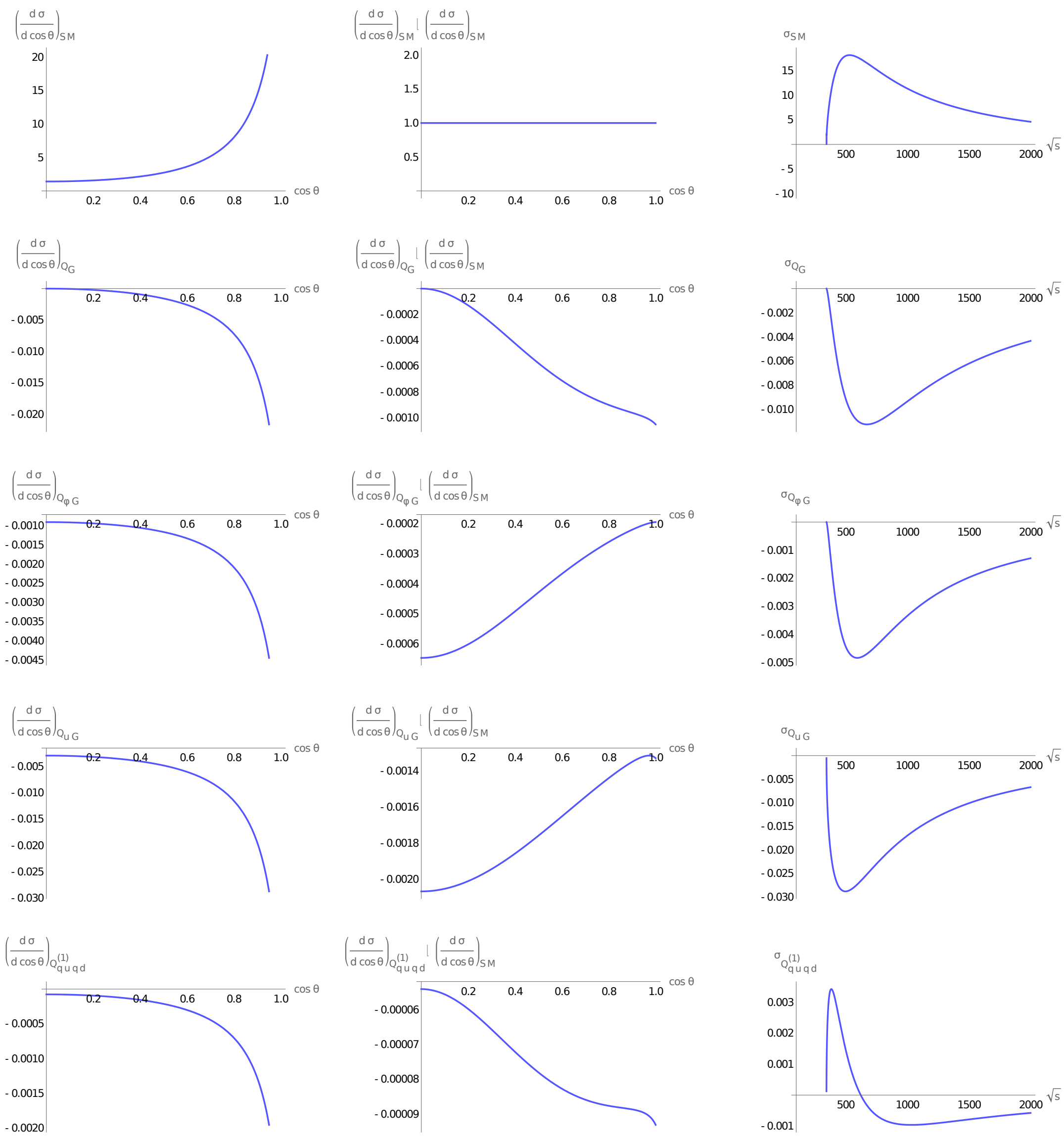

Figure 1: Numerical plots for the SM result (first row), Q_G (second row), $Q_{\varphi G}$ (third row), Q_{uG} (fourth row) and $Q^{(1)}_{qugd}$ (last row). The left and right columns show the differential (for $\sqrt{s} = 1$ TeV) and total cross-sections in pb, respectively. The middle column represents the ratio between the differential corrections and the SM result.

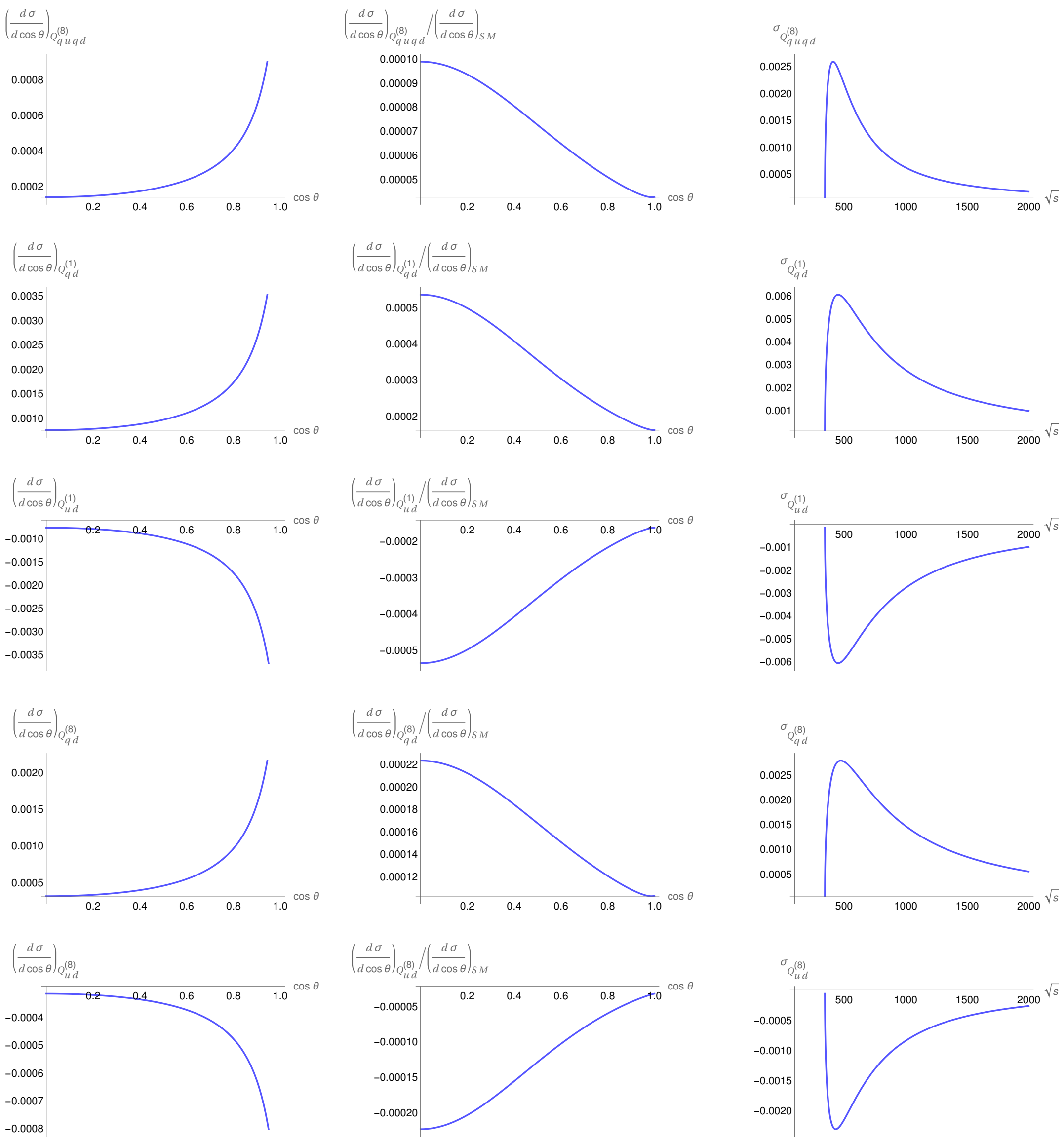

Figure 2: Numerical plots for $Q^{(8)}_{quqd}$ (first row), $Q^{(1)}_{qd}$ (second row), $Q^{(1)}_{ud}$ (third row), $Q^{(8)}_{qd}$ (fourth row) and $Q^{(8)}_{ud}$ (last row). See Figure 1 for further details.

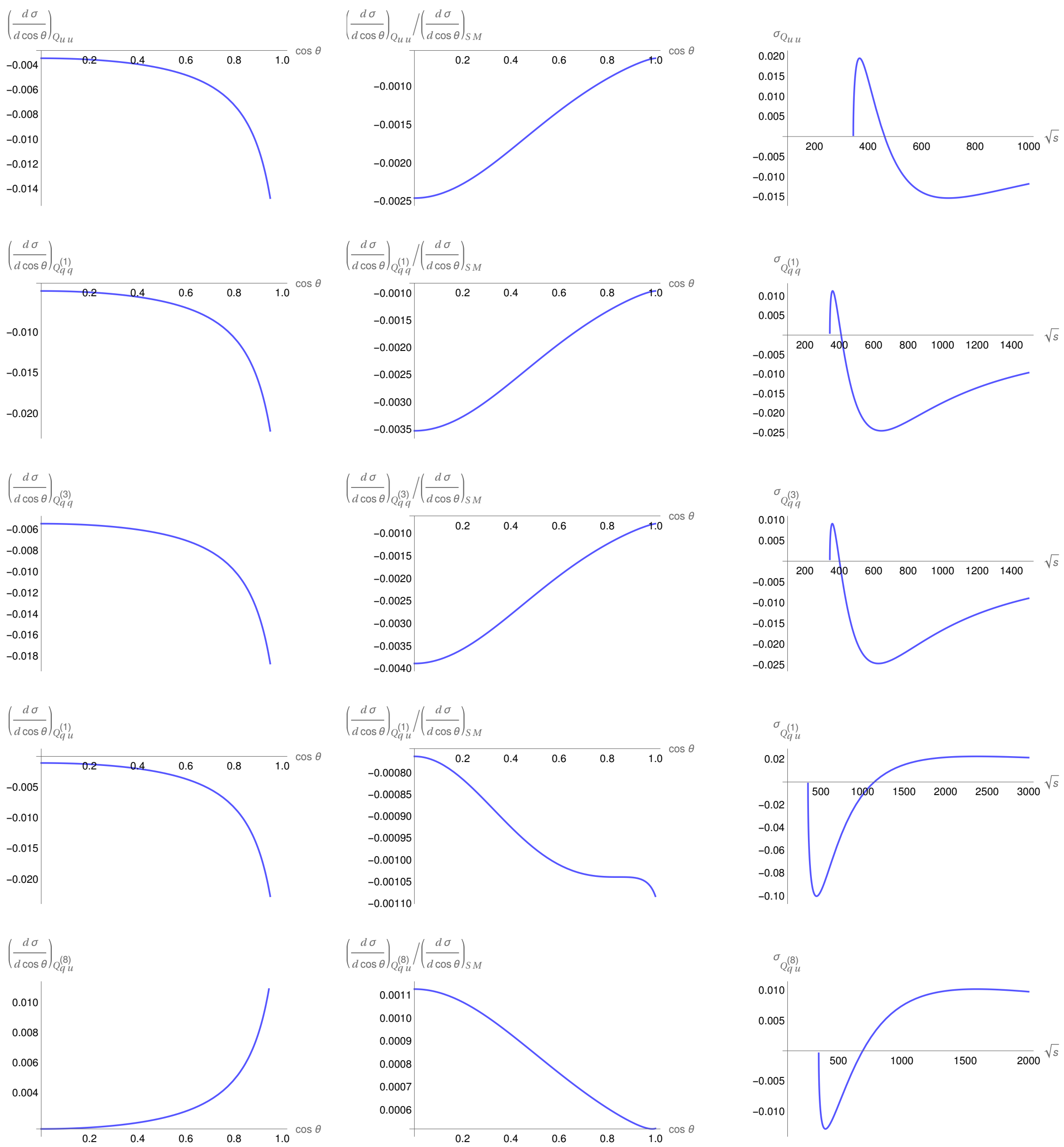

Figure 3: Numerical plots for Q_{uu} (first row), $Q_{qq}^{(1)}$ (second row), $Q_{qq}^{(3)}$ (third row), $Q_{qu}^{(1)}$ (fourth row) and $Q_{qu}^{(8)}$ (last row). See Figure 1 for further details.

mass at $\mu = m_b$. The cutoff scale is set to $\Lambda = 1$ TeV and we fix the renormalization scale to $\mu = m_t$. The Wilson coefficients with field strength tensors, i.e. C_G, $C_{\varphi G}$ and C_{uG} are nominally set to $1/(16\pi^2)$, all others are assumed to be 1. Since it is only the ratio between the Wilson-coefficients and the cutoff scale that enters the analytic formulas, we can safely extend the latter beyond 1 TeV without spoiling the SMEFT expansion by implicitly adjusting the parameters. We plot the absolute values of the differential cross-section corrections for $\sqrt{s} = 1$ TeV together with their ratios to the SM result, as well as the corrections to the total cross-section by integrating over the remaining angle as a function of the center-of-mass energy $\sqrt{s}$ in Figures 1-3. Due to the cylindrical symmetry, the angular dependence of our cross-section formulas (4.45)-(4.58) can be reduced to only one angle via $d\Omega = 2\pi d\theta$. The relative corrections to the SM never exceed the per-mille range, which is far beyond the current experimental reachability. We can nevertheless make some qualitative observations. First, on one hand, for the operators Q_G, $Q^{(1)}_{quqd}$ and $Q^{(1)}_{qu}$, the relative correction of the differential cross-section to the SM reaches is maximum for the forward-backward scattering case, which would make their detection even harder due to beamline constraints. All other operators, on the other hand, reach their maximal relative impact for high scattering angles. Second, the relative total cross-section (not plotted) for the fastest growing operator $Q^{(1)}_{qu}$ hits the percent level at around $\sqrt{s} \approx 3.5$ TeV. Possible resonances above 1 TeV could, however, spoil the applicability of SMEFT already before this benchmark. Last and most interestingly, we observe a change of sign of the correction to the total cross-section shortly after the top-pair production threshold $\sqrt{s} = 2m_t$ for the operators $Q^{(1)}_{quqd}$, Q_{uu}, $Q^{(1)}_{qq}$, $Q^{(3)}_{qq}$, $Q^{(1)}_{qu}$ and $Q^{(8)}_{qu}$. After subtracting the SM background from experimental data, such a signature could prove to be valuable for the hypothetical extraction of non-vanishing values for their Wilson coefficients.

Of course, other processes for which the impact of the operators under consideration is enhanced compared to our case are possible. For instance, four-top production channels at particle colliders feature the plain four-top operator already at tree-level [113]. This, however, comes with the cost of having to produce four on-shell top-quarks in the first place. Concerning the operator Q_{uu}, the combined upper limit from the ATLAS experiment for four-top production implies $|C_{uu}| \leq 1.9$ for $\Lambda = 1$ TeV [114].

Apart from the top sector, the occurrence of hypothetical strong couplings in the context of new physics seems plausible in the Higgs sector for this process, where an enhancement of certain Wilson coefficients involving the Higgs field could be possible. Scenarios with strong dynamics of electroweak symmetry breaking can be described in very general terms by the EWChL, see also the next section. In such cases, the operator $Q_{\varphi G}$ can in principle be generated without the extra loop factor $1/(16\pi^2)$, since the Higgs fields are no longer associated with weak couplings, which essentially reduces the chiral dimension. On one hand, depending on the scenario, this would also enhance the one-loop contribution (4.29) such that their respective hierarchy is restored [74]. For instance, albeit the chiral dimension of $Q_{\varphi G}$ would be reduced to $d_\chi = 4$ (there are always weak gauge couplings associated with field strength tensors), we would simultaneously also reduce the chiral dimensions of $Q_{\varphi,kin}$ and $C_{f\varphi}$ (see Table 1 in Section 5) to $d_\chi = 2$. The oper-

ator Q_{uG}, on the other hand, is always loop-suppressed with respect to the four-fermion ones, even for strong-coupling scenarios in the Higgs sector, see also Chapter 2.1 in [115]. The EWChL framework has such subtleties automatically incorporated.
The EWChL coefficient c_{ggh} is related to the SMEFT coefficient $C_{\varphi G}$ via

$$C_{\varphi G} = \frac{\Lambda^2 \alpha_s}{8\pi v^2} c_{ggh} \approx 0.08\ c_{ggh} \tag{4.61}$$

Its experimental value is approximately given by $c_{ggh} = -0.01 \pm 0.08$ [116]. The remaining tree-level operators are at best constrained by $|C_{uG}| \leq 0.78$ and $|C_G| \leq 0.037$ for $\Lambda = 1$ TeV [103, 117–121]. The uncertainties of the coefficients are in fact quite large. Given the current data, it is therefore not possible to postulate significant deviations from their natural values of $1/(16\pi^2) \approx 0.0063$.
We have compared our analytic results to the numerical Monte Carlo implementation SMEFT@NLO [122] for MadGraph5_aMC@NLO [123, 124] for selected center-of-mass energies and scattering angles with $m_b = 0$ (this is required by SMEFT@NLO[37]) and fixed α_s. For the tree-level-topology operators, as well as the bottom-quark loops, we find sufficient agreement with our formulas. In contrast, our top-quark-loop results differ from the SMEFT@NLO output by a few percent[38].

Appendix: Explicit calculations of the loop diagrams

For the process in mind, there are two new vertices that play a role at the one-loop level. With open colour indices c_i and spinor indices s_i and taking only the third quark generation into account, these vertices are of the four-fermion type and are given by

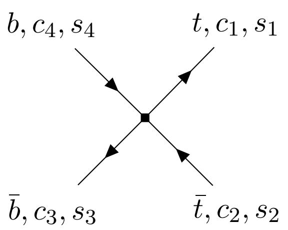

$$\equiv V^{(b)}_{c_1c_2c_3c_4s_1s_2s_3s_4} \equiv V^{(b,1)}_{s_1s_2s_3s_4}\delta_{c_3c_4}\delta_{c_1c_2} + V^{(b,2)}_{s_1s_2s_3s_4}\delta_{c_3c_2}\delta_{c_4c_1} =$$

$$\begin{aligned}
= i\delta_{c_3c_4}\delta_{c_1c_2}\Bigg(&(\gamma_\alpha P_L)_{s_3s_4}(\gamma^\alpha P_L)_{s_1s_2}\left(2C^{(1)}_{qq} - 2C^{(3)}_{qq}\right) + \\
&+(\gamma_\alpha P_R)_{s_3s_4}(\gamma^\alpha P_R)_{s_1s_2}\left(C^{(1)}_{ud} - \frac{1}{6}C^{(8)}_{ud}\right) + \\
&+(\gamma_\alpha P_L)_{s_3s_4}(\gamma^\alpha P_R)_{s_1s_2}\left(C^{(1)}_{qu} - \frac{1}{6}C^{(8)}_{qu}\right) +
\end{aligned}$$

---

[37] Providing the full m_b-dependence (including the renormalization group equation (4.41) for the chromomagnetic operator!), our analytic formulas therefore complement the numerical discussion.

[38] This might partly be due to ambiguous contractions for the four-top vertex together with large numerical cancellations when the full m_t-dependence is taken into account. In fact, we were able to achieve adequate accordance when manipulating the counterterms within the program.

$$+(\gamma_\alpha P_R)_{s_3s_4}(\gamma^\alpha P_L)_{s_1s_2}\left(C^{(1)}_{qd}-\frac{1}{6}C^{(8)}_{qd}\right)+$$
$$+(P_L)_{s_3s_4}(P_L)_{s_1s_2}\left(C^{(1)*}_{quqd}-\frac{1}{6}C^{(8)*}_{quqd}\right)+$$
$$+(P_R)_{s_3s_4}(P_R)_{s_1s_2}\left(C^{(1)}_{quqd}-\frac{1}{6}C^{(8)}_{quqd}\right)+$$
$$+(P_L)_{s_3s_2}(P_L)_{s_1s_4}\frac{1}{2}C^{(8)*}_{quqd}+(P_R)_{s_3s_2}(P_R)_{s_1s_4}\frac{1}{2}C^{(8)}_{quqd}\Bigg)+$$
$$+i\delta_{c_3c_2}\delta_{c_4c_1}\Bigg((\gamma_\alpha P_L)_{s_3s_2}(\gamma^\alpha P_L)_{s_1s_4}(-4)C^{(3)}_{qq}+$$
$$+(\gamma_\alpha P_R)_{s_3s_4}(\gamma^\alpha P_R)_{s_1s_2}\frac{1}{2}C^{(8)}_{ud}+$$
$$+(\gamma_\alpha P_L)_{s_3s_4}(\gamma^\alpha P_R)_{s_1s_2}\frac{1}{2}C^{(8)}_{qu}+$$
$$+(\gamma_\alpha P_R)_{s_3s_4}(\gamma^\alpha P_L)_{s_1s_2}\frac{1}{2}C^{(8)}_{qd}+$$
$$+(P_L)_{s_3s_2}(P_L)_{s_1s_4}\left(C^{(1)*}_{quqd}-\frac{1}{6}C^{(8)*}_{quqd}\right)+$$
$$+(P_R)_{s_3s_2}(P_R)_{s_1s_4}\left(C^{(1)}_{quqd}-\frac{1}{6}C^{(8)}_{quqd}\right)+$$
$$+(P_L)_{s_3s_4}(P_L)_{s_1s_2}\frac{1}{2}C^{(8)*}_{quqd}+(P_R)_{s_3s_4}(P_R)_{s_1s_2}\frac{1}{2}C^{(8)}_{quqd}\Bigg) \qquad (4.62)$$

and

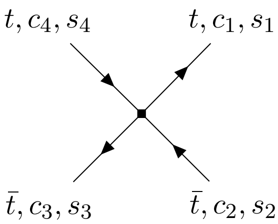

$$\equiv V^{(t)}_{c_1c_2c_3c_4s_1s_2s_3s_4}\equiv V^{(t,1)}_{s_1s_2s_3s_4}\delta_{c_3c_4}\delta_{c_1c_2}+V^{(t,2)}_{s_1s_2s_3s_4}\delta_{c_3c_2}\delta_{c_4c_1}=$$

$$=i\delta_{c_3c_4}\delta_{c_1c_2}\Bigg((\gamma_\alpha P_L)_{s_3s_4}(\gamma^\alpha P_L)_{s_1s_2}\left(2C^{(1)}_{qq}+2C^{(3)}_{qq}\right)+$$
$$+(\gamma_\alpha P_R)_{s_3s_4}(\gamma^\alpha P_R)_{s_1s_2}2C_{uu}+$$
$$+(\gamma_\alpha P_L)_{s_3s_4}(\gamma^\alpha P_R)_{s_1s_2}\left(C^{(1)}_{qu}-\frac{1}{6}C^{(8)}_{qu}\right)+$$
$$+(\gamma_\alpha P_R)_{s_3s_4}(\gamma^\alpha P_L)_{s_1s_2}\left(C^{(1)}_{qu}-\frac{1}{6}C^{(8)}_{qu}\right)+$$
$$+(\gamma_\alpha P_L)_{s_3s_2}(\gamma^\alpha P_R)_{s_1s_4}\left(-\frac{1}{2}\right)C^{(8)}_{qu}+$$

$$
\begin{aligned}
&+(\gamma_\alpha P_R)_{s_3 s_2}(\gamma^\alpha P_L)_{s_1 s_4}\left(-\frac{1}{2}\right)C_{qu}^{(8)}\Bigg)+\\
+i\delta_{c_3c_2}\delta_{c_4c_1}\Bigg(&(\gamma_\alpha P_L)_{s_3 s_2}(\gamma^\alpha P_L)_{s_1 s_4}\left(-2C_{qq}^{(1)}-2C_{qq}^{(3)}\right)+\\
&+(\gamma_\alpha P_R)_{s_3 s_2}(\gamma^\alpha P_R)_{s_1 s_4}(-2)C_{uu}+\\
&+(\gamma_\alpha P_L)_{s_3 s_2}(\gamma^\alpha P_R)_{s_1 s_4}\left(-C_{qu}^{(1)}+\frac{1}{6}C_{qu}^{(8)}\right)+\\
&+(\gamma_\alpha P_R)_{s_3 s_2}(\gamma^\alpha P_L)_{s_1 s_4}\left(-C_{qu}^{(1)}+\frac{1}{6}C_{qu}^{(8)}\right)+\\
&+(\gamma_\alpha P_L)_{s_3 s_4}(\gamma^\alpha P_R)_{s_1 s_2}\frac{1}{2}C_{qu}^{(8)}+\\
&+(\gamma_\alpha P_R)_{s_3 s_4}(\gamma^\alpha P_L)_{s_1 s_2}\frac{1}{2}C_{qu}^{(8)}\Bigg)
\end{aligned}
\tag{4.63}
$$

Where we have suppressed the $1/\Lambda^2$ factors. The particle-anti-particle assignments are, of course, arbitrary and the Feynman rules were chosen such that we need to include an extra minus sign for each fermion loop irrespective of its index structure (trace or non-trace), see also [125].

The most obvious thing to do is to close the loop on one side resulting in a modified quark propagator

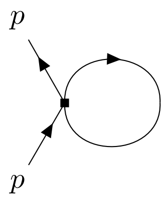

$$\equiv i\Sigma \tag{4.64}$$

It could replace the internal propagator of the t- and u-channel diagrams in the SM. However, since the loop does not depend on the external momentum p, the OS condition $\Sigma(p)+\delta=0$ leads to an exact cancellation by the counterterm δ, so these tadpole diagrams can be annihilated by their respective counterterms [8].

The next possibility is the attachment of one or two gluons to the closed loop resulting in modified three- and four-point functions. Adding one gluon gives the following modified quark-quark-gluon vertex (the incoming gluon g has colour A and the loop momenta are denoted by $\tilde{k}$ and $\tilde{p}$; of course, the latter are not independent of each other but rather depend on only one unconstrained loop momentum k)

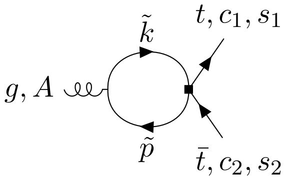

$$= -ig_sT^A_{c_1c_2}\Bigg(\int\frac{d^4k}{(2\pi)^4}\frac{V^{(b,2)}_{s_1s_2s_3s_4}\big((\tilde{\not{k}}+m_b)\gamma^\sigma(\tilde{\not{p}}+m_b)\big)_{s_4s_3}}{(\tilde{k}^2-m_b^2+i\eta)(\tilde{p}^2-m_b^2+i\eta)}+$$

$$+\int \frac{d^4k}{(2\pi)^4}\frac{V^{(t,2)}_{s_1s_2s_3s_4}\big((\tilde{\not k}+m_t)\gamma^\sigma(\tilde{\not p}+m_t)\big)_{s_4s_3}}{(\tilde{k}^2-m_t^2+i\eta)(\tilde{p}^2-m_t^2+i\eta)}\Bigg) \tag{4.65}$$

We will, as usual, drop the $i\eta$-terms from now on. The so-obtained modified quark-quark-gluon vertex thus does not depend on $V^{(b/t,1)}$.
Adding a second gluon yields two diagrams depending on the direction of the loop momentum (clockwise or anti-clockwise). The result is a modified quark-quark-gluon-gluon vertex which now depends on both $V^{(b/t,1)}$ and $V^{(b/t,2)}$. For the sake of notation, we focus on one of the two four-fermion vertices and drop the index b or t. We also suppress the Wilson coefficients as well as spinor indices and introduce Γ_1 and Γ_2 denoting a certain combination of left- and right-handed projectors appearing in the four-fermion vertices (e.g. $\Gamma_1=\gamma_\alpha P_R$, etc.). The expression $\Gamma_1(...)\Gamma_2$ is therefore a short notation for $\big(\Gamma_1(...)\Gamma_2\big)_{s_1s_2}$ or $Tr\big(\Gamma_1(...)\big)(\Gamma_2)_{s_1s_2}$ depending on the context. Let us also introduce the notation $\widetilde{\Gamma}$ denoting the parts of the four-fermion vertex appearing in $V^{(b/t,1)}$, whereas Γ refers to $V^{(b/t,2)}$. All in all, we find the following loop contributions

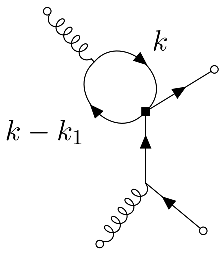

$$\equiv i\mathcal{M}^{(loops,1)}_{SMEFT}=g_s^2(T^BT^C)_{c_1c_2}\cdot$$

$$\cdot\,\bar{u}\Bigg(\int\frac{d^4k}{(2\pi)^4}\frac{\Gamma_1(\not k+m)\gamma^\mu(\not k-\not k_1+m)\Gamma_2}{(k^2-m^2)((k-k_1)^2-m^2)}\frac{\not k_2-\not p_2+m_t}{-2p_2\cdot k_2}\gamma^\nu\Bigg)v\epsilon_\mu\epsilon_\nu \tag{4.66}$$

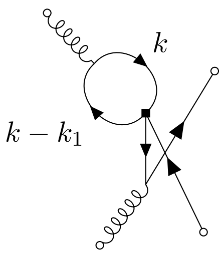

$$\equiv i\mathcal{M}^{(loops,2)}_{SMEFT}=g_s^2(T^CT^B)_{c_1c_2}\cdot$$

$$\cdot\,\bar{u}\Bigg(\gamma^\nu\frac{\not p_1-\not k_2+m_t}{-2p_1\cdot k_2}\int\frac{d^4k}{(2\pi)^4}\frac{\Gamma_1(\not k+m)\gamma^\mu(\not k-\not k_1+m)\Gamma_2}{(k^2-m^2)((k-k_1)^2-m^2)}\Bigg)v\epsilon_\mu\epsilon_\nu \tag{4.67}$$

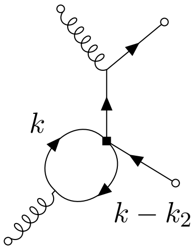

$$\equiv i\mathcal{M}^{(loops,3)}_{SMEFT} = g_s^2 (T^B T^C)_{c_1 c_2} \cdot$$

$$\cdot\, \bar{u}\left(\gamma^\mu \frac{\not{p}_1 - \not{k}_1 + m_t}{-2p_1 \cdot k_1} \int \frac{d^4k}{(2\pi)^4} \frac{\Gamma_1(\not{k}+m)\gamma^\nu(\not{k}-\not{k}_2+m)\Gamma_2}{(k^2-m^2)((k-k_2)^2-m^2)}\right) v \epsilon_\mu \epsilon_\nu \tag{4.68}$$

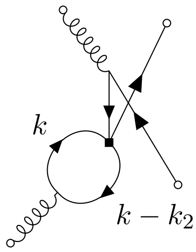

$$\equiv i\mathcal{M}^{(loops,4)}_{SMEFT} = g_s^2 (T^C T^B)_{c_1 c_2} \cdot$$

$$\cdot\, \bar{u}\left(\int \frac{d^4k}{(2\pi)^4} \frac{\Gamma_1(\not{k}+m)\gamma^\nu(\not{k}-\not{k}_2+m)\Gamma_2}{(k^2-m^2)((k-k_2)^2-m^2)} \frac{\not{k}_1 - \not{p}_2 + m_t}{-2p_2 \cdot k_1} \gamma^\mu\right) v \epsilon_\mu \epsilon_\nu \tag{4.69}$$

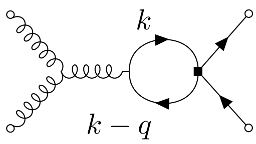

$$\equiv i\mathcal{M}^{(loops,5)}_{SMEFT} = i g_s^2 f^{ABC} T^A_{c_1 c_2} \frac{1}{q^2}\left(2k_2^\mu g^{\sigma\nu} + g^{\mu\nu}(k_1-k_2)^\sigma - 2k_1^\nu g^{\sigma\mu}\right) \cdot$$

$$\cdot\, \bar{u}\left(\int \frac{d^4k}{(2\pi)^4} \frac{\Gamma_1(\not{k}+m)\gamma_\sigma(\not{k}-\not{q}+m)\Gamma_2}{(k^2-m^2)((k-q)^2-m^2)}\right) v \epsilon_\mu \epsilon_\nu \tag{4.70}$$

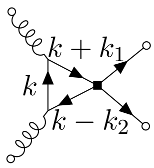

$$\equiv i\mathcal{M}^{(loops,6)}_{SMEFT} =$$

$$\begin{aligned} =& g_s^2 (T^B T^C)_{c_1 c_2} \bar{u}\left(\int \frac{d^4k}{(2\pi)^4} \frac{\Gamma_1(\not{k}+\not{k}_1+m)\gamma^\mu(\not{k}+m)\gamma^\nu(\not{k}-\not{k}_2+m)\Gamma_2}{(k^2-m^2)((k+k_1)^2-m^2)((k-k_2)^2-m^2)}\right) v \epsilon_\mu \epsilon_\nu + \\ +& g_s^2 Tr(T^B T^C)\delta_{c_1 c_2} \bar{u}\left(\int \frac{d^4k}{(2\pi)^4} \frac{\widetilde{\Gamma}_1(\not{k}+\not{k}_1+m)\gamma^\mu(\not{k}+m)\gamma^\nu(\not{k}-\not{k}_2+m)\widetilde{\Gamma}_2}{(k^2-m^2)((k+k_1)^2-m^2)((k-k_2)^2-m^2)}\right) v \epsilon_\mu \epsilon_\nu \end{aligned} \tag{4.71}$$

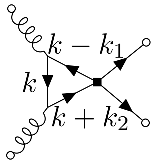

$$\equiv i\mathcal{M}^{(loops,7)}_{SMEFT} =$$

$$
\begin{aligned}
=&g_s^2(T^CT^B)_{c_1c_2}\bar{u}\left(\int\frac{d^4k}{(2\pi)^4}\frac{\Gamma_1(\not{k}+\not{k}_2+m)\gamma^\nu(\not{k}+m)\gamma^\mu(\not{k}-\not{k}_1+m)\Gamma_2}{(k^2-m^2)((k+k_2)^2-m^2)((k-k_1)^2-m^2)}\right)v\epsilon_\mu\epsilon_\nu+\\
+&g_s^2Tr(T^BT^C)\delta_{c_1c_2}\bar{u}\left(\int\frac{d^4k}{(2\pi)^4}\frac{\widetilde{\Gamma}_1(\not{k}+\not{k}_2+m)\gamma^\nu(\not{k}+m)\gamma^\mu(\not{k}-\not{k}_1+m)\widetilde{\Gamma}_2}{(k^2-m^2)((k+k_2)^2-m^2)((k-k_1)^2-m^2)}\right)v\epsilon_\mu\epsilon_\nu
\end{aligned}
\tag{4.72}
$$

Before we go on with the explicit calculation of the loop functions, in order to be sure not to miss any contributions, we should superficially check the gauge invariance of the sum of these amplitudes, i.e. the Ward identity. This can be done by letting $\epsilon_\mu \longrightarrow k_{1\mu}$ (the analysis for $\epsilon_\nu \longrightarrow k_{2\nu}$ works analogously). We find

$$
\begin{aligned}
i\mathcal{M}^{(loops,1)}_{SMEFT} \rightarrow &g_s^2(T^BT^C)_{c_1c_2}\bar{u}\left(\left(\int\frac{d^4k}{(2\pi)^4}\frac{\Gamma_1(\not{k}-\not{k}_1+m)\Gamma_2}{((k-k_1)^2-m^2)}+\right.\right.\\
&\left.\left.-\frac{\Gamma_1(\not{k}+m)\Gamma_2}{(k^2-m^2)}\right)\frac{\not{k}_2-\not{p}_2+m_t}{-2p_2\cdot k_2}\gamma^\nu\right)v\epsilon_\nu
\end{aligned}
\tag{4.73}
$$

$$
\begin{aligned}
i\mathcal{M}^{(loops,2)}_{SMEFT} \rightarrow &g_s^2(T^CT^B)_{c_1c_2}\bar{u}\left(\gamma^\nu\frac{\not{p}_1-\not{k}_2+m_t}{-2p_1\cdot k_2}\left(\int\frac{d^4k}{(2\pi)^4}\frac{\Gamma_1(\not{k}-\not{k}_1+m)\Gamma_2}{((k-k_1)^2-m^2)}+\right.\right.\\
&\left.\left.-\frac{\Gamma_1(\not{k}+m)\Gamma_2}{(k^2-m^2)}\right)\right)v\epsilon_\nu
\end{aligned}
\tag{4.74}
$$

$$i\mathcal{M}^{(loops,3)}_{SMEFT} \rightarrow -g_s^2(T^BT^C)_{c_1c_2}\bar{u}\left(\int\frac{d^4k}{(2\pi)^4}\frac{\Gamma_1(\not{k}+m)\gamma^\nu(\not{k}-\not{k}_2+m)\Gamma_2}{(k^2-m^2)((k-k_2)^2-m^2)}\right)v\epsilon_\nu \tag{4.75}$$

$$i\mathcal{M}^{(loops,4)}_{SMEFT} \rightarrow g_s^2(T^CT^B)_{c_1c_2}\bar{u}\left(\int\frac{d^4k}{(2\pi)^4}\frac{\Gamma_1(\not{k}+m)\gamma^\nu(\not{k}-\not{k}_2+m)\Gamma_2}{(k^2-m^2)((k-k_2)^2-m^2)}\right)v\epsilon_\nu \tag{4.76}$$

$$i\mathcal{M}^{(loops,5)}_{SMEFT} \rightarrow ig_s^2f^{ABC}T^A_{c_1c_2}\bar{u}\left(\int\frac{d^4k}{(2\pi)^4}\frac{\Gamma_1(\not{k}+m)\gamma^\nu(\not{k}-\not{q}+m)\Gamma_2}{(k^2-m^2)((k-q)^2-m^2)}\right)v\epsilon_\nu+ \tag{4.77}$$

$$-ig_s^2f^{ABC}T^A_{c_1c_2}\bar{u}\left(\int\frac{d^4k}{(2\pi)^4}\frac{\Gamma_1(\not{k}-\not{q}+m)\Gamma_2}{((k-q)^2-m^2)}-\frac{\Gamma_1(\not{k}+m)\Gamma_2}{(k^2-m^2)}\right)v\epsilon_\nu \tag{4.78}$$

$$i\mathcal{M}^{(loops,6)}_{SMEFT} \rightarrow g_s^2(T^BT^C)_{c_1c_2}\bar{u}\left(\int\frac{d^4k}{(2\pi)^4}\frac{\Gamma_1(\not{k}+m)\gamma^\nu(\not{k}-\not{k}_2+m)\Gamma_2}{(k^2-m^2)((k-k_2)^2-m^2)}\right)v\epsilon_\nu+ \tag{4.79}$$

$$-g_s^2(T^BT^C)_{c_1c_2}\bar{u}\left(\int\frac{d^4k}{(2\pi)^4}\frac{\Gamma_1(\not{k}+\not{k}_1+m)\gamma^\nu(\not{k}-\not{k}_2+m)\Gamma_2}{((k+k_1)^2-m^2)((k-k_2)^2-m^2)}\right)v\epsilon_\nu+ \tag{4.80}$$

$$+g_s^2Tr(T^BT^C)\delta_{c_1c_2}\bar{u}\left(\int\frac{d^4k}{(2\pi)^4}\frac{\widetilde{\Gamma}_1(\not{k}+m)\gamma^\nu(\not{k}-\not{k}_2+m)\widetilde{\Gamma}_2}{(k^2-m^2)((k-k_2)^2-m^2)}\right)v\epsilon_\nu+ \tag{4.81}$$

$$-g_s^2 Tr(T^B T^C)\delta_{c_1c_2}\bar{u}\left(\int \frac{d^4k}{(2\pi)^4}\frac{\widetilde{\Gamma}_1(\not{k}+\not{k}_1+m)\gamma^\nu(\not{k}-\not{k}_2+m)\widetilde{\Gamma}_2}{((k+k_1)^2-m^2)((k-k_2)^2-m^2)}\right)v\epsilon_\nu \tag{4.82}$$

$$i\mathcal{M}_{SMEFT}^{(loops,7)} \to g_s^2(T^C T^B)_{c_1c_2}\bar{u}\left(\int \frac{d^4k}{(2\pi)^4}\frac{\Gamma_1(\not{k}+\not{k}_2+m)\gamma^\nu(\not{k}-\not{k}_1+m)\Gamma_2}{((k+k_2)^2-m^2)((k-k_1)^2-m^2)}\right)v\epsilon_\nu + \tag{4.83}$$

$$-g_s^2(T^C T^B)_{c_1c_2}\bar{u}\left(\int \frac{d^4k}{(2\pi)^4}\frac{\Gamma_1(\not{k}+\not{k}_2+m)\gamma^\nu(\not{k}+m)\Gamma_2}{((k+k_2)^2-m^2)(k^2-m^2)}\right)v\epsilon_\nu + \tag{4.84}$$

$$+g_s^2 Tr(T^B T^C)\delta_{c_1c_2}\bar{u}\left(\int \frac{d^4k}{(2\pi)^4}\frac{\widetilde{\Gamma}_1(\not{k}+\not{k}_2+m)\gamma^\nu(\not{k}-\not{k}_1+m)\widetilde{\Gamma}_2}{((k+k_2)^2-m^2)((k-k_1)^2-m^2)}\right)v\epsilon_\nu + \tag{4.85}$$

$$-g_s^2 Tr(T^B T^C)\delta_{c_1c_2}\bar{u}\left(\int \frac{d^4k}{(2\pi)^4}\frac{\widetilde{\Gamma}_1(\not{k}+\not{k}_2+m)\gamma^\nu(\not{k}+m)\widetilde{\Gamma}_2}{((k+k_2)^2-m^2)(k^2-m^2)}\right)v\epsilon_\nu \tag{4.86}$$

The cancellation pattern then works as follows:

$$\begin{aligned}
(4.73), (4.74), (4.78) &\longrightarrow 0\\
(4.75) &\longleftrightarrow (4.79)\\
(4.76) &\longleftrightarrow (4.84)\\
(4.77) &\longleftrightarrow (4.80), (4.83)\\
(4.81) &\longleftrightarrow (4.86)\\
(4.82) &\longleftrightarrow (4.85)
\end{aligned}$$

The Ward identity therefore seems to be fulfilled, at least at first sight. In order to perform these various cancellations, however, it is necessary to shift loop momenta. This is actually not a valid manipulation as the four-fermion vertex structure denoted by Γ_1, etc. contains γ^5 forcing us to work strictly in four dimensions where bubble- and triangular diagrams are quadratically and linearly divergent, respectively. Shifting integration variables could therefore introduce non-vanishing boundary terms. We will nonetheless apply dimensional regularization with a naïve prescription for γ^5, i.e. with anti commuting γ^5 [126]. In particular, the formula $Tr(\gamma^\mu\gamma^\nu\gamma^\alpha\gamma^\beta\gamma^5) = -4i\epsilon^{\mu\nu\alpha\beta}$ continues to hold in $d \neq 4$ dimensions[39]. In Appendix F, we show an explicit example calculation of how this affects the triangle diagrams. Further comments can be found in [127–134].
As usual, we define $d = 4-2\epsilon$ and let $\int \frac{d^4k}{(2\pi)^4} \longrightarrow \mu^{2\epsilon}\int \frac{d^dk}{(2\pi)^d}$, where μ is the usual renormalization (more precise: regularization) scale. The final result should unambiguously be defined by being finite, renormalization scale independent and gauge invariant, i.e. obeying the Ward identity. We will actually leave Γ_1, etc. open and adjust them to the respective cases afterwards. As shown above, this guarantees the Ward identity to be fulfilled at every intermediate step of the calculation.

[39] This is the same convention used in FeynCalc [92].

The straightforward computation of the respective diagrams leads to

$$i\mathcal{M}_{SMEFT}^{(loops,1)} = g_s^2 (T^B T^C)_{c_1 c_2} \frac{i}{16\pi^2} \left(\frac{1}{\epsilon} + \ln\frac{4\pi}{e^\gamma} + \ln\frac{\mu^2}{m^2} \right) \cdot \cdot \bar{u} \Big(\Gamma_1 m i \sigma^{\mu\alpha} k_{1\alpha} \Gamma_2 \frac{\not{k}_2 - \not{p}_2 + m_t}{-2p_2 \cdot k_2} \gamma^\nu \Big) v \epsilon_\mu \epsilon_\nu \quad (4.87)$$

$$i\mathcal{M}_{SMEFT}^{(loops,2)} = g_s^2 (T^C T^B)_{c_1 c_2} \frac{i}{16\pi^2} \left(\frac{1}{\epsilon} + \ln\frac{4\pi}{e^\gamma} + \ln\frac{\mu^2}{m^2} \right) \cdot \cdot \bar{u} \Big(\gamma^\nu \frac{\not{p}_1 - \not{k}_2 + m_t}{-2p_1 \cdot k_2} \Gamma_1 m i \sigma^{\mu\alpha} k_{1\alpha} \Gamma_2 \Big) v \epsilon_\mu \epsilon_\nu \quad (4.88)$$

$$i\mathcal{M}_{SMEFT}^{(loops,3)} = g_s^2 (T^B T^C)_{c_1 c_2} \frac{i}{16\pi^2} \left(\frac{1}{\epsilon} + \ln\frac{4\pi}{e^\gamma} + \ln\frac{\mu^2}{m^2} \right) \cdot \cdot \bar{u} \Big(\gamma^\mu \frac{\not{p}_1 - \not{k}_1 + m_t}{-2p_1 \cdot k_1} \Gamma_1 m i \sigma^{\nu\alpha} k_{2\alpha} \Gamma_2 \Big) v \epsilon_\mu \epsilon_\nu \quad (4.89)$$

$$i\mathcal{M}_{SMEFT}^{(loops,4)} = g_s^2 (T^C T^B)_{c_1 c_2} \frac{i}{16\pi^2} \left(\frac{1}{\epsilon} + \ln\frac{4\pi}{e^\gamma} + \ln\frac{\mu^2}{m^2} \right) \cdot \cdot \bar{u} \Big(\Gamma_1 m i \sigma^{\nu\alpha} k_{2\alpha} \Gamma_2 \frac{\not{k}_1 - \not{p}_2 + m_t}{-2p_2 \cdot k_1} \gamma^\mu \Big) v \epsilon_\mu \epsilon_\nu \quad (4.90)$$

$$i\mathcal{M}_{SMEFT}^{(loops,5)} = g_s^2 i f^{ABC} T^A_{c_1 c_2} \frac{i}{16\pi^2} \frac{1}{q^2} \big(2k_2^\mu g^{\sigma\nu} + g^{\mu\nu}(k_1 - k_2)^\sigma - 2k_1^\nu g^{\sigma\mu} \big) \cdot \cdot \bar{u}\Gamma_1 \left(\left(\frac{1}{\epsilon} + \ln\frac{4\pi}{e^\gamma} + \ln\frac{\mu^2}{m^2} \right) \left(\frac{1}{3} q^2 \gamma_\sigma + m i \sigma_{\sigma\alpha} q^\alpha \right) + X_1 q^2 \gamma_\sigma + X_2 m i \sigma_{\sigma\alpha} q^\alpha \right) \Gamma_2 v \epsilon_\mu \epsilon_\nu \quad (4.91)$$

$$\begin{aligned} i\mathcal{M}_{SMEFT}^{(loops,6)} = & g_s^2 (T^B T^C)_{c_1 c_2} \frac{i}{16\pi^2} \bar{u}\Gamma_1 \left(\left(\frac{1}{\epsilon} + \ln\frac{4\pi}{e^\gamma} + \ln\frac{\mu^2}{m^2} \right) \Big(m i \sigma^{\mu\nu} + \frac{1}{3}(\not{k}_2 - \not{k}_1) g^{\mu\nu} + \right. \\ & + \frac{2}{3}(k_1^\nu \gamma^\mu - k_2^\mu \gamma^\nu) \Big) + S_1 m i \sigma^{\mu\nu} + S_2 i\gamma^5 \gamma_\lambda \epsilon^{\lambda\mu\nu\alpha} k_{1\alpha} + S_3 i\gamma^5 \gamma_\lambda \epsilon^{\lambda\mu\nu\alpha} k_{2\alpha} + \\ & + S_4 g^{\mu\nu} \not{k}_1 + S_5 g^{\mu\nu} \not{k}_2 + S_6 k_1^\nu \gamma^\mu + S_7 k_2^\mu \gamma^\nu + \\ & + S_8 m g^{\mu\nu} + S_9 \frac{1}{m} k_1^\nu k_2^\mu + S_{10} \frac{1}{m^2} k_1^\nu k_2^\mu \not{k}_1 + S_{11} \frac{1}{m^2} k_1^\nu k_2^\mu \not{k}_2 + S_{12} \frac{1}{m} i\sigma^{\alpha\mu} k_{1\alpha} k_1^\nu + \\ & + S_{13} \frac{1}{m} i\sigma^{\alpha\nu} k_{2\alpha} k_2^\mu + S_{14} \frac{1}{m} i\sigma^{\alpha\mu} k_{2\alpha} k_1^\nu + S_{15} \frac{1}{m} i\sigma^{\alpha\nu} k_{1\alpha} k_2^\mu + \\ & + S_{16} \frac{1}{m^2} i\gamma^5 \gamma_\lambda \epsilon^{\lambda\alpha\beta\mu} k_{1\alpha} k_{2\beta} k_1^\nu + S_{17} \frac{1}{m^2} i\gamma^5 \gamma_\lambda \epsilon^{\lambda\alpha\beta\nu} k_{1\alpha} k_{2\beta} k_2^\mu + \\ & + S_{18} \frac{1}{m} i\sigma^{\alpha\beta} k_{1\alpha} k_{2\beta} g^{\mu\nu} + S_{19} \frac{\not{k}_1}{m^2} i\gamma^5 \epsilon^{\alpha\beta\mu\nu} k_{1\alpha} k_{2\beta} + \\ & \left. + S_{20} \frac{\not{k}_2}{m^2} i\gamma^5 \epsilon^{\alpha\beta\mu\nu} k_{1\alpha} k_{2\beta} + S_{21} \frac{1}{m} i\gamma^5 \epsilon^{\alpha\beta\mu\nu} k_{1\alpha} k_{2\beta} \right) \Gamma_2 v \epsilon_\mu \epsilon_\nu + \end{aligned}$$

$$+g_s^2 Tr(T^B T^C)\delta_{c_1c_2}\frac{i}{16\pi^2}\bar{u}\widetilde{\Gamma}_1\Bigg(\text{same expression}\Bigg)\widetilde{\Gamma}_2 v\epsilon_\mu\epsilon_\nu \quad (4.92)$$

$$\begin{aligned}
i\mathcal{M}_{SMEFT}^{(loops,7)} =& g_s^2(T^C T^B)_{c_1c_2}\frac{i}{16\pi^2}\bar{u}\Gamma_1\Bigg(\Bigg(\frac{1}{\epsilon}+\ln\frac{4\pi}{e^\gamma}+\ln\frac{\mu^2}{m^2}\Bigg)\Bigg(mi\sigma^{\nu\mu}+\frac{1}{3}(\not{k}_1-\not{k}_2)g^{\mu\nu}+\\
&+\frac{2}{3}(k_2^\mu\gamma^\nu-k_1^\nu\gamma^\mu)\Bigg)+S_1 mi\sigma^{\nu\mu}+S_2 i\gamma^5\gamma_\lambda\epsilon^{\lambda\nu\mu\alpha}k_{2\alpha}+S_3 i\gamma^5\gamma_\lambda\epsilon^{\lambda\nu\mu\alpha}k_{1\alpha}+\\
&+S_4 g^{\mu\nu}\not{k}_2+S_5 g^{\mu\nu}\not{k}_1+S_6 k_2^\mu\gamma^\nu+S_7 k_1^\nu\gamma^\mu+\\
&+S_8 m g^{\mu\nu}+S_9\frac{1}{m}k_2^\mu k_1^\nu+S_{10}\frac{1}{m^2}k_2^\mu k_1^\nu\not{k}_2+S_{11}\frac{1}{m^2}k_2^\mu k_1^\nu\not{k}_1+S_{12}\frac{1}{m}i\sigma^{\alpha\nu}k_{2\alpha}k_2^\mu+\\
&+S_{13}\frac{1}{m}i\sigma^{\alpha\mu}k_{1\alpha}k_1^\nu+S_{14}\frac{1}{m}i\sigma^{\alpha\nu}k_{1\alpha}k_2^\mu+S_{15}\frac{1}{m}i\sigma^{\alpha\mu}k_{2\alpha}k_1^\nu+\\
&+S_{16}\frac{1}{m^2}i\gamma^5\gamma_\lambda\epsilon^{\lambda\alpha\beta\nu}k_{2\alpha}k_{1\beta}k_2^\mu+S_{17}\frac{1}{m^2}i\gamma^5\gamma_\lambda\epsilon^{\lambda\alpha\beta\mu}k_{2\alpha}k_{1\beta}k_1^\nu+\\
&+S_{18}\frac{1}{m}i\sigma^{\alpha\beta}k_{2\alpha}k_{1\beta}g^{\mu\nu}+S_{19}\frac{\not{k}_2}{m^2}i\gamma^5\epsilon^{\alpha\beta\nu\mu}k_{2\alpha}k_{1\beta}+\\
&+S_{20}\frac{\not{k}_1}{m^2}i\gamma^5\epsilon^{\alpha\beta\nu\mu}k_{2\alpha}k_{1\beta}+S_{21}\frac{1}{m}i\gamma^5\epsilon^{\alpha\beta\nu\mu}k_{2\alpha}k_{1\beta}\Bigg)\Gamma_2 v\epsilon_\mu\epsilon_\nu+\\
&+g_s^2 Tr(T^B T^C)\delta_{c_1c_2}\frac{i}{16\pi^2}\bar{u}\widetilde{\Gamma}_1\Bigg(\text{same expression}\Bigg)\widetilde{\Gamma}_2 v\epsilon_\mu\epsilon_\nu
\end{aligned} \quad (4.93)$$

The short notations for non-trivial Feynman parameter integrals (X are the bubbles, S the triangles) are defined by

$$X_1 \equiv -\int_0^1 dx\; 2x(1-x)\ln\left(1-2x(1-x)\frac{k_1\cdot k_2}{m^2}\right) \quad (4.94)$$

$$X_2 \equiv -\int_0^1 dx\ln\left(1-2x(1-x)\frac{k_1\cdot k_2}{m^2}\right) \quad (4.95)$$

$$\begin{aligned}
S_1 \equiv& -\frac{1}{2}-2\int_0^1 dz\int_0^{1-z}dy\ln\left(1-2yz\frac{k_1\cdot k_2}{m^2}\right)+\\
&+\int_0^1 dz\int_0^{1-z}dy\frac{1+(2yz-1)\frac{k_1\cdot k_2}{m^2}}{1-2yz\frac{k_1\cdot k_2}{m^2}}
\end{aligned} \quad (4.96)$$

$$\begin{aligned}
S_2 \equiv& \frac{1}{3}+\int_0^1 dz\int_0^{1-z}dy(1-3y)\ln\left(1-2yz\frac{k_1\cdot k_2}{m^2}\right)+\\
&+\int_0^1 dz\int_0^{1-z}dy\frac{(y-1)+y(y-1)(2z-1)\frac{k_1\cdot k_2}{m^2}}{1-2yz\frac{k_1\cdot k_2}{m^2}}
\end{aligned} \quad (4.97)$$

$$S_3 \equiv -\frac{1}{3}-\int_0^1 dz\int_0^{1-z}dy(1-3z)\ln\left(1-2yz\frac{k_1\cdot k_2}{m^2}\right)+$$

$$- \int_0^1 dz \int_0^{1-z} dy \frac{(z-1) + yz(2z-1)\frac{k_1\cdot k_2}{m^2}}{1-2yz\frac{k_1\cdot k_2}{m^2}} \tag{4.98}$$

$$S_4 \equiv \frac{1}{3} + \int_0^1 dz \int_0^{1-z} dy (1-y) \ln\left(1 - 2yz\frac{k_1 \cdot k_2}{m^2}\right) +$$

$$+ \int_0^1 dz \int_0^{1-z} dy \frac{(y-1) + 2yz(y-1)\frac{k_1\cdot k_2}{m^2}}{1-2yz\frac{k_1\cdot k_2}{m^2}} \tag{4.99}$$

$$S_5 \equiv -\frac{1}{3} - \int_0^1 dz \int_0^{1-z} dy (1-z) \ln\left(1 - 2yz\frac{k_1 \cdot k_2}{m^2}\right) +$$

$$- \int_0^1 dz \int_0^{1-z} dy \frac{(z-1) + 2yz(z-1)\frac{k_1\cdot k_2}{m^2}}{1-2yz\frac{k_1\cdot k_2}{m^2}} \tag{4.100}$$

$$S_6 \equiv -\frac{2}{3} - \int_0^1 dz \int_0^{1-z} dy (1+y) \ln\left(1 - 2yz\frac{k_1 \cdot k_2}{m^2}\right) +$$

$$+ \int_0^1 dz \int_0^{1-z} dy \frac{(y+1) + 2y^2z\frac{k_1\cdot k_2}{m^2}}{1-2yz\frac{k_1\cdot k_2}{m^2}} \tag{4.101}$$

$$S_7 \equiv \frac{2}{3} + \int_0^1 dz \int_0^{1-z} dy (1+z) \ln\left(1 - 2yz\frac{k_1 \cdot k_2}{m^2}\right) +$$

$$- \int_0^1 dz \int_0^{1-z} dy \frac{(z+1) + 2yz^2\frac{k_1\cdot k_2}{m^2}}{1-2yz\frac{k_1\cdot k_2}{m^2}} \tag{4.102}$$

$$S_8 \equiv \frac{1}{2} - \int_0^1 dz \int_0^{1-z} dy \frac{1 + (2yz-1)\frac{k_1\cdot k_2}{m^2}}{1-2yz\frac{k_1\cdot k_2}{m^2}}, \; S_9 \equiv \int_0^1 dz \int_0^{1-z} dy \frac{4yz-1}{1-2yz\frac{k_1\cdot k_2}{m^2}} \tag{4.103}$$

$$S_{10} \equiv \int_0^1 dz \int_0^{1-z} dy \frac{2yz(1-2y)}{1-2yz\frac{k_1\cdot k_2}{m^2}}, \; S_{11} \equiv -\int_0^1 dz \int_0^{1-z} dy \frac{2yz(1-2z)}{1-2yz\frac{k_1\cdot k_2}{m^2}} \tag{4.104}$$

$$S_{12} \equiv -\int_0^1 dz \int_0^{1-z} dy \frac{2y}{1-2yz\frac{k_1\cdot k_2}{m^2}}, \; S_{13} \equiv \int_0^1 dz \int_0^{1-z} dy \frac{2z}{1-2yz\frac{k_1\cdot k_2}{m^2}} \tag{4.105}$$

$$S_{14} \equiv -\int_0^1 dz \int_0^{1-z} dy \frac{1}{1-2yz\frac{k_1\cdot k_2}{m^2}}, \; S_{15} \equiv \int_0^1 dz \int_0^{1-z} dy \frac{1}{1-2yz\frac{k_1\cdot k_2}{m^2}} \tag{4.106}$$

$$S_{16} \equiv -\int_0^1 dz \int_0^{1-z} dy \frac{y(y+2z-1)}{1-2yz\frac{k_1\cdot k_2}{m^2}}, \; S_{17} \equiv \int_0^1 dz \int_0^{1-z} dy \frac{yz}{1-2yz\frac{k_1\cdot k_2}{m^2}} \tag{4.107}$$

$$S_{18} \equiv -\int_0^1 dz \int_0^{1-z} dy \frac{1}{1-2yz\frac{k_1\cdot k_2}{m^2}}, \; S_{19} \equiv -\int_0^1 dz \int_0^{1-z} dy \frac{y(1-y)}{1-2yz\frac{k_1\cdot k_2}{m^2}} \tag{4.108}$$

$$S_{20} \equiv -\int_0^1 dz \int_0^{1-z} dy \frac{yz}{1-2yz\frac{k_1\cdot k_2}{m^2}}, \; S_{21} = -\int_0^1 dz \int_0^{1-z} dy \frac{1}{1-2yz\frac{k_1\cdot k_2}{m^2}} \tag{4.109}$$

Note that these expressions can always be modified using the identities

$$\int_0^1 dz \int_0^{1-z} dy \; f(y,z) = \int_0^1 dz \int_0^{1-z} dy \; f(z,y) = \int_0^1 dx \int_0^{1-x} dy \; f(y, 1-x-y) =$$

$$= \int_0^1 dw \int_0^1 d\xi \ wf(w - w\xi, w\xi) = \int_0^1 dw \int_0^1 d\xi \ wf(1-w, w\xi) \tag{4.110}$$

It is obvious that our presentation contains a horrendous amount of redundancy. Indeed, numerically evaluating the integrals as functions of $\frac{k_1 \cdot k_2}{m^2}$ leads to the following relations[40]

$$S_{14} = -S_{15} = S_{18} = S_{21} = S_9 - 4S_{17}, \quad S_4 = -S_5 = -X_1 - \frac{k_1 \cdot k_2}{m^2} S_{10}, \tag{4.111}$$

$$S_6 = -S_7 = 2X_1, \quad S_{10} = -S_{11}, \quad S_{12} = -S_{13}, \tag{4.112}$$

$$S_{17} = -S_{20} = -\frac{1}{2}\left(S_{16} + S_{19}\right), \tag{4.113}$$

$$S_2 = \frac{k_1 \cdot k_2}{m^2} S_{16}, \quad S_3 = \frac{k_1 \cdot k_2}{m^2} S_{17}, \quad S_8 = -\frac{k_1 \cdot k_2}{m^2} S_9, \tag{4.114}$$

$$S_1 - \frac{k_1 \cdot k_2}{m^2} S_{14} = -\frac{k_1 \cdot k_2}{m^2} S_{12} = X_2 \tag{4.115}$$

With a minimal set of structure functions (we chooseX_1, X_2, S_9, S_{10} and S_{17}; let us also keep S_{14} for notational clarity, remembering that it actually equals $S_9 - 4S_{17}$) and using $g^{\alpha\beta}\epsilon^{\mu\nu\lambda\rho} = g^{\alpha\mu}\epsilon^{\beta\nu\lambda\rho} - g^{\alpha\nu}\epsilon^{\beta\mu\lambda\rho} + g^{\alpha\lambda}\epsilon^{\beta\mu\nu\rho} - g^{\alpha\rho}\epsilon^{\beta\mu\nu\lambda}$, the sum of the triangle diagrams is given by

$$\begin{aligned}
& i\mathcal{M}^{(loops,6)}_{SMEFT} + i\mathcal{M}^{(loops,7)}_{SMEFT} = \\
&= g_s^2 i f^{ABC} T^A_{c_1 c_2} \frac{i}{16\pi^2} \bar{u}\Gamma_1 \Bigg(\left(\frac{1}{\epsilon} + \ln\frac{4\pi}{e^\gamma} + \ln\frac{\mu^2}{m^2} \right) \cdot \\
&\qquad \cdot \left(m i\sigma^{\mu\nu} + \frac{1}{3}(\not{k}_2 - \not{k}_1) g^{\mu\nu} + \frac{2}{3}(k_1^\nu \gamma^\mu - k_2^\mu \gamma^\nu) \right) + \\
&\quad + X_1 \Big(2k_1^\nu \gamma^\mu - 2k_2^\mu \gamma^\nu + g^{\mu\nu}(\not{k}_2 - \not{k}_1) \Big) + \\
&\quad + X_2 \frac{m}{k_1 \cdot k_2} \Big((k_1 \cdot k_2) i\sigma^{\mu\nu} + i\sigma^{\alpha\nu} k_{2\alpha} k_2^\mu - i\sigma^{\alpha\mu} k_{1\alpha} k_1^\nu \Big) + \\
&\quad + S_{10} \frac{1}{m^2} (\not{k}_1 - \not{k}_2) \Big(k_1^\nu k_2^\mu - (k_1 \cdot k_2) g^{\mu\nu} \Big) + \\
&\quad + S_{14} \frac{1}{m} \Big((k_1 \cdot k_2) i\sigma^{\mu\nu} + i\sigma^{\alpha\mu} k_{2\alpha} k_1^\nu - i\sigma^{\alpha\nu} k_{1\alpha} k_2^\mu + i\sigma^{\alpha\beta} k_{1\alpha} k_{2\beta} g^{\mu\nu} \Big) \Bigg) \Gamma_2 v \epsilon_\mu \epsilon_\nu + \\
&+ g_s^2 \{T^B, T^C\}_{c_1 c_2} \frac{i}{16\pi^2} \bar{u}\Gamma_1 \Bigg(S_9 \frac{1}{m} \Big(k_1^\nu k_2^\mu - (k_1 \cdot k_2) g^{\mu\nu} \Big) + S_{14} \frac{1}{m} i\gamma^5 \epsilon^{\alpha\beta\mu\nu} k_{1\alpha} k_{2\beta} + \\
&\quad + 2S_{17} \frac{1}{m^2} \Big((k_1 \cdot k_2) i\gamma^5 \gamma_\lambda \epsilon^{\lambda\alpha\mu\nu} (k_2 - k_1)_\alpha - i\gamma^5 \gamma_\lambda \epsilon^{\lambda\alpha\beta\mu} k_{1\alpha} k_{2\beta} k_1^\nu + \\
&\quad + i\gamma^5 \gamma_\lambda \epsilon^{\lambda\alpha\beta\nu} k_{1\alpha} k_{2\beta} k_2^\mu \Big) \Bigg) \Gamma_2 v \epsilon_\mu \epsilon_\nu + \\
&+ g_s^2 Tr(T^B T^C) \delta_{c_1 c_2} \frac{i}{16\pi^2} \bar{u}\widetilde{\Gamma}_1 \Bigg(2S_9 \frac{1}{m} \Big(k_1^\nu k_2^\mu - (k_1 \cdot k_2) g^{\mu\nu} \Big) + 2S_{14} \frac{1}{m} i\gamma^5 \epsilon^{\alpha\beta\mu\nu} k_{1\alpha} k_{2\beta} +
\end{aligned}$$

[40] Analytically, this can be justified upon integration by parts, see [135].

$$+ 4S_{17}\frac{1}{m^2}\Big((k_1 \cdot k_2) i\gamma^5\gamma_\lambda \epsilon^{\lambda\alpha\mu\nu}(k_2 - k_1)_\alpha - i\gamma^5\gamma_\lambda\epsilon^{\lambda\alpha\beta\mu}k_{1\alpha}k_{2\beta}k_1^\nu +$$

$$+ i\gamma^5\gamma_\lambda\epsilon^{\lambda\alpha\beta\nu}k_{1\alpha}k_{2\beta}k_2^\mu\Big)\Bigg)\widetilde{\Gamma}_2 v\epsilon_\mu\epsilon_\nu \tag{4.116}$$

From the vertex factor written above, we can now read off the respective contributions of every four-fermion operator. Symbolically, the final result is then given by

$$\begin{aligned} i\mathcal{M}^{(loops)}_{SMEFT} &= \sum_{k\in Q} i\mathcal{M}^{(loops,k)}_{SMEFT} \\ Q &= \{Q^{(1)}_{quqd}, Q^{(1)*}_{quqd}, Q^{(8)}_{quqd} Q^{(8)*}_{quqd}, Q^{(1)}_{qd}, Q^{(8)}_{qd}, Q^{(1)}_{ud}, Q^{(8)}_{ud}, Q_{uu}, Q^{(1)}_{qq}, Q^{(3)}_{qq}, Q^{(1)}_{qu}, Q^{(8)}_{qu}\} \end{aligned} \tag{4.117}$$

However, it is easier to organize the terms according to their colour- and Dirac structures. Let us therefore write

$$i\mathcal{M}^{(loops)}_{SMEFT} = \sum_{k=I}^{V} i\mathcal{M}^{(loops,k)}_{SMEFT}$$

which closes the gap to (4.30). The masses appearing in the structure functions will be distinguished by superscripts b or t. As a crosscheck, we have also derived these expressions using tensor integral reduction methods.

5. The decay process $h \to gg$ with anomalous Higgs couplings at NLO in QCD

Our second example concerns the decay of a Higgs boson associated with the production of two gluons at NLO in QCD. Based on the power-counting arguments discussed in Section 3, we assume the existence of anomalous couplings in the Higgs sector resulting from the dynamics of potential heavy particle states beyond the SM. Similar setups and processes in the context of the pure SM have intensively been investigated in the literature [136–149]. Our analysis is based on [150].

5.1. Introduction and motivation

When generalizing the notion of anomalous Higgs couplings for a broader class of scenarios, one inevitably arrives at the formalism of the EWChL [36, 46, 151–160]. We use this opportunity to introduce the basics of the EWChL as well as its connection to SMEFT for the process under consideration.
In broad terms, solely based on the loop expansion and featuring the Higgs boson as a singlet rather than a doublet, the EWChL is an EFT that most effectively reconciles the nature of perturbative QFT along with the real physical states. Its basic idea relies on a more general interpretation of the electroweak Goldstone bosons in terms of an a priori unknown symmetry-breaking pattern. A similar situation applies to low-energy QCD when the theory becomes non-perturbative. Chiral symmetry breaking is the transition from the high-energy states (quarks, gluons) to the low-energy regime where the degrees of freedom are given by pions, kaons, eta-particle, etc. The latter can be reinterpreted as the (pseudo-)Goldstone bosons from an (approximate) flavour-symmetry-breaking pattern $SU(3)_L \times SU(3)_R \to SU(3)_V$. The most general Lagrangian collects the Goldstone fields in their exponential representation [26, 161]. The spectrum can straightforwardly be enlarged by singlets like the $f_0(500)$-resonance in terms of scalar functions [162–167]. In the case of the electroweak sector of the SM, the role of $SU(3)_L \times SU(3)_R$ is played by *custodial symmetry* $SU(2)_L \times SU(2)_R$ and the pions together with the $f_0(500)$-resonance are replaced by the electroweak Goldstone bosons φ^i and the Higgs boson h realized as a singlet. The Lagrangian is constructed in terms of the chiral dimensions given in (3.41). Since bosons do not increase the chiral dimension, its LO form already features an infinite tower of Higgs boson interactions. Although this looks unwieldy at first glance, it offers the advantage over SMEFT in that every term can be associated with a *fixed number* of Higgs bosons. This makes the EWChL the EFT of choice for fixed-number Higgs processes.
The LO Lagrangian ($d_\chi = 2$) is the same as (2.11) with the last two lines replaced by

$$\frac{v^2}{4}\,\langle D_\mu U^\dagger D^\mu U\rangle\, F(\eta) + \frac{v^2}{2}\partial_\mu\eta\partial^\mu\eta - V(\eta) - \bar{\psi} m(\eta, U)\psi \tag{5.1}$$

where $\eta \equiv h/v$ and $U \equiv \exp\{2i\varphi^\alpha\tau^\alpha/v\}$. The covariant derivative is given by

$$D_\mu U = \partial_\mu U - ig' B_\mu U \tau^3 + igW_\mu U \tag{5.2}$$

and the mass matrix reads

$$m(\eta, U) \equiv U\mathcal{M}(\eta)P_R + \mathcal{M}^\dagger(\eta)U^\dagger P_L, \tag{5.3}$$

with $\psi = (u, d, \nu, e)^T$ and $\mathcal{M}(\eta) = \mathrm{diag}\big(\mathcal{M}_u(\eta), \mathcal{M}_d(\eta), \mathcal{M}_\nu(\eta), \mathcal{M}_e(\eta)\big)$. As usual, generation indices are suppressed. Without loss of generality, we expand the scalar functions around their minimum according to

$$F(\eta) = 1 + \sum_{n=1}^{\infty} F_n\eta^n, \quad V(\eta) = v^4\sum_{n=2}^{\infty} V_n\eta^n, \quad \mathcal{M}_f(\eta) = \sum_{n=0}^{\infty}\mathcal{M}_{f,n}\eta^n \tag{5.4}$$

for $f = \{u, d, \nu, e\}$ and identify the fermion masses as $m_f = \mathcal{M}_{f,0}$. Constructed in this way, the EWChL at LO contains the SM as a limit when renormalizability is required and the doublet structure of the Higgs field is restored. It is more general in the sense that it allows for arbitrary coefficients in the Higgs sector deviating from the SM. For instance, single Higgs couplings between fermions and the W-boson can now be parameterized by arbitrary numbers multiplying the SM Feynman rules. These anomalous couplings are denoted by $c_f = \mathcal{M}_{f,1}/m_f$ and $c_W = F_1/2$, respectively [168]. The SM requires $\mathcal{M}_{f,1} = m_f$ and $F_1 = 2$ and thus $c_f = c_W = 1$.
The construction of the EWChL at NLO ($d_\chi = 4$ or one-loop order) works analogously [46, 169, 170]. Interestingly, this introduces local interactions between the Higgs boson and the massless gauge bosons, i.e. the photon and the gluon, which can be parameterized by anomalous couplings $c_{\gamma\gamma h}$ and c_{ggh}. In the pure SM, there exists no contact interaction between the neutral and colourless Higgs boson and the massless photons or gluons[41]. However, a Higgs decay to two gluons or photons can still be realized by virtue of closed fermion loops (coloured fermions, i.e. quarks, for the gluon case). Similar setups might be realized in the context of new heavy particles beyond the SM which generate non-vanishing values for $c_{\gamma\gamma h}$ and c_{ggh}. Although being implemented by local operators within the framework of the EWChL, these hypothetical effects are by construction loop suppressed.
The relevant part of the EWChL for the decay of a Higgs boson to two gluons can then be written down as[42]

$$\mathcal{L}_{eff} = -\sum_f m_f c_f \frac{h}{v}\bar{f}f + \frac{\alpha_s}{8\pi}c_{ggh}\frac{h}{v}G^A_{\mu\nu}G^{A\mu\nu} + 2c_W m_W^2\frac{h}{v}W^+_\mu W^{-\mu} + \frac{\alpha}{8\pi}c_{\gamma\gamma h}\frac{h}{v}F_{\mu\nu}F^{\mu\nu} \tag{5.5}$$

where we have made the loop factors as well as the necessary weak couplings (the strong coupling constant $g_s = 2\sqrt{\pi\alpha_s}$ and the elementary charge $e = 2\sqrt{\pi\alpha} = gg'/\sqrt{g^2+g'^2}$)

[41] The heavy-top limit (see below) is sometimes said to introduce a contact interaction *in the pure SM*. As such a language can, however, lead to confusing communication, we will not adopt this jargon. In this work, unless otherwise explicitly specified, the SM has all particles, including the top-quark, fully resolved, i.e. we fix $c_{ggh} = c_{\gamma\gamma h} = 0$ for the SM.

[42] Our main focus lies on the gluon decay channel for which only the first two terms in (5.5) are relevant. We will eventually turn to the photon case and hence the remaining terms of (5.5) at the end of this section.

explicit. The thus-obtained anomalous coefficients c_f, c_W, c_{ggh} and $c_{\gamma\gamma h}$ can then be taken as $\mathcal{O}(1)$-numbers.
So far, our discussion seems to be restricted to the framework of the EWChL which may differ from the same setup in SMEFT. This is, however, not the case. Consider, for example, the diagrams

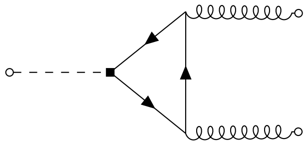

and

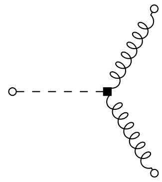

(5.6)

where as before black squares represent new-physics insertions parameterized by c_f and c_{ggh} or Warsaw-basis Wilson coefficients[43]. The loop diagram also appears in the pure SM, which is why we refer to it as SM-like, whereas the local Higgs gluon interaction is non-SM-like. We will turn to their calculation in the next subsections. These diagrams are not only the unique LO diagrams for $h \to gg$ within the EWChL, but also in SMEFT[44]. In particular, the SMEFT diagrams

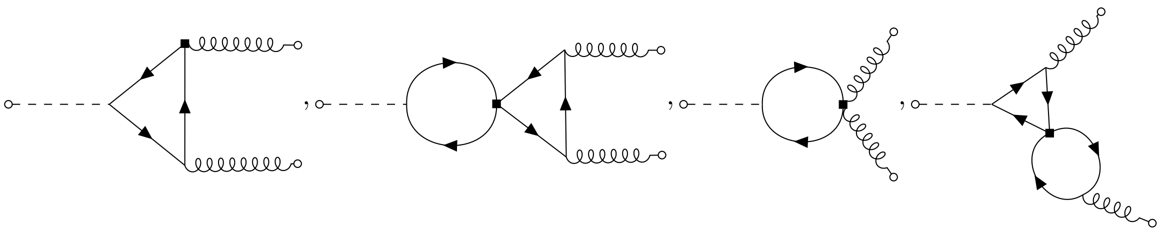

(5.7)

are all of the same subleading order, namely $d_\chi = 6$, and can consistently be neglected. It is therefore possible to take over (5.5) to the SMEFT framework. The respective translation between the various SMEFT and EWChL coefficients is given in Table 1.

[43]We will also apply the convention to use black dots (or squares) for EWChL insertions of $d_\chi = 2$ (or $d_\chi = 4$) below.

[44]There seems to be quite some confusion in the community about the terms "LO" and "NLO" in the context of new physics concerning the comparison between SMEFT and the EWChL. Strictly speaking, it is advantageous to refer to the SM as the LO SMEFT Lagrangian. We have explicitly *not* done so in this work to catch up with the conventions used in the literture. In this language (neglecting the Weinberg operator) the Warsaw basis then builds up SMEFT at NLO - all effects are suppressed with respect to the LO terms by one suppression component, namely $1/\Lambda^2$. For instance, the coefficient c_{ggh} in SMEFT is an NLO effect - exactly as in the EWChL. In fact, it is even less: For weakly coupled scenarios - and SMEFT is explicitly constructed for such scenarios - it comes with an extra loop suppression $1/(16\pi^2)$, formally pushing it to the NNLO. This apparent discrepancy can be understood when referring back to the purpose of the EWChL as the more general EFT for new physics in the Higgs sector. Indeed, strong coupling scenarios are explicitly allowed, which would render c_{ggh} a genuine NLO effect with only one suppression factor. This comes with the cost of enhancing anomalous non-field-strength Higgs-operators of arbitrary canonical dimension to the LO, i.e. they are completely unsuppressed and potentially of the same order as the SM. According to this view, the diagrams (5.6) are the LO contributions to $h \to gg$ in the EWChL, but the NLO ones in SMEFT.

Anomalous EWChL coupling	SMEFT coefficient
c_f	$1+\frac{v^2}{\Lambda^2}C_{\varphi,kin}-\frac{v^3}{\sqrt{2}m_f\Lambda^2}C_{f\varphi}$
c_W	$1+\frac{v^2}{\Lambda^2}C_{\varphi,kin}$
c_{ggh}	$\frac{32\pi^2v^2}{g_s^2\Lambda^2}C_{\varphi G}$
$c_{\gamma\gamma h}$	$\frac{32\pi^2v^2}{\Lambda^2}\left(\frac{C_{\varphi W}}{g^2}+\frac{C_{\varphi B}}{g'^2}-\frac{C_{\varphi WB}}{gg'}\right)$

Table 1: Relation between the anomalous couplings in (5.5) interpreted as the fundamental parameters of the EWChL and the SMEFT Wilson coefficients given in (2.17)-(2.49). For notational simplicity, we have defined $C_{\varphi,kin}\equiv C_{\varphi\Box}-C_{\varphi D}/4$. See also [150, 171–173].

It is now a mere philosophical question of whether one thinks in terms of the EWChL or SMEFT when it comes to Higgs processes. The former, however, has several advantages in this regard. As stated above, having the actual physical object, the Higgs boson h, implemented on a fundamental level, the Higgs interaction vertex structure is more clear in the framework of the EWChL. For instance, for the single Higgs anomalous coupling to two gluons, it is possible to sum up the contributions from all chiral dimensions in a single object c_{ggh} which is already present at the $d_\chi=4$-Lagrangian[45]. In fact, due to their vanishing contribution to the chiral dimension, this observation can be generalized to an arbitrary number of Higgs bosons. Note that this is not the case in SMEFT, which features the unphysical Higgs doublet as a building block. Here, a generic $(2n+4)$-dimensional operator $Q_{\varphi G}^{2n+4}\equiv(\varphi^\dagger\varphi)^n G_{\mu\nu}^A G^{A\mu\nu}$ has an impact on processes with up to $2n$ Higgs bosons. Extending the idea of resumming the infinite tower of Higgs singlets interactions to the doublet case results in the recently developed framework of *geometric* SMEFT (abbreviated geoSMEFT) [174–177], to which we turn back at the end of this section.

Let us now perform the explicit calculation of the diagrams (5.6). These are LO QCD contributions, i.e. their amplitudes scale as $\sim g_s^2$ and the decay rate is proportional to $g_s^4\sim\alpha_s^2$. However, it is a well-known fact for the case at hand that NLO QCD effects scaling like $\sim g_s^6$ on the decay-rate level are essential for reasonable phenomenological analyses. We therefore extend our treatment to include NLO QCD corrections. This is a cumbersome exercise that includes the calculation of virtual diagrams scaling like $\sim g_s^4$ on the amplitude level, as well as real radiation contributions $\sim g_s^3$ with soft or collinear coloured final states. The former interfere with the LO diagrams, the latter with themselves. In order to not lose the overview of the various contributions, we split the calculation apart into smaller subsections starting with a detailed calculation of the LO diagrams.

[45]It is common practice to absorb higher-chiral-dimension contributions into c_{ggh} since their corresponding operators can always be brought to the form $hG_{\mu\nu}^A G^{A\mu\nu}$ by the common methods (equations of motion, integrating by parts, etc.). See also [150].

5.2. Detailed calculation at LO in QCD

SM-like contribution

We first turn to the SM-like contribution to $h \to gg$ featuring a modified $h\bar{f}f$-coupling. As this calculation also features the building blocks for subsequent chapters, we show most of the mathematical details within the main text. The total amplitude $i\mathcal{M}_{SM}^{LO}$ in the SM at LO in QCD for this process consists of two contributions $i\mathcal{M}_{1,SM}^{LO}$ and $i\mathcal{M}_{2,SM}^{LO}$ that are related by reverting the fermion flow. They are given by (see Appendix C for our conventions)

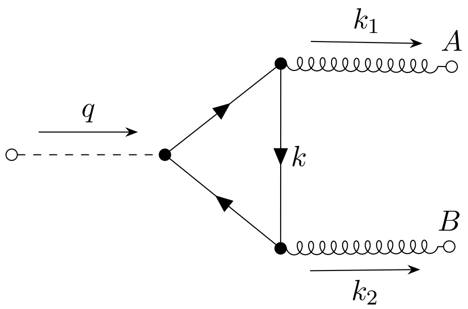

$$\equiv i\mathcal{M}_{1,SM}^{LO} = -\frac{g_s^2 c_f y_f}{\sqrt{2}} Tr(T^B T^A)\epsilon_\mu^*(k_1)\epsilon_\nu^*(k_2) I_{1,2}^{\mu\nu} \tag{5.8}$$

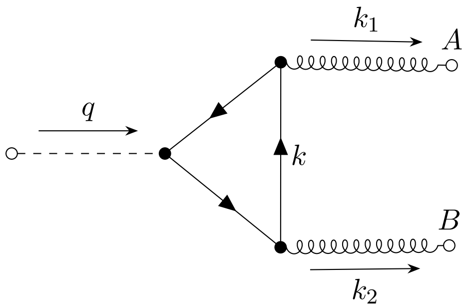

$$\equiv i\mathcal{M}_{2,SM}^{LO} = -\frac{g_s^2 c_f y_f}{\sqrt{2}} Tr(T^A T^B)\epsilon_\mu^*(k_1)\epsilon_\nu^*(k_2) I_{2,1}^{\nu\mu} \tag{5.9}$$

where the two outgoing on-shell gluon momenta are given by k_1 and k_2 with $k_1^2 = k_2^2 = 0$, respectively, and the incoming Higgs momentum is given by $q = k_1 + k_2$ with $q^2 = m_h^2$. The momentum integral in dimensional regularization with $d = 4 - 2\epsilon$ is given by

$$I_{1,2}^{\mu\nu} = \mu^{2\epsilon} \int \frac{d^d k}{(2\pi)^d} \frac{Tr\big((\not{k} - \not{k}_2 + m_f)\gamma^\nu(\not{k} + m_f)\gamma^\mu(\not{k} + \not{k}_1 + m_f)\big)}{\big((k-k_2)^2 - m_f^2 + i\eta\big)(k^2 - m_f^2 + i\eta)\big((k+k_1)^2 - m_f^2 + i\eta\big)} \tag{5.10}$$

with $I_{2,1}^{\nu\mu}$ related by interchanging $k_1 \leftrightarrow k_2$ and $\mu \leftrightarrow \nu$. We will apply similar notational conventions throughout this entire section. Note that we have left the gluon colour indices A and B open, which will simplify the notation. Due to the cyclicity of the trace, the LO colour structure is particularly simple. It is also useful to distinguish between the fermion mass m_f participating in the loop and the Yukawa coupling $y_f = \sqrt{2}m_f/v$.

Note that for $h \to gg$, the loop fermions are mandatorily quarks, so $f = \{t, b, c, s, u, d\}$ (see (5.258) for an explicit distinction between quarks and leptons in the context of $h \to \gamma\gamma$). The total LO amplitude for a single fermion is given by the sum of the two contributions (5.8) and (5.9)

$$i\mathcal{M}_{SM}^{LO} = i\mathcal{M}_{1,SM}^{LO} + i\mathcal{M}_{2,SM}^{LO} = -\frac{g_s^2 c_f y_f}{\sqrt{2}} Tr(T^A T^B)\epsilon_\mu^*(k_1)\epsilon_\nu^*(k_2)(I_{1,2}^{\mu\nu} + I_{2,1}^{\nu\mu}) \tag{5.11}$$

We now have to evaluate the loop integral (5.10). Since there exists no Higgs-gluon-gluon vertex in the SM to absorb an eventual divergence coming from the momentum integration, we expect the final result to be finite despite the integral itself being superficially divergent. The numerator is given by

$$\begin{aligned} Tr\big((\not{k} - \not{k}_2 + m_f)\gamma^\nu(\not{k} + m_f)\gamma^\mu(\not{k} + \not{k}_1 + m_f)\big) = \\ =4m_f\big((4g^{\mu\alpha}g^{\nu\beta} - g^{\mu\nu}g^{\alpha\beta})k_\alpha k_\beta + \\ + (2g^{\nu\alpha}k_1^\mu - 2g^{\mu\alpha}k_2^\nu)k_\alpha + (m_f^2 - k_1 \cdot k_2)g^{\mu\nu} + k_1^\nu k_2^\mu - k_1^\mu k_2^\nu\big) \end{aligned} \tag{5.12}$$

Crucially, the vanishing of an odd number of Dirac matrices causes the $\mathcal{O}(k^3)$-term to disappear. Due to the transversality of the gluon polarization vectors, i.e. $k_1^\mu \epsilon_\mu^*(k_1) = 0$ and $k_2^\nu \epsilon_\nu^*(k_2) = 0$, we can drop the $\mathcal{O}(k^1)$-contribution as a whole and the last term of the $\mathcal{O}(k^0)$-contribution. Furthermore, we observe that $I_{1,2}^{\mu\nu} = I_{2,1}^{\nu\mu}$. Employing the notation of Appendix E, we end up with

$$I_{1,2}^{\mu\nu} = 4m_f\big((4g^{\mu\alpha}g^{\nu\beta} - g^{\mu\nu}g^{\alpha\beta})C_{\alpha\beta} + (m_f^2 - k_1 \cdot k_2)g^{\mu\nu}C + k_1^\nu k_2^\mu C\big) \tag{5.13}$$

Reducing the tensor integral $C_{\alpha\beta}$ to scalar integrals and defining $\tau_f = k_1 \cdot k_2/(2m_f^2)$ results in

$$I_{1,2}^{\mu\nu} = -\frac{4m_f}{k_1 \cdot k_2}(k_1^\nu k_2^\mu - k_1 \cdot k_2 g^{\mu\nu})J(\tau_f) \tag{5.14}$$

with $J(\tau_f) \equiv i\tilde{J}(\tau_f)/(16\pi^2) = \epsilon B - 2m_f^2(\tau_f - 1)C$ to leading order in ϵ, which is finite as expected. The loop function $\tilde{J}(\tau_f)$ is evaluated in Appendix E and given by

$$\tilde{J}(\tau_f) = \begin{cases} 1 + \left(1 - \frac{1}{\tau_f}\right)\arcsin^2\sqrt{\tau_f} & \text{for } 0 < \tau_f < 1 \\ 1 - \frac{1}{4}\left(1 - \frac{1}{\tau_f}\right)\left(\ln\left(\frac{1-\sqrt{1-\frac{1}{\tau_f}}}{1+\sqrt{1-\frac{1}{\tau_f}}}\right) + i\pi\right)^2 & \text{for } 1 \le \tau_f < \infty \end{cases} \tag{5.15}$$

We will give a more general expression for higher ϵ orders below. For notational simplicity, the dependence on τ_f of the scalar integrals B and C has been suppressed. Using $Tr(T^A T^B) = T_F \delta^{AB}$ with $T_F = 1/2$ and $k_1 \cdot k_2 = q^2/2 = m_h^2/2$, the total amplitude is given by

$$i\mathcal{M}_{SM}^{LO} = \frac{i g_s^2 c_f y_f m_f}{2\sqrt{2}\pi^2 m_h^2}\delta^{AB}\epsilon_\mu^*(k_1)\epsilon_\nu^*(k_2)(k_1^\nu k_2^\mu - k_1 \cdot k_2 g^{\mu\nu})\tilde{J}(\tau_f) \tag{5.16}$$

The amplitude $\mathcal{M}_{SM}^{LO}$ has an imaginary part in the kinematic regime $2m_f < m_h$, which - in accordance with the optical theorem - is to be expected, as the loop-fermions can go on-shell.
For a $1 \to 2$ decay, it is straightforward to compute the total decay rate Γ once the squared amplitude $|\mathcal{M}|^2$ is known. The differential decay rate in the Higgs boson's rest frame is given by [61]

$$d\Gamma = \frac{|\boldsymbol{k_1}|}{32\pi^2 m_h^2} \overline{|\mathcal{M}|^2} d\Omega_3 \tag{5.17}$$

where the overline in $\overline{|\mathcal{M}|^2}$ denotes a sum over final spins and colours as before and $d\Omega_3$ is the differential solid angle that can trivially be integrated to 4π, because there is no angular dependence. This yields the total decay rate Γ. The absolute value of the spatial momentum of either outgoing gluon is $|\boldsymbol{k_1}| = m_h/2$. Finally, (5.17) has to be corrected by a symmetry factor of $1/2$ due to the two final state gluons being indistinguishable. Actually, introducing the symmetry factor on the level of the differential decay rate is not strictly correct. Instead, it appears when the phase space integral is carried out and accounts for an overcounting of distinguishable final states. We will nevertheless introduce these factors already at the differential level. Note that (5.17) is not restricted to LO calculations, hence the suppression of further labels.
Returning to our case, squaring $i\mathcal{M}_{SM}^{LO}$ and performing the spin and colour sums is straightforward. For the colour sum, we use $\delta^{AB}\delta^{BA} = N_c^2 - 1$, where N_c is the number of quark colours, i.e. $N_c = 3$ for QCD. The spin sum[46] is equivalent to adding up the individual helicity amplitudes. Employing the notation of Appendix B, we have

$$H_{++}^{gg} = -\langle 12\rangle^2, \; H_{--}^{gg} = -[12]^2, \; H_{+-}^{gg} = 0, \; H_{-+}^{gg} = 0 \tag{5.19}$$

with[47]

$$H_{\lambda_1\lambda_2}^{gg} \equiv 2\epsilon_{\mu\lambda_1}^*(k_1,k_2)\epsilon_{\nu\lambda_2}^*(k_2,k_1)(k_1^\nu k_2^\mu - k_1 \cdot k_2 g^{\mu\nu}) \tag{5.20}$$

Using $\langle 12\rangle^* = [21]$ and $\langle 12\rangle[21] = m_h^2$, the polarization sums evaluate to

$$\sum_{\lambda_{1,2}=\pm} |H_{\lambda_1\lambda_2}^{gg}|^2 = |H_{++}^{gg}|^2 + |H_{--}^{gg}|^2 + |H_{+-}^{gg}|^2 + |H_{-+}^{gg}|^2 = 2m_h^4 \tag{5.21}$$

We finally arrive at

$$\overline{|\mathcal{M}_{SM}^{LO}|^2} = 128 g_s^4 c_f^2 y_f^2 m_f^2 |J(\tau_f)|^2 \tag{5.22}$$

[46]In contrast to QED, the spin sum for non-Abelian gauge bosons should take ghost contributions into account and is given by the formula [135]

$$\sum_{\text{polarizations},\; n} \epsilon_\alpha(k)\epsilon_\beta^*(k) = -g_{\alpha\beta} + \frac{k_\alpha n_\beta + k_\beta n_\alpha}{k \cdot n} - \frac{n^2 k_\alpha k_\beta}{(k \cdot n)^2} \tag{5.18}$$

holding for arbitrary linearly independent four-momenta k and n. It is convenient to choose the reference momentum $n = k_2$ for the spin sum related to $k = k_1$ and vice versa in order to drop the last term in (5.18). This is also done in (5.20).

[47]We have so far suppressed the gluon helicity indices λ_1 and λ_2.

and thus - with an obvious notational convention - a total decay rate of

$$\Gamma_{SM}^{LO\times LO} = \frac{4g_s^4 c_f^2 y_f^2 m_f^2}{\pi m_h} |J(\tau_f)|^2 \tag{5.23}$$

where

$$|J(\tau_f)|^2 = \begin{cases} \frac{1}{256\pi^4}\left(1+\left(1-\frac{1}{\tau_f}\right)\arcsin^2\sqrt{\tau_f}\right)^2 & \text{for } 0<\tau_f<1 \\ \frac{1}{256\pi^4}\left|1-\frac{1}{4}\left(1-\frac{1}{\tau_f}\right)\left(\ln\left(\frac{1-\sqrt{1-\frac{1}{\tau_f}}}{1+\sqrt{1-\frac{1}{\tau_f}}}\right)+i\pi\right)^2\right|^2 & \text{for } 1\leq\tau_f<\infty \end{cases} \tag{5.24}$$

Before moving on, we should get an overview of the numerical impact for different quarks running through the loop. The SM result for one quark ($c_f = 1$ for only one f) can be obtained by plugging in the parameters (without errors) from Appendix A. We find

$$\Gamma_{SM}^{LO\times LO} = \begin{cases} 2.15117542\cdot 10^{-1}\ \text{MeV} & \text{for the top-quark with OS mass as input} \\ 1.60163440\cdot 10^{-3}\ \text{MeV} & \text{for the bottom-quark with } \overline{\text{MS}} \text{ mass as input} \end{cases} \tag{5.25}$$

In the light of these numbers, one could conclude that the effects of lighter quarks can be neglected and only the top-quark has a significant impact on the total decay rate. However, the previous discussion misses interference effects between the various quark channels. To take them into account, we add up the individual amplitudes (5.16) for a single fermion f (or better quark) and obtain[48]

$$\sum_f i\mathcal{M}_{SM}^{LO} = \frac{8g_s^2}{\sqrt{2}m_h^2}\delta^{AB}\epsilon_\mu^*(k_1)\epsilon_\nu^*(k_2)(k_1^\nu k_2^\mu - k_1\cdot k_2 g^{\mu\nu})\sum_f c_f y_f m_f J(\tau_f) \tag{5.26}$$

Repeating the same steps as before for the top- and bottom-quark results in

$$\begin{aligned}\Gamma_{SM}^{LO\times LO} =& \frac{4g_s^4}{\pi m_h}\left(c_t^2 y_t^2 m_t^2|J(\tau_t)|^2 + c_b^2 y_b^2 m_b^2|J(\tau_b)|^2 + 2c_t c_b y_t y_b m_t m_b \operatorname{Re}\{J(\tau_t)^* J(\tau_b)\}\right) = \\ =&(2.15117542\cdot 10^{-1} c_t^2 + 1.60163440\cdot 10^{-3} c_b^2 - 2.24018695\cdot 10^{-2} c_t c_b)\ \text{MeV}\end{aligned} \tag{5.27}$$

which gives a total decay rate of $\Gamma_{SM}^{LO\times LO} = 1.94317307\cdot 10^{-1}$ MeV for the top- and bottom-quark at LO for the pure SM. This demonstrates the importance for including lighter quarks in a proper numerical analysis. We will do so in Subsection 5.8.

[48]From now on, the sum over loop fermions f is always implicitly understood.

Non-SM-like contribution

As discussed above, the EWChL allows for scenarios with arbitrary c_{ggh} (in combination with non-vanishing c_f, also for the top-quark). These non-SM-like contributions are given by the single diagram

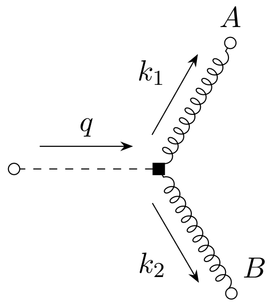

$$\equiv i\mathcal{M}^{LO}_{NSM} = \frac{ig_s^2 c_{ggh}}{8\pi^2 v}\delta^{AB}\epsilon^*_\mu(k_1)\epsilon^*_\nu(k_2)(k_1^\nu k_2^\mu - k_1 \cdot k_2 g^{\mu\nu}) \quad (5.28)$$

In terms of the helicity amplitudes (5.20), we have

$$i\mathcal{M}^{LO}_{NSM} = \frac{ig_s^2 c_{ggh}}{16\pi^2 v}\delta^{AB} H^{gg}_{\lambda_1\lambda_2} \quad (5.29)$$

Combining the amplitudes (5.26) and (5.29) finally yields

$$i\mathcal{M}^{LO} \equiv i\mathcal{M}^{LO}_{NSM} + i\mathcal{M}^{LO}_{SM} = \frac{i\alpha_s}{4\pi}\delta^{AB} H^{gg}_{\lambda_1\lambda_2}\left(\frac{c_{ggh}}{v} + \sum_f \frac{y_f c_f}{\sqrt{2}m_f}\frac{\tilde{J}(\tau_f)}{\tau_f}\right) \quad (5.30)$$

and thus

$$\overline{|\mathcal{M}^{LO}|^2} = \frac{\alpha_s^2 m_h^4}{8\pi^2}(N_c^2 - 1)\left|\frac{c_{ggh}}{v} + \sum_f \frac{y_f c_f}{\sqrt{2}m_f}\frac{\tilde{J}(\tau_f)}{\tau_f}\right|^2 \quad (5.31)$$

The total LO decay rate is then given by

$$\Gamma^{LO\times LO} = \frac{\alpha_s^2 m_h^3}{256\pi^3}(N_c^2 - 1)\Bigg(\frac{c_{ggh}^2}{v^2} + 2\frac{c_{ggh}}{v}\sum_f \frac{y_f c_f}{\sqrt{2}m_f}\frac{\mathrm{Re}\{\tilde{J}(\tau_f)\}}{\tau_f} + \\ + \left|\sum_f \frac{y_f c_f}{\sqrt{2}m_f}\frac{\tilde{J}(\tau_f)}{\tau_f}\right|^2\Bigg) \quad (5.32)$$

Heavy-top limit

It is also worth considering the limit $m_t \to \infty$ in (5.16), subsequently denoted as the heavy-top limit. With $\arcsin(x) = x + x^3/6 + 3x^5/40 + \mathcal{O}(x^7)$, we obtain

$$\frac{J(\tau_t)}{\tau_t} = \frac{i}{24\pi^2} + \frac{7i\tau_t}{720\pi^2} + \frac{i\tau_t^2}{252\pi^2} + \frac{13i\tau_t^3}{6300\pi^2} + \mathcal{O}\left(\tau_t^4\right) \quad (5.33)$$

and therefore (setting $y_t/m_t = \sqrt{2}/v$ and $c_t = 1$)

$$\lim_{\tau_t \to 0} i\mathcal{M}_{SM}^{LO} = \frac{ig_s^2}{12\pi^2 v}\delta^{AB}\epsilon_\mu^*(k_1)\epsilon_\nu^*(k_2)(k_1^\nu k_2^\mu - k_1 \cdot k_2 g^{\mu\nu}) \tag{5.34}$$

for the top-quark contribution. The heavy-top limit corresponds to an EFT in which a heavy quark (e.g. the top) is integrated out and its loop contribution to $h \to gg$ is replaced by a local interaction giving rise to the amplitude (5.34). Upon "zooming out", the complicated loop function collapses to a pure number and the fermion does not act as a separate degree of freedom any more. It can therefore be viewed as taking $c_t \to 0$ in the EFT and introducing a new direct coupling between the Higgs boson and two gluons of the form (5.28) with

$$c_{ggh} = \frac{2}{3} + \frac{7}{45}\tau_t + \frac{4}{63}\tau_t^2 + \frac{52}{1575}\tau_t^3 + \mathcal{O}\left(\tau_t^4\right) \tag{5.35}$$

for $c_t = 1$ and $y_t = \sqrt{2}m_t/v$ in the full theory, that is the SM. The so-obtained c_{ggh} should be distinguished from the corresponding EWChL parameter. It solely depends on the "high energy" parameters c_t, y_t and m_t (namely $c_{ggh} = 2c_t y_t v/(3\sqrt{2}m_t)$ at lowest order). In reality, $\tau_t \approx 0.13$ and $J(\tau_t)/\tau_t \approx i/(23.25\pi^2)$, so the lowest order term in the heavy-top limit is already quite accurate. There will be corrections of higher order in g_s, which we will come to later (see (5.308)).

Appendix: Higher orders in ϵ

For later use, we will now expand the amplitude to $\mathcal{O}(\epsilon^2)$. In fact, carefully keeping track of higher order terms in ϵ in (5.13) with (E.21), we actually find

$$\begin{aligned} I_{1,2}^{\mu\nu} = &-\frac{4m_f}{k_1 \cdot k_2}(k_1^\nu k_2^\mu - k_1 \cdot k_2 g^{\mu\nu})\Big((\epsilon + \epsilon^2 + \epsilon^3)\widetilde{B} + \\ &- 2m_f^2(\tau_f - 1 - \epsilon - \epsilon^2)C\Big) + \mathcal{O}(\epsilon^3) \end{aligned} \tag{5.36}$$

which reduces to the previous result (5.14) when ϵ is sent to 0. Note that $\widetilde{B}$ actually starts with $1/\epsilon$. The tricky part is to expand $\tilde{B}$ and C to higher orders in ϵ. Using (D.13), we get

$$\begin{aligned} \widetilde{B} =& \mu^{2\epsilon}\int \frac{d^dk}{(2\pi)^d}\frac{1}{(k^2 - m_f^2)\big((k+q)^2 - m_f^2\big)} = \\ &= \frac{i}{16\pi^2}\left(\frac{4\pi\mu^2}{m_f^2}\right)^\epsilon \Gamma(\epsilon)\int_0^1 dx \frac{1}{(1 - 4x(1-x)\tau_f)^\epsilon} \end{aligned} \tag{5.37}$$

$$\begin{aligned} C =& \mu^{2\epsilon}\int \frac{d^dk}{(2\pi)^d}\frac{1}{(k^2 - m_f^2)\big((k+k_1)^2 - m_f^2\big)\big((k-k_2)^2 - m_f^2\big)} = \\ &= -\frac{i}{16\pi^2 m_f^2}\left(\frac{4\pi\mu^2}{m_f^2}\right)^\epsilon \Gamma(1+\epsilon)\int_0^1 dz \int_0^{1-z} dy \frac{1}{(1 - 4yz\tau_f)^{1+\epsilon}} \end{aligned} \tag{5.38}$$

for arbitrary $\epsilon = (4-d)/2$. Again, these expressions reduce to the ones listed in Appendix E for $\epsilon \to 0$. For (5.36) to be accurate, we need $\widetilde{B}$ to $\mathcal{O}(\epsilon)$ and C to $\mathcal{O}(\epsilon^2)$, which is achieved by expanding the integrands keeping in mind that $\Gamma(\epsilon) = e^{-\gamma\epsilon}(1/\epsilon + \pi^2\epsilon/12) + \mathcal{O}(\epsilon^2)$ and $\Gamma(1+\epsilon) = e^{-\gamma\epsilon}(1+\pi^2\epsilon^2/12) + \mathcal{O}(\epsilon^3)$. This yields [141]

$$\widetilde{B} = \frac{i}{16\pi^2}\left(\frac{4\pi\mu^2}{m_f^2}\right)^{\epsilon}\frac{\Gamma(1+\epsilon)}{1-\epsilon}\left(\frac{\widetilde{B}_{-1}}{\epsilon} + \widetilde{B}_0 + \widetilde{B}_1\epsilon\right) + \mathcal{O}(\epsilon^2) \tag{5.39}$$

$$C = \frac{i}{16\pi^2 m_f^2}\left(\frac{4\pi\mu^2}{m_f^2}\right)^{\epsilon}\frac{\Gamma(1+\epsilon)}{1-\epsilon}\left(C_0 + C_1\epsilon + C_2\epsilon^2\right) + \mathcal{O}(\epsilon^3) \tag{5.40}$$

with

$$\widetilde{B}_{-1} = 1 \tag{5.41}$$

$$\widetilde{B}_0 = \frac{1}{1-\theta_f}\big(-\theta_f + (\theta_f+1)H(\{0\};\theta_f) + 1\big) \tag{5.42}$$

$$\begin{aligned}\widetilde{B}_1 = \frac{1}{1-\theta_f}\Big(&\frac{1}{6}(12 - 12\theta_f - \pi^2 - \pi^2\theta_f) + \\ &+ (\theta_f+1)\big(H(\{0\};\theta_f) - 2H(\{-1,0\};\theta_f) + H(\{0,0\};\theta_f)\big)\Big)\end{aligned} \tag{5.43}$$

$$C_0 = -\frac{\theta_f H(\{0,0\};\theta_f)}{(\theta_f-1)^2} \tag{5.44}$$

$$\begin{aligned}C_1 = \frac{\theta_f}{(1-\theta_f)^2}\Big(&\frac{\pi^2}{6}H(\{0\};\theta_f) + 2H(\{0,-1,0\};\theta_f) + \\ &+ H(\{0,0\};\theta_f) - H(\{0,0,0\};\theta_f) + 3\zeta(3)\Big)\end{aligned} \tag{5.45}$$

$$\begin{aligned}C_2 = \frac{\theta_f}{(1-\theta_f)^2}\Big(&-\frac{\pi^2}{3}H(\{0,-1\};\theta_f) - \frac{1}{6}\big(\pi^2 - 12\zeta(3)\big)H(\{0\};\theta_f) - 3\zeta(3) + \frac{\pi^4}{72} + \\ &+ 2H(\{0,0,-1,0\};\theta_f) - 2H(\{0,-1,0\};\theta_f) + \\ &+ \frac{\pi^2}{6}H(\{0,0\};\theta_f) - 4H(\{0,-1,-1,0\};\theta_f) + \\ &+ 2H(\{0,-1,0,0\};\theta_f) + H(\{0,0,0\};\theta_f) - H(\{0,0,0,0\};\theta_f)\Big)\end{aligned} \tag{5.46}$$

where θ_f is defined via

$$\theta_f \equiv \frac{\sqrt{1-\frac{1}{\tau_f}} - 1}{\sqrt{1-\frac{1}{\tau_f}} + 1} \tag{5.47}$$

Note that upon sending $\tau_f \to \tau_f + i\eta$, one also has $\theta_f \to \theta_f + i\eta$, which is important for obtaining the correct analytic continuations. The functions $H(\{...\};\theta_f)$ denote the harmonic polylogarithms (HPL functions, see [178] for an implementation) normalized such that $H(\{0\};\theta_f) = \ln\theta_f$ and $\zeta(3) \approx 1.202$ is Apéry's constant defined via the Riemann zeta function $\zeta(s) = \sum_{k=1}^{\infty} k^{-s}$. The generalization of (5.15) then reads

$$J(\tau_f, \epsilon) = (\epsilon + \epsilon^2 + \epsilon^3)\widetilde{B} - 2m_f^2(\tau_f - 1 - \epsilon - \epsilon^2)C + \mathcal{O}(\epsilon^3) \tag{5.48}$$

with $\widetilde{B}$ and C given by (5.39) and (5.40). For later purposes, we introduce

$$\frac{4}{3}F_0^H(\epsilon) \equiv \frac{2\tilde{J}(\tau_f, \epsilon)}{\tau_f} \tag{5.49}$$

with $J(\tau_f, \epsilon) \equiv \tilde{J}(\tau_f, \epsilon)/(16\pi^2)$ as before. Explicitly, we then find

$$F_0^H(\epsilon) = -i\frac{\pi^2}{24\tau_f}\left((\epsilon + \epsilon^2 + \epsilon^3)\widetilde{B} - 2m_f^2(\tau_f - 1 - \epsilon - \epsilon^2)C\right) \tag{5.50}$$

Dropping terms of $\mathcal{O}(\epsilon^3)$. We remark that when working with $\epsilon \neq 0$, not only the amplitude, but also the phase space gets ϵ-corrections. Indeed, the strictly four-dimensional formula (5.17) should be viewed as the special case of the more general expression [61]

$$d\Gamma = \frac{1}{2m_h}\frac{1}{S}\overline{|\mathcal{M}|^2}d\Phi_n \tag{5.51}$$

which is valid for arbitrary space time dimensions $d = 4 - 2\epsilon$ and n final state particles (here we have $n = 2$). Again, the symmetry factor S is equal to the number of indistinguishable permutations of the final state particles (so $S = 2$ for our case) and the two-body phase space integration measure is given by [179]

$$d\Phi_2 = (2\pi)^{2\epsilon-2}\frac{2^{2\epsilon-3}}{(m_h^2)^\epsilon}d\Omega_{3-2\epsilon} \xrightarrow{\epsilon\to 0} \frac{1}{32\pi^2}d\Omega_3 \tag{5.52}$$

with $d\Omega_N$ being the N-dimensional solid angle such that

$$\Omega_N \equiv \int d\Omega_N = \frac{2\pi^{\frac{N}{2}}}{\Gamma\left(\frac{N}{2}\right)} \tag{5.53}$$

is the volume of the N-dimensional hypersphere. The total phase space volume can be obtained immediately as

$$\Phi_2 \equiv \int d\Phi_2 = \frac{2^{2\epsilon-3}\pi^{\epsilon-1}}{(m_h^2)^\epsilon}\frac{\Gamma(1-\epsilon)}{\Gamma(2-2\epsilon)} \xrightarrow{\epsilon\to 0} \frac{1}{8\pi} \tag{5.54}$$

5.3. Virtual QCD corrections

Non-SM-like contribution

We now turn to the virtual $\mathcal{O}(g_s^4)$-corrections to the amplitude (5.30). In contrast to the LO calculation, we consider the local Higgs-gluon-gluon interaction first and turn to the SM-like contributions later.

The QCD corrections to the diagram (5.28) are given by one-loop diagrams featuring gluons. From (5.5), we see that the Feynman rules for local Higgs-triple gluon or Higgs-quadruple gluon vertices are simply given by $-g_s^2 c_{ggh}/(8\pi^2 v)$ times the corresponding three- or four-gluon Feynman rule displayed in Appendix C. We only consider diagrams with at most one effective vertex. These are given by[49]

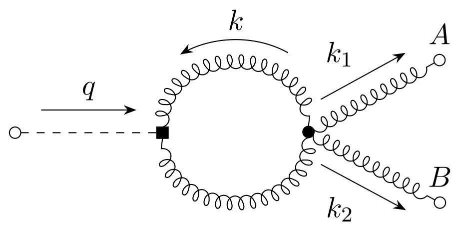

$$\equiv i\mathcal{M}^V_{1,NSM} \tag{5.55}$$

and

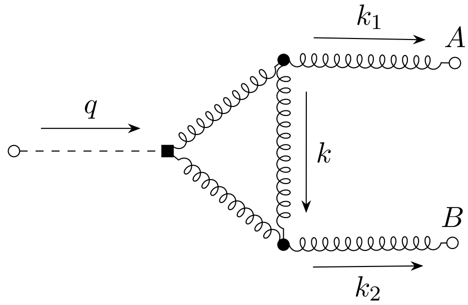

$$\equiv i\mathcal{M}^V_{2,NSM} \tag{5.56}$$

The total virtual amplitude $i\mathcal{M}^V_{NSM} \equiv i\mathcal{M}^V_{1,NSM} + i\mathcal{M}^V_{2,NSM}$ is given by

$$i\mathcal{M}^V_{NSM} = \frac{ig_s^4 N_c c_{ggh}}{64\pi^4 v \epsilon^2} \epsilon^*_\mu(k_1)\epsilon^*_\nu(k_2)\delta^{AB} \left(\frac{\mu^2 4\pi}{-m_h^2 e^\gamma}\right)^\epsilon \left(1 - \frac{\pi^2}{12}\epsilon^2\right)(g^{\mu\nu} k_1 \cdot k_2 - k_1^\nu k_2^\mu) + \mathcal{O}(\epsilon) \tag{5.57}$$

or, in its full glory

$$\begin{aligned} i\mathcal{M}^V_{NSM} = & \frac{ig_s^4 N_c c_{ggh}}{64\pi^4 v} \epsilon^*_\mu(k_1)\epsilon^*_\nu(k_2)\delta^{AB} (g^{\mu\nu} k_1 \cdot k_2 - k_1^\nu k_2^\mu) \cdot \\ & \cdot \left(\frac{1}{\epsilon^2} + \frac{1}{\epsilon}\left(\ln\frac{4\pi}{e^\gamma} + L\right) + \frac{1}{2}\ln^2\frac{4\pi}{e^\gamma} + \ln\frac{4\pi}{e^\gamma} L + \frac{1}{2}L^2 - \frac{\pi^2}{12}\right) + \mathcal{O}(\epsilon) \end{aligned} \tag{5.58}$$

where we have defined[50]

$$L \equiv \ln\frac{\mu^2}{-m_h^2} = \ln\frac{\mu^2}{m_h^2} + i\pi \tag{5.59}$$

The calculational details are left for the appendix to this chapter. Featuring UV, as well as IR poles, this amplitude requires renormalization, which we turn to now.

[49] Generally, we label the virtual corrections with V and the real radiation contributions with R (see below).

[50] We have to choose the $+i\pi$-convention due to the $i\eta$-prescription.

Renormalization

We will now renormalize the amplitude (5.57) by absorbing the UV divergencies into a counterterm of the form (5.28). With $g_s^2 = 4\pi\alpha_s$, the combined amplitudes (5.28) and (5.57) are given by

$$
\begin{aligned}
i\mathcal{M}_{NSM}^{LO+V} =& \frac{i\alpha_s c_{ggh}}{4\pi v}\delta^{AB} H^{gg}_{\lambda_1\lambda_2}\left(1 - \frac{\alpha_s}{2\pi}N_c\left(\frac{\mu^2 4\pi}{-m_h^2 e^{\gamma}}\right)^{\epsilon}\left(\frac{1}{\epsilon^2} - \frac{\pi^2}{12}\right)\right) \\
&\equiv \frac{\alpha_s}{4\pi} i\mathcal{M}^{(0)}_{NSM} + \left(\frac{\alpha_s}{4\pi}\right)^2 i\mathcal{M}^{(1)}_{NSM} \qquad (5.60)
\end{aligned}
$$

with $H^{gg}_{\lambda_1\lambda_2}$ defined in (5.20) and

$$
i\mathcal{M}^{(0)}_{NSM} = \frac{i c_{ggh}}{v}\delta^{AB} H^{gg}_{\lambda_1\lambda_2} \qquad (5.61)
$$

$$
i\mathcal{M}^{(1)}_{NSM} = -2i\mathcal{M}^{(0)}_{NSM} N_c S_\epsilon \left(\frac{\mu^2}{-m_h^2}\right)^{\epsilon}\left(\frac{1}{\epsilon^2} - \frac{\pi^2}{12}\right) \qquad (5.62)
$$

where we have introduced $S_\epsilon \equiv (4\pi/e^{\gamma})^{\epsilon}$. This factor is common to all loop computations that are carried out in dimensional regularization. Let us now, for the sake of generality in the following derivations, drop all the labels and consider the amplitude

$$
i\mathcal{M} \equiv \frac{\alpha_s}{4\pi} i\mathcal{M}^{(0)} + \left(\frac{\alpha_s}{4\pi}\right)^2 i\mathcal{M}^{(1)} \qquad (5.63)
$$

We now redefine the parameters of the theory by introducing counterterms Z_α and Z_G for the coupling constant α_s and the external gluon wavefunctions $\epsilon^*_{\mu_i}(k_i)$ (the labels μ_i and k_i stand for generic Lorentz indices and four-momenta), respectively[51]. The explicit formulas are given by [138, 143]

$$
\frac{\alpha_s}{4\pi} \longrightarrow \frac{\alpha_s}{4\pi}\left(\frac{\mu_R^2}{\mu^2}\right)^{\epsilon} Z_\alpha \equiv \frac{\alpha_s}{4\pi}\left(\frac{\mu_R^2}{\mu^2}\right)^{\epsilon} S_\epsilon^{-1}\left(1 + \frac{\alpha_s}{4\pi}\delta Z_\alpha\right) + \mathcal{O}(\alpha_s^3) \qquad (5.64)
$$

$$
\epsilon^*_{\mu_i}(k_i) \longrightarrow \sqrt{Z_G}\epsilon^*_{\mu_i}(k_i) \equiv \sqrt{1 + \frac{\alpha_s}{4\pi}\delta Z_G}\epsilon^*_{\mu_i}(k_i) + \mathcal{O}(\alpha_s^2) \qquad (5.65)
$$

$$
m_f^2 \longrightarrow Z_{m_f^2} m_f^2 \equiv m_f^2 + \frac{\alpha_s}{4\pi}\delta m_f^2 + \mathcal{O}(\alpha_s^2) \qquad (5.66)
$$

where μ_R is the renormalization scale, which essentially trades against the artificial regularization scale μ. For an amplitude with n_g external gluons (we have $n_g = 2$), the shift (5.65) just means that an overall factor of $Z_G^{n_g/2} = 1 + n_g\alpha_s\delta Z_G/(8\pi) + \mathcal{O}(\alpha_s^2)$ has to be introduced. The right-hand sides of (5.64)-(5.66) feature the renormalized coupling constant *after the shift* (5.64), so no additional adjustment of α_s is required in the latter two equations, i.e. (5.64) is only applied to the α_s-factors displayed on the right-hand

[51] As we want to apply the same formulas for the two-loop amplitudes featuring fermion loops (see below), we pretend that there is also a dependence on the fermion mass and renormalize the latter as well via $Z_{m_f^2}$.

side of (5.63). The mass renormalization (5.66) is the only manipulation that does not affect overall factors only. An amplitude exposed to (5.66) then changes according to

$$i\mathcal{M} = i\mathcal{M} + \frac{\alpha_s}{4\pi}\delta m_f^2 \frac{\partial}{\partial m_f^2} i\mathcal{M} + \mathcal{O}(\alpha_s^2) \tag{5.67}$$

It is important to carefully keep track of the order in α_s one is working at. Applying the combined shifts to (5.63) eventually results in a renormalized amplitude $i\mathcal{M}_r$ given by

$$\begin{aligned} i\mathcal{M}_r =& Z_G^{n_g/2}\left(\frac{\alpha_s}{4\pi}\left(\frac{\mu_R^2}{\mu^2}\right)^{\epsilon} Z_\alpha \left(i\mathcal{M}^{(0)} + \frac{\alpha_s}{4\pi}\delta m_f^2 \frac{\partial}{\partial m_f^2} i\mathcal{M}^{(0)}\right) + \right. \\ &\left. + \left(\frac{\alpha_s}{4\pi}\right)^2 \left(\frac{\mu_R^2}{\mu^2}\right)^{2\epsilon} Z_\alpha^2 i\mathcal{M}^{(1)}\right) + \mathcal{O}(\alpha_s^3) = \\ =& \underbrace{\frac{\alpha_s}{4\pi}\left(\frac{\mu_R^2}{\mu^2}\right)^{\epsilon} S_\epsilon^{-1} i\mathcal{M}^{(0)}}_{i\mathcal{M}_r^{(0)}} + \left(\frac{\alpha_s}{4\pi}\right)^2 \underbrace{\left(\frac{\mu_R^2}{\mu^2}\right)^{2\epsilon} S_\epsilon^{-2}\left(i\mathcal{M}^{(1)} - i\mathcal{M}^{\otimes}\right)}_{i\mathcal{M}_r^{(1)}} + \mathcal{O}(\alpha_s^3) \end{aligned} \tag{5.68}$$

where

$$i\mathcal{M}^{\otimes} = -\left(\frac{\mu_R^2}{\mu^2}\right)^{-\epsilon} S_\epsilon \left(\frac{n_g}{2}\delta Z_G + \delta Z_\alpha + \delta m_f^2 \frac{\partial}{\partial m_f^2}\right) i\mathcal{M}^{(0)} \tag{5.69}$$

summarizes the counterterms. Their explicit forms to $\mathcal{O}(\alpha_s^0)$ in the OS scheme (we will also use other schemes, see below) are given by [143]

$$\delta Z_G = -\left(\frac{\mu_R^2}{m_t^2}\right)^{\epsilon} \frac{2}{3\epsilon} \tag{5.70}$$

$$\delta Z_\alpha = -\frac{1}{\epsilon}\beta_0 - \delta Z_G \tag{5.71}$$

$$\delta m_f^2 = -\left(\frac{\mu_R^2}{m_f^2}\right)^{\epsilon} 6 m_f^2 C_F \left(\frac{1}{\epsilon} + \frac{4}{3}\right) + \mathcal{O}(\epsilon) \tag{5.72}$$

where $\beta_0 = 11C_A/3 - 2N_f/3$ is the LO term in the QCD beta-function with $N_f = 5$ light, i.e. massless quark flavours contributing to the gluon self energy[52] and the Casimir operators are given by $C_A = N_c$ and $C_F = (N_c^2-1)/(2N_c)$ and reduce to 3 and 4/3 for $N_c = 3$, respectively. In (5.70) and (5.71), the fermion mass has to be the top mass m_t, as all other masses are approximated as massless and their effects are included in β_0. For $n_g = 2$, however, δZ_α cancels anyways in (5.69). The mass renormalization (5.72), on the other hand, applies to all possible masses appearing in the loops. In practice, this means that while all quark masses are considered as massive when going through the loop, when appearing as external real radiation states to cancel the virtual IR infinities,

[52] This always includes the bottom-quark, irrespective its non-vanishing mass as a loop participant.

all quarks but the top can be treated as massless.
With $n_g = 2$, we are finally left with

$$i\mathcal{M}^{\otimes} = S_\epsilon \left(\frac{1}{\epsilon}\beta_0 + \beta_0 \ln \frac{\mu^2}{\mu_R^2} + 6m_f^2 C_F \left(\frac{1}{\epsilon} + \frac{4}{3} + \ln \frac{\mu^2}{m_f^2} \right) \frac{\partial}{\partial m_f^2} \right) i\mathcal{M}^{(0)} + \mathcal{O}(\epsilon) \quad (5.73)$$

At NLO, UV divergencies of a given virtual amplitude $i\mathcal{M}^{(1)}$ manifest themselves as single poles in $1/\epsilon$. They are canceled by the $1/\epsilon$-term in (5.73).
For our case (5.60), remembering that (5.61) is actually independent of m_f, we obtain

$$i\mathcal{M}_{r,NSM}^{LO+V} = \frac{\alpha_s}{4\pi} i\mathcal{M}_{r,NSM}^{(0)} + \left(\frac{\alpha_s}{4\pi}\right)^2 i\mathcal{M}_{r,NSM}^{(1)} \quad (5.74)$$

with

$$i\mathcal{M}_{r,NSM}^{(0)} = \left(\frac{\mu_R^2}{\mu^2}\right)^\epsilon S_\epsilon^{-1} \frac{ic_{ggh}}{v} \delta^{AB} H_{\lambda_1\lambda_2}^{gg} \quad (5.75)$$

$$i\mathcal{M}_{r,NSM}^{(1)} = \left(\frac{\mu_R^2}{\mu^2}\right)^\epsilon S_\epsilon^{-1} \frac{ic_{ggh}}{v} \delta^{AB} H_{\lambda_1\lambda_2}^{gg} N_c I(\epsilon) + \mathcal{O}(\epsilon) \quad (5.76)$$

where we defined

$$I(\epsilon) = -\frac{2}{\epsilon^2} - \frac{1}{\epsilon}\left(\frac{\beta_0}{N_c} + 2\tilde{L}\right) - \tilde{L}^2 + \frac{\pi^2}{6} \quad (5.77)$$

with

$$\tilde{L} \equiv \ln \frac{\mu_R^2}{-m_h^2} = \ln \frac{\mu_R^2}{m_h^2} + i\pi \quad (5.78)$$

Note that the renormalized coupling constant α_s implicitly depends on the renormalization scale μ_R and has to be adjusted accordingly. The final result (5.74) is now free from UV divergencies, but still contains IR poles. These need to be canceled by real radiation contributions. Before turning to them, let us first move to the virtual SM-like diagrams.

SM-like contribution

We now consider the two-loop diagrams featuring the SM-like coupling c_f, see Figures 4 and 5. Their direct computation reveals UV as well as IR divergencies that need renormalization as in the non-SM-like case. However, the explicit expressions are now far more involved [137, 140–142]. Note that only [141] includes the full unrenormalized and IR divergent bare amplitudes. The unrenormalized LO quark-loop amplitude (see Section 5.2) plus its divergent two-loop correction is given by

$$i\mathcal{M}_{SM}^{LO+V} \equiv \frac{i\alpha_s}{4\pi} H_{\lambda_1\lambda_2}^{gg} \delta^{AB} \sum_f \frac{y_f c_f}{2\sqrt{2}m_f} \left(\frac{2\tilde{J}(\tau_f,\epsilon)}{\tau_f} + \frac{\alpha_s}{\pi}\mathcal{A}_{gg} \right) \quad (5.79)$$

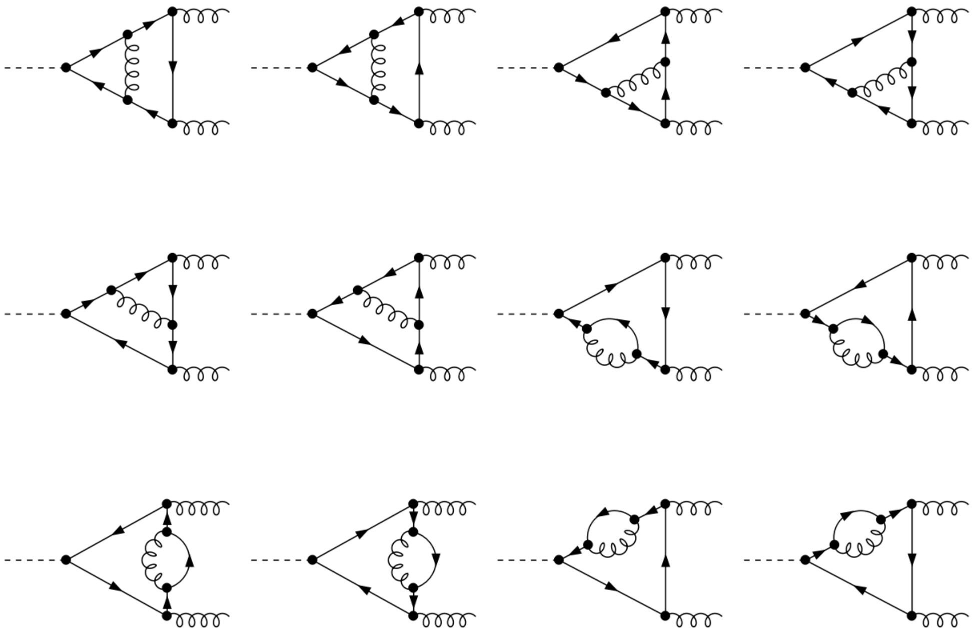

Figure 4: Two-loop diagrams (the layout was generated with [180]) representing the Abelian (proportional to C_F) corrections of $\mathcal{O}(\alpha_s^2)$ to the amplitude for $h \to gg$.

where $\tilde{J}(\tau_f, \epsilon)$ is defined in (5.48). The first term is just the c_f-part of (5.30), that now has to be evaluated up to $\mathcal{O}(\epsilon^2)$, whereas $\mathcal{A}_{gg}$ denotes its unrenormalized QCD correction, i.e. a quite complicated object. Upon renormalization (see (5.64)-(5.66)), we effectively replace

$$\frac{\alpha_s}{\pi}\left(\frac{2\tilde{J}(\tau_f,\epsilon)}{\tau_f} + \frac{\alpha_s}{\pi}\mathcal{A}_{gg}\right) \longrightarrow \frac{\alpha_s}{\pi}\left(\frac{\mu_R^2}{\mu^2}\right)^{\epsilon} S_\epsilon^{-1}\left(\frac{2\tilde{J}(\tau_f,\epsilon)}{\tau_f} + \frac{\alpha_s}{\pi}\left(\frac{\mu_R^2}{\mu^2}\right)^{\epsilon} S_\epsilon^{-1}(\mathcal{A}_{gg} - \mathcal{A}_{gg}^{\otimes})\right) \tag{5.80}$$

where the counterterm (5.69) reads

$$\mathcal{A}_{gg}^{\otimes} = -\frac{1}{4}\left(\frac{\mu_R^2}{\mu^2}\right)^{-\epsilon} S_\epsilon \left(-\frac{1}{\epsilon}\beta_0 + \delta m_f^2 \frac{\partial}{\partial m_f^2}\right)\frac{2\tilde{J}(\tau_f,\epsilon)}{\tau_f} \tag{5.81}$$

The explicit form of the counterterm up to $\mathcal{O}(\epsilon)$ depends on the scheme and is given by (see (5.72))

$$\delta m_f^2 = -6 m_f^2 C_F \begin{cases} \frac{1}{\epsilon} + \frac{4}{3} + \ln\frac{\mu_R^2}{m_f^2} & (OS) \\ \frac{1}{\epsilon} + \ln\frac{\mu_R^2}{\mu_f^2} & (\overline{\text{MS}}) \\ \frac{1}{\epsilon} + \frac{4}{3} + \ln\frac{\mu_R^2}{\mu_f^2} & (\text{scheme in [137, 140]}) \end{cases} \tag{5.82}$$

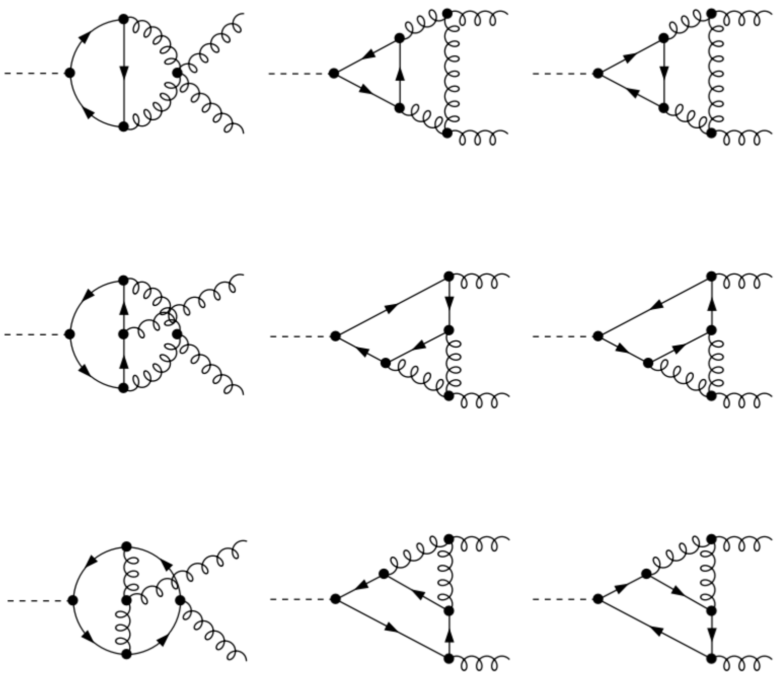

Figure 5: Non-Abelian (proportional to C_A) two-loop diagrams featuring three- and four-gluon vertices, which supplement the ones in Figure 4.

where μ_f is the scale at which the fermion mass is renormalized. We now employ the notation of [140] by writing (see also (5.49))

$$\frac{4}{3}F_0^H \equiv 2\tilde{J}(\tau_f)\tau_f \tag{5.83}$$

where $\tilde{J}(\tau_f)$ is given by (5.15). Furthermore, we write the ϵ-dependence in $F_0^H(\epsilon)$ only when higher order ϵ-terms are actually needed. This is the case for the LO term, as it eventually interferes with the NLO result which contains IR poles of $\mathcal{O}(\epsilon^{-2})$, as well as for the term in (5.81) which gets multiplied by β_0/ϵ (and of course anything contained in $\mathcal{A}_{gg}$). We finally end up with[53]

$$\frac{\alpha_s}{\pi}\left(\frac{4}{3}F_0^H(\epsilon) + \frac{\alpha_s}{\pi}\mathcal{A}_{gg}\right) \longrightarrow \frac{\alpha_s}{\pi}\left(\frac{\mu_R^2}{\mu^2}\right)^{\epsilon} S_\epsilon^{-1}\Bigg(\frac{4}{3}F_0^H(\epsilon)+$$

[53]Using

$$\frac{\partial}{\partial m_f^2} = -\frac{\tau_f}{m_f^2}\frac{\partial}{\partial \tau_f} \tag{5.84}$$

and

$$\frac{\partial}{\partial \tau_f}\frac{4}{3}F_0^H = \frac{2}{\tau_f^3}\big(-\tau_f + (2-\tau_f)f(\tau_f) + \tau_f(\tau_f-1)f'(\tau_f)\big) \equiv -\frac{2}{3\tau_f}F_0^H C_2^H \tag{5.85}$$

$$+\frac{\alpha_s}{\pi}\left(\frac{\mu_R^2}{\mu^2}\right)^{\epsilon} S_\epsilon^{-1}\left(\left(\frac{\mu_R^2}{\mu^2}\right)^{-\epsilon} S_\epsilon\left(\frac{1}{6}\frac{\delta m_f^2}{m_f^2}F_0^H C_2^H - \frac{1}{3\epsilon}\beta_0 F_0^H(\epsilon)\right)+\mathcal{A}_{gg}\right)\right) \tag{5.87}$$

The two-loop amplitude is now given by

$$\mathcal{A}_{gg} = \left(\frac{\mu_R^2}{\mu^2}\right)^{-\epsilon} S_\epsilon\left(-\frac{2}{3}N_c\left(\frac{\mu_R^2}{-m_h^2}\right)^{\epsilon}\left(\frac{1}{\epsilon^2}-\frac{\pi^2}{12}\right)F_0^H(\epsilon)+\right.$$
$$\left.+C_F F_0^H C_2^H\left(\frac{1}{\epsilon}+\frac{4}{3}+\ln\frac{\mu_R^2}{m_f^2}\right)+\mathcal{A}_{fin}\right)+\mathcal{O}(\epsilon) \tag{5.88}$$

Note that we have replaced the dependence on μ (which comes into play via dimensional regularization of the divergent two-loop diagrams) by the renormalization scale μ_R to $\mathcal{O}(\epsilon)$ by pulling out the factor $(\mu_R^2/\mu^2)^{-\epsilon}$. The finite terms read [140]

$$\mathcal{A}_{fin} \equiv C_F F_0^H C_1^H + \frac{2}{9}C_A\left(F_0^H B_1^H - 2F_0^H C_1^H\right) \tag{5.89}$$

where[54]

$$F_0^H C_1^H = -\frac{\theta_f(1+\theta_f+\theta_f^2+\theta_f^3)}{(1-\theta_f)^5}\big(108\mathrm{Li}_4(\theta_f)+144\mathrm{Li}_4(-\theta_f)-64\mathrm{Li}_3(\theta_f)\ln\theta_f+$$
$$-64\mathrm{Li}_3(-\theta_f)\ln\theta_f+14\mathrm{Li}_2(\theta_f)\ln^2\theta_f+8\mathrm{Li}_2(-\theta_f)\ln^2\theta_f+$$
$$+\frac{1}{12}\ln^4\theta_f+4\zeta(2)\ln^2\theta_f+16\zeta(3)\ln\theta_f+18\zeta(4)\big)-\frac{20\theta_f}{(1-\theta_f)^2}+$$
$$+\frac{\theta_f(1+\theta_f)^2}{(1-\theta_f)^4}\big(-32\mathrm{Li}_3(-\theta_f)+16\mathrm{Li}_2(-\theta_f)\ln\theta_f-4\zeta(2)\ln\theta_f\big)+$$
$$-\frac{4\theta_f(7-2\theta_f+7\theta_f^2)}{(1-\theta_f)^4}\mathrm{Li}_3(\theta_f)+\frac{8\theta_f(3-2\theta_f+3\theta_f^2)}{(1-\theta_f)^4}\mathrm{Li}_2(\theta_f)\ln\theta_f+$$

---

where a prime denotes derivation with respect to τ_f and

$$f(\tau_f) = -\frac{1}{4}\ln^2\left(\frac{\sqrt{1-\frac{1}{\tau_f}}-1}{\sqrt{1-\frac{1}{\tau_f}}+1}\right) = \begin{cases}\arcsin^2\sqrt{\tau_f} & \text{for } 0<\tau_f<1\\ -\frac{1}{4}\left(\ln\left(\frac{1-\sqrt{1-\frac{1}{\tau_f}}}{1+\sqrt{1-\frac{1}{\tau_f}}}\right)+i\pi\right)^2 & \text{for } 1\le\tau_f<\infty\end{cases} \tag{5.86}$$

[54] The HPL functions were already introduced in the appendix to Section 5.2 and the polylogarithms and zeta-functions are defined via

$$\mathrm{Li}_n(x) = \sum_{k=1}^{\infty}\frac{x^k}{k^n} = \int_0^x \frac{\mathrm{Li}_{n-1}(t)}{t}dt, \qquad \zeta(n) = \mathrm{Li}_n(1) \tag{5.90}$$

with the special cases

$$\mathrm{Li}_0(x) = \frac{x}{1-x}, \quad \mathrm{Li}_1(x) = -\ln(1-x), \quad \zeta(2) = \frac{\pi^2}{2}, \quad \zeta(4) = \frac{\pi^4}{90} \tag{5.91}$$

$$+\frac{2\theta_f(5-6\theta_f+5\theta_f^2)}{(1-\theta_f)^4}\ln(1-\theta_f)\ln^2\theta_f+\frac{\theta_f(3+25\theta_f-7\theta_f^2+3\theta_f^3)}{3(1-\theta_f)^5}\ln^3\theta_f+$$
$$+\frac{4\theta_f(1-14\theta_f+\theta_f^2)}{(1-\theta_f)^4}\zeta(3)+\frac{12\theta_f^2}{(1-\theta_f)^4}\ln^2\theta_f-\frac{12\theta_f(1+\theta_f)}{(1-\theta_f)^3}\ln\theta_f \tag{5.92}$$

and

$$F_0^H B_1^H=\frac{\theta_f(1+\theta_f)^2}{(1-\theta_f)^4}\Big(72H(\{1,0,-1,0\};\theta_f)+6\ln(1-\theta_f)\ln^3\theta_f-36\zeta(2)\mathrm{Li}_2(\theta_f)+$$
$$-36\zeta(2)\ln(1-\theta_f)\ln\theta_f-108\zeta(3)\ln(1-\theta_f)-64\mathrm{Li}_3(-\theta_f)$$
$$+32\mathrm{Li}_2(-\theta_f)\ln\theta_f-8\zeta(2)\ln\theta_f\Big)+$$
$$-\frac{36\theta_f(5+5\theta_f+11\theta_f^2+11\theta_f^3)}{(1-\theta_f)^5}\mathrm{Li}_4(-\theta_f)-\frac{36\theta_f(5+5\theta_f+7\theta_f^2+7\theta_f^3)}{(1-\theta_f)^5}\mathrm{Li}_4(\theta_f)+$$
$$+\frac{4\theta_f(1+\theta_f)(23+41\theta_f^2)}{(1-\theta_f)^5}\Big(\mathrm{Li}_3(\theta_f)+\mathrm{Li}_3(-\theta_f)\Big)\ln\theta_f+$$
$$-\frac{16\theta_f(1+\theta_f+\theta_f^2+\theta_f^3)}{(1-\theta_f)^5}\mathrm{Li}_2(-\theta_f)\ln^2\theta_f+\frac{\theta_f(1+\theta_f-17\theta_f^2-17\theta_f^3)}{(1-\theta_f)^5}\zeta(2)\ln^2\theta_f+$$
$$+\frac{\theta_f(5+5\theta_f-13\theta_f^2-13\theta_f^3)}{24(1-\theta_f)^5}\ln^4\theta_f-\frac{2\theta_f(5+5\theta_f+23\theta_f^2+23\theta_f^3)}{(1-\theta_f)^5}\mathrm{Li}_2(\theta_f)\ln^2\theta_f+$$
$$+\frac{2\theta_f(11+11\theta_f-43\theta_f^2-43\theta_f^3)}{(1-\theta_f)^5}\zeta(3)\ln\theta_f+\frac{36\theta_f(1+\theta_f-3\theta_f^2-3\theta_f^3)}{(1-\theta_f)^5}\zeta(4)+$$
$$-\frac{2\theta_f(55+82\theta_f+55\theta_f^2)}{(1-\theta_f)^4}\mathrm{Li}_3(\theta_f)+\frac{2\theta_f(51+74\theta_f+51\theta_f^2)}{(1-\theta_f)^4}\mathrm{Li}_2(\theta_f)\ln\theta_f+$$
$$+\frac{\theta_f(47+66\theta_f+47\theta_f^2)}{(1-\theta_f)^4}\ln(1-\theta_f)\ln^2\theta_f+\frac{\theta_f(6+59\theta_f+58\theta_f^2+33\theta_f^3)}{3(1-\theta_f)^5}\ln^3\theta_f+$$
$$+\frac{2\theta_f(31+34\theta_f+31\theta_f^2)}{(1-\theta_f)^4}\zeta(3)+\frac{3\theta_f(3+22\theta_f+3\theta_f^2)}{2(1-\theta_f)^4}\ln^2\theta_f+$$
$$-\frac{24\theta_f(1+\theta_f)}{(1-\theta_f)^3}\ln\theta_f-\frac{94\theta_f}{(1-\theta_f)^2} \tag{5.93}$$

with θ_f defined in (5.47).
Finally, we can write down a compact form of the renormalized SM-like NLO amplitude, namely

$$i\mathcal{M}_{r,SM}^{LO+V}=\frac{i\alpha_s}{4\pi}H_{\lambda_1\lambda_2}^{gg}\delta^{AB}\left(\frac{\mu_R^2}{\mu^2}\right)^{\epsilon}S_\epsilon^{-1}\sum_f\frac{y_f c_f}{2\sqrt{2}m_f}\Bigg(\frac{4}{3}F_0^H(\epsilon)+$$
$$+\frac{\alpha_s}{\pi}\left(\mathcal{A}_{fin}+\frac{N_c}{3}I(\epsilon)F_0^H(\epsilon)+C_F F_0^H C_2^H X(\mu_f^2)\right)\Bigg) \tag{5.94}$$

where

$$X(\mu_f^2) = \begin{cases} 0 & (OS) \\ \frac{4}{3} + \ln \frac{\mu_f^2}{m_f^2} & (\overline{\text{MS}}) \\ \ln \frac{\mu_f^2}{m_f^2} & (\text{scheme in [137, 140]}) \end{cases} \tag{5.95}$$

Combined together with (5.74), we obtain the fully-fledged NLO QCD amplitude

$$\begin{aligned} i\mathcal{M}_r^{LO+V} = &\frac{i\alpha_s}{4\pi} H_{\lambda_1\lambda_2}^{gg} \delta^{AB} \left(\frac{\mu_R^2}{\mu^2}\right)^{\epsilon} S_\epsilon^{-1} \Bigg(\frac{c_{ggh}}{v} \left(1 + \frac{\alpha_s}{4\pi} N_c I(\epsilon)\right) + \\ &+ \sum_f \frac{y_f c_f}{2\sqrt{2} m_f} \left(\frac{4}{3} F_0^H(\epsilon) + \frac{\alpha_s}{\pi} \left(\mathcal{A}_{fin} + \frac{N_c}{3} I(\epsilon) F_0^H(\epsilon) + C_F F_0^H C_2^H X(\mu_f^2) \right) \right) \Bigg) \end{aligned} \tag{5.96}$$

resulting in

$$\begin{aligned} d\Gamma^{LO\times V} = &\frac{\alpha_s^3 m_h^3}{16\pi^3} (N_c^2 - 1) \left(\frac{\mu_R^2}{\mu^2}\right)^{2\epsilon} S_\epsilon^{-2} \operatorname{Re}\Bigg\{ \left(\frac{c_{ggh}}{v} + \sum_f \frac{y_f c_f}{2\sqrt{2} m_f} \frac{4}{3} \left(F_0^H(\epsilon)\right)^* \right) \times \\ &\times \left(\frac{c_{ggh}}{4v} N_c I(\epsilon) + \sum_f \frac{y_f c_f}{2\sqrt{2} m_f} \left(\mathcal{A}_{fin} + \frac{N_c}{3} I(\epsilon) F_0^H(\epsilon) + C_F F_0^H C_2^H X(\mu_f^2) \right) \right) \Bigg\} d\Phi_2 \end{aligned} \tag{5.97}$$

This expression is, however, not finite upon sending $\epsilon \to 0$. It contains the object $I(\epsilon)$ which collects the IR behavior of the virtual amplitudes. According to the Kinoshita-Lee-Nauenberg (KLN) theorem [181, 182], the IR singularities of the $LO \times V$ decay rate - it is of $\mathcal{O}(\alpha_s^3)$ - have to be canceled against phase space singularities of the $R \times R$ decay rate which is also of $\mathcal{O}(\alpha_s^3)$. The latter consists of the real radiation corrections - with amplitudes of $\mathcal{O}(g_s^3)$ - which we will turn to in the next two subsections.

Appendix: Explicit calculation of the one-loop integrals

This appendix highlights the calculational details for the virtual one-loop diagrams (5.55) and (5.56). The first contribution is given by (see Appendix C for the conventions and abbreviations)

$$i\mathcal{M}_{1,NSM}^V = -\frac{g_s^4 c_{ggh}}{16\pi^2 v} \epsilon_\mu^*(k_1) \epsilon_\nu^*(k_2) I^{AB\mu\nu} \tag{5.98}$$

with

$$I^{AB\mu\nu} \equiv W_{\alpha\beta\gamma\sigma}^{ABCC} g^{\mu\alpha} g^{\nu\beta} \mu^{2\epsilon} \int \frac{d^d k}{(2\pi)^d} \frac{(k^2 + q\cdot k) g^{\gamma\sigma} - k^\gamma k^\sigma - q^\gamma k^\sigma}{k^2 (k+q)^2} \tag{5.99}$$

An extra symmetry factor of 1/2 had to be introduced in (5.98) as the gluon is its own anti-particle. The $i\eta$-prescription has been suppressed. It can be restored upon noting that $q^2 = m_h^2$ should be replaced by $m_h^2 + i\eta$ in the denominator, so $-m_h^2 \to m_h^2 e^{-i\pi}$ inside logarithms.
Introducing the Feynman parameter x and shifting $k \to k - xq$, we arrive at

$$I^{AB\mu\nu} = W^{ABCC}_{\alpha\beta\gamma\sigma} g^{\mu\alpha} g^{\nu\beta} \int_0^1 dx \, \mu^{2\epsilon} \int \frac{d^dk}{(2\pi)^d} \frac{N^{\gamma\sigma}}{(k^2 + x(1-x)q^2)^2} \tag{5.100}$$

where the numerator is given by

$$N^{\gamma\sigma} \equiv (g^{\delta\tau} g^{\gamma\sigma} - g^{\delta\gamma} g^{\sigma\tau}) k_\delta k_\tau - x(1-x)(q^2 g^{\gamma\sigma} - q^\gamma q^\sigma) \tag{5.101}$$

Employing (D.17) and (D.18) and carefully taking care of all $\mathcal{O}(\epsilon)$-terms, we end up with

$$\begin{aligned} i\mathcal{M}^V_{1,NSM} =& \frac{i g_s^4 c_{ggh}}{256\pi^4 v} \epsilon^*_\mu(k_1) \epsilon^*_\nu(k_2) f^{ACD} f^{BCD} \left(\frac{13}{6} \left(\frac{1}{\epsilon} + \ln\frac{4\pi}{e^\gamma} + \ln\frac{\mu^2}{q^2} + i\pi + \frac{44}{39} \right) q^2 g^{\mu\nu} + \right. \\ & \left. + \frac{1}{3} \left(\frac{1}{\epsilon} + \ln\frac{4\pi}{e^\gamma} + \ln\frac{\mu^2}{q^2} + i\pi + \frac{5}{3} \right) k_1^\nu k_2^\mu \right) + \mathcal{O}(\epsilon) = \\ =& \frac{i g_s^4 c_{ggh}}{128\pi^4 v} \epsilon^*_\mu(k_1) \epsilon^*_\nu(k_2) f^{ACD} f^{BCD} \left(\frac{\mu^2 4\pi}{-m_h^2 e^\gamma} \right)^\epsilon \cdot \\ & \cdot \left(\left(\frac{13}{6\epsilon} + \frac{22}{9} \right) g^{\mu\nu} k_1 \cdot k_2 + \left(\frac{1}{6\epsilon} + \frac{5}{18} \right) k_1^\nu k_2^\mu \right) + \mathcal{O}(\epsilon) \end{aligned} \tag{5.102}$$

where we have used $\ln(-q^2) = \ln(q^2) - i\pi$. Note that the final result is IR finite. This could have been anticipated since the Higgs-gluon-gluon vertex in fact vanishes when one of the gluon propagators gets on-shell, so the IR-divergent region does not contribute.
The second diagram reads

$$i\mathcal{M}^V_{2,NSM} = \frac{g_s^4 c_{ggh}}{8\pi^2 v} \epsilon^*_\mu(k_1) \epsilon^*_\nu(k_2) \tilde{I}^{AB\mu\nu} \tag{5.103}$$

$$\tag{5.104}$$

where

$$\tilde{I}^{AB\mu\nu} \equiv \mu^{2\epsilon} \int \frac{d^dk}{(2\pi)^d} \frac{N^{AB\mu\nu}}{k^2 (k+k_1)^2 (k-k_2)^2} \tag{5.105}$$

with

$$\begin{aligned} N^{AB\mu\nu} \equiv & \big((k+k_1) \cdot (k-k_2) g^{\sigma\gamma} - (k+k_1)^\gamma (k-k_2)^\sigma \big) \cdot \\ & \cdot V^{ACD}_{\sigma\tau\alpha}(k+k_1, k_1, k) g^{\mu\tau} g^{\nu\delta} g^{\alpha\beta} V^{BDC}_{\beta\delta\gamma}(k, k_2, k-k_2) \end{aligned} \tag{5.106}$$

Unfortunately, apart from the colour part (which is simply $-f^{ACD}f^{BDC}$), the expanded expression for the numerator is quite lengthy. Ultimately, we have to calculate the integral

$$\mu^{2\epsilon}\int\frac{d^dk}{(2\pi)^d}\frac{A^{\alpha\beta\gamma\sigma\mu\nu}k_\alpha k_\beta k_\gamma k_\sigma+A^{\alpha\gamma\sigma\mu\nu}k_\alpha k_\gamma k_\sigma+A^{\gamma\sigma\mu\nu}k_\gamma k_\sigma+A^{\gamma\mu\nu}k_\gamma+A^{\mu\nu}}{k^2(k+k_1)^2(k-k_2)^2} \tag{5.107}$$

with

$$A^{\alpha\beta\gamma\sigma\mu\nu}\equiv g^{\alpha\beta}g^{\gamma\sigma}g^{\mu\nu}+(4d-5)g^{\alpha\beta}g^{\gamma\mu}g^{\sigma\nu} \tag{5.108}$$

$$A^{\alpha\gamma\sigma\mu\nu}\equiv(4d-6)g^{\mu\gamma}g^{\nu\sigma}(k_1^\alpha-k_2^\alpha)+3g^{\gamma\sigma}g^{\mu\nu}(k_1^\alpha-k_2^\alpha)-g^{\gamma\sigma}g^{\mu\alpha}k_1^\nu+g^{\gamma\sigma}g^{\nu\alpha}k_2^\mu \tag{5.109}$$

$$\begin{aligned}A^{\gamma\sigma\mu\nu}\equiv{}&4(4-d)g^{\mu\gamma}g^{\nu\sigma}k_1\cdot k_2+2g^{\mu\nu}(k_1^\sigma k_1^\gamma+k_2^\sigma k_2^\gamma)+9g^{\gamma\sigma}(k_1^\nu k_2^\mu-k_1\cdot k_2g^{\mu\nu})+\\&-6g^{\nu\sigma}k_2^\mu k_1^\gamma-6g^{\mu\sigma}k_1^\nu k_2^\gamma-2g^{\nu\sigma}k_2^\mu k_2^\gamma-2g^{\mu\sigma}k_1^\nu k_1^\gamma\end{aligned} \tag{5.110}$$

$$A^{\gamma\mu\nu}\equiv 6(k_1^\gamma-k_2^\gamma)(k_1^\nu k_2^\mu-g^{\mu\nu}k_1\cdot k_2) \tag{5.111}$$

$$A^{\mu\nu}=4k_1\cdot k_2(g^{\mu\nu}k_1\cdot k_2-k_1^\nu k_2^\mu) \tag{5.112}$$

Introducing Feynman parameters y and z and shifting $k\to k-yk_1+zk_2$, we obtain

$$\tilde{I}^{AB\mu\nu}=-2f^{ACD}f^{BDC}\int_0^1dz\int_0^{1-z}dy\mu^{2\epsilon}\int\frac{d^dk}{(2\pi)^d}\frac{\tilde{A}^{\alpha\beta\gamma\sigma\mu\nu}k_\alpha k_\beta k_\gamma k_\sigma+\tilde{A}^{\gamma\sigma\mu\nu}k_\gamma k_\sigma+\tilde{A}^{\mu\nu}}{(k^2+2yzk_1\cdot k_2)^3} \tag{5.113}$$

where

$$\tilde{A}^{\alpha\beta\gamma\sigma\mu\nu}\equiv g^{\alpha\beta}g^{\gamma\sigma}g^{\mu\nu}+(4d-5)g^{\alpha\beta}g^{\gamma\mu}g^{\sigma\nu} \tag{5.114}$$

$$\begin{aligned}\tilde{A}^{\gamma\sigma\mu\nu}\equiv{}&g^{\mu\nu}\big((4y^2-6y+2)k_1^\gamma k_1^\sigma+(4z^2-6z+2)k_2^\gamma k_2^\sigma+\\&+(6y-8yz+6z)k_1^\gamma k_2^\sigma-(4yz-3y-3z+9)g^{\gamma\sigma}k_1\cdot k_2\big)+\\&+2g^{\mu\sigma}k_1^\nu\big((4dy^2-5y^2-2dy+4y-1)k_1^\gamma-(4dyz-2dy-5yz+3y+z+3)k_2^\gamma\big)+\\&+2g^{\nu\sigma}k_2^\mu\big((4dz^2-5z^2-2dz+4z-1)k_2^\gamma-(4dyz-2dz-5yz+3z+y+3)k_1^\gamma\big)+\\&+2g^{\gamma\mu}g^{\sigma\nu}k_1\cdot k_2(-4dyz+2dy+2dz-2d+5yz-3y-3z+8)+\\&-g^{\gamma\sigma}k_1^\nu k_2^\mu(4dyz-5yz+y+z-9)\end{aligned} \tag{5.115}$$

$$\begin{aligned}\tilde{A}^{\mu\nu}\equiv{}&2g^{\mu\nu}(k_1\cdot k_2)^2(2y^2z^2-3y^2z+y^2-3yz^2+9yz-3y+z^2-3z+2)+\\&+2k_1^\nu k_2^\mu k_1\cdot k_2(4dy^2z^2-5y^2z^2-2dy^2z+\\&+4y^2z-y^2-2dyz^2+4yz^2+2dyz-11yz+3y-z^2+3z-2)\end{aligned} \tag{5.116}$$

Using (D.13), (D.14) and (D.15), we eventually find

$$\begin{aligned}&2\int_0^1dz\int_0^{1-z}dy\mu^{2\epsilon}\int\frac{d^dk}{(2\pi)^d}\frac{\tilde{A}^{\alpha\beta\gamma\sigma\mu\nu}k_\alpha k_\beta k_\gamma k_\sigma}{(k^2+2yzk_1\cdot k_2)^3}=\\&=-\frac{i}{16\pi^2}\left(\frac{\mu^2 4\pi}{-m_h^2e^\gamma}\right)^\epsilon g^{\mu\nu}k_1\cdot k_2\left(\frac{15}{8\epsilon}+\frac{65}{16}\right)+\mathcal{O}(\epsilon^2)\end{aligned} \tag{5.117}$$

$$2\int_0^1 dz \int_0^{1-z} dy \mu^{2\epsilon} \int \frac{d^dk}{(2\pi)^d} \frac{\tilde{A}^{\gamma\sigma\mu\nu} k_\gamma k_\sigma}{(k^2 + 2yzk_1 \cdot k_2)^3} =$$
$$= \frac{i}{16\pi^2} \left(\frac{\mu^2 4\pi}{-m_h^2 e^\gamma} \right)^\epsilon \left(-\left(\frac{127}{24\epsilon} + \frac{1723}{144} \right) g^{\mu\nu} k_1 \cdot k_2 + \left(\frac{29}{6\epsilon} + \frac{871}{72} \right) k_1^\nu k_2^\mu \right) + \mathcal{O}(\epsilon) \tag{5.118}$$

$$2\int_0^1 dz \int_0^{1-z} dy \mu^{2\epsilon} \int \frac{d^dk}{(2\pi)^d} \frac{\tilde{A}^{\mu\nu}}{(k^2 + 2yzk_1 \cdot k_2)^3} =$$
$$= \frac{i}{16\pi^2} \left(\frac{\mu^2 4\pi}{-m_h^2 e^\gamma} \right)^\epsilon \left(\left(\frac{2}{\epsilon^2} + \frac{5}{\epsilon} + \frac{163}{12} - \frac{\pi^2}{6} \right) g^{\mu\nu} k_1 \cdot k_2 + \right.$$
$$\left. - \left(\frac{2}{\epsilon^2} + \frac{5}{\epsilon} + \frac{99}{8} - \frac{\pi^2}{6} \right) k_1^\nu k_2^\mu \right) + \mathcal{O}(\epsilon) \tag{5.119}$$

When the dust settles, we arrive at

$$i\mathcal{M}^V_{2,NSM} = \frac{ig_s^4 c_{ggh}}{128\pi^4 v} \epsilon^*_\mu(k_1)\epsilon^*_\nu(k_2) f^{ACD} f^{BCD} \left(\frac{\mu^2 4\pi}{-m_h^2 e^\gamma} \right)^\epsilon \left(1 - \frac{\pi^2}{12}\epsilon^2 \right) \cdot$$
$$\cdot \left(\left(\frac{2}{\epsilon^2} - \frac{13}{6\epsilon} - \frac{22}{9} \right) g^{\mu\nu} k_1 \cdot k_2 - \left(\frac{2}{\epsilon^2} + \frac{1}{6\epsilon} + \frac{5}{18} \right) k_1^\nu k_2^\mu \right) + \mathcal{O}(\epsilon) \tag{5.120}$$

The $\mathcal{O}(1/\epsilon^2)$-term indicates an IR pole. This had to be expected as one of the loop gluons might get on-shell resulting in a diverging propagator. The IR poles will drop out in the full decay rate by virtue of phase space integration associated with soft real radiation diagrams. The final combined result (5.57) is obtained upon using $f^{ACD} f^{BCD} = N_c \delta^{AB}$. It is worth noting that all $\mathcal{O}(1/\epsilon)$-terms cancel in an almost magical way in (5.102) and (5.120) leaving only the explicit IR pole $1/\epsilon^2$ behind.
One might think that the following three contributions should also be taken into account (symmetry factors have been dropped):

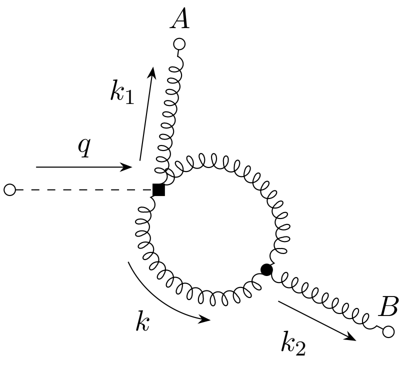

$$\equiv i\mathcal{M}^V_{3,NSM} = -\frac{g_s^4 c_{ggh}}{8\pi^2 v} \epsilon^*_\mu(k_1)\epsilon^*_\nu(k_2) J^{AB\mu\nu}_{1,2} \tag{5.121}$$

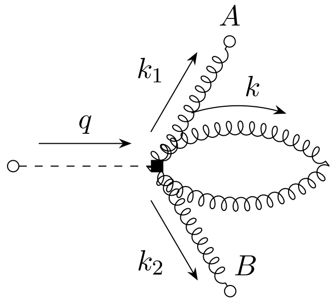

$$\equiv i\mathcal{M}^{V}_{5,NSM} = \frac{g_s^4 c_{ggh}}{8\pi^2 v}\epsilon^*_\mu(k_1)\epsilon^*_\nu(k_2)J^{AB\mu\nu} \tag{5.122}$$

where we have defined

$$J^{AB\mu\nu}_{1,2} \equiv \mu^{2\epsilon}\int \frac{d^dk}{(2\pi)^d}\frac{V^{CAD}_{\alpha\gamma\beta}(k-k_2,k_1,k)g^{\mu\gamma}g^{\nu\delta}g^{\alpha\sigma}g^{\beta\lambda}V^{DBC}_{\lambda\delta\sigma}(k,k_2,k-k_2)}{k^2(k-k_2)^2} \tag{5.123}$$

and

$$J^{AB\mu\nu} \equiv W^{ABCC}_{\alpha\beta\lambda\sigma}g^{\mu\alpha}g^{\nu\beta}g^{\lambda\sigma}\mu^{2\epsilon}\int\frac{d^dk}{(2\pi)^d}\frac{1}{k^2} \tag{5.124}$$

The amplitude $i\mathcal{M}^V_{4,NSM}$ is related to $i\mathcal{M}^V_{3,NSM}$ by interchanging the external gluons, which leads to the replacement of $J^{AB\mu\nu}_{1,2}$ by $J^{BA\nu\mu}_{2,1}$. Thee loop integrals $J^{AB\mu\nu}_{1,2}$ and $J^{AB\mu\nu}$ vanish due to being scaleless (see Appendix D), so the amplitudes $i\mathcal{M}^V_{3,NSM}$, $i\mathcal{M}^V_{4,NSM}$ and $i\mathcal{M}^V_{5,NSM}$ are in fact zero.

5.4. Real QCD corrections ($h \to g\bar{q}q$)

Non-SM-like contribution

Real radiation contributions are associated with soft and collinear emission channels which can not be distinguished from a gluon. In the case of one gluon and two massless quarks in the final state, there is one diagram with effective Higgs-gluon-gluon-vertex to consider, namely

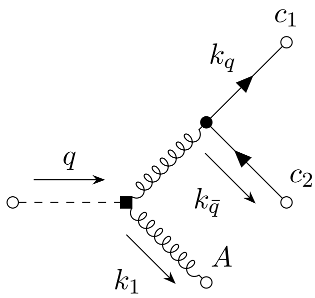

$$\equiv i\mathcal{M}^{R,g\bar{q}q}_{NSM} \tag{5.125}$$

for which we define $s_{1q} = (k_1+k_q)^2$, $s_{1\bar{q}} = (k_1+k_{\bar{q}})^2$ and $s_{q\bar{q}} = (k_q+k_{\bar{q}})^2$ with $m_h^2 = s_{1q}+s_{1\bar{q}}+s_{q\bar{q}}$ and find

$$i\mathcal{M}^{R,g\bar{q}q}_{NSM} = \frac{ig_s^3 c_{ggh}}{16\pi^2 v s_{q\bar{q}}}\epsilon^*_\mu(k_1)T^A_{c_1c_2}\bar{u}(k_q)\big((m_h^2 - s_{q\bar{q}})\gamma^\mu - 2\not{k}_1(k_q^\mu + k_{\bar{q}}^\mu)\big)v(k_{\bar{q}}) \tag{5.126}$$

This expression can easily be converted into the spinor-helicity formalism using the relations

$$H^{gq\bar{q}}_{+++} = 0,\ H^{gq\bar{q}}_{---} = 0,\ H^{gq\bar{q}}_{+--} = 0,\ H^{gq\bar{q}}_{-++} = 0,$$
$$H^{gq\bar{q}}_{+-+} = -\frac{\langle 1q\rangle^2}{\langle q\bar{q}\rangle},\ H^{gq\bar{q}}_{-+-} = \frac{[1q]^2}{[q\bar{q}]},\ H^{gq\bar{q}}_{++-} = \frac{\langle 1\bar{q}\rangle^2}{\langle q\bar{q}\rangle},\ H^{gq\bar{q}}_{--+} = -\frac{[1\bar{q}]^2}{[q\bar{q}]} \tag{5.127}$$

where

$$H^{gq\bar{q}}_{\lambda_1\lambda_q\lambda_{\bar{q}}} \equiv \frac{1}{\sqrt{2}s_{q\bar{q}}}\epsilon^*_{\mu\lambda_1}(k_1, k_q + k_{\bar{q}})\bar{u}_{\lambda_q}(k_q)\big((m_h^2 - s_{q\bar{q}})\gamma^\mu - 2\not{k}_1(k_q^\mu + k_{\bar{q}}^\mu)\big)v_{\lambda_{\bar{q}}}(k_{\bar{q}}) \tag{5.128}$$

for the gluon, quark and anti- quark helicities λ_1, λ_q and $\lambda_{\bar{q}}$, yielding the compact form

$$i\mathcal{M}^{R,g\bar{q}q}_{NSM} = \frac{ig_s^3 c_{ggh}\sqrt{2}}{16\pi^2 v}T^A_{c_1c_2}H^{gq\bar{q}}_{\lambda_1\lambda_q\lambda_{\bar{q}}} \tag{5.129}$$

SM-like contribution

We now have the contribution

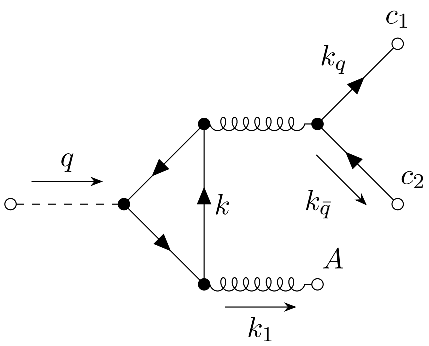

$$\equiv i\mathcal{M}^{R,g\bar{q}q}_{1,SM} \tag{5.130}$$

and its fermion flow reversed relative $i\mathcal{M}^{R,g\bar{q}q}_{2,SM}$. Explicit calculations can be found in the appendix to this subsection. The final result $i\mathcal{M}^{R,g\bar{q}q}_{SM} = i\mathcal{M}^{R,g\bar{q}q}_{1,SM} + i\mathcal{M}^{R,g\bar{q}q}_{2,SM}$ is given by

$$\begin{aligned} i\mathcal{M}^{R,g\bar{q}q}_{SM} =& \frac{ig_s^3}{16\pi^2 s_{q\bar{q}}}T^A_{c_1c_2}\epsilon^*_\mu(k_1)\bar{u}(k_q)\gamma_\nu v(k_{\bar{q}})\cdot \\ &\cdot \sum_f \frac{y_f c_f}{\sqrt{2}m_f}\left(2k_1^\nu(k_q^\mu + k_{\bar{q}}^\mu) - (m_h^2 - s_{q\bar{q}})g^{\mu\nu}\right)\frac{F(\tau_f,\kappa_f)}{(\kappa_f - \tau_f)^2} \end{aligned} \tag{5.131}$$

where the loop-function $F(\tau_f, \kappa_f)$ is defined below (see (5.146) and (5.148)). Using (5.128), this can be cast in the form

$$i\mathcal{M}^{R,g\bar{q}q}_{SM} = -\frac{ig_s^3\sqrt{2}}{16\pi^2}T^A_{c_1c_2}H^{gq\bar{q}}_{\lambda_1\lambda_q\lambda_{\bar{q}}}\sum_f \frac{y_f c_f}{\sqrt{2}m_f}\frac{F(\tau_f,\kappa_f)}{(\kappa_f - \tau_f)^2} \tag{5.132}$$

The final result for the real radiation quark channel thus reads

$$
\begin{aligned}
i\mathcal{M}^{R,g\bar{q}q} \equiv& i\mathcal{M}^{R,g\bar{q}q}_{NSM} + i\mathcal{M}^{R,g\bar{q}q}_{SM} = \\
=& \frac{ig_s^3\sqrt{2}}{16\pi^2} T^A_{c_1c_2} H^{gq\bar{q}}_{\lambda_1\lambda_q\lambda_{\bar{q}}} \left(\frac{c_{ggh}}{v} - \sum_f \frac{y_f c_f}{\sqrt{2}m_f} \frac{F(\tau_f,\kappa_f)}{(\kappa_f-\tau_f)^2} \right)
\end{aligned} \tag{5.133}
$$

To check the consistency of our results, let us now consider the heavy-top limit for this amplitude (see also (5.34)). Writing $\kappa_t = r\tau_t$ with $r = s_{\bar{q}q}/m_h^2$, there is only one parameter entering the limit. We find

$$
\begin{aligned}
-\frac{F(\tau_f,\kappa_f)}{(\kappa_f-\tau_f)^2} =& \frac{2}{3} + \frac{7}{45}\tau_t + \frac{4}{63}\tau_t^2 + \frac{52}{1575}\tau_t^3 + \left(\frac{11}{45}\tau_t + \frac{32}{315}\tau_t^2 + \frac{4}{75}\tau_t^3\right) r + \\
&+ \left(\frac{44}{315}\tau_t^2 + \frac{116}{1575}\tau_t^3\right) r^2 + \frac{148}{1575}\tau_t^3 r^3 + \mathcal{O}\left(\tau_t^4\right)
\end{aligned} \tag{5.134}
$$

The $\mathcal{O}(r^0)$-terms can be matched to (5.35) for $c_t = 1$ and Yukawa-like Higgs-top coupling and are thus associated with a diagram of the form (5.125) in the heavy-top limit. The remaining $\mathcal{O}(r^k)$-terms with $k \geq 1$ correspond to a local interaction

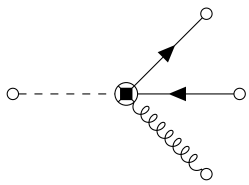

(5.135)

where the encircled square symbolizes a local interaction with $d_\chi \geq 6$. For instance, for $k = 1$, the local operator

$$
\frac{g_s^3 c_{g\bar{q}qh}}{16\pi^2 v m_t^2} \bar{q}\gamma^\mu T^A q G^A_{\mu\nu}\partial^\nu h \tag{5.136}
$$

with

$$
c_{g\bar{q}qh} = \frac{11}{180} + \frac{8}{315}\tau_t + \frac{1}{75}\tau_t^2 + \mathcal{O}\left(\tau_t^3\right) \tag{5.137}
$$

for $c_t = 1$ and Yukawa-like Higgs-top coupling has chiral dimension $d_\chi = 6$ and scales like $\sim 1/(16\pi^2 m_t^2)$. For higher k, derivatives on the quark current are needed. These come with extra suppression of the heavy mass m_t via the increasing power of τ_t. In any case, EWChL contributions like (5.135)-(5.136) with m_t replaced by some heavy mass scale are beyond the scope of this work.

Appendix: Calculational details for the SM-like contribution

The quantitative expressions for the two contributions are given by

$$
i\mathcal{M}^{R,g\bar{q}q}_{1,SM} = \frac{g_s^3 y_f c_f}{\sqrt{2}(k_q+k_{\bar{q}})^2} T^B_{c_1c_2} Tr(T^B T^A)\epsilon^*_\mu(k_1)\bar{u}(k_q)\gamma_\nu v(k_{\bar{q}}) I^{\mu\nu} \tag{5.138}
$$

and

$$i\mathcal{M}^{R,g\bar{q}q}_{2,SM} = \frac{g_s^3 y_f c_f}{\sqrt{2}(k_q+k_{\bar{q}})^2} T^B_{c_1c_2} Tr(T^B T^A)\epsilon^*_\mu(k_1)\bar{u}(k_q)\gamma_\nu v(k_{\bar{q}})J^{\mu\nu} \tag{5.139}$$

with

$$I^{\mu\nu} \equiv \mu^{2\epsilon}\int \frac{d^dk}{(2\pi)^d}\frac{Tr\big((\not{k}-\not{k}_q-\not{k}_{\bar{q}}+m_f)\gamma^\nu(\not{k}+m_f)\gamma^\mu(\not{k}+\not{k}_1+m_f)\big)}{\big((k+k_1)^2-m_f^2\big)(k^2-m_f^2)\big((k-k_q-k_{\bar{q}})^2-m_f^2\big)} \tag{5.140}$$

$$J^{\mu\nu} \equiv \mu^{2\epsilon}\int \frac{d^dk}{(2\pi)^d}\frac{Tr\big((\not{k}-\not{k}_1+m_f)\gamma^\mu(\not{k}+m_f)\gamma^\nu(\not{k}+\not{k}_q+\not{k}_{\bar{q}}+m_f)\big)}{\big((k-k_1)^2-m_f^2\big)(k^2-m_f^2)\big((k+k_q+k_{\bar{q}})^2-m_f^2\big)} \tag{5.141}$$

The Dirac equation implies $\bar{u}(k_q)(\not{k}_q+\not{k}_{\bar{q}})v(k_{\bar{q}}) = 0$, so we can take over the results from the LO SM calculation in Subsection 5.2, where the same role is played by the transversality condition $k_2^\nu\epsilon^*_\nu(k_2) = 0$. Defining $k_{q\bar{q}} \equiv k_q + k_{\bar{q}}$ and dropping terms proportion to k_1^μ and $k_{q\bar{q}}^\nu$, we find the numerator of $I^{\mu\nu}$ to be given by

$$\begin{aligned}&Tr\big((\not{k}-\not{k}_{q\bar{q}}+m_f)\gamma^\nu(\not{k}+m_f)\gamma^\mu(\not{k}+\not{k}_1+m_f)\big) = \\ &= 4m_f\big((4g^{\mu\alpha}g^{\nu\beta}-g^{\mu\nu}g^{\alpha\beta})k_\alpha k_\beta + (m_f^2 - k_1\cdot k_{q\bar{q}})g^{\mu\nu} + k_1^\nu k_{q\bar{q}}^\mu\big)\end{aligned} \tag{5.142}$$

Using the same arguments as in Subsection 5.2, we find $I^{\mu\nu} = J^{\mu\nu}$ and thus $i\mathcal{M}^{R,g\bar{q}q}_{SM} \equiv i\mathcal{M}^{R,g\bar{q}q}_{1,SM} + i\mathcal{M}^{R,g\bar{q}q}_{1,SM} = 2i\mathcal{M}^{R,g\bar{q}q}_{1,SM}$. The situation is, however, a bit more involved, since $k_1^2 = 0$, but $k_{q\bar{q}}^2 = s_{q\bar{q}} \neq 0$. Shifting the loop momentum $k \to k - yk_1 + zk_{q\bar{q}}$ and introducing Feynman parameters, we arrive at

$$I^{\mu\nu} = \int_0^1 dz\int_0^{1-z} dy\mu^{2\epsilon}\int\frac{d^dk}{(2\pi)^d}\frac{N^{\mu\nu}}{\big(k^2-m_f^2+yz(m_h^2-s_{q\bar{q}})+z(1-z)s_{q\bar{q}}\big)^3} \tag{5.143}$$

where

$$\begin{aligned}N^{\mu\nu} =& 4m_f\big((8g^{\mu\alpha}g^{\nu\beta}-2g^{\mu\nu}g^{\alpha\beta})k_\alpha k_\beta + \\ &+ 2m_f^2 g^{\mu\nu} - 2z^2 s_{q\bar{q}}g^{\mu\nu} - (1-2yz)(m_h^2-s_{q\bar{q}})g^{\mu\nu} + (2-8yz)k_1^\nu k_{q\bar{q}}^\mu\big)\end{aligned} \tag{5.144}$$

Performing the momentum integral and defining $\tau_f \equiv m_h^2/4m_f^2$ as before and $\kappa_f \equiv s_{q\bar{q}}/4m_f^2$ results in the gauge invariant expression

$$\begin{aligned}I^{\mu\nu} =& \frac{im_f}{8\pi^2}\Bigg(g^{\mu\nu} + \\ &- 2\int_0^1 dz\int_0^{1-z} dy\frac{g^{\mu\nu} - 2(1-2yz)(\tau_f-\kappa_f)g^{\mu\nu} - 4z^2\kappa_f g^{\mu\nu} + (1-4yz)\frac{k_1^\nu k_{q\bar{q}}^\mu}{m_f^2}}{1-4yz\tau_f - 4\big(z(1-z)-yz\big)\kappa_f}\Bigg) = \\ =& \frac{im_f}{8\pi^2}\left(\frac{k_1^\nu k_{q\bar{q}}^\mu}{m_f^2} - 2(\tau_f-\kappa_f)g^{\mu\nu}\right)\frac{F(\tau_f,\kappa_f)}{(\kappa_f-\tau_f)^2}\end{aligned} \tag{5.145}$$

with

$$
\begin{aligned}
F(\tau_f,\kappa_f) \equiv&\kappa_f\sqrt{\frac{1}{\tau_f}-1}\arctan\left(\frac{1}{\sqrt{\frac{1}{\tau_f}-1}}\right)-\sqrt{1-\kappa_f}\sqrt{\kappa_f}\arctan\left(\frac{1}{\sqrt{\frac{1}{\kappa_f}-1}}\right)+\kappa_f-\tau_f+\\
&+\frac{\kappa_f-\tau_f+1}{2}\left[\mathrm{Li}_2\left(\frac{2}{1+\sqrt{1-\frac{1}{\tau_f}}}\right)+\mathrm{Li}_2\left(\frac{2}{1-\sqrt{1-\frac{1}{\tau_f}}}\right)+\right.\\
&\left.-\mathrm{Li}_2\left(\frac{2}{1+\sqrt{1-\frac{1}{\kappa_f}}}\right)-\mathrm{Li}_2\left(\frac{2}{1-\sqrt{1-\frac{1}{\kappa_f}}}\right)\right]+\\
&+\kappa_f\sqrt{1-\frac{1}{\tau_f}}\mathrm{Artanh}\left(\frac{1}{\sqrt{1-\frac{1}{\tau_f}}}\right)-\sqrt{\kappa_f-1}\sqrt{\kappa_f}\mathrm{Artanh}\left(\frac{1}{\sqrt{1-\frac{1}{\kappa_f}}}\right)
\end{aligned}
\tag{5.146}
$$

When working with FeynCalc [92] using Mathematica [183], it is important to write $\sqrt{\kappa_f-1}\sqrt{\kappa_f}$ instead of $\sqrt{\kappa_f^2-\kappa_f}$, etc.; otherwise the wrong analytic continuation will be implemented. Note that

$$
\begin{aligned}
\lim_{\kappa_f\to 0}F(\tau_f,\kappa_f)=&-\frac{(\tau_f-1)\mathrm{Li}_2\left(\frac{2}{1+\sqrt{1-\frac{1}{\tau_f}}}\right)+(\tau_f-1)\mathrm{Li}_2\left(\frac{2}{1-\sqrt{1-\frac{1}{\tau_f}}}\right)+2\tau_f}{2}=\\
=&i16\pi^2\tau_f J(\tau_f)
\end{aligned}
\tag{5.147}
$$

with $J(\tau_f)$ from (5.15). One can rewrite the dilogarithms in terms of ordinary logarithms squared (see Appendix E). The correct analytic continuation is achieved by sending $m_f^2\to m_f^2-i\eta$ and therefore $\tau_f\to\tau_f+i\eta$ and $\kappa_f\to\kappa_f+i\eta$.
It is worth noting that $F(\tau_f,\kappa_f)$ can be related to $A_5(\tau_f,\kappa_f)$ defined via equation (A.14) in [184] and $\mathcal{A}$ from equation (A.19) in [136] by

$$
F(\tau_f,\kappa_f)=\tau_f(\kappa_f-\tau_f)A_5(\tau_f,\kappa_f)=\frac{1}{2m_f^2}(\kappa_f-\tau_f)\mathcal{A}
\tag{5.148}
$$

where

$$
\begin{aligned}
A_5(\tau_f,\kappa_f)=&\frac{1}{4\tau_f}\left(4+\frac{4\kappa_f}{\tau_f-\kappa_f}\left(W_1(s_{q\bar{q}})-W_1(m_h^2)\right)+\right.\\
&\left.+\left(1-\frac{1}{\tau_f-\kappa_f}\right)\left(W_2(s_{q\bar{q}})-W_2(m_h^2)\right)\right)
\end{aligned}
\tag{5.149}
$$

with

$$
W_1(a)\equiv 2+\int_0^1 dx\ln\left(1-x(1-x)\frac{a}{m_f^2}-i\epsilon\right)=
$$

$$= \begin{cases} 2\sqrt{\frac{4m_f^2}{a}-1}\arcsin\sqrt{\frac{a}{4m_f^2}} & \text{for } 0 < a < 4m_f^2 \\ \sqrt{1-\frac{4m_f}{a}}(2\arccos\sqrt{\frac{a}{4m_f^2}} - i\pi) & \text{for } 4m_f^2 \leq a < \infty \end{cases} \tag{5.150}$$

$$W_2(a) \equiv 2\int_0^1 \frac{dx}{x}\ln\left(1 - x(1-x)\frac{a}{m_f^2} - i\epsilon\right) =$$

$$= \begin{cases} -4\arcsin^2\sqrt{\frac{a}{4m_f^2}} & \text{for } 0 < a < 4m_f^2 \\ \left(2\arccos\sqrt{\frac{a}{4m_f^2}} - i\pi\right)^2 & \text{for } 4m_f^2 \leq a < \infty \end{cases} \tag{5.151}$$

5.5. Real QCD corrections ($h \to ggg$)

Non-SM-like contribution

In addition to the gluon-light-quarks radiation channels, amplitudes with three final-state gluons have to be dealt with. The non-SM-like diagrams involve effective Higgs-multiple-gluon vertices. We have

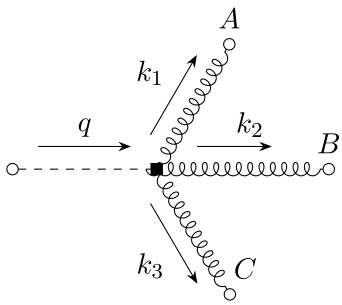

$$\equiv i\mathcal{M}^{R,ggg}_{1,NSM} =$$

$$= \frac{ig_s^3 c_{ggh}}{8\pi^2 v}\epsilon^{*\mu}(k_1)\epsilon^{*\nu}(k_2)\epsilon^{*\lambda}(k_3)V^{ABC}_{\mu\nu\lambda}(-k_1, k_2, k_3) \tag{5.152}$$

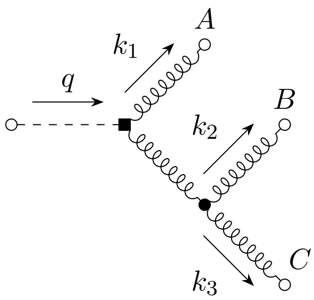

$$\equiv \; i\mathcal{M}^{R,ggg}_{2,NSM} = \frac{ig_s^3 c_{ggh}}{8\pi^2 v(k_2+k_3)^2}\epsilon^*_\mu(k_1)\epsilon^{*\nu}(k_2)\epsilon^{*\lambda}(k_3)\cdot$$

$$\cdot \left(k_1\cdot(k_2+k_3)g^{\alpha\mu} - k_1^\alpha(k_2^\mu + k_3^\mu)\right)V^{ABC}_{\alpha\nu\lambda}(k_2+k_3, k_2, k_3) \tag{5.153}$$

and $i\mathcal{M}^{R,ggg}_{3,NSM}$ and $i\mathcal{M}^{R,ggg}_{4,NSM}$, which are related to $i\mathcal{M}^{R,ggg}_{2,NSM}$ by permuting $\{k_1, \mu, A\} \longleftrightarrow \{k_2, \nu, B\} \longleftrightarrow \{k_3, \lambda, C\}$. The triple-gluon vertex $V^{ABC}_{\mu\nu\lambda}(k_1, k_2, k_3)$ is explicitly written out in Appendix C. It is worth defining $s_{ij} \equiv (k_i + k_j)^2$ for $i, j = 1, 2, 3$ with $m_h^2 = s_{12} + s_{13} + s_{23}$. A lengthy, but straightforward computation shows that $i\mathcal{M}^{R,ggg}_{NSM} \equiv \sum_{k=1}^4 i\mathcal{M}^{R,ggg}_{k,NSM}$ is indeed gauge invariant as it should, i.e. sending $\epsilon^*(k_i) \to k_i$ yields zero. The final result reads

$$i\mathcal{M}^{R,ggg}_{NSM} = \frac{g_s^3 c_{ggh}}{8\pi^2 v}\epsilon^*_\mu(k_1)\epsilon^*_\nu(k_2)\epsilon^*_\lambda(k_3) f^{ABC}\mathcal{F}^{\mu\nu\lambda} \tag{5.154}$$

where

$$\begin{aligned}\mathcal{F}^{\mu\nu\lambda} =& g^{\mu\nu}(k_2^\lambda - k_1^\lambda) + g^{\mu\lambda}(k_1^\nu - k_3^\nu) + g^{\nu\lambda}(k_3^\mu - k_2^\mu) + \\ &+ \frac{(s_{12}+s_{13})(k_2^\lambda g^{\mu\nu} - k_3^\nu g^{\mu\lambda}) + 2(k_2^\mu + k_3^\mu)(k_1^\lambda k_3^\nu - k_1^\nu k_2^\lambda) + g^{\nu\lambda}(k_3^\mu s_{12} - k_2^\mu s_{13})}{s_{23}} + \\ &- \frac{(s_{23}+s_{13})(k_2^\mu g^{\lambda\nu} - k_1^\nu g^{\mu\lambda}) + 2(k_2^\lambda + k_1^\lambda)(k_3^\mu k_1^\nu - k_3^\nu k_2^\mu) + g^{\nu\mu}(k_1^\lambda s_{23} - k_2^\lambda s_{13})}{s_{12}} + \\ &- \frac{(s_{12}+s_{23})(k_1^\lambda g^{\mu\nu} - k_3^\mu g^{\nu\lambda}) + 2(k_1^\nu + k_3^\nu)(k_2^\lambda k_3^\mu - k_2^\mu k_1^\lambda) + g^{\mu\lambda}(k_3^\nu s_{12} - k_1^\nu s_{23})}{s_{13}}\end{aligned} \tag{5.155}$$

We can rewrite this expression in terms of helicity amplitudes as shown in Appendix B. The actual conversion is tedious, but again straightforward. We finally arrive at

$$\begin{aligned}&H^{ggg}_{+++} = -\frac{m_h^4}{[12][23][31]},\ H^{ggg}_{---} = \frac{m_h^4}{\langle 12\rangle\langle 23\rangle\langle 31\rangle},\ H^{ggg}_{+--} = -\frac{[23]^3}{[21][13]},\ H^{ggg}_{-++} = \frac{\langle 23\rangle^3}{\langle 21\rangle\langle 13\rangle} \\ &H^{ggg}_{+-+} = -\frac{\langle 13\rangle^3}{\langle 12\rangle\langle 23\rangle},\ H^{ggg}_{-+-} = \frac{[13]^3}{[12][23]},\ H^{ggg}_{++-} = \frac{\langle 12\rangle^3}{\langle 13\rangle\langle 32\rangle},\ H^{ggg}_{--+} = -\frac{[12]^3}{[13][32]}\end{aligned} \tag{5.156}$$

where[55]

$$H^{ggg}_{\lambda_1\lambda_2\lambda_3} \equiv \sqrt{2}\epsilon^*_{\mu\lambda_1}(k_1,k_2)\epsilon^*_{\nu\lambda_2}(k_2,k_3)\epsilon^*_{\lambda\lambda_3}(k_3,k_1)\mathcal{F}^{\mu\nu\lambda} \tag{5.157}$$

and thus

$$i\mathcal{M}^{R,ggg}_{NSM} = \frac{g_s^3 c_{ggh}}{8\sqrt{2}\pi^2 v} f^{ABC} H^{ggg}_{\lambda_1\lambda_2\lambda_3} \tag{5.158}$$

SM-like contribution

The real radiation amplitudes for $h \to ggg$ for the SM-like contributions consist of six genuine triangle amplitudes $i\mathcal{M}^{R,ggg}_{1,SM}$ to $i\mathcal{M}^{R,ggg}_{6,SM}$ and six box diagrams $i\mathcal{M}^{R,ggg}_{7,SM}$ to $i\mathcal{M}^{R,ggg}_{12,SM}$. Within each group, the diagrams are related to each other by permuting the final state gluons (three possibilities for a given fermion flow direction) and reverting

[55]Note that λ is a Lorentz index, whereas λ_i with $i = 1, 2, 3$ are the helicity indices for the three gluons.

the fermion flow (two possibilities for each final state permutation). Let us start with the first triangle diagram

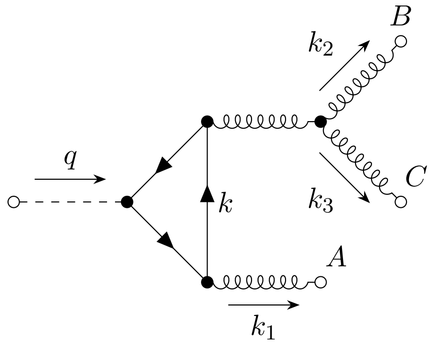

$$\equiv i\mathcal{M}^{R,ggg}_{1,SM} \tag{5.159}$$

Defining $\kappa_{f,ij} \equiv s_{ij}/4m_f^2$, the final expression reads

$$\begin{aligned} i\mathcal{M}^{R,ggg}_{1,SM} =& \frac{ig_s^3}{32\pi^2 s_{23}} V^{ABC}_{\delta\nu\lambda}(k_{23}, k_2, k_3)\epsilon^*_\mu(k_1)\epsilon^{*\nu}(k_2)\epsilon^{*\lambda}(k_3)\cdot \\ &\cdot \sum_f \frac{y_f c_f}{\sqrt{2}m_f}\left(2k_1^\delta k_{23}^\mu - (m_h^2 - s_{23})g^{\mu\delta}\right)\frac{F(\tau_f, \kappa_{f,23})}{(\kappa_{f,23} - \tau_f)^2} \end{aligned} \tag{5.160}$$

where the complex function F was already defined in (5.146). The amplitude $i\mathcal{M}^{R,ggg}_{2,SM}$ can be obtained from $i\mathcal{M}^{R,ggg}_{1,SM}$ by reverting the fermion flow, resulting in the same expression[56]. The remaining amplitudes $i\mathcal{M}^{R,ggg}_{3,SM}$ and $i\mathcal{M}^{R,ggg}_{5,SM}$ and their reversed fermion flow analogues $i\mathcal{M}^{R,ggg}_{4,SM}$ and $i\mathcal{M}^{R,ggg}_{6,SM}$ are related to $i\mathcal{M}^{R,ggg}_{1,SM}$ and $i\mathcal{M}^{R,ggg}_{2,SM}$ by exchanging the external particles. For instance, with a self-explaining notation, we have

$$i\mathcal{M}^{R,ggg}_{1,SM}(k_1, k_2, k_3; A, B, C) = i\mathcal{M}^{R,ggg}_{3,SM}(k_2, k_1, k_3; B, A, C) = i\mathcal{M}^{R,ggg}_{5,SM}(k_3, k_2, k_1; C, B, A) \tag{5.161}$$

All in all, defining $V^{ABC}_{\alpha\beta\gamma}(p_1, p_2, p_3) = f^{ABC}\tilde{V}_{\alpha\beta\gamma}(p_1, p_2, p_3)$, we get

$$\begin{aligned} \sum_{k=1}^{6} i\mathcal{M}^{R,ggg}_{k,SM} =& \sum_f \frac{ig_s^3}{16\pi^2}\frac{y_f c_f}{\sqrt{2}m_f} f^{ABC}\epsilon^*_\mu(k_1)\epsilon^*_\nu(k_2)\epsilon^*_\lambda(k_3)\cdot \\ &\cdot\Bigg(\tilde{V}_{\delta\nu\lambda}(k_{23}, k_2, k_3)\left(2k_1^\delta k_{23}^\mu - (m_h^2 - s_{23})g^{\mu\delta}\right)\frac{F(\tau_f, \kappa_{f,23})}{s_{23}(\kappa_{f,23} - \tau_f)^2} + \\ &- \tilde{V}_{\delta\mu\lambda}(k_{13}, k_1, k_3)\left(2k_2^\delta k_{13}^\nu - (m_h^2 - s_{13})g^{\nu\delta}\right)\frac{F(\tau_f, \kappa_{f,13})}{s_{13}(\kappa_{f,13} - \tau_f)^2} + \\ &- \tilde{V}_{\delta\nu\mu}(k_{12}, k_2, k_1)\left(2k_3^\delta k_{12}^\lambda - (m_h^2 - s_{12})g^{\lambda\delta}\right)\frac{F(\tau_f, \kappa_{f,12})}{s_{12}(\kappa_{f,12} - \tau_f)^2}\Bigg) \end{aligned} \tag{5.162}$$

[56] In the notation of the appendix to this subsection, reverting the fermion flow implies the exchange of μ with δ and k_1 with k_{23} in $I^{\mu\delta}_{1,23}$, which does not change anything.

where we have lowered all polarization indices μ, ν and λ for the sake of notation. The second class of diagrams starts with the box

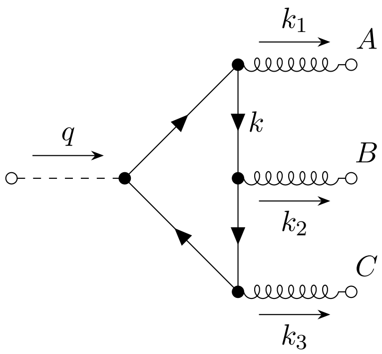

$$\equiv i\mathcal{M}^{R,ggg}_{7,SM} \tag{5.163}$$

As before, reverting the fermion flow generates the next amplitude $i\mathcal{M}^{R,ggg}_{8,SM}$. This implies exchanging $A, \mu, k_1 \longleftrightarrow C, \lambda, k_3$. The remaining ones $i\mathcal{M}^{R,ggg}_{9,SM}$ to $i\mathcal{M}^{R,ggg}_{12,SM}$ can be obtained from all other permutations. Using $Tr(T^AT^BT^C) - Tr(T^AT^CT^B) = \frac{i}{2}f^{ABC}$, the final result for the box amplitudes is then given by

$$\sum_{k=7}^{12} i\mathcal{M}^{R,ggg}_{k,SM} = -\sum_f \frac{ig_s^3 y_f c_f}{2\sqrt{2}} f^{ABC} \epsilon^*_\mu(k_1)\epsilon^*_\nu(k_2)\epsilon^*_\lambda(k_3)\left(J^{\lambda\nu\mu}_{3,2,1} + J^{\nu\mu\lambda}_{2,1,3} + J^{\mu\lambda\nu}_{1,3,2}\right) \tag{5.164}$$

where $J^{\mu\nu\lambda}_{1,2,3}$ is calculated explicitly in the appendix to this subsection and defined in (5.196).

The full expression obtained by combining (5.162) and (5.164) is quite complicated and unhandy. However, it can be numerically matched to the formulas given in [184] and [137]. These are given by

$$i\mathcal{M}^{R,ggg}_{SM} \equiv \sum_{k=1}^{12} i\mathcal{M}^{R,ggg}_{k,SM} = -\sum_f \frac{g_s^3 m_h^4 y_f c_f}{16\pi^2\sqrt{2}m_f}\epsilon^{*\mu}(k_1)\epsilon^{*\nu}(k_2)\epsilon^{*\lambda}(k_3) f^{ABC}\mathcal{A}_{\mu\nu\lambda}(1,2,3) \tag{5.165}$$

where

$$\begin{aligned}\mathcal{A}_{\mu\nu\lambda}(1,2,3) \equiv & A_{\mu\nu\lambda}(1,2,3) - A_{\nu\mu\lambda}(2,1,3) - A_{\lambda\nu\mu}(3,2,1) + \\ & - A_{\mu\lambda\nu}(1,3,2) + A_{\nu\lambda\mu}(2,3,1) + A_{\lambda\mu\nu}(3,1,2)\end{aligned} \tag{5.166}$$

with

$$\begin{aligned}A_{\mu\nu\lambda}(1,2,3) \equiv & \left(\frac{8k_{1\lambda}k_{1\nu}k_{2\mu}}{s_{12}^2 s_{13}} - \frac{4k_{1\lambda}g_{\mu\nu}}{s_{12}s_{13}}\right) A_2(s_{12}, s_{13}, s_{23}) \\ & + \left(\frac{2k_{1\nu}k_{8\lambda}k_{3\mu}}{3s_{12}s_{13}s_{23}} + \frac{4k_{1\lambda}g_{\mu\nu}}{s_{12}s_{13}}\right) A_3(s_{12}, s_{13}, s_{23})\end{aligned} \tag{5.167}$$

and (in the notation of [184])

$$A_2(s_{12},s_{13},s_{23}) \equiv b_2(s_{12},s_{13},s_{23}) + b_2(s_{12},s_{23},s_{13}) \tag{5.168}$$

$$\begin{aligned} A_3(s_{12},s_{13},s_{23}) \equiv & \frac{1}{2}\Big(A_2(s_{12},s_{13},s_{23}) + A_2(s_{23},s_{12},s_{13}) + A_2(s_{13},s_{23},s_{12}) + \\ & -b_4(s_{12},s_{13},s_{23}) - b_4(s_{23},s_{12},s_{13}) - b_4(s_{13},s_{23},s_{12})\Big) \end{aligned} \tag{5.169}$$

The functions b_2 and b_4 are defined via (always remember $m_f^2 \to m_f^2 - i\epsilon$)

$$\begin{aligned} b_2(a,b,c) \equiv & \frac{m_f^2}{m_h^4}\left(\frac{a(c-a)}{a+c} + \frac{2bc(c+2a)}{(a+c)^2}\big(W_1(b) - W_1(m_h^2)\big) + \right. \\ & + \left(m_f^2 - \frac{a}{4}\right)\left(\frac{1}{2}W_2(a) + \frac{1}{2}W_2(m_h^2) - W_2(b) + W_3(a,b,c,m_h^2)\right) + \\ & + a^2\left(\frac{2m_f^2}{(a+c)^2} - \frac{1}{2(a+c)}\right)\big(W_2(b) - W_2(m_h^2)\big) + \frac{bc}{2a}\big(W_2(m_h^2) - 2W_2(b)\big) + \\ & \left. + \frac{1}{8}\left(a - 12m_f^2 - \frac{4bc}{a}\right)W_3(b,a,c,m_h^2)\right) \end{aligned} \tag{5.170}$$

and

$$b_4(a,b,c) \equiv \frac{m_f^2}{m_h^2}\left(-\frac{2}{3} + \left(\frac{m_f^2}{m_h^2} - \frac{1}{4}\right)\big(W_2(a) - W_2(m_h^2) + W_3(a,b,c,m_h^2)\big)\right) \tag{5.171}$$

where, in addition to $W1$ and $W2$ defined in (5.150) and (5.151),

$$W_3(a,b,c,d) \equiv I_3(a,b,c,d) - I_3(a,b,c,a) - I_3(a,b,c,c) \tag{5.172}$$

The integral I_3 is given in [137] and reads

$$\begin{aligned} I_3(a,b,c,d) \equiv & \int_0^1 \frac{dx}{x(1-x) + \frac{bm_f^2}{ac}} \ln\left(1 - x(1-x)\frac{d}{m_f^2}\right) = \\ = & \frac{2}{\beta_+(a,b,c) - \beta_-(a,b,c)}\left(\mathrm{Li}_2\left(\frac{\beta_-(a,b,c)}{\beta_-(a,b,c) - \alpha_-(d)}\right) + \right. \\ & + \mathrm{Li}_2\left(\frac{\beta_-(a,b,c)}{\beta_-(a,b,c) - \alpha_+(d)}\right) - \mathrm{Li}_2\left(\frac{\beta_+(a,b,c)}{\beta_+(a,b,c) - \alpha_-(d)}\right) + \\ & \left. + \ln\left(-\frac{\beta_+(a,b,c)}{\beta_-(a,b,c)}\right)\ln\left(1 + \frac{bd}{ac}\right) - \mathrm{Li}_2\left(\frac{\beta_+(a,b,c)}{\beta_+(a,b,c) - \alpha_+(d)}\right)\right) \end{aligned} \tag{5.173}$$

with

$$\beta_\pm(a,b,c) \equiv \frac{1}{2}\left(1 \pm \sqrt{1 + \frac{4m_f^2 b}{ac}}\right) \tag{5.174}$$

$$\alpha_\pm(d) \equiv \frac{1}{2}\left(1 \pm \sqrt{1 - \frac{4m_f^2}{d}}\right) \tag{5.175}$$

Defining

$$\tilde{a}(d) \equiv \sqrt{\frac{4m_f^2}{d} - 1} \tag{5.176}$$

$$r^2(a,b,c,d) \equiv \frac{\tilde{a}^2(d) + 1}{\tilde{a}^2(d) + (2\beta_+(a,b,c) - 1)^2} \tag{5.177}$$

$$\cos\big(\theta(a,b,c,d)\big) \equiv \frac{r(a,b,c,d)(\tilde{a}^2(d) - 2\beta_+(a,b,c) - 1)}{1 + \tilde{a}^2(d)} \tag{5.178}$$

$$\cos\big(\phi(a,b,c,d)\big) \equiv \frac{r(a,b,c,d)(\tilde{a}^2(d) + 2\beta_+(a,b,c) - 1)}{1 + \tilde{a}^2(d)} \tag{5.179}$$

$$\tag{5.180}$$

with θ and ϕ between 0 and π, the two relevant special cases are

$$I_3(a,b,c,d) \equiv \begin{cases} I_3^<(a,b,c,d) & \text{for } 0 < d < 4m_f^2 \\ I_3^>(a,b,c,d) & \text{for } 4m_f^2 \le d < \infty \end{cases} \tag{5.181}$$

where

$$\begin{aligned} I_3^<(a,b,c,d) \equiv & \frac{2}{2\beta_+(a,b,c) - 1}\Big(2\mathrm{Li}_2\big(r(a,b,c,d), \theta(a,b,c,d)\big) + \\ & - 2\mathrm{Li}_2\big(r(a,b,c,d), \phi(a,b,c,d)\big) + \\ & + \big(\phi(a,b,c,d) - \theta(a,b,c,d)\big)\big(\phi(a,b,c,d) + \theta(a,b,c,d) - \pi\big)\Big) \end{aligned} \tag{5.182}$$

and

$$\begin{aligned} I_3^>(a,b,c,d) \equiv & \frac{2}{2\beta_+(a,b,c) - 1}\left(-\mathrm{Li}_2\left(\frac{\alpha_+(d)}{\alpha_+(d) + \beta_+(a,b,c) - 1}\right) + \right. \\ & + \mathrm{Li}_2\left(\frac{\alpha_+(d) - 1}{\alpha_+(d) + \beta_+(a,b,c) - 1}\right) + \\ & + \mathrm{Li}_2\left(\frac{\alpha_+(d)}{\alpha_+(d) - \beta_+(a,b,c)}\right) - \mathrm{Li}_2\left(\frac{\alpha_+(d) - 1}{\alpha_+(d) - \beta_+(a,b,c)}\right) + \\ & + \ln\left(\frac{\alpha_+(d)}{1 - \alpha_+(d)}\right) \ln\left(\frac{\alpha_+(d) + \beta_+(a,b,c) - 1}{\beta_+(a,b,c) - \alpha_+(d)}\right) + \\ & \left. - i\pi \ln\left(\frac{\alpha_+(d) + \beta_+(a,b,c) - 1}{\beta_+(a,b,c) - \alpha_+(d)}\right)\right) \end{aligned} \tag{5.183}$$

The dilogarithm with two arguments[57] is defined via

$$\mathrm{Li}_2(x,y) = -\frac{1}{2}\int_0^x \frac{dz}{z}\ln\bigl(1-2z\cos y+z^2\bigr) = \frac{1}{2}\left(\mathrm{Li}_2(xe^{iy})-\mathrm{Li}_2(xe^{-iy})\right) \tag{5.185}$$

The special cases (5.182) and (5.183) can straightforwardly be obtained from the general form (5.173) using

$$\mathrm{Li}_2(1-x) = \frac{1}{6}\pi^2 - \mathrm{Li}_2(x) - \ln(1-x)\ln x \tag{5.186}$$

Again, we rewrite the amplitude in terms of helicity amplitudes in the notation of Appendix B. As the amplitudes themselves now depend on the helicity configuration - MHV (maximally helicity violating) vs. NMHV (next-to maximally helicity violating), this is an involved task. To shorten the notation, we introduce the abbreviation

$$\mathcal{P}_{\lambda_1\lambda_2\lambda_3} \equiv \epsilon^*_{\mu\lambda_1}(k_1,k_2)\epsilon^*_{\nu\lambda_2}(k_2,k_3)\epsilon^*_{\lambda\lambda_3}(k_3,k_1)\frac{m_h^4\mathcal{A}^{\mu\nu\lambda}(1,2,3)}{\sqrt{2}} \tag{5.187}$$

yielding

$$i\mathcal{M}^{R,ggg}_{SM} = -\sum_f \frac{g_s^3 y_f c_f}{16\pi^2 m_f} f^{ABC}\mathcal{P}_{\lambda_1\lambda_2\lambda_3} \tag{5.188}$$

Writing $A_4(s_{12},s_{13},s_{23}) \equiv b_4(s_{12},s_{13},s_{23}) + b_4(s_{23},s_{12},s_{13}) + b_4(s_{13},s_{23},s_{12})$ as in [184] and applying the notation (5.157), we find

$$\begin{aligned}
\mathcal{P}_{+++} =& -\frac{m_h^4}{[12][23][31]}\frac{2}{3}\Bigl(3A_2(s_{12},s_{23},s_{13}) + 3A_2(s_{13},s_{12},s_{23}) + 3A_2(s_{23},s_{13},s_{12}) + \\
&+ A_3(s_{12},s_{13},s_{23}) - 3A_3(s_{12},s_{23},s_{13}) - 3A_3(s_{13},s_{12},s_{23}) + A_3(s_{13},s_{23},s_{12}) + \\
&+ A_3(s_{23},s_{12},s_{13}) - 3A_3(s_{23},s_{13},s_{12})\Bigr) = 2A_4(s_{12},s_{13},s_{23})H^{ggg}_{+++} \\
\mathcal{P}_{+--} =& -\frac{[23]^3}{[21][13]}\frac{2m_h^4}{3s_{23}^2}\Bigl(3A_2(s_{23},s_{13},s_{12}) + A_3(s_{12},s_{13},s_{23}) + A_3(s_{13},s_{23},s_{12}) + \\
&+ A_3(s_{23},s_{12},s_{13}) - 3A_3(s_{23},s_{13},s_{12})\Bigr) = \frac{2m_h^4}{s_{23}^2}A_2(s_{23},s_{12},s_{13})H^{ggg}_{+--} \\
\mathcal{P}_{---} =& 2A_4(s_{12},s_{13},s_{23})H^{ggg}_{---}, \ \mathcal{P}_{-++} = \frac{2m_h^4}{s_{23}^2}A_2(s_{23},s_{12},s_{13})H^{ggg}_{-++} \\
\mathcal{P}_{+-+} =& \frac{2m_h^4}{s_{13}^2}A_2(s_{13},s_{23},s_{12})H^{ggg}_{+-+}, \ \mathcal{P}_{-+-} = \frac{2m_h^4}{s_{13}^2}A_2(s_{13},s_{23},s_{12})H^{ggg}_{-+-}
\end{aligned}$$

[57] For one argument, see 5.90. It is given by

$$\mathrm{Li}_2(x) \equiv -\int_0^x \frac{\ln(1-z)}{z}dz = \int_1^{1-x}\frac{\ln(z)}{1-z}dz \tag{5.184}$$

$$\mathcal{P}_{++-} = \frac{2m_h^4}{s_{12}^2} A_2(s_{12}, s_{13}, s_{23}) H^{ggg}_{++-}, \ \mathcal{P}_{--+} = \frac{2m_h^4}{s_{12}^2} A_2(s_{12}, s_{13}, s_{23}) H^{ggg}_{--+} \tag{5.189}$$

It seems reasonable to pull out the polarization factor $H^{ggg}_{\lambda_1\lambda_2\lambda_3}$ by introducing

$$\mathcal{P}_{\lambda_1\lambda_2\lambda_3} \equiv H^{ggg}_{\lambda_1\lambda_2\lambda_3} \mathcal{Q}^f_{\lambda_1\lambda_2\lambda_3}(s_{12}, s_{13}, s_{23}) \tag{5.190}$$

where we have reintroduced the label f to denote the dependence on the fermion mass m_f, which we have suppressed so far for notational simplicity. The explicit expressions for $\mathcal{Q}^f_{\lambda_1\lambda_2\lambda_3}(s_{12}, s_{13}, s_{23})$ can be read off from (5.189).
Combining both amplitudes (5.158) and (5.188) yields

$$\begin{aligned} i\mathcal{M}^{R,ggg} \equiv & i\mathcal{M}^{R,ggg}_{NSM} + i\mathcal{M}^{R,ggg}_{SM} = \\ = & \frac{\alpha_s^{3/2}}{\sqrt{2\pi}} f^{ABC} H^{ggg}_{\lambda_1\lambda_2\lambda_3} \left(\frac{c_{ggh}}{v} - \sum_f \frac{y_f c_f}{\sqrt{2} m_f} \mathcal{Q}^f_{\lambda_1\lambda_2\lambda_3}(s_{12}, s_{13}, s_{23}) \right) \end{aligned} \tag{5.191}$$

Note that in contrast to all other amplitudes, there is no overall polarization factor. Instead, the functional form of the amplitude depends on the latter in a non-trivial way.

Appendix: Calculational details for the SM-like contributions

For the triangle graphs, we find

$$i\mathcal{M}^{R,ggg}_{1,SM} = \frac{g_s^3 y_f c_f}{\sqrt{2} k_{23}^2} Tr(T^A T^D) V^{DBC}_{\delta\nu\lambda}(k_{23}, k_2, k_3) \epsilon^*_\mu(k_1) \epsilon^{*\nu}(k_2) \epsilon^{*\lambda}(k_3) I^{\mu\delta}_{1,23} \tag{5.192}$$

where we defined $k_{ij} \equiv k_i + k_j$ and

$$I^{\mu\delta}_{1,23} \equiv \mu^{2\epsilon} \int \frac{d^d k}{(2\pi)^d} \frac{Tr\big((\not{k} - \not{k}_{23} + m_f)\gamma^\delta(\not{k} + m_f)\gamma^\mu(\not{k} + \not{k}_1 + m_f)\big)}{\big((k+k_1)^2 - m_f^2\big)(k^2 - m_f^2)\big((k-k_{23})^2 - m_f^2\big)} \tag{5.193}$$

Fortunately, we have $k^\delta_{23} V^{DBC}_{\delta\nu\lambda}(k_{23}, k_2, k_3) = 0$ (see Appendix C for the notation), so we can use the results of Subsection 5.4.
Turning to the box graphs, we have

$$i\mathcal{M}^{R,ggg}_{7,SM} = -\frac{g_s^3 y_f c_f}{\sqrt{2}} Tr(T^C T^B T^A) \epsilon^*_\mu(k_1) \epsilon^{*\nu}(k_2) \epsilon^{*\lambda}(k_3) J^{\mu\nu\lambda}_{1,2,3} \tag{5.194}$$

with

$$J^{\mu\nu\lambda}_{1,2,3} \equiv \mu^{2\epsilon} \int \frac{d^d k}{(2\pi)^d} \frac{Tr\big((\not{k} - \not{k}_{23} + m_f)\gamma^\lambda(\not{k} - \not{k}_2 + m_f)\gamma^\nu(\not{k} + m_f)\gamma^\mu(\not{k} + \not{k}_1 + m_f)\big)}{\big((k+k_1)^2 - m_f^2\big)(k^2 - m_f^2)\big((k-k_2)^2 - m_f^2\big)\big((k-k_{23})^2 - m_f^2\big)} \tag{5.195}$$

Proceeding the usual way - that is, introducing Feynman parameters and so on - will lead to expressions that cannot be integrated analytically by the standard methods[58]. Instead

[58] We have numerically checked the equality of the so-obtained Feynman-parameter integrals with (5.196). The explicit expressions are, however, too lengthy for the limited space in this work.

of doing so, we evaluate the integral in terms of scalar Passarino-Veltman amplitudes as in Appendix E, although with slightly different normalizations. We denote the box, triangle and bubble contributions by D, C (or $\tilde{C}$) and B (or $\tilde{B}$), respectively. The full expression (5.195) is then expanded according to (remember $s_{ij} = 2k_i \cdot k_j$)

$$\begin{aligned} J^{\mu\nu\lambda}_{1,2,3} \equiv & f^{\mu\nu\lambda}_{D}(k_1,k_2,k_3) + f^{\mu\nu\lambda}_{\tilde{B}}(k_1,k_2,k_3) + \\ & + f^{\mu\nu\lambda}_{B}(k_1,k_2,k_3) - f^{\lambda\nu\mu}_{B}(k_3,k_2,k_1) + \\ & + f^{\mu\nu\lambda}_{C}(k_1,k_2,k_3) - f^{\lambda\nu\mu}_{C}(k_3,k_2,k_1) + \\ & + f^{\mu\nu\lambda}_{\tilde{C}}(k_1,k_2,k_3) - f^{\lambda\nu\mu}_{\tilde{C}}(k_3,k_2,k_1) = -J^{\lambda\nu\mu}_{3,2,1} \end{aligned} \tag{5.196}$$

where

$$\begin{aligned} f^{\mu\nu\lambda}_{D}(k_1,k_2,k_3) = & \frac{i\pi^2 m_f D_0(0,0,0,m_h^2,s_{12},s_{23},m_f^2,m_f^2,m_f^2,m_f^2)}{(2\pi)^d s_{12}s_{13}^3 s_{23}} \cdot \\ & \cdot \Big(4s_{13}^2 s_{23}\big(s_{12}-4m_f^2\big)\big(s_{23}k_2^\mu k_1^\nu k_1^\lambda - s_{13}k_2^\mu k_1^\nu k_2^\lambda\big) + \\ & + 4s_{12}s_{13}s_{23}\big(s_{13}(s_{13}-4m_f^2) - 2s_{12}s_{23}\big)\big(k_2^\mu k_3^\nu k_1^\lambda - k_3^\mu k_1^\nu k_2^\lambda\big) + \\ & + 4s_{12}s_{13}^2\big(s_{23}-4m_f^2\big)\big(s_{13}k_2^\mu k_3^\nu k_2^\lambda - s_{12}k_3^\mu k_3^\nu k_2^\lambda\big) + \\ & + 4s_{12}s_{23}\big(s_{13}(s_{13}-12m_f^2) - 4s_{12}s_{23}\big)\big(s_{23}k_3^\mu k_1^\nu k_1^\lambda - s_{12}k_3^\mu k_3^\nu k_1^\lambda\big) + \\ & + 2s_{12}s_{13}s_{23}\big(s_{13}(s_{12}+s_{13}-8m_f^2) - 2s_{12}s_{23}\big)g^{\mu\nu}\big(s_{13}k_2^\lambda - s_{23}k_1^\lambda\big) + \\ & + 4s_{12}s_{13}s_{23}\big(4s_{13}m_f^2 + s_{12}s_{23}\big)g^{\mu\lambda}\big(s_{23}k_1^\nu - s_{12}k_3^\nu\big) + \\ & + 2s_{12}s_{13}s_{23}\big(s_{13}(s_{13}+s_{23}-8m_f^2) - 2s_{12}s_{23}\big)g^{\nu\lambda}\big(s_{12}k_3^\mu - s_{13}k_2^\mu\big)\Big) \end{aligned} \tag{5.197}$$

$$\begin{aligned} f^{\mu\nu\lambda}_{\tilde{B}}(k_1,k_2,k_3) = & - \frac{8i\pi^2 m_f B_0(m_h^2,m_f^2,m_f^2)}{(2\pi)^d(d-2)s_{12}s_{13}^2 s_{23}(m_h^2-s_{23})^2(m_h^2-s_{12})^2} \cdot \\ & \cdot \Big(-2s_{13}s_{23}(s_{13}+s_{23})^2\big((d-4)s_{12}m_h^2 + (d-2)s_{13}s_{23}\big)k_2^\mu k_1^\nu k_1^\lambda + \\ & + 2(d-2)s_{13}^2 s_{23}(m_h^2-s_{23})(s_{13}+s_{23})^2 k_2^\mu k_1^\nu k_2^\lambda + \\ & + 2(d-2)s_{12}s_{13}s_{23}(m_h^2+s_{13})(m_h^2-s_{23})(s_{13}+s_{23})k_2^\mu k_3^\nu k_1^\lambda + \\ & - 2(d-2)s_{12}s_{13}^2(m_h^2-s_{23})^2(s_{13}+s_{23})k_2^\mu k_3^\nu k_2^\lambda + \\ & - 2s_{12}s_{23}(s_{13}+s_{23})\big(dm_h^2 s_{23}^2 + (d-4)m_h^2 s_{13}^2 + \\ & - m_h^4(ds_{23}+2s_{13}) - (d-2)s_{13}^2 s_{23}\big)k_3^\mu k_1^\nu k_1^\lambda + \\ & - 2(d-2)s_{12}s_{13}s_{23}(m_h^2+s_{13})(m_h^2-s_{23})(s_{13}+s_{23})k_3^\mu k_1^\nu k_2^\lambda + \\ & - 2s_{12}s_{23}(m_h^2-s_{23})\big(d(m_h^4 s_{12} - m_h^2(s_{12}^2+s_{13}^2) + s_{12}s_{13}^2) + \\ & + 2s_{13}(m_h^4 + 2m_h^2 s_{13} - s_{12}s_{13})\big)k_3^\mu k_3^\nu k_1^\lambda + \\ & + 2s_{12}s_{13}(m_h^2-s_{23})^2\big((d-2)s_{12}s_{13} + (d-4)s_{23}m_h^2\big)k_3^\mu k_3^\nu k_2^\lambda + \end{aligned}$$

$$
\begin{aligned}
&+ s_{12}s_{13}s_{23}(m_h^2 - s_{23})(s_{13}+s_{23})g^{\mu\nu}\big((m_h^2((d-4)s_{13}-2s_{23})+\\
&-(d-2)s_{13}s_{23})k_1^\lambda + (d-2)s_{13}(m_h^2-s_{23})k_2^\lambda\big)+\\
&-2m_h^2 s_{12}s_{13}s_{23}(m_h^2-s_{23})(s_{13}+s_{23})g^{\mu\lambda}\big((s_{13}+s_{23})k_1^\nu - (m_h^2-s_{23})k_3^\nu\big)+\\
&-s_{12}s_{13}s_{23}(m_h^2-s_{23})(s_{13}+s_{23})g^{\nu\lambda}\big((d-2)s_{13}(s_{13}+s_{23})k_2^\mu+\\
&-\big((d-2)s_{12}s_{13}-m_h^2((d-4)s_{13}-2s_{12})\big)k_3^\mu\big)\Big)
\end{aligned} \tag{5.198}
$$

$$
\begin{aligned}
f_B^{\mu\nu\lambda}(k_1,k_2,k_3) = &-\frac{8i\pi^2 m_f B_0(s_{23},m_f^2,m_f^2)}{(2\pi)^d(d-2)s_{12}s_{13}^2 s_{23}(m_h^2-s_{23})^2}\cdot\\
&\cdot\Big(2s_{13}s_{23}^2\big((d-4)s_{12}+(d-2)s_{13}\big)k_2^\mu k_1^\nu k_1^\lambda+\\
&+2(d-2)s_{13}s_{23}(m_h^2-s_{23})(s_{12}k_3^\mu k_1^\nu k_2^\lambda - s_{12}k_2^\mu k_3^\nu k_1^\lambda - s_{13}k_2^\mu k_1^\nu k_2^\lambda)+\\
&-2s_{12}s_{23}^2\big(2s_{13}+d(m_h^2-s_{23})\big)k_3^\mu k_1^\nu k_1^\lambda+\\
&+2s_{12}s_{23}(m_h^2-s_{23})(ds_{12}+2s_{13})k_3^\mu k_3^\nu k_1^\lambda+\\
&-2(d-4)s_{12}s_{13}(m_h^2-s_{23})^2 k_3^\mu k_3^\nu k_2^\lambda+\\
&+2s_{12}s_{13}s_{23}^2(m_h^2-s_{23})g^{\mu\nu}k_1^\lambda+\\
&+2s_{12}s_{13}s_{23}\big(m_h^2-s_{23})g^{\mu\lambda}\big(s_{23}k_1^\nu-(m_h^2-s_{23})k_3^\nu\big)+\\
&+s_{12}s_{13}s_{23}\big(m_h^2-s_{23})g^{\nu\lambda}\big((d-2)s_{13}k_2^\mu+((d-4)s_{13}-2s_{12})k_3^\mu\big)\Big)
\end{aligned} \tag{5.199}
$$

$$
\begin{aligned}
f_C^{\mu\nu\lambda}(k_1,k_2,k_3) = &\frac{i\pi^2 m_f C_0(0,s_{12},m_h^2,m_f^2,m_f^2,m_f^2)}{(2\pi)^d s_{12}^2 s_{13}^3 s_{23}^2(s_{13}+s_{23})}\cdot\\
&\cdot\Big(4s_{13}^2 s_{23}(s_{13}+s_{23})^2(s_{12}-4m_f^2)(s_{23}k_2^\mu k_1^\nu k_1^\lambda - s_{13}k_2^\mu k_1^\nu k_2^\lambda)+\\
&+8s_{12}^2 s_{13}s_{23}^2(s_{13}+s_{23})^2(k_3^\mu k_1^\nu k_2^\lambda - k_2^\mu k_3^\nu k_1^\lambda)+\\
&-4s_{12}s_{13}^3(s_{13}+s_{23})^2(s_{23}-4m_f^2)k_2^\mu k_3^\nu k_2^\lambda+\\
&+4s_{12}s_{23}^2(s_{13}+s_{23})^2\big(s_{13}(s_{13}-4m_f^2)-4s_{12}s_{23}\big)k_3^\mu k_1^\nu k_1^\lambda+\\
&+2s_{12}^2 s_{23}\big(2(s_{13}+s_{23})(4s_{12}s_{13}s_{23}+4s_{12}s_{23}^2+s_{13}^3-s_{13}^2 s_{23})+\\
&-8s_{13}m_f^2(s_{13}^2-2s_{13}s_{23}-s_{23}^2)\big)k_3^\mu k_3^\nu k_1^\lambda+\\
&-4s_{12}^2 s_{13}^2\big(4m_f^2(s_{13}^2+2s_{13}s_{23}-s_{23}^2)-s_{13}^2 s_{23}+s_{23}^3\big)k_3^\mu k_3^\nu k_2^\lambda+\\
&+2s_{12}s_{13}s_{23}(s_{13}+s_{23})^2\big(s_{12}(s_{13}-2s_{23})-4s_{13}m_f^2\big)g^{\mu\nu}\big(s_{13}k_2^\lambda - s_{23}k_1^\lambda\big)+\\
&-2s_{12}s_{13}s_{23}(s_{13}+s_{23})g^{\mu\lambda}\big(s_{23}(s_{13}+s_{23})(s_{13}(s_{13}-4m_f^2)-2s_{12}s_{23})k_1^\nu+\\
&+s_{12}\big((s_{13}+s_{23})(2s_{12}s_{23}+s_{13}^2)-4s_{13}m_f^2(s_{13}-s_{23})\big)k_3^\nu\big)+\\
&+2s_{12}s_{13}s_{23}(s_{13}+s_{23})g^{\nu\lambda}\big(s_{13}(s_{13}+s_{23})(s_{23}(2s_{12}+s_{13})-4s_{13}m_f^2)k_2^\mu+\\
&+s_{12}(4s_{13}m_f^2(s_{13}-s_{23})-s_{23}(2s_{12}-s_{13})(s_{13}+s_{23}))k_3^\mu\big)\Big)
\end{aligned} \tag{5.200}
$$

$$
\begin{aligned}
f_{\tilde{C}}^{\mu\nu\lambda}(k_1,k_2,k_3) =& \frac{i\pi^2 m_f C_0(0,0,s_{12},m_f^2,m_f^2,m_f^2)}{(2\pi)^d s_{12}s_{13}^3 s_{23}^2}\cdot \\
&\cdot\Big(-4s_{13}^2 s_{23}(s_{12}-4m_f^2)(s_{23}k_2^\mu k_1^\nu k_1^\lambda + s_{13}k_2^\mu k_1^\nu k_2^\lambda)+ \\
&+8s_{12}^2 s_{13} s_{23}^2 (k_2^\mu k_3^\nu k_1^\lambda - k_3^\mu k_1^\nu k_2^\lambda)+ \\
&+4s_{12}s_{13}^2(s_{23}-4m_f^2)(s_{12}k_3^\mu k_3^\nu k_2^\lambda - s_{13}k_2^\mu k_3^\nu k_2^\lambda)+ \\
&+4s_{12}s_{23}\big(s_{13}(s_{13}-4m_f^2)-4s_{12}s_{23}\big)(s_{12}k_3^\mu k_3^\nu k_1^\lambda - s_{23}k_3^\mu k_1^\nu k_1^\lambda)+ \\
&+2s_{12}s_{13}s_{23}g^{\mu\nu}\big(s_{23}(s_{13}(s_{12}-4m_f^2)-2s_{12}s_{23})k_1^\lambda+ \\
&+s_{13}(s_{13}(s_{12}-4m_f^2)+2s_{12}s_{23})k_2^\lambda\big)+ \\
&+2s_{12}s_{13}s_{23}g^{\mu\lambda}\big(s_{13}(s_{13}-4m_f^2)-2s_{12}s_{23}\big)(s_{23}k_1^\nu - s_{12}k_3^\nu)+ \\
&-2s_{12}s_{13}s_{23}(s_{13}(s_{23}-4m_f^2)-2s_{12}s_{23})g^{\nu\lambda}(s_{12}k_3^\mu - s_{13}k_2^\mu)\Big)
\end{aligned}
\tag{5.201}
$$

With $q = k_1 + k_2 + k_3$ and $\kappa_{f,ij} = s_{ij}/4m_f^2$ as before, the Passarino-Veltman amplitudes are given by

$$
\begin{aligned}
\frac{i\pi^2}{(2\pi)^d}B_0(s_{ij},m_f^2,m_f^2) &\equiv \mu^{2\epsilon}\int\frac{d^dk}{(2\pi)^d}\frac{1}{(k^2-m_f^2)\big((k-k_{ij})^2-m_f^2\big)} = \\
&= \frac{i}{16\pi^2}\left(\frac{1}{\epsilon}+\ln\frac{4\pi}{e^\gamma}+\ln\frac{\mu^2}{m_f^2}+2+\right. \\
&\left.+\sqrt{1-\frac{1}{\kappa_{f,ij}}}\ln\left(1-2\kappa_{f,ij}\left(1-\sqrt{1-\frac{1}{\kappa_{f,ij}}}\right)\right)\right)
\end{aligned}
\tag{5.202}
$$

$$
\begin{aligned}
\frac{i\pi^2}{(2\pi)^d}B_0(m_h^2,m_f^2,m_f^2) &\equiv \mu^{2\epsilon}\int\frac{d^dk}{(2\pi)^d}\frac{1}{(k^2-m_f^2)\big((k-q)^2-m_f^2\big)} = \\
&= \frac{i}{16\pi^2}\left(\frac{1}{\epsilon}+\ln\frac{4\pi}{e^\gamma}+\ln\frac{\mu^2}{m_f^2}+2+\sqrt{1-\frac{1}{\tau_f}}\ln\left(1-2\tau_f\left(1-\sqrt{1-\frac{1}{\tau_f}}\right)\right)\right)
\end{aligned}
\tag{5.203}
$$

$$
\begin{aligned}
&\frac{i\pi^2}{(2\pi)^d}C_0(0,0,s_{ij},m_f^2,m_f^2,m_f^2) \equiv \\
&\quad\equiv \mu^{2\epsilon}\int\frac{d^dk}{(2\pi)^d}\frac{1}{(k^2-m_f^2)\big((k-k_i)^2-m_f^2\big)\big((k-k_{ij})^2-m_f^2\big)} \\
&\quad= \frac{i}{32\pi^2 s_{ij}}\ln^2\left(1-2\kappa_{f,ij}\left(1-\sqrt{1-\frac{1}{\kappa_{f,ij}}}\right)\right)
\end{aligned}
\tag{5.204}
$$

$$
\frac{i\pi^2}{(2\pi)^d}C_0(0,s_{ij},m_h^2,m_f^2,m_f^2,m_f^2) \equiv
$$

$$\overset{k_i,k_j\neq k_k}{\equiv} \mu^{2\epsilon}\int \frac{d^dk}{(2\pi)^d}\frac{1}{(k^2-m_f^2)\big((k-k_k)^2-m_f^2\big)\big((k-q)^2-m_f^2\big)}$$

$$= \frac{i}{32\pi^2(m_h^2-s_{ij})}\left(\ln^2\left(1-2\tau_f\left(1-\sqrt{1-\frac{1}{\tau_f}}\right)\right)+\right.$$

$$\left.-\ln^2\left(1-2\kappa_{f,ij}\left(1-\sqrt{1-\frac{1}{\kappa_{f,ij}}}\right)\right)\right) \tag{5.205}$$

$$\frac{i\pi^2}{(2\pi)^d}D_0(0,0,0,m_h^2,s_{12},s_{23},m_f^2,m_f^2,m_f^2,m_f^2)\equiv$$

$$\equiv \mu^{2\epsilon}\int \frac{d^dk}{(2\pi)^d}\frac{1}{(k^2-m_f^2)\big((k-k_1)^2-m_f^2\big)\big((k-k_{12})^2-m_f^2\big)\big((k-q)^2-m_f^2\big)} =$$

$$= -\frac{i}{16\pi^2}\frac{1}{s_{12}s_{23}}W_3(s_{12},s_{13},s_{23},m_h^2) \tag{5.206}$$

A compact expression for W_3 is defined above (see (5.172)) and $s_{13} = m_h^2 - s_{12} - s_{23}$ [136].

5.6. Antenna subtraction

$h \to g\bar{q}q$-channel

In the case of a $1 \to 3$ decay, the relation between the spin- and colour-summed amplitude squared and the differential decay rate of the Higgs boson is given by (see (5.51))

$$d\Gamma = \frac{1}{2m_h}\frac{1}{S}\overline{|\mathcal{M}|^2}d\Phi_3 \tag{5.207}$$

For $h \to gq\bar{q}$, we have $S = 1$, because all particles in the final state are distinguishable. Using $Tr(T^AT^A) = (N_c^2-1)/2$ and (see (5.128))

$$\sum_{\lambda_{1,q,\bar{q}}=\pm}|H^{gq\bar{q}}_{\lambda_1\lambda_q\lambda_{\bar{q}}}|^2 = \frac{1}{2}\frac{s_{1q}^2+s_{1\bar{q}}^2}{s_{q\bar{q}}} \tag{5.208}$$

it is given by

$$\overline{|\mathcal{M}^{R,g\bar{q}q}|^2} = \frac{\alpha_s^3}{2\pi}(N_c^2-1)\frac{s_{1q}^2+s_{1\bar{q}}^2}{s_{q\bar{q}}}\left|\frac{c_{ggh}}{v}-\sum_f\frac{y_fc_f}{\sqrt{2}m_f}\frac{F(\tau_f,\kappa_f)}{(\kappa_f-\tau_f)^2}\right|^2 \tag{5.209}$$

where (5.133) has been used. Upon applying the renormalization prescriptions (5.64)-(5.66), we simply pick up an overall factor of $(\mu_R^2/\mu^2)^{3\epsilon}S_\epsilon^{-3}$ in (5.209), as all other effects are of higher order in α_s. We finally obtain the real radiation decay rate

$$d\Gamma^{R,g\bar{q}q} = \left(\frac{\mu_R^2}{\mu^2}\right)^{3\epsilon}S_\epsilon^{-3}\frac{\alpha_s^3}{4\pi m_h}(N_c^2-1)\frac{s_{1q}^2+s_{1\bar{q}}^2}{s_{q\bar{q}}}\left|\frac{c_{ggh}}{v}-\sum_f\frac{y_fc_f}{\sqrt{2}m_f}\frac{F(\tau_f,\kappa_f)}{(\kappa_f-\tau_f)^2}\right|^2 d\Phi_3 \tag{5.210}$$

The difficult part is the phase space integration over $d\Phi_3$. All real radiation amplitudes are in fact finite, so the three-body phase space integration must contain divergencies in order to cancel the explicit IR divergencies associated with ϵ-poles (i.e. the object $I(\epsilon)$) in the NLO virtual $h \to gg$ decay rate (5.97). Working with dimensional regularization in the virtual case, one is therefore motivated to perform the phase space integration in $d = 4 - 2\epsilon$ dimensions, too. Equation (A4) in [179] gives the relevant expression as

$$d\Phi_3 = \frac{(2\pi)^{2\epsilon-3}}{2^{4-2\epsilon}\Gamma(2-2\epsilon)} \frac{(m_h^2)^{\epsilon-1}}{\left(s_{1q}s_{q\bar{q}}(m_h^2 - s_{1q} - s_{q\bar{q}})\right)^{\epsilon}} ds_{q\bar{q}}ds_{1q} \overset{\epsilon\to 0}{\longrightarrow} \frac{ds_{q\bar{q}}ds_{1q}}{128\pi^3 m_h^2} \tag{5.211}$$

where $s_{1\bar{q}}$ has been eliminated by a delta distribution enforcing $s_{1q} + s_{1\bar{q}} + s_{q\bar{q}} = m_h^2$ (one does a similar thing when dealing with Feynman parameters for triangle diagrams). Due to the Higgs boson being a scalar, there is no need for a non-trivial angular integration. Performing the integrals over $s_{q\bar{q}}$ from 0 to $m_h^2 - s_{1q}$ and s_{1q} from 0 to m_h^2 yields the total phase space volume

$$\Phi_3 \equiv \int d\Phi_3 = \frac{2^{4\epsilon-7}\pi^{2\epsilon-3}(m_h^2)^{1-2\epsilon}\Gamma(1-\epsilon)^3}{\Gamma(3-3\epsilon)\Gamma(2-2\epsilon)} \overset{\epsilon\to 0}{\longrightarrow} \frac{m_h^2}{256\pi^3} \tag{5.212}$$

As mentioned before, the divergent phase space integral combines with the explicit IR poles in terms of ϵ of the virtual amplitudes yielding a finite result. Rather than having a highly unstable numerical cancellation between the phase space integral and the poles, it would be convenient to have an analytic cancellation by coming across the relevant expressions featuring ϵ within the phase space integral itself. We do this by employing the antenna subtraction scheme [185–188].

Symbolically, we can write

$$\Gamma^R + \Gamma^V = \underbrace{\int_3 d\Gamma^R - \int_3 d\Gamma^S}_{\int_3 d\Gamma^{R-S}} + \underbrace{\int_3 d\Gamma^S + \int_2 d\Gamma^V}_{\int_2 (d\Gamma^V - d\Gamma^T)\, \equiv\, \int_2 d\Gamma^{V-T}} \tag{5.213}$$

where the integral subindices denote whether the two- or three-body phase space integration has to be performed (i.e. integration over $d\Phi_2$ or $d\Phi_3$, etc.). The renormalized real radiation differential decay rate and its virtual counterpart are denoted by $d\Gamma^R$ (see 5.210 or a similar expression for $h \to ggg$) and $d\Gamma^V$ (see (5.97)), respectively, and the subtraction term $d\Gamma^S$ is chosen such that $\int_3 d\Gamma^{R-S}$ is finite and can be integrated numerically without any peculiarities. It is possible to set $\epsilon \to 0$ here[59]. Correspondingly, the combination $\int_3 d\Gamma^S + \int_2 d\Gamma^V$ should be finite as well. However, as the last term contains poles in ϵ, one has to keep ϵ arbitrary here. In fact, it is possible to choose $d\Gamma^S$ such that the three-body phase space $d\Phi_3$ integral factorizes into the two-body phase space $d\Phi_2$ and the so-called unresolved antenna phase space $d\Phi_X$ yielding [189]

$$\int_3 d\Gamma^S = \int_2 \int_X d\Gamma^S \equiv - \int_2 d\Gamma^T \tag{5.214}$$

[59]The combination $d\Gamma^{R-S}$ actually vanishes for the non-SM-like case, as the explicit form of the antenna function (5.218) is chosen such that it exactly cancels the c_{ggh}-part of the physical amplitude squared in (5.209).

where the integration $\int_X$ can be done analytically.
For the case at hand, the explicit form of the subtraction term is given by [187]

$$d\Gamma^{S,g\bar{q}q} \equiv \frac{1}{2m_h}\frac{\alpha_s^3}{4\pi}\left(\frac{\mu_R^2}{\mu^2}\right)^{\epsilon} S_\epsilon^{-1} G_0^3 \overline{|\mathcal{M}_r^{(0)}|^2} d\Phi_3 \tag{5.215}$$

where (see (5.30), (5.75) and (5.94))

$$i\mathcal{M}_r^{(0)} = iH_{\lambda_1\lambda_2}^{gg}\delta^{AB}\left(\frac{\mu_R^2}{\mu^2}\right)^{\epsilon} S_\epsilon^{-1}\left(\frac{c_{ggh}}{v} + \sum_f \frac{y_f c_f}{2\sqrt{2}m_f}\frac{4}{3}F_0^H(\epsilon)\right) \tag{5.216}$$

and thus

$$\overline{|\mathcal{M}_r^{(0)}|^2} = 2m_h^4(N_c^2-1)\left(\frac{\mu_R^2}{\mu^2}\right)^{2\epsilon} S_\epsilon^{-2}\left|\frac{c_{ggh}}{v} + \sum_f \frac{y_f c_f}{2\sqrt{2}m_f}\frac{4}{3}F_0^H(\epsilon)\right|^2 \tag{5.217}$$

This corresponds to (5.2) with $\epsilon \neq 0$. The object

$$G_0^3 \equiv \frac{\mu^{2\epsilon}}{m_h^4}\left(\frac{s_{1q}^2 + s_{1\bar{q}}^2}{s_{q\bar{q}}}\right)\left(1 - \frac{\epsilon}{2} - \frac{\epsilon^2}{4} - \left(\frac{1}{8} - \frac{50\zeta(3)}{3}\right)\epsilon^3 + \mathcal{O}(\epsilon^4)\right) \tag{5.218}$$

is the adequate gluon-quark-antiquark antenna function. Note that the symbols s_{1q}, $s_{1\bar{q}}$ and $s_{q\bar{q}}$ in (5.218) are in fact different from the Mandelstam variables defined for the physical process $h \to gq\bar{q}$. Indeed, they refer to the momenta of the three partons that are involved in the IR singularity giving rise to a separate phase space Φ_X that should not be confused with the physical one defined in (5.211); see [190, 191] and [187] for the technical details concerning the dipole or antenna interpretation of Φ_X, respectively. Using $d\Phi_X = d\Phi_3/\Phi_2$ for this additional phase space (which follows from the integral over $d\Phi_2$ being constant, see [179, 187, 192]), where Φ_2 for arbitrary ϵ is given in (5.54), the integrated form of the antenna function reads

$$\begin{aligned}\mathcal{G}_0^3 \equiv 8\pi^2 S_\epsilon^{-1}\int d\Phi_X G_0^3 = \left(\frac{\mu^2}{m_h^2}\right)^{\epsilon}\Bigg(&-\frac{1}{3\epsilon} - \frac{7}{6} + \frac{1}{36}\left(7\pi^2 - 135\right)\epsilon + \\ &+\left(-\frac{25\zeta(3)}{9} - \frac{93}{8} + \frac{49\pi^2}{72}\right)\epsilon^2\Bigg) + \mathcal{O}(\epsilon^3)\end{aligned} \tag{5.219}$$

For our purpose, we only need the $\mathcal{O}(\epsilon^{-1})$ and $\mathcal{O}(\epsilon^0)$ terms. The final result is then given by

$$\begin{aligned}d\Gamma^{T,g\bar{q}q} &= -\int_X d\Gamma^{S,g\bar{q}q} = -\left(\int d\Phi_X G_0^3\right)\frac{1}{2m_h}\frac{\alpha_s^3}{4\pi}\left(\frac{\mu_R^2}{\mu^2}\right)^{\epsilon} S_\epsilon^{-1}\overline{|\mathcal{M}_r^{(0)}|^2} d\Phi_2 = \\ &= \left(\frac{1}{3\epsilon} + \frac{7}{6}\right)\frac{1}{2m_h}\left(\frac{\mu_R^2}{m_h^2}\right)^{\epsilon}\frac{\alpha_s^3}{32\pi^3}\overline{|\mathcal{M}_r^{(0)}|^2} d\Phi_2 + \mathcal{O}(\epsilon)\end{aligned} \tag{5.220}$$

with $\overline{|\mathcal{M}_r^{(0)}|^2}$ defined in (5.217). This expression has to be multiplied by the number N_f of light quarks in the final state, which - as stated before - equals 5 in our case (all final

state quarks but the top are considered as massless).
The combination $d\Gamma^{(R-S),g\bar{q}q}$ gives a non-zero contribution only in the SM-like case, namely (we are allowed to set $\epsilon \to 0$ here)

$$d\Gamma^{(R-S),g\bar{q}q} = \frac{\alpha_s^3}{4\pi m_h} N_f(N_c^2-1)\frac{s_{1q}^2+s_{1\bar{q}}^2}{s_{q\bar{q}}}\left(\left|\frac{c_{ggh}}{v} - \sum_f \frac{y_f c_f}{\sqrt{2}m_f}\frac{F(\tau_f,\kappa_f)}{(\kappa_f-\tau_f)^2}\right|^2 + \right.$$
$$\left. -\left|\frac{c_{ggh}}{v} + \sum_f \frac{y_f c_f}{2\sqrt{2}m_f}\frac{4}{3}F_0^H\right|^2\right) d\Phi_3 \quad (5.221)$$

which is independent of c_{ggh}^2. Remember that κ_f depends on $s_{q\bar{q}}$. The phase space integral over $d\Phi_3$ in (5.221) has to be done numerically.

$h \to ggg$-channel

We now apply (5.207) with $S = 6$ for three indistinguishable final gluon states and (5.211) with s_{1q}, $s_{1\bar{q}}$ and $s_{q\bar{q}}$ replaced by s_{12}, s_{13} and s_{23}, respectively. The renormalized amplitude squared is given by (see (5.191))

$$\overline{|\mathcal{M}_r^{R,ggg}|^2} = \left(\frac{\mu_R^2}{\mu^2}\right)^{3\epsilon} S_\epsilon^{-3}\frac{\alpha_s^3}{2\pi}N_c(N_c^2-1)\cdot$$
$$\cdot \sum_{\lambda_{1,2,3}=\pm}\left|H^{ggg}_{\lambda_1\lambda_2\lambda_3}\right|^2\left|\frac{c_{ggh}}{v} - \sum_f \frac{y_f c_f}{\sqrt{2}m_f}\mathcal{Q}^f_{\lambda_1\lambda_2\lambda_3}(s_{12},s_{13},s_{23})\right|^2 \quad (5.222)$$

with the helicities defined in (5.157). Their squares read

$$\left|H^{ggg}_{+++}\right|^2 = \left|H^{ggg}_{---}\right|^2 = \frac{m_h^8}{s_{12}s_{13}s_{23}},\quad \left|H^{ggg}_{+--}\right|^2 = \left|H^{ggg}_{-++}\right|^2 = \frac{s_{23}^3}{s_{12}s_{13}}$$
$$\left|H^{ggg}_{+-+}\right|^2 = \left|H^{ggg}_{-+-}\right|^2 = \frac{s_{13}^3}{s_{12}s_{23}},\quad \left|H^{ggg}_{++-}\right|^2 = \left|H^{ggg}_{--+}\right|^2 = \frac{s_{12}^3}{s_{13}s_{23}} \quad (5.223)$$

and the relevant sum evaluates to

$$\sum_{\lambda_{1,2,3}=\pm}\left|H^{ggg}_{\lambda_1\lambda_2\lambda_3}\right|^2\left|\mathcal{Q}^f_{\lambda_1\lambda_2\lambda_3}(s_{12},s_{13},s_{23})\right|^2 = \sum_{\lambda_{1,2,3}=\pm}|\mathcal{P}_{\lambda_1\lambda_2\lambda_3}|^2 = \frac{8m_h^8}{s_{12}s_{13}s_{23}}A_6(s_{12},s_{13},s_{23}) \quad (5.224)$$

where

$$A_6(s_{12},s_{13},s_{23}) \equiv \left|A_4(s_{12},s_{13},s_{23})\right|^2 + \left|A_2(s_{12},s_{13},s_{23})\right|^2 +$$
$$+\left|A_2(s_{13},s_{23},s_{12})\right|^2 + \left|A_2(s_{23},s_{12},s_{13})\right|^2 \quad (5.225)$$

We can take over (5.215) for $d\Gamma^{S,ggg}$ with G_0^3 replaced by

$$F_0^3 = \frac{2\mu^{2\epsilon}}{m_h^4}\left(\frac{m_h^4 s_{12}}{s_{13}s_{23}} + \frac{m_h^4 s_{13}}{s_{12}s_{23}} + \frac{m_h^4 s_{23}}{s_{12}s_{13}} + \right.$$

$$+\frac{s_{12}s_{13}}{s_{23}}+\frac{s_{13}s_{23}}{s_{12}}+\frac{s_{12}s_{23}}{s_{13}}+4m_h^2\Big)\left(1-\frac{\epsilon^3}{3}-\frac{11\epsilon^4}{9}+\mathcal{O}(\epsilon^5)\right) \tag{5.226}$$

and an extra factor of $N_c/3$ in order to adjust the colour- and symmetry factors for three gluons (1/6 for the final state permutations and an extra factor of 2 due to the overall relative normalization between the ggg and $gq\bar{q}$ channels which can ultimately be traced back to a reflection symmetry in the former). We obtain

$$d\Gamma^{S,ggg}=\frac{N_c}{2m_h}\frac{\alpha_s^3}{12\pi}\left(\frac{\mu_R^2}{\mu^2}\right)^\epsilon S_\epsilon^{-1}F_0^3\overline{|\mathcal{M}_r^{(0)}|^2}d\Phi_3 \tag{5.227}$$

with $\overline{|\mathcal{M}_r^{(0)}|^2}$ again given by (5.217). The integrated form of F_0^3 is given by

$$\mathcal{F}_0^3 \equiv 8\pi^2 S_\epsilon^{-1}\int d\Phi_X F_0^3=\left(\frac{\mu^2}{m_h^2}\right)^\epsilon\Bigg(\frac{3}{\epsilon^2}+\frac{11}{2\epsilon}-\frac{7\pi^2}{4}+\frac{73}{4}+ \\ +\left(\frac{451}{8}-25\zeta(3)-\frac{77\pi^2}{24}\right)\epsilon+\left(\frac{2729}{16}-\frac{275\zeta(3)}{6}-\frac{511\pi^2}{48}-\frac{71\pi^4}{480}\right)\epsilon^2\Bigg)+\mathcal{O}(\epsilon^3) \tag{5.228}$$

The subtraction term for the virtual amplitude is reads

$$d\Gamma^{T,ggg}=-\left(\frac{3}{\epsilon^2}+\frac{11}{2\epsilon}-\frac{7\pi^2}{4}+\frac{73}{4}\right)\frac{N_c}{2m_h}\left(\frac{\mu_R^2}{m_h^2}\right)^\epsilon\frac{\alpha_s^3}{96\pi^3}\overline{|\mathcal{M}_r^{(0)}|^2}d\Phi_2+\mathcal{O}(\epsilon) \tag{5.229}$$

where the definition (5.220) was used.
Applying $m_h^2=s_{12}+s_{13}+s_{23}$ yields

$$m_h^4F_0^3=\frac{m_h^8+s_{12}^4+s_{13}^4+s_{23}^4}{s_{12}s_{13}s_{23}}+\mathcal{O}(\epsilon)=\frac{1}{2}\sum_{\lambda_{1,2,3}=\pm}\left|H^{ggg}_{\lambda_1\lambda_2\lambda_3}\right|^2+\mathcal{O}(\epsilon) \tag{5.230}$$

and thus (we set $\epsilon=0$)

$$d\Gamma^{(R-S),ggg}=\frac{\alpha_s^3}{24\pi m_h}N_c(N_c^2-1)\cdot \\ \cdot\sum_{\lambda_{1,2,3}=\pm}\left|H^{ggg}_{\lambda_1\lambda_2\lambda_3}\right|^2\left(\left|\frac{c_{ggh}}{v}-\sum_f\frac{y_fc_f}{\sqrt{2}m_f}\mathcal{Q}^f_{\lambda_1\lambda_2\lambda_3}(s_{12},s_{13},s_{23})\right|^2+ \\ -\left|\frac{c_{ggh}}{v}+\sum_f\frac{y_fc_f}{2\sqrt{2}m_f}\frac{4}{3}F_0^H\right|^2\right)d\Phi_3 \tag{5.231}$$

Again, setting $c_f=0$ yields a vanishing contribution.
Let us now combine the virtual decay rate (5.97) with its subtraction terms (5.220) and (5.229). Indeed, rewriting the expressions using (5.217) and neglecting terms of $\mathcal{O}(\epsilon)$ gives

$$d\Gamma^{LO\times V}=\frac{N_c}{2m_h}\frac{\alpha_s^3}{32\pi^3}\overline{|\mathcal{M}_r^{(0)}|^2}\,\mathrm{Re}\left\{\frac{I(\epsilon)}{2}\right\}d\Phi_2+$$

$$+\frac{\alpha_s^3 m_h^3}{16\pi^3}(N_c^2-1)\,\mathrm{Re}\Bigg\{\left(\frac{c_{ggh}}{v}+\sum_f \frac{y_f c_f}{2\sqrt{2}m_f}\frac{4}{3}(F_0^H)^*\right)\times$$

$$\times\left(\sum_f \frac{y_f c_f}{2\sqrt{2}m_f}\left(\mathcal{A}_{fin}+C_F F_0^H C_2^H X(\mu_f^2)\right)\right)\Bigg\}d\Phi_2 \tag{5.232}$$

and

$$d\Gamma^T \equiv d\Gamma^{T,g\bar{q}q}+d\Gamma^{T,ggg}=$$

$$=\frac{N_c}{2m_h}\frac{\alpha_s^3}{32\pi^3}\overline{|\mathcal{M}_r^{(0)}|^2}\left(\frac{\mu_R^2}{m_h^2}\right)^\epsilon\left(\frac{N_f}{3N_c\epsilon}+\frac{7N_f}{6N_c}-\frac{1}{\epsilon^2}-\frac{11}{6\epsilon}-\frac{7\pi^2}{12}+\frac{73}{12}\right)d\Phi_2 \tag{5.233}$$

For $C_A = N_c$, we find

$$\left(\frac{\mu_R^2}{m_h^2}\right)^\epsilon\left(\frac{N_f}{3N_c\epsilon}+\frac{7N_f}{6N_c}-\frac{1}{\epsilon^2}-\frac{11}{6\epsilon}-\frac{7\pi^2}{12}+\frac{73}{12}\right)=$$

$$=\mathrm{Re}\left\{\frac{I(\epsilon)}{2}\right\}-\frac{\beta_0\ln\frac{\mu_R^2}{m_h^2}}{2N_c}+\frac{7N_f}{6N_c}-\frac{73}{12}+\mathcal{O}(\epsilon) \tag{5.234}$$

This confirms the cancellation of the IR divergencies contained in the object $I(\epsilon)$. Note that the non-trivial explicit ϵ-dependence of the object $F_0^H(\epsilon)$ (see (5.50)) has actually never been used as it is canceled in the final expression.

We are now ready to write down the full virtual decay rate together with its subtraction terms. It is given by

$$\Gamma^{V-T}=\int\left(d\Gamma^{LO\times V}-d\Gamma^T\right)=\frac{\alpha_s^3 m_h^3}{128\pi^4}(N_c^2-1)\,\mathrm{Re}\Bigg\{\left(\frac{c_{ggh}}{v}+\sum_f \frac{y_f c_f}{2\sqrt{2}m_f}\frac{4}{3}(F_0^H)^*\right)\cdot$$

$$\cdot\left(\sum_f \frac{y_f c_f}{2\sqrt{2}m_f}\left(\mathcal{A}_{fin}+C_F F_0^H C_2^H X(\mu_f^2)\right)\right)\Bigg\}+$$

$$+\frac{\alpha_s^3 m_h^3}{512\pi^4}(N_c^2-1)\left|\frac{c_{ggh}}{v}+\sum_f \frac{y_f c_f}{2\sqrt{2}m_f}\frac{4}{3}F_0^H\right|^2\left(\beta_0\ln\frac{\mu_R^2}{m_h^2}-\frac{7N_f}{3}+\frac{73N_c}{6}\right) \tag{5.235}$$

where (5.54) has been used. The beta-function can be found below (5.72) and F_0^H, $\mathcal{A}_{fin}$, C_2^H and $X(\mu_f^2)$ are given by (5.83), (5.89), (5.85) and (5.95), respectively.

The list of required expressions for a numerical analysis $h\to gg$ at NLO QCD based on actual numbers is hereby complete. Before doing so, we briefly turn to a related process, namely $h\to\gamma\gamma$, which we have almost already completed en passant.

5.7. $h \to \gamma\gamma$ at NLO in QCD

LO conributions

Having exploited the non-Abelian case, i.e. $h \to gg$, it should be straightforward to obtain results for $h \to \gamma\gamma$ by taking the Abelian limit of our formulas. In addition, however, we need to take into account the coupling between the photon and the massive gauge bosons. This will introduce interesting new insights that are absent in the gluon case, as we will discuss in this subsection [193–204].
Using the results of Subsection 5.2, one can immediately write down the SM-like amplitude for $h \to \gamma\gamma$ induced by fermion loops. In contrast to $h \to gg$, these could now also be leptons. The diagrams are given by

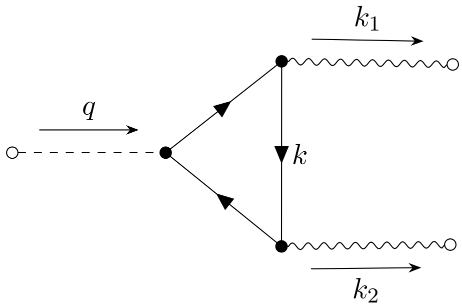

$$\equiv i\mathcal{M}^{\gamma\gamma,LO}_{1,SM} = -\frac{q_f^2 y_f c_f}{\sqrt{2}} \epsilon^*_\mu(k_1)\epsilon^*_\nu(k_2) I^{\mu\nu}_{1,2} \tag{5.236}$$

and its fermion flow reversed version $i\mathcal{M}^{\gamma\gamma,LO}_{2,SM}$ with $I^{\mu\nu}_{1,2}$ replaced by $I^{\nu\mu}_{2,1}$, where $q_f \equiv Q_f e$ denotes the charge of the fermion going through the loop ($Q_f = 0$ and $Q_f = -1$ for neutrinos and charged leptons and $Q_f = 2/3$ and $Q_f = -1/3$ for up- and down-type quarks, respectively) and $I^{\mu\nu}_{1,2}$ given in (5.10) as before. We end up with

$$\begin{aligned} i\mathcal{M}^{\gamma\gamma,LO}_{1,SM} + i\mathcal{M}^{\gamma\gamma,LO}_{2,SM} &= \frac{ie^2}{8\pi^2} H^{\gamma\gamma}_{\lambda_1\lambda_2} \sum_f c_f \frac{Q_f^2 y_f}{\sqrt{2} m_f} \frac{\tilde{J}(\tau_f)}{\tau_f} \\ \tilde{J}(\tau_f) &= \begin{cases} 1 + \left(1 - \frac{1}{\tau_f}\right) \arcsin^2 \sqrt{\tau_f} & \text{for } 0 < \tau_f < 1 \\ 1 - \frac{1}{4}\left(1 - \frac{1}{\tau_f}\right) \left(\ln \left(\frac{1-\sqrt{1-\frac{1}{\tau_f}}}{1+\sqrt{1-\frac{1}{\tau_f}}} \right) + i\pi \right)^2 & \text{for } 1 \leq \tau_f < \infty \end{cases} \end{aligned} \tag{5.237}$$

where

$$H^{\gamma\gamma}_{\lambda_1\lambda_2} \equiv 2\epsilon^*_{\lambda_1\mu}(k_1)\epsilon^*_{\lambda_2\nu}(k_2)(k_1^\nu k_2^\mu - k_1 \cdot k_2 g^{\mu\nu}) \tag{5.238}$$

as in (5.20). Compared to (5.16), there is an extra factor of 2 resulting from the normalization of the $SU(3)$ generators, i.e. $Tr(T^A T^B) = \delta^{AB}/2$. If the loop-fermions are quarks, there is an extra factor of $\delta_{c_1c_1} = N_c$ resulting from the implicit colour-index contraction across the loop-propagators.
As mentioned before, there are additional contributions arising from W-boson loops. In

unitary gauge, the first one is given by

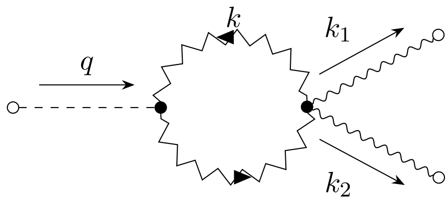

$$\equiv i\mathcal{M}_{3,SM}^{\gamma\gamma,LO} \tag{5.239}$$

and the second and third ones by

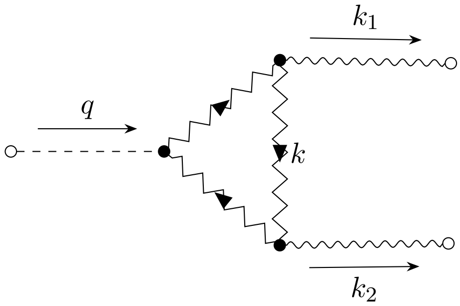

$$\equiv i\mathcal{M}_{4,SM}^{\gamma\gamma,LO} \tag{5.240}$$

and its gauge boson flow reverted relative $i\mathcal{M}_{5,SM}^{\gamma\gamma,LO}$. The explicit calculations are carried out in the appendix to this subsection. The final result is given by

$$i\mathcal{M}_{3,SM}^{\gamma\gamma,LO} + i\mathcal{M}_{4,SM}^{\gamma\gamma,LO} + i\mathcal{M}_{5,SM}^{\gamma\gamma,LO} = -\frac{ig^2e^2vc_V}{64\pi^2m_W^2}H_{\lambda_1\lambda_2}^{\gamma\gamma}F\left(\tau_W\right)$$

$$F\left(\tau_W\right) = \begin{cases} 2+\frac{3}{\tau_W}+3\left(\frac{2}{\tau_W}-\frac{1}{\tau_W^2}\right)\arcsin^2\sqrt{\tau_W} & \text{for } 0<\tau_W<1 \\ 2+\frac{3}{\tau_W}-\frac{3}{4}\left(\frac{2}{\tau_W}-\frac{1}{\tau_W^2}\right)\left(\ln\left(\frac{1-\sqrt{1-\frac{1}{\tau_W}}}{1+\sqrt{1-\frac{1}{\tau_W}}}\right)+i\pi\right)^2 & \text{for } 1\leq\tau_W<\infty \end{cases} \tag{5.241}$$

where $\tau_W \equiv m_h^2/4m_W^2 \approx 0.60706$.

In addition to the SM-like couplings c_f and c_W, we have the direct coupling between the Higgs boson and two photons in the context of an EFT. Following (5.5), we have

$$\mathcal{L}_{int} \supset \frac{e^2}{32\pi^2 v}c_{\gamma\gamma h}hF_{\mu\nu}F^{\mu\nu} \tag{5.242}$$

where $F_{\mu\nu}$ is the Abelian field strength tensor for photons. The relevant contribution is given by

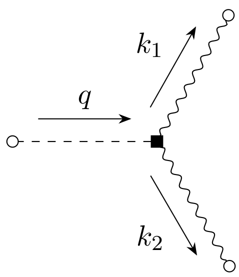

$$\equiv i\mathcal{M}_{NSM}^{\gamma\gamma,LO} = \frac{ie^2c_{\gamma\gamma h}}{16\pi^2 v}H_{\lambda_1\lambda_2}^{\gamma\gamma} \tag{5.243}$$

and the full LO result is then given by adding up (5.237), (5.241) and (5.243).

The role of the Goldstone bosons

There have recently been suggestions that (5.241) or (5.293) might in fact be wrong [205, 206]. Instead, the expression

$$\frac{3}{\tau_W} - \frac{3}{4}\left(\frac{2}{\tau_W} - \frac{1}{\tau_W^2}\right)\ln^2\left(\frac{\sqrt{1-\frac{1}{\tau_W}}-1}{\sqrt{1-\frac{1}{\tau_W}}+1}\right) \tag{5.244}$$

is envoked, i.e. the first term in (5.241) is missing. However, the argumentation is based on a blank-faced non-necessity of regularization for divergent momentum integrals when the final result turns out to be finite, which is the case for $h \to \gamma\gamma$ in the SM. While this argument is not only false [207], expression (5.244) has the wrong behavior when the particle in the loop becomes massless [208, 209].
Naïvely taking the coupling between the Higgs and the loop particle to be proportional to the mass of the latter ($y_f \sim m_f$ or $g^2 \sim m_W^2$), we expect no coupling at all and hence no Higgs decay into photons when $m_f, m_W \to 0$. For the fermion loop, we find

$$\lim_{\tau_f \to \infty} \frac{J(\tau_f)}{\tau_f} = 0 \tag{5.245}$$

confirming our guess, but for the W-boson loop we have

$$\lim_{\tau_W \to \infty} F(\tau_W) = 2 \tag{5.246}$$

while (5.244) would yield 0. We now show that the (correct) non-decoupling between the Higgs and the W-bosons shown by (5.246) has its origin in the pure Higgs-sector, namely the Goldstone bosons of electroweak symmetry breaking - that is the longitudinal modes of the W-bosons.
To be more specific, imagine a world without W-bosons. We are interested in calculating the amplitude for $h \to \gamma\gamma$ within the pure Higgs sector. Setting $g = 0$ in the SM Lagrangian while keeping e finite does not work because of the interplay between g and g'. Somehow identifying the latter with e assigns a charge to all components of the complex scalar doublet φ. We therefore have to consider the Lagrangian

$$\mathcal{L} = (D_\mu\varphi)^\dagger D^\mu\varphi + m^2\varphi^\dagger\varphi - \frac{\lambda}{2}(\varphi^\dagger\varphi)^2 \tag{5.247}$$

with $D^\mu\varphi = \partial^\mu\varphi + iQA^\mu\varphi$, see (2.11). We identify A^μ with the electromagnetic field and Q as the charge operator

$$Q = e\begin{pmatrix} 1 & 0 \\ 0 & 0 \end{pmatrix} \tag{5.248}$$

As in the SM, the scalar field develops a vacuum expectation value given by $v = \sqrt{2m^2/\lambda}$ and we can introduce the real scalar fields φ_0, φ_1, φ_2 and h and write

$$\varphi = \begin{pmatrix} \varphi_+ \\ \frac{1}{\sqrt{2}}(v + h + i\varphi_0) \end{pmatrix} \tag{5.249}$$

where $\varphi_\pm \equiv (\varphi_1 \pm i\varphi_2)/\sqrt{2}$ with a slightly different notation compared to (2.12). The scalars $\varphi_\pm$ and φ_0 are the massless Goldstone bosons, while the massive field h can be identified with the SM Higgs boson. When the W- and Z-bosons are reintroduced, the Goldstones become the longitudinal modes of the former. However, without massive vector bosons, the Goldstones remain in the physical particle spectrum - as is the case for non-unitary gauges in the full SM with massive vector bosons.
We now evaluate the couplings between the photon A^μ, the Higgs h and the charged Goldstones $\varphi_\pm$. Expanding the kinetic term of the scalar doublet yields

$$\begin{aligned}(D_\mu\varphi)^\dagger D^\mu\varphi =& \partial_\mu\varphi_-\partial^\mu\varphi_+ \frac{1}{2}\partial_\mu h\partial^\mu h + \frac{1}{2}\partial_\mu\varphi_0\partial^\mu\varphi_0 + \\ &+ ieA^\mu(\varphi_+\partial_\mu\varphi_- - \varphi_-\partial_\mu\varphi_+) + e^2 A_\mu A^\mu \varphi_-\varphi_+\end{aligned} \tag{5.250}$$

The relevant Feynman rules are given by

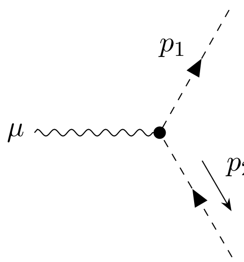

$$\equiv -ie(p_1^\mu - p_2^\mu) \tag{5.251}$$

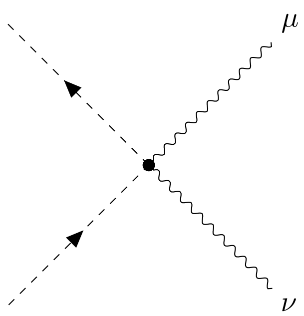

$$\equiv = 2ie^2 g^{\mu\nu} \tag{5.252}$$

The Higgs potential contains the terms

$$m^2\varphi^\dagger\varphi - \frac{\lambda}{2}(\varphi^\dagger\varphi)^2 \supset -\frac{1}{2}\lambda v^2 h^2 - \lambda v \varphi_-\varphi_+ h \tag{5.253}$$

giving rise to the Feynman rules

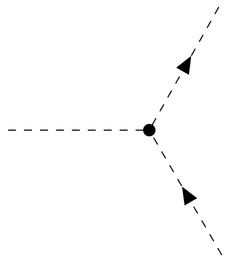

$$\equiv -i\lambda v$$

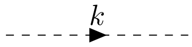

$$\equiv \frac{i}{k^2} \tag{5.254}$$

and the masses $m_h^2 = \lambda v^2$ and $m_{\varphi_\pm} = m_{\varphi_0} = 0$ as expected.
Next, we evaluate the loop diagrams generating $h \to \gamma\gamma$. They are given by

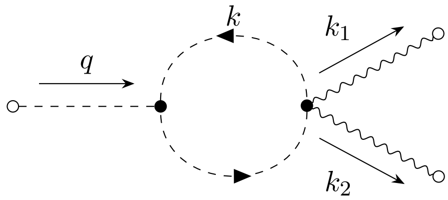

$$\equiv -2\lambda v e^2 g^{\mu\nu}\epsilon^*_\mu(k_1)\epsilon^*_\nu(k_2)\mu^{2\epsilon}\int \frac{d^dk}{(2\pi)^d}\frac{1}{k^2(k-q)^2} =$$

$$= -\frac{i}{8\pi^2}\lambda v e^2 g^{\mu\nu}\epsilon^*_\mu(k_1)\epsilon^*_\nu(k_2)\left(\frac{1}{\epsilon} + \ln\frac{4\pi}{e^\gamma} + \ln\frac{\mu^2}{-q^2} + 2\right) \tag{5.255}$$

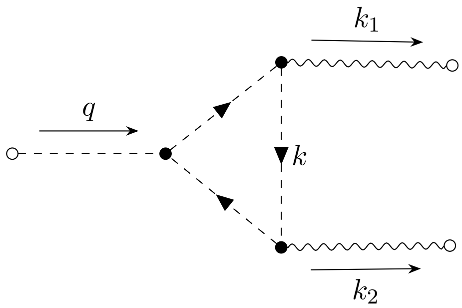

$$\equiv \lambda v e^2 \epsilon^*_\mu(k_1)\epsilon^*_\nu(k_2)\mu^{2\epsilon}\int \frac{d^dk}{(2\pi)^d}\frac{(2k^\mu + k_1^\mu)(2k^\nu - k_2^\nu)}{k^2(k+k_1)^2(k-k_2)^2} =$$

$$= \frac{i}{16\pi^2}\lambda v e^2 g^{\mu\nu}\epsilon^*_\mu(k_1)\epsilon^*_\nu(k_2)\left(\frac{1}{\epsilon} + \ln\frac{4\pi}{e^\gamma} + \ln\frac{\mu^2}{-q^2} + 3\right) +$$
$$-\frac{i}{8q^2\pi^2}\lambda v e^2 k_1^\nu k_2^\mu \epsilon^*_\mu(k_1)\epsilon^*_\nu(k_2) \tag{5.256}$$

The second diagram has a fermion-flow reversed version yielding the same analytical expression. Combining all three results using $q^2 = \lambda v^2 = m_h^2$ leads to

$$\frac{ie^2}{4\pi^2 v}(k_1\cdot k_2 g^{\mu\nu} - k_1^\nu k_2^\mu)\epsilon^*_\mu(k_1)\epsilon^*_\nu(k_2) \tag{5.257}$$

which is precisely the first term of (5.293) in (5.290).
This calculation demonstrates a non-decoupling behavior of the Higgs boson from photons, even if massive fermions or vector bosons are absent. This is in strong contrast to

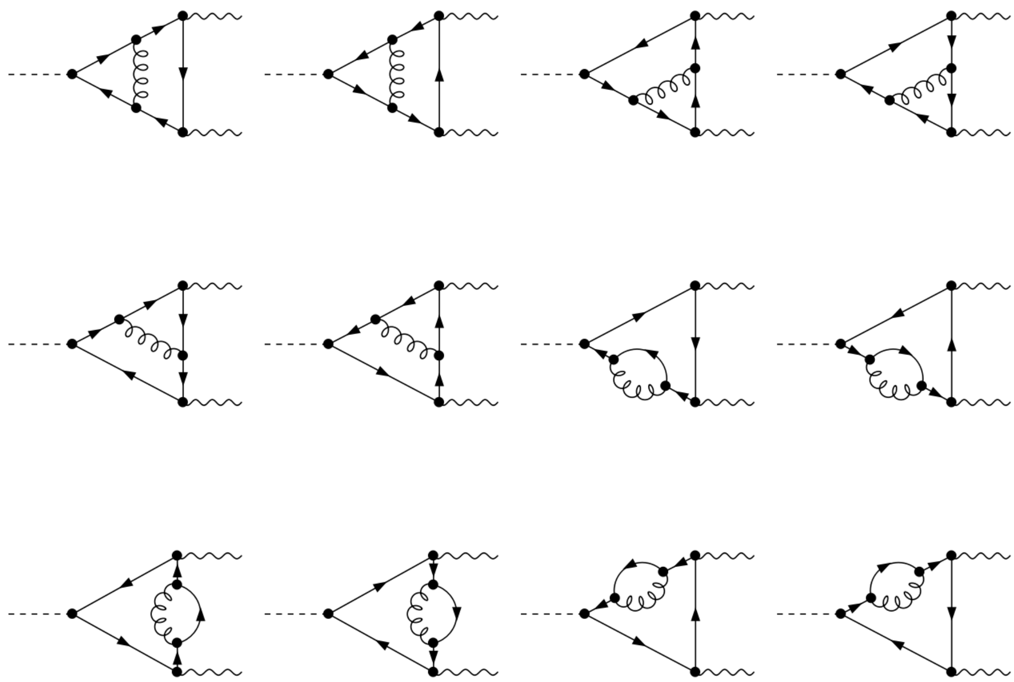

Figure 6: All two-loop diagrams that represent the corrections of $\mathcal{O}(\alpha_s)$ to the quark loop amplitude for $h \to \gamma\gamma$, see also Figure 4. The lepton- and W-boson loops don't get QCD corrections since there is no coupling between leptons or W-bosons and gluons.

gluons, which would indeed decouple from the Higgs particle in this limit - a relic from QCD being unaffected by electroweak symmetry breaking.

NLO conributions

There is no coupling between photons and gluons in the SM, so all QCD corrections to $h \to \gamma\gamma$ are of genuine two-loop topology (in contrast to Subsection 5.3). The relevant diagrams are displayed in Figure 6.
Only the quark loops obtain QCD corrections. With $\alpha = e^2/(4\pi)$ and $Q_l = -1$, the fermion loops (5.237) - LO plus QCD corrections - are given by

$$i\mathcal{M}_{SM}^{\gamma\gamma,LO+V} \equiv \frac{i\alpha}{2\pi} H_{\lambda_1\lambda_2}^{\gamma\gamma} \left(\sum_l \left(c_l \frac{y_l}{\sqrt{2}m_l} \frac{\tilde{J}(\tau_l)}{\tau_l} \right) + \sum_q c_q \frac{N_c Q_q^2 y_q}{2\sqrt{2}m_q} \left(\frac{2\tilde{J}(\tau_q)}{\tau_q} + \frac{\alpha_s}{\pi}\mathcal{A}_{\gamma\gamma} \right) \right) \tag{5.258}$$

where the subindices l and q refer to leptons and quarks, respectively. Details can be found in [137, 140, 142, 210, 211]. We have suppressed the terms associated with $c_{\gamma\gamma h}$ and c_W. The expression $\mathcal{A}_{\gamma\gamma}$ refers to the unrenormalized QCD correction and thus contains divergencies in the first place. Luckily, in contrast to Subsection 5.3, there are no IR poles, as there cannot be a cancellation mechanism to account for them. Indeed, the corresponding real radiation amplitude $h \to \gamma\gamma g$ does not exist due to gluon colour conservation. However, $\mathcal{A}_{\gamma\gamma}$ still contains UV poles. These need to be canceled by appropriate counterterms in the form of the LO amplitude. In fact, the first term in

$$\frac{2\tilde{J}(\tau_q)}{\tau_q} + \frac{\alpha_s}{\pi}\mathcal{A}_{\gamma\gamma} \tag{5.259}$$

changes according to (5.64)-(5.66). As there are no gluons in the final state and the LO amplitude is $\mathcal{O}(\alpha_s^0)$, only the mass renormalization comes into play. We have (in the notation of [140], see also (5.83))

$$\frac{2\tilde{J}(\tau_q)}{\tau_q} = \frac{4}{3}F_0^H \longrightarrow \frac{4}{3}F_0^H + \frac{\alpha_s}{4\pi}\delta m_q^2 \frac{\partial}{\partial m_q^2}\frac{4}{3}F_0^H \tag{5.260}$$

and

$$\frac{\alpha_s}{\pi}\mathcal{A}_{\gamma\gamma} \longrightarrow \left(\frac{\mu_R^2}{\mu^2}\right)^{\epsilon} S_\epsilon^{-1}\frac{\alpha_s}{\pi}\mathcal{A}_{\gamma\gamma} \tag{5.261}$$

yielding (see also Subsection 5.3)

$$\frac{4}{3}F_0^H + \frac{\alpha_s}{\pi}\mathcal{A}_{\gamma\gamma} \longrightarrow \frac{4}{3}F_0^H + \left(\frac{\mu_R^2}{\mu^2}\right)^{\epsilon} S_\epsilon^{-1}\frac{\alpha_s}{\pi}\left(\left(\frac{\mu_R^2}{\mu^2}\right)^{-\epsilon} S_\epsilon \frac{1}{6}\frac{\delta m_q^2}{m_q^2}F_0^H C_2^H + \mathcal{A}_{\gamma\gamma}\right) \tag{5.262}$$

The explicit form of the mass counterterm is again given by (5.82). The unrenormalized amplitude $\mathcal{A}_{\gamma\gamma}$ is proportional to $C_F = (N_c^2-1)/(2N_c)$ and can be written as

$$\mathcal{A}_{\gamma\gamma} \equiv \left(\frac{\mu_R^2}{\mu^2}\right)^{-\epsilon} S_\epsilon\left(C_F F_0^H C_2^H\left(\frac{1}{\epsilon} + \frac{4}{3} + \ln\frac{\mu_R^2}{m_q^2}\right) + C_F F_0^H C_1^H\right) + \mathcal{O}(\epsilon) \tag{5.263}$$

where $F_0^H C_1^H$ and $F_0^H C_2^H$ were defined in (5.92) and (5.85), respectively, with θ_f replaced by θ_q. The renormalized final result of (5.258) is then given by

$$\begin{aligned} i\mathcal{M}_{r,SM}^{\gamma\gamma,LO+V} = \frac{i\alpha}{2\pi}H_{\lambda_1\lambda_2}^{\gamma\gamma}\Bigg(&\sum_l\left(c_l\frac{y_l}{\sqrt{2}m_l}\frac{\tilde{J}(\tau_l)}{\tau_l}\right)+ \\ &+\sum_q c_q\frac{N_c Q_q^2 y_q}{2\sqrt{2}m_q}\left(\frac{4}{3}F_0^H + \frac{\alpha_s}{\pi}C_F\left(F_0^H C_1^H + F_0^H C_2^H X(\mu_f^2)\right)\right)\Bigg) \end{aligned} \tag{5.264}$$

where $X(\mu_f^2)$ was defined in (5.95). The final expressions (5.264), (5.241) and (5.243) provide the basic ingredients for a numerical study of $h \to \gamma\gamma$ at NLO QCD, to which we turn to in the last subsection.

Appendix: Calculation of the W-boson loops

Evaluating the W-boson loops requires a lot of calculational endurance and patience. The first question one is confronted with addresses the choice of the gauge. For example, we could work in *Feynman gauge*, resulting in a particularly easy-to-handle form of the W-propagator. This, however, comes with the disadvantage of explicitly having to include the electroweak Goldstone bosons separately in the analysis, resulting in more than ten diagrams! Although each diagram might ultimately turn out to be simple, their sheer number makes the bookkeeping rather uncomfortable and prone to error. We will therefore work in *unitary gauge*, where the effects of the Goldstones are processed by the W-propagators. We only have to evaluate two diagrams in this case - though two quite spicy ones. They are given by (5.239) and (5.240).
In formulas, we have

$$i\mathcal{M}_{3,SM}^{\gamma\gamma,LO} \equiv \frac{g^2 e^2 v c_V}{2m_W^4}\epsilon_\mu^*(k_1)\epsilon_\nu^*(k_2)I^{\mu\nu} \tag{5.265}$$

with

$$I^{\mu\nu} = \mu^{2\epsilon}\int \frac{d^dk}{(2\pi)^d}\frac{\left(g^{\mu\alpha}g^{\nu\beta}+g^{\mu\beta}g^{\nu\alpha}-2g^{\mu\nu}g^{\alpha\beta}\right)\left(m_W^2 g^{\gamma\sigma}-k^\gamma k^\sigma\right)g_{\sigma\beta}\left(m_W^2 g_{\gamma\alpha}-p_\gamma p_\alpha\right)}{\left(k^2-m_W^2\right)\left(p^2-m_W^2\right)} \tag{5.266}$$

with $p \equiv k+q$. The coupling constant g plays the same role as the Yukawa coupling and may be eliminated using $g = 2m_W/v$. Employing the usual tricks yields

$$I^{\mu\nu} = \int_0^1 dx\ \mu^{2\epsilon}\int \frac{d^dk}{(2\pi)^d}\frac{N^{\mu\nu}}{\left(k^2-m_W^2+x(1-x)q^2\right)^2} \tag{5.267}$$

with

$$\begin{aligned} N^{\mu\nu} \equiv &(2g^{\alpha\beta}g^{\mu\gamma}g^{\nu\sigma}-2g^{\mu\nu}g^{\alpha\beta}g^{\gamma\sigma})k_\alpha k_\beta k_\gamma k_\sigma + \\ &+\big(4(m_W^2+x(1-x)q^2)g^{\mu\nu}g^{\alpha\beta}-2(1-2x)^2 g^{\mu\nu}q^\alpha q^\beta + \\ &-2(2m_W^2+x(1-x)q^2)g^{\mu\alpha}g^{\nu\beta}-2x(1-x)q^\mu q^\nu g^{\alpha\beta} + \\ &+(1-2x)^2 q^\alpha(g^{\nu\beta}q^\mu+g^{\mu\beta}q^\nu)\big)k_\alpha k_\beta + \\ &+\big(2m_W^2 q^2(1-2x+2x^2)-2x^2(1-x)^2q^4+2(1-d)m_W^4\big)g^{\mu\nu} + \\ &+\big(2x^2(1-x)^2q^2-2m_W^2(1-2x+2x^2)\big)q^\mu q^\nu \end{aligned} \tag{5.268}$$

Using (D.13)-(D.15) and splitting $I^{\mu\nu}$ into three parts $I_{k^4}^{\mu\nu}$, $I_{k^2}^{\mu\nu}$ and $I_{k^0}^{\mu\nu}$ corresponding to the number of loop momenta in the numerator of (5.268), we obtain the expressions

$$\begin{aligned} I_{k^4}^{\mu\nu} = &\frac{i}{16\pi^2}g^{\mu\nu}m_W^4\Bigg(\left(-\frac{9}{2}+\frac{3q^2}{2m_W^2}-\frac{3q^4}{20m_W^4}\right)\left(\frac{1}{\epsilon}+\ln\frac{4\pi}{e^\gamma}+\ln\frac{\mu^2}{m_W^2}\right)-\frac{9}{4}+\frac{3q^2}{4m_W^2} + \\ &-\frac{3q^4}{40m_W^4}+\frac{9}{2}\int_0^1 dx\ \left(1-x(1-x)\frac{q^2}{m_W^2}\right)^2\ln\left(1-x(1-x)\frac{q^2}{m_W^2}\right)\Bigg) \end{aligned} \tag{5.269}$$

$$
\begin{aligned}
I^{\mu\nu}_{k^2} =& \frac{i}{16\pi^2} g^{\mu\nu} m_W^4 \Bigg(\left(\left(6 - \frac{q^2}{6m_W^2} - \frac{q^4}{5m_W^4}\right) \left(\frac{1}{\epsilon} + \ln\frac{4\pi}{e^\gamma} + \ln\frac{\mu^2}{m_W^2}\right) + 2 - \frac{q^2}{6m_W^2} - \frac{q^4}{15m_W^4} + \right. \\
& - \int_0^1 dx \, \Bigg(6 - (5x^2 - 5x + 1)\frac{q^2}{m_W^2} + \\
& \qquad + x(1-x)(11x^2 - 11x + 1)\frac{q^4}{m_W^4}\Bigg) \ln\left(1 - x(1-x)\frac{q^2}{m_W^2}\right)\Bigg) + \\
& + \frac{i}{16\pi^2} q^\mu q^\nu m_W^2 \Bigg(\left(-\frac{1}{3} + \frac{q^2}{10m_W^2}\right) \left(\frac{1}{\epsilon} + \ln\frac{4\pi}{e^\gamma} + \ln\frac{\mu^2}{m_W^2}\right) + \frac{q^2}{30m_W^2} + \\
& - \int_0^1 dx \, \left(8x^2 - 8x + 1\right) \left(1 - x(1-x)\frac{q^2}{m_W^2}\right) \ln\left(1 - x(1-x)\frac{q^2}{m_W^2}\right)\Bigg)
\end{aligned} \tag{5.270}
$$

$$
\begin{aligned}
I^{\mu\nu}_{k^0} =& \frac{i}{16\pi^2} g^{\mu\nu} m_W^4 \Bigg(\left(-6 + \frac{4q^2}{3m_W^2} - \frac{q^4}{15m_W^4}\right) \left(\frac{1}{\epsilon} + \ln\frac{4\pi}{e^\gamma} + \ln\frac{\mu^2}{m_W^2}\right) + 4 + \\
& - \int_0^1 dx \, \Bigg(-6 + 2(1 - 2x + 2x^2)\frac{q^2}{m_W^2} + \\
& \qquad - 2x^2(1-x)^2\frac{q^4}{m_W^4}\Bigg) \ln\left(1 - x(1-x)\frac{q^2}{m_W^2}\right)\Bigg) + \\
& + \frac{i}{16\pi^2} q^\mu q^\nu m_W^2 \Bigg(\left(-\frac{4}{3} + \frac{q^2}{15m_W^2}\right) \left(\frac{1}{\epsilon} + \ln\frac{4\pi}{e^\gamma} + \ln\frac{\mu^2}{m_W^2}\right) + \\
& + \int_0^1 dx \, \left(2(1 - 2x + 2x^2) - 2x^2(1-x)^2\frac{q^2}{m_W^2}\right) \ln\left(1 - x(1-x)\frac{q^2}{m_W^2}\right)\Bigg)
\end{aligned} \tag{5.271}
$$

Adding up all three contributions yields

$$
\begin{aligned}
I^{\mu\nu} =& \frac{i}{16\pi^2} g^{\mu\nu} q^2 m_W^2 \Bigg(\left(-\frac{9m_W^2}{2q^2} + \frac{8}{3} - \frac{5q^2}{12m_W^2}\right) \left(\frac{1}{\epsilon} + \ln\frac{4\pi}{e^\gamma} + \ln\frac{\mu^2}{m_W^2}\right) + \\
& \qquad + \frac{15m_W^2}{4q^2} + \frac{7}{12} - \frac{17q^2}{120m_W^2} + \\
& + \int_0^1 dx \, \Bigg(\frac{9m_W^2}{2q^2} + 10x^2 - 10x - 1 + \\
& \qquad - \frac{1}{2}x(1-x)(35x^2 - 35x + 2)\frac{q^2}{m_W^2}\Bigg) \ln\left(1 - x(1-x)\frac{q^2}{m_W^2}\right)\Bigg) + \\
& + \frac{i}{16\pi^2} q^\mu q^\nu m_W^2 \Bigg(\left(-\frac{5}{3} + \frac{q^2}{6m_W^2}\right) \left(\frac{1}{\epsilon} + \ln\frac{4\pi}{e^\gamma} + \ln\frac{\mu^2}{m_W^2}\right) + \frac{q^2}{30m_W^2} +
\end{aligned}
$$

$$+\int_0^1 dx\ \left(1-4x^2+4x+(-10x^4+20x^3-11x^2+x)\frac{q^2}{m_W^2}\right)\cdot$$
$$\cdot\ln\left(1-x(1-x)\frac{q^2}{m_W^2}\right)\Bigg) \quad (5.272)$$

The remaining contributions come from the triangle graphs

$$i\mathcal{M}^{\gamma\gamma,LO}_{4,SM} = \frac{g^2e^2vc_V}{2m_W^6}\epsilon^*_\mu(k_1)\epsilon^*_\nu(k_2)J^{\mu\nu}_{1,2} \quad (5.273)$$

$$i\mathcal{M}^{\gamma\gamma,LO}_{5,SM} = \frac{g^2e^2vc_V}{2m_W^6}\epsilon^*_\mu(k_1)\epsilon^*_\nu(k_2)J^{\nu\mu}_{2,1} \quad (5.274)$$

where

$$J^{\mu\nu}_{1,2} \equiv \mu^{2\epsilon}\int\frac{d^dk}{(2\pi)^d}\frac{n^{\mu\nu}}{\left(k^2-m_W^2\right)\left((k+k_1)^2-m_W^2\right)\left((k-k_2)^2-m_W^2\right)} \quad (5.275)$$

with

$$n^{\mu\nu} \equiv \tilde{V}^{\mu\beta\gamma}(-k_1,-k-k_1,k)\tilde{V}^{\nu\delta\sigma}(-k_2,-k,k-k_2)g_{\lambda\beta}\cdot$$
$$\cdot\left(m_W^2g_{\gamma\delta}-k_\gamma k_\delta\right)\left(m_W^2g^{\alpha\lambda}-(k+k_1)^\alpha(k+k_1)^\lambda\right)\left(m_W^2g_{\sigma\alpha}-(k-k_2)_\sigma(k-k_2)_\alpha\right) \quad (5.276)$$

The object $\tilde{V}^{\mu\nu\lambda}(p_1,p_2,p_3)$ was defined above (5.162). Employing Feynman parameters and shifting $k\to k-yk_1+zk_2$, we get

$$J^{\mu\nu}_{1,2} = 2\int_0^1 dz\int_0^{1-z}dy\ \mu^{2\epsilon}\int\frac{d^dk}{(2\pi)^d}\frac{N^{\mu\nu}}{(k^2-m_W^2+yzq^2)^3} \quad (5.277)$$

where

$$N^{\mu\nu} \equiv N^{\mu\nu}_{k^8}+N^{\mu\nu}_{k^6}+N^{\mu\nu}_{k^4}+N^{\mu\nu}_{k^2}+N^{\mu\nu}_{k^0} \quad (5.278)$$

The individual contributions are given by

$$N^{\mu\nu}_{k^8} = 0 \quad (5.279)$$

$$N^{\mu\nu}_{k^6} = m_W^2(g^{\mu\nu}g^{\alpha\beta}g^{\gamma\delta}g^{\lambda\sigma}-g^{\mu\alpha}g^{\nu\beta}g^{\gamma\delta}g^{\lambda\sigma})k_\alpha k_\beta k_\gamma k_\delta k_\lambda k_\sigma \quad (5.280)$$

$$N^{\mu\nu}_{k^4} = m_W^2\Bigg(\frac{1}{2}g^{\alpha\mu}g^{\beta\nu}\Big(g^{\gamma\delta}\left(6m_W^2+q^2(4yz-y-z+1)\right)+$$
$$-4y(2y-1)k_1^\gamma k_1^\delta-4z(2z-1)k_2^\gamma k_2^\delta+4(4yz-y-z)k_1^\gamma k_2^\delta\Big)+$$

$$
\begin{aligned}
&-\frac{1}{2}g^{\alpha\beta}g^{\gamma\delta}\Big(g^{\mu\nu}\big(6m_W^2+q^2(6yz-y-z+1)\big)-2yzk_1^\nu k_2^\mu\Big)+\\
&+g^{\alpha\beta}\Big(4g^{\mu\nu}\big(y(3y-1)k_1^\gamma k_1^\delta+z(3z-1)k_2^\gamma k_2^\delta-(6yz-y-z)k_1^\gamma k_2^\delta\big)+\\
&+g^{\nu\gamma}k_2^\mu\big(z(1-4z)k_2^\delta-z(1-4y)k_1^\delta\big)+\\
&+g^{\mu\gamma}k_1^\nu\big(y(1-4y)k_1^\delta-y(1-4z)k_2^\delta\big)\Big)\Bigg)k_\alpha k_\beta k_\gamma k_\delta
\end{aligned}
\tag{5.281}
$$

$$
\begin{aligned}
N^{\mu\nu}_{k^2}=&m_W^2\Bigg(\frac{1}{2}g^{\alpha\beta}\Big(2g^{\mu\nu}\big(2m_W^4+m_W^2q^2(6yz-y-z-1)+q^4yz(3yz-y-z+1)\big)+\\
&+k_1^\nu k_2^\mu\big(q^2yz(y+z-1-4yz)-2m_W^2(3yz+y+z-4)\big)\Big)+\\
&+\frac{1}{2}g^{\mu\alpha}g^{\nu\beta}\Big(4(2d-3)m_W^4+m_W^2q^2(3+y+z-6yz)+q^4yz(y+z-1-2yz)\Big)+\\
&-2g^{\mu\nu}\Big(\big(m_W^2y(6y-2)+q^2y^2(6yz-y-3z+1)\big)k_1^\alpha k_1^\beta+\\
&+\big(m_W^2z(6z-2)+q^2z^2(6yz-3y-z+1)\big)k_2^\alpha k_2^\beta+\\
&-2\big(m_W^2(6yz-y-z+1)+q^2yz(6yz-2y-2z+1)\big)k_1^\alpha k_2^\beta\Big)+\\
&+2k_1^\nu k_2^\mu\big(y^2z(2y-1)k_1^\alpha k_1^\beta+yz^2(2z-1)k_2^\alpha k_2^\beta+yz(y+z-4yz)k_1^\alpha k_2^\beta\big)+\\
&+k_1^\nu g^{\mu\alpha}\Big(\big(m_W^2y(6y+1)+q^2y^2(4yz-y-2z+1)\big)k_1^\beta+\\
&+\big(m_W^2(y-2z-4-6yz)+q^2yz(2y-4yz+z-1)\big)k_2^\beta\Big)+\\
&+k_2^\mu g^{\nu\alpha}\Big(\big(m_W^2z(6z+1)+q^2z^2(4yz-2y-z+1)\big)k_2^\beta+\\
&+\big(m_W^2(z-2y-4-6yz)+q^2yz(2z-4yz+y-1)\big)k_1^\beta\Big)\Bigg)k_\alpha k_\beta
\end{aligned}
\tag{5.282}
$$

$$
\begin{aligned}
N^{\mu\nu}_{k^0}=&\frac{m_W^2}{2}\Bigg(k_1^\nu k_2^\mu\Big(2m_W^4\big((6-4d)yz+y+z+4\big)+\\
&+m_W^2q^2yz(6yz+y+z-3)+q^4y^2z^2(2yz-y-z+1)\Big)+\\
&-g^{\mu\nu}q^2\Big(m_W^4(4yz-y-z+5)+2m_W^2q^2yz(3yz-y-z)+\\
&+q^4y^2z^2(2yz-y-z+1)\Big)\Bigg)
\end{aligned}
\tag{5.283}
$$

It can be viewed as a lucky coincidence that the $\mathcal{O}(k^8)$-term vanishes. Otherwise, the complexity it would have induced to the lower order terms would have made the whole calculation hardly tackleable by hand. It also has to vanish for consistency reasons, as it scales like $d^4k\ k^8/k^6 \sim dk\ k^5$, but the highest order term in $i\mathcal{M}_3$ scales like

$d^4k\ k^4/k^4 \sim dk\ k^3$, so there would be nothing for the resulting divergencies to cancel against.
As before, we split $J^{\mu\nu}_{1,2}$ apart according to the number of loop momenta in the numerator. We obtain

$$J^{\mu\nu}_{1,2,k^8} = 0 \tag{5.284}$$

$$J^{\mu\nu}_{1,2,k^6} = \frac{i}{16\pi^2} g^{\mu\nu} m_W^6 \Bigg(\left(\frac{9}{2} - \frac{3q^2}{4m_W^2} + \frac{q^4}{20m_W^4} \right) \left(\frac{1}{\epsilon} + \ln\frac{4\pi}{e^\gamma} + \ln\frac{\mu^2}{m_W^2} \right) + \frac{9}{8} - \frac{3q^2}{16m_W^2} + \\ + \frac{q^4}{80m_W^4} - 9\int_0^1 dz \int_0^{1-z} dy\ \left(1 - yz\frac{q^2}{m_W^2}\right)^2 \ln\left(1 - yz\frac{q^2}{m_W^2}\right) \Bigg) \tag{5.285}$$

$$J^{\mu\nu}_{1,2,k^4} = \frac{i}{16\pi^2} g^{\mu\nu} m_W^6 \Bigg(\left(-\frac{27}{4} - \frac{11q^2}{48m_W^2} + \frac{151q^4}{1440m_W^4} \right) \left(\frac{1}{\epsilon} + \ln\frac{4\pi}{e^\gamma} + \ln\frac{\mu^2}{m_W^2} \right) + \\ + \frac{q^2}{12m_W^2} + \frac{q^4}{120m_W^4} + \\ + \frac{1}{8}\int_0^1 dz \int_0^{1-z} dy\ \left(108 + (256yz - 40y - 40z + 18)\frac{q^2}{m_W^2} \right) \cdot \\ \cdot \left(1 - yz\frac{q^2}{m_W^2}\right) \ln\left(1 - yz\frac{q^2}{m_W^2}\right) \Bigg) + \\ + \frac{i}{16\pi^2} k_1^\nu k_2^\mu m_W^4 \Bigg(\left(\frac{1}{6} - \frac{2q^2}{45m_W^2} \right) \left(\frac{1}{\epsilon} + \ln\frac{4\pi}{e^\gamma} + \ln\frac{\mu^2}{m_W^2} \right) - \frac{1}{24} - \frac{q^2}{90m_W^2} + \\ - 2\int_0^1 dz \int_0^{1-z} dy\ (10yz - y - z) \left(1 - yz\frac{q^2}{m_W^2}\right) \ln\left(1 - yz\frac{q^2}{m_W^2}\right) \Bigg) \tag{5.286}$$

$$J^{\mu\nu}_{1,2,k^2} = \frac{i}{16\pi^2} g^{\mu\nu} m_W^6 \Bigg(\left(\frac{9}{2} - \frac{17q^2}{48m_W^2} + \frac{77q^4}{1440m_W^4} \right) \left(\frac{1}{\epsilon} + \ln\frac{4\pi}{e^\gamma} + \ln\frac{\mu^2}{m_W^2} \right) + \\ - 3 + \frac{7q^2}{12m_W^2} - \frac{q^4}{40m_W^4} + \\ - \frac{1}{4}\int_0^1 dz \int_0^{1-z} dy\ \Bigg(36 + (66yz - 11y - 11z - 1)\frac{q^2}{m_W^2} + \\ + yz(46yz - 15y - 15z + 11)\frac{q^4}{m_W^4} \Bigg) \ln\left(1 - yz\frac{q^2}{m_W^2}\right) \Bigg) + \\ + \frac{i}{16\pi^2} k_1^\nu k_2^\mu m_W^4 \Bigg(\left(\frac{2}{3} - \frac{7q^2}{180m_W^2} \right) \left(\frac{1}{\epsilon} + \ln\frac{4\pi}{e^\gamma} + \ln\frac{\mu^2}{m_W^2} \right) - \frac{37}{24} + \frac{11q^2}{720m_W^2} +$$

$$-\frac{1}{4}\int_0^1 dz \int_0^{1-z} dy\, \left(-2(24yz+5y+5z-8)+\right.$$
$$\left.-4yz(10yz-3y-3z+2)\frac{q^2}{m_W^2}\right)\ln\left(1-yz\frac{q^2}{m_W^2}\right)\Bigg) \tag{5.287}$$

$$\begin{aligned}
J^{\mu\nu}_{1,2,k^0} =& \frac{i}{16\pi^2}g^{\mu\nu}m_W^6\left(\int_0^1 dz\int_0^{1-z} dy\, \frac{1}{2\left(1-yz\frac{q^2}{m_W^2}\right)}\left((4yz-y-z+5)\frac{q^2}{m_W^2}+\right.\right.\\
&\left.\left.+yz(6yz-2y-2z)\frac{q^4}{m_W^4}+y^2z^2(2yz-y-z+1)\frac{q^6}{m_W^6}\right)\right)+\\
&-\frac{i}{16\pi^2}k_1^\nu k_2^\mu m_W^4\left(\int_0^1 dz\int_0^{1-z} dy\, \frac{1}{2\left(1-yz\frac{q^2}{m_W^2}\right)}\left(-20yz+2y+2z+8+\right.\right.\\
&\left.\left.+yz(6yz+y+z-3)\frac{q^2}{m_W^2}+y^2z^2(2yz-y-z+1)\frac{q^4}{m_W^4}\right)\right)
\end{aligned} \tag{5.288}$$

Adding up all contributions, we find

$$\begin{aligned}
J^{\mu\nu}_{1,2} =& \frac{i}{16\pi^2}g^{\mu\nu}q^2m_W^4\left(\left(\frac{9m_W^2}{4q^2}-\frac{4}{3}+\frac{5q^2}{24m_W^2}\right)\left(\frac{1}{\epsilon}+\ln\frac{4\pi}{e^\gamma}+\ln\frac{\mu^2}{m_W^2}\right)+\right.\\
&-\frac{15m_W^2}{8q^2}+\frac{23}{48}-\frac{q^2}{240m_W^2}+\\
&+\int_0^1 dz\int_0^{1-z} dy\,\left(-\frac{9m_W^2}{2q^2}+20yz-\frac{9y}{4}-\frac{9z}{4}+\frac{5}{2}+\right.\\
&\qquad\left.+\left(-5yz-\frac{105y^2z^2}{2}+\frac{35y^2z}{4}+\frac{35yz^2}{4}\right)\frac{q^2}{m_W^2}\right)\ln\left(1-yz\frac{q^2}{m_W^2}\right)+\\
&+\frac{1}{2\left(1-yz\frac{q^2}{m_W^2}\right)}\left(4yz-y-z+5+\right.\\
&\qquad\left.\left.+yz(6yz-2y-2z)\frac{q^2}{m_W^2}+y^2z^2(2yz-y-z+1)\frac{q^4}{m_W^4}\right)\right)+\\
&+\frac{i}{16\pi^2}k_1^\nu k_2^\mu m_W^4\left(\left(\frac{5}{6}-\frac{q^2}{12m_W^2}\right)\left(\frac{1}{\epsilon}+\ln\frac{4\pi}{e^\gamma}+\ln\frac{\mu^2}{m_W^2}\right)-\frac{19}{12}+\frac{q^2}{240m_W^2}+\right.\\
&+\int_0^1 dz\int_0^{1-z} dy\,\left(-4+\frac{9y}{2}+\frac{9z}{2}-8yz+\right.\\
&\qquad\left.+\left(30y^2z^2-5y^2z-5yz^2+2yz\right)\frac{q^2}{m_W^2}\right)\ln\left(1-yz\frac{q^2}{m_W^2}\right)+\\
&-\frac{1}{2\left(1-yz\frac{q^2}{m_W^2}\right)}\left(-20yz+2y+2z+8+\right.
\end{aligned}$$

$$+ yz(6yz + y + z - 3)\frac{q^2}{m_W^2} + y^2z^2(2yz - y - z + 1)\frac{q^4}{m_W^4}\Big)\Big) \tag{5.289}$$

This result is symmetric under the exchange $\mu \leftrightarrow \nu$ and $k_1 \leftrightarrow k_2$, so $J_{1,2}^{\mu\nu} = J_{2,1}^{\nu\mu}$. The divergent pieces cancel the ones from (5.272). The final result for the W-loop contribution to $h \to \gamma\gamma$ is therefore given by

$$\begin{aligned} i\mathcal{M}_{3,SM}^{\gamma\gamma,LO} + i\mathcal{M}_{4,SM}^{\gamma\gamma,LO} + i\mathcal{M}_{5,SM}^{\gamma\gamma,LO} &= \frac{g^2e^2vc_V}{2m_W^4}\epsilon_\mu^*(k_1)\epsilon_\nu^*(k_2)\left(I^{\mu\nu} + \frac{2J_{1,2}^{\mu\nu}}{m_W^2}\right) = \\ &= \frac{ig^2e^2vc_V}{32m_W^2}\epsilon_\mu^*(k_1)\epsilon_\nu^*(k_2)\Big(F\left(\tau_W\right)k_1\cdot k_2 g^{\mu\nu} + G\left(\tau_W\right)k_1^\nu k_2^\mu\Big) \end{aligned} \tag{5.290}$$

where

$$\begin{aligned} F\left(\tau_W\right) = &\frac{37}{12} - \frac{6}{5}\tau_W + \\ &+ \int_0^1 dx\,\left(\frac{9}{4\tau_W} + 20x^2 - 20x - 2 + \right. \\ &\qquad \left. - 4x(1-x)(35x^2 - 35x + 2)\tau_W\right)\ln\left(1 - 4x(1-x)\tau_W\right) + \\ &- \int_0^1 dz\int_0^{1-z} dy\,\left(\frac{9}{2\tau_W} - 80yz + 9y + 9z - 10 + \right. \\ &\qquad \left. + 20yz\left(4 + 42yz - 7y - 7z\right)\tau_W\right)\ln\left(1 - 4yz\tau_W\right) + \\ &+ \frac{2}{1 - yz\frac{q^2}{m_W^2}}\left(4yz - y - z + 5 + 8yz(3yz - y - z)\tau_W + 16y^2z^2(2yz - y - z + 1)\tau_W^2\right) \end{aligned} \tag{5.291}$$

and

$$\begin{aligned} G\left(\tau_W\right) = &\frac{\tau_W}{6} - \frac{19}{6} + \\ &+ \int_0^1 dx\,\left(1 - 4x^2 + 4x - 4x(10x^3 - 20x^2 + 11x - 1)\tau_W\right)\ln\left(1 - 4x(1-x)\tau_W\right) + \\ &- \int_0^1 dz\int_0^{1-z} dy\,\left(8 - 9y - 9z + 16yz - 8yz\left(30yz - 5y - 5z + 2\right)\tau_W\right)\ln\left(1 - 4yz\tau_W\right) + \\ &+ \frac{2}{1 - 4yz\tau_W}\left(10yz - y - z - 4 - 2yz(6yz + y + z - 3)\tau_W - 8y^2z^2(2yz - y - z + 1)\tau_W^2\right) \end{aligned} \tag{5.292}$$

Evaluating the parameter integrals yields after some algebra

$$F\left(\tau_W\right) = -G\left(\tau_W\right) = 2 + \frac{3}{\tau_W} - \frac{3}{4}\left(\frac{2}{\tau_W} - \frac{1}{\tau_W^2}\right)\ln^2\left(\frac{\sqrt{1 - \frac{1}{\tau_W}} - 1}{\sqrt{1 - \frac{1}{\tau_W}} + 1}\right) \tag{5.293}$$

where

$$\ln^2\left(\frac{\sqrt{1-\frac{1}{\tau_W}}-1}{\sqrt{1-\frac{1}{\tau_W}}+1}\right)=\begin{cases}-4\arcsin^2\sqrt{\tau_W} & \text{for } 0<\tau_W<1\\ \left(\ln\left(\frac{1-\sqrt{1-\frac{1}{\tau_W}}}{1+\sqrt{1-\frac{1}{\tau_W}}}\right)+i\pi\right)^2 & \text{for } 1\leq\tau_W<\infty\end{cases} \tag{5.294}$$

5.8. Phenomenological results

We now turn to a numerical analysis of our decay-rate formulas. This subsection is based on the numbers presented in [150]. The input parameters are defined in Appendix A. We use the OS quark masses as input parameters and convert them into running masses via the scheme in [137, 140]. This corresponds to the last possibility in (5.95). To the relevant order in α_s, the corresponding formula that converts an OS mass m_f to its running version $m_f(\mu_f^2)$ reads[60]

$$m_f(\mu_f^2)=m_f\left(1-\frac{\alpha_s(\mu_f^2)}{\pi}\ln\frac{\mu_f^2}{m_f^2}\right)+\mathcal{O}(\alpha_s^2) \tag{5.295}$$

Solving the one-loop renormalization group equation $d\alpha_s/d\ln\mu_f^2=-\alpha_s\beta_0/(4\pi)+\mathcal{O}(\alpha_s^2)$, this formula is equivalent to [137]

$$m_f(\mu_f^2)=m_f\left(\frac{\alpha_s(\mu_f^2)}{\alpha_s(m_f^2)}\right)^{\frac{4}{\beta_0}}\left(1+\mathcal{O}(\alpha_s^2)\right) \tag{5.296}$$

which is the expression we employ for our analysis. For numerical implementations, the package CRunDec [212–214] can be employed for the conversion between the mass schemes and the running strong coupling with $N_f=5$ light flavours at the two-loop level. This introduces an artificial renormalization scale dependence for our results, both at LO and at NLO in QCD - in addition to the NLO function $X(\mu_f^2)$ and the logarithmic dependence on μ_R. The degree of dependence on these scales can be illustrated by fixing them to selected values and varying between half and double these values. It is common to choose $\mu_f=m_f$ and $\mu_R=m_h$. The parametric uncertainties are obtained upon varying one input parameter at a time and adding up the respective contributions in quadrature. This, of course, assumes the independency of our input parameter uncertainties.
Featuring easily tackleable analytic expressions without phase space singularities, we begin with the process $h\to\gamma\gamma$ and consider $h\to gg$ afterwards.

[60] This formula can be derived by formally equating the bare masses squared in terms of the different renormalization schemes in (5.82) and taking the square root.

Numerics for $h \to \gamma\gamma$

The QCD corrections to $h \to \gamma\gamma$ do not change the final results significantly. Indeed, employing a self-explaining notation, the central values for the SM result are given by

$$\Gamma_{h\to\gamma\gamma} = \begin{cases} 9.41\,\text{keV} & \text{(LO QCD)} \\ 9.54\,\text{keV} & \text{(NLO QCD)} \end{cases} \tag{5.297}$$

The scale dependence from varying the quark-mass renormalization scales μ_q between half and double their values are negligible in both cases (going from LO to NLO reduces them by another order of magnitude).

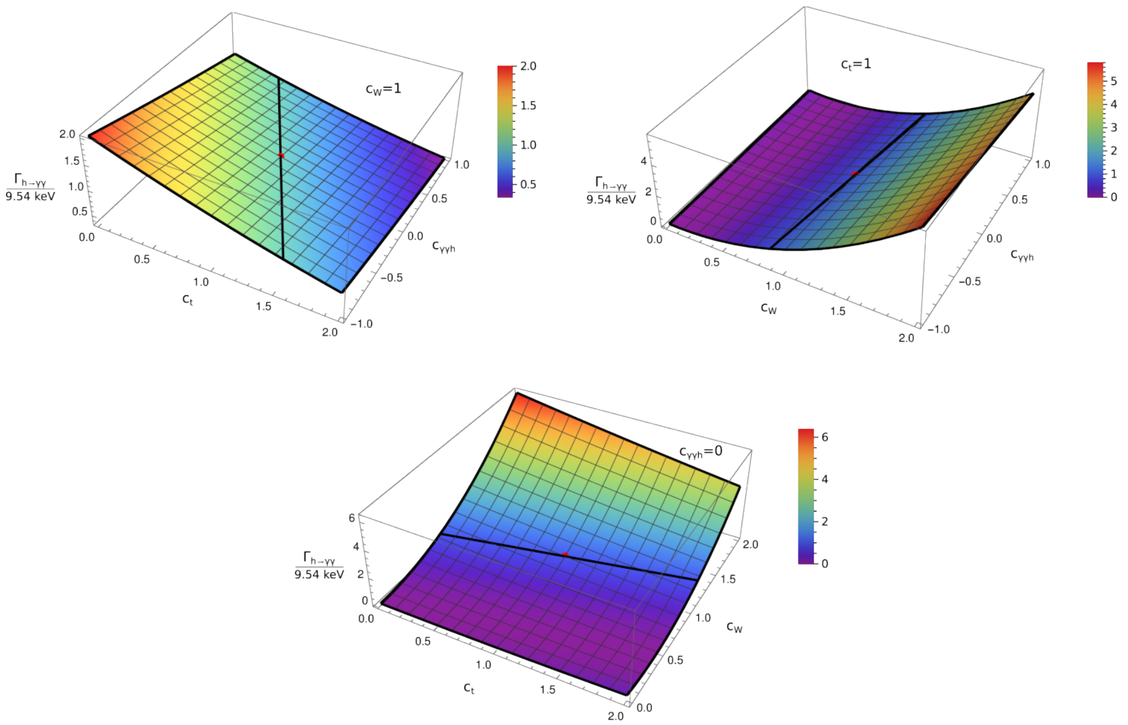

Figure 7: Contour plots for $h \to \gamma\gamma$ generated by varying two parameters at a time showing the steeper gradient away from the SM result in the c_W-direction. We have set $c_b = c_c = c_\tau = 1$ in all plots. The SM central value of 9.54 keV is marked with a black line and the SM configuration $c_t = c_W = 1$ together with $c_{\gamma\gamma h} = 0$ is given by a red dot in the center of the respective plot.

Allowing arbitrary anomalous couplings and dropping contributions below one per mille, we arrive at [150]

$$\Gamma_{h\to\gamma\gamma} = \big(15.098c_W^2 - 6.451c_t c_W - 3.624c_{\gamma\gamma h}c_W + 0.774c_{\gamma\gamma h}c_t + 0.689c_t^2 + \\ +0.217c_{\gamma\gamma h}^2 + 0.097c_b c_W + 0.085c_\tau c_W + 0.079c_c c_W - 0.021c_b c_t +$$

$$-0.018c_tc_\tau - 0.017c_cc_t - 0.012c_bc_{\gamma\gamma h} - 0.010c_{\gamma\gamma h}c_\tau - 0.009c_cc_{\gamma\gamma h}\big)\ \text{keV} \tag{5.298}$$

at NLO QCD, where we have ordered the terms by phenomenological impact. Fixing all anomalous couplings but two to their SM values enables us to plot the new-physics deviations of the decay rate. In Figure 7, we have concentrated ourselves on the most promising anomalous couplings, i.e. c_W, c_t and $c_{\gamma\gamma h}$. The rate of change away from the SM central value of 9.54 keV is significantly larger for varying c_W than in the other directions, hinting towards the high sensitivity of the decay $h \to \gamma\gamma$ to the W-boson loops, as is also indicated by the numbers in (5.298). In this context, speculative new-physics models influencing the Higgs-W-boson coupling should therefore be easier accessible than other scenarios.

Numerics for $h \to gg$

The numerical results for $h \to gg$ as given in (5.235) are based on a C++ program for which the Monte Carlo algorithm SUAVE implemented in the CUBA library [215] is used for the real radiation phase space integration after the antenna subtraction has been performed. In the vicinity of $c_{ggh} \approx -2c_t/3$, however, one inevitably encounters a negative total decay rate. This can be understood upon noting that there are indeed parameter space regions where the LO QCD amplitude vanishes identically, effectively pushing its (negative) interference term with the virtual amplitude to the LO. The only term that could fix this unphysical behavior is the virtual amplitude squared, which we have neglected in our α_s-expansion[61]. A rigorous expansion in α_s on the rate level is never a perfect square, so parameter space regions where the total decay rate becomes negative are unavoidable. We will now try to understand this on a quantitative level and argue for an *ad hoc* fix to cure the decay rate near its singular regions.
The decay rates (5.32) and (5.235) serve as our starting points. We now perform the heavy-top limit with $y_t = \sqrt{2}m_t/v$ and $N_c = 3$ to reduce the complexity of our expressions[62]. For $m_t \to \infty$, we have

$$F_0^H \longrightarrow 1 \tag{5.299}$$

$$\mathcal{A}_{fin} \longrightarrow \frac{11}{3} \tag{5.300}$$

$$F_0^H C_1^H \longrightarrow -1 \tag{5.301}$$

$$F_0^H C_2^H \longrightarrow 0 \tag{5.302}$$

$$F_0^H B_1^H \longrightarrow \frac{11}{2} \tag{5.303}$$

resulting in

$$\Gamma^{LO\times LO} \longrightarrow \Gamma_\infty^{LO\times LO} \equiv \frac{\alpha_s^2 m_h^3}{32\pi^3 v^2}\left(c_{ggh} + \frac{2}{3}c_t\right)^2 \tag{5.304}$$

[61] A thorough treatment would require double-real-radiation contributions, etc. and is beyond the scope of this work

[62] The phase space integrations (5.221) and (5.231) vanish identically in the heavy-top limit.

$$\Gamma^{LO\times LO} + \Gamma^{(V-T)} \longrightarrow \Gamma_{\infty}^{NLO} \equiv \Gamma_{\infty}^{LO\times LO}\left(1+\frac{\alpha_s}{\pi}\left(\mathcal{R}+\frac{11}{3}\frac{c_t}{c_{ggh}+\frac{2}{3}c_t}\right)\right)+\mathcal{O}(\alpha_s^4) \tag{5.305}$$

The first factor is simply $\Gamma^{LO\times LO}$ from (5.32) in the heavy-top limit (5.35) and

$$\mathcal{R} = \frac{1}{2}\left(\frac{73}{2}-\frac{7N_f}{3}+\frac{3\beta_0}{3}\log\frac{\mu_R^2}{m_h^2}\right) \tag{5.306}$$

is the real-radiation contribution, which is always positive for realistic values of N_f. The $\mathcal{O}(\alpha_s^4)$ correction explicitly indicated refers to the aforementioned NNLO corrections. While the result vanishes for $c_{ggh} = -2c_t/3$, it can become negative for $c_{ggh} \approx -2c_t/3$. This is an artifact of the truncation in the α_s-expansion that can be fixed by "completing the square".

The heavy-top-limit result can be mapped to a tree-level calculation of the effective Lagrangian

$$\mathcal{L}_{eff} = \mathcal{C}hG^a_{\mu\nu}G^{a\mu\nu} \tag{5.307}$$

with

$$\mathcal{C} = \frac{\alpha_s}{8\pi v}\left(c_{ggh}+\frac{2}{3}c_t\left(1+11\frac{\alpha_s}{4\pi}\right)\right) \tag{5.308}$$

which results in a decay rate of

$$\Gamma_{eff} = \frac{2m_h^3}{\pi}\mathcal{C}^2 = \Gamma_{\infty}^{LO\times LO}\left(1+\frac{11\alpha_s}{3\pi}\frac{c_t}{c_{ggh}+\frac{2}{3}c_t}+\frac{121\alpha_s^2}{36\pi^2}\frac{c_t^2}{\left(c_{ggh}+\frac{2}{3}c_t\right)^2}\right) \tag{5.309}$$

with $\Gamma_{\infty}^{LO\times LO}$ given above. For the effective Lagrangian, this result is exact to $\mathcal{O}(\alpha_s^4)$ and differs from (5.305) at this order. In contrast to the latter, however, (5.309) is a perfect square. In addition, setting $c_{ggh} = -2c_t/3$, we obtain the (positive) result

$$\Gamma_{eff} \longrightarrow \frac{121\alpha_s^4 m_h^3 c_t^2}{1152\pi^5 v^2} \tag{5.310}$$

This term might now serve as a regulator for (5.305) near the singular configuration $c_{ggh} \approx -2c_t/3$. We therefore *define* our parameter-space regularized to include the fix (5.310). The result is given by

$$\Gamma_{\infty}^{NLO} \longrightarrow \Gamma_{\infty}^{LO\times LO}\left(1+\frac{\alpha_s}{\pi}\left(\mathcal{R}+\frac{11}{3}\frac{c_t}{c_{ggh}+\frac{2}{3}c_t}\right)\right)+\frac{121\alpha_s^4 m_h^3 c_t^2}{1152\pi^5 v^2}+\mathcal{O}(\alpha_s^4) = \tag{5.311}$$

$$= \Gamma_{\infty}^{LO\times LO}\left(\left(1+\frac{11\alpha_s}{6\pi}\frac{c_t}{c_{ggh}+\frac{2}{3}c_t}\right)^2+\frac{\alpha_s}{\pi}\mathcal{R}\right)+\mathcal{O}(\alpha_s^4) \tag{5.312}$$

	LO			NLO		
A_{tg}	0.56937	$\pm1.5\%$	$^{+23\%}_{-17\%}$	0.88041	$\pm1.8\%$	$^{+11\%}_{-11\%}$
A_{gg}	0.41360	$\pm1.5\%$	$^{+23\%}_{-17\%}$	0.59755	$\pm1.7\%$	$^{+9.5\%}_{-9.6\%}$
A_{tt}	0.19595	$\pm1.5\%$	$^{+23\%}_{-17\%}$	0.32290	$\pm1.8\%$	$^{+13\%}_{-11\%}$
A_{tt} + fix (5.310)				0.32468	$\pm1.8\%$	$^{+13\%}_{-12\%}$
A_{bg}	−0.03442	$\pm2.0\%$	$^{+23\%}_{-17\%}$	−0.04837	$\pm2.2\%$	$^{+8.8\%}_{-9.2\%}$
A_{bt}	−0.02369	$\pm2.0\%$	$^{+23\%}_{-17\%}$	−0.03569	$\pm2.2\%$	$^{+11\%}_{-10\%}$
A_{bb}	0.00218	$\pm4.0\%$	$^{+23\%}_{-17\%}$	0.00328	$\pm4.0\%$	$^{+11\%}_{-10\%}$

Table 2: LO and NLO values for the coefficients in (5.314). The first uncertainty refers to the parametric uncertainty, the second one is related to the renormalization scale variation. For the former, we have to take their respective correlations into account when calculating the error of the LO and NLO decay rates, see also [150].

.

It turns out that the same fix (5.310) provides the necessary regulatory properties for the full decay rate when the top-mass dependence is restored[63]. This is, of course, not a rigorous procedure and should be taken with caution. The phenomenological impact of the fix away from the singular regions, however, is almost negligible. In the following analysis, we will always include the fix.

Including parametric, as well as scale uncertainties resulting from varying the renormalization scale μ_R between half and double the Higgs mass m_h, and employing the same self-explaining notation as in the $h \to \gamma\gamma$ case, the SM results are given by

$$\Gamma_{h\to gg} = \begin{cases} \left(0.1744 \pm 1.5\%(\text{parametric})^{+23\%}_{-17\%}(\text{scale})\right)\text{MeV} & (\text{LO QCD}) \\ \left(0.2923 \pm 1.8\%(\text{parametric})^{+13\%}_{-12\%}(\text{scale})\right)\text{MeV} & (\text{NLO QCD}) \end{cases} \tag{5.313}$$

With arbitrary anomalous couplings, we obtain

$$\Gamma_{h\to gg} = \left(A_{tg}c_{ggh}c_t + A_{gg}c_{ggh}^2 + A_{tt}c_t^2 + A_{bg}c_{ggh}c_b + A_{bt}c_tc_b + A_{bb}c_b^2\right)\text{MeV} \tag{5.314}$$

where the coefficients can be read off from Table 2. Referring to the anomalous couplings c_{ggh}, c_t, etc. as the fundamental parameters of the EWChL [216] and including only

[63] In fact, this is not strictly true when lower-mass quarks, such as the bottom- or charm-quark are included. However, the problematic regions are far off from phenomenologically reasonable regions, so we don't worry about them here.

top-quark contributions, we arrive at the following NLO QCD formula

$$\frac{\Gamma^{\rm EWChL}_{h\to gg}}{\Gamma^{\rm SM}_{h\to gg}} = 1 + 2\ \delta_{c_t} + 2.7116\ c_{ggh} + \delta_{c_t}^2 + 1.8404\ c_{ggh}^2 + 2.7116\ \delta_{c_t} c_{ggh}\,, \tag{5.315}$$

with the definition $\delta_{c_t} \equiv c_t - 1$, which can be matched to the corresponding expression in SMEFT using the relations of Table 1. Employing the definition $\tilde{C}_i \equiv C_i v^2/\Lambda^2$, one then obtains

$$\begin{aligned}\frac{\Gamma^{\rm SMEFT}_{h\to gg}}{\Gamma^{\rm SM}_{h\to gg}} &= 1 + 2\left(\tilde{C}_{\varphi\Box} - \frac{1}{4}\tilde{C}_{\varphi D}\right) - 2.0164\ \tilde{C}_{t\varphi} + 578.04\ \tilde{C}_{\varphi G} \\ &+ \left(\tilde{C}_{\varphi\Box} - \frac{1}{4}\tilde{C}_{\varphi D}\right)^2 - 2.0164\left(\tilde{C}_{\varphi\Box} - \frac{1}{4}\tilde{C}_{\varphi D}\right)\tilde{C}_{t\varphi} \\ &+ 1.0164\ \tilde{C}_{t\varphi}^2 + 8.3632\cdot 10^4\ \tilde{C}_{\varphi G}^2 \\ &+ 578.04\left(\tilde{C}_{\varphi\Box} - \frac{1}{4}\tilde{C}_{\varphi D}\right)\tilde{C}_{\varphi G} - 582.77\ \tilde{C}_{t\varphi}\tilde{C}_{\varphi G}\,.\end{aligned} \tag{5.316}$$

However, in contrast to the former expression, the last one is far from being systematically consistent. On one hand, it lacks the implicit loop factors of field-strength operators. Including them would, as an example, lower the coefficient associated with $\tilde{C}_{\varphi G}$ from 578.04 to 3.6605. In fact, all coefficients would then be given by $\mathcal{O}(1)$-numbers. On the other hand, it contains dimension-six squared contributions ($\sim 1/\Lambda^4$ on the decay-rate level), but neglects genuine dimension-eight operators. This can be fixed by enlarging Table 1 to include dimension-eight effects (see [175, 176, 217] for the phenomenological implications, where it has been argued that including QCD corrections to the dimension-six terms $\sim C^6_{\varphi G}$ spoils the degeneracy of c_{ggh} within SMEFT[64]). For instance, kinematic differences between the related processes $h \to gg$ and $gg \to h$ introduce a mismatch between the ratio of $C^6_{\varphi G}$ and its eight-dimensional relative $C^8_{\varphi G}$ inside c_{ggh}. Within ordinary SMEFT, this arises naturally when the perturbative expansion is truncated systematically. It is, however, an artifact of not treating $C^6_{\varphi G}$ and $C^8_{\varphi G}$ on equal footing when it comes to QCD corrections. In fact, the main advantage of working with only one object c_{ggh} is the possibility to calculate radiative corrections once and for all as there is no reason to distinguish the EFT-dependent ingredients that eventually sum up to c_{ggh}. Viewing c_{ggh} as a single object with respect to QCD corrections also makes their common origin in geoSMEFT more manifest. Processes involving more than two external Higgs states then require additional coefficients, e.g. c_{gghh}, accounting for a parameter degeneracy in the EWChL [171, 216, 218–224]. In SMEFT at canonical dimension eight, both c_{ggh} and c_{gghh} are represented by (different) linear combinations of $C^6_{\varphi G}$ and $C^8_{\varphi G}$. To be more specific, enlarging the Lagrangian (5.5) by a term[65]

$$\frac{\alpha_s}{16\pi v^2} c_{gghh} h^2 G^A_{\mu\nu} G^{A\mu\nu} \tag{5.317}$$

[64]Here, we employ the notation $C^6_{\varphi G} \equiv C_{\varphi G}$.

[65]Note that our conventions differ slightly to the ones used in [216].

leads to

$$c_{ggh} = \frac{32\pi^2}{g_s^2}\left(\frac{v^2}{\Lambda^2}C^6_{\varphi G} + \frac{v^4}{\Lambda^4}C^8_{\varphi G}\right) \tag{5.318}$$

$$c_{gghh} = \frac{32\pi^2}{g_s^2}\left(\frac{v^2}{\Lambda^2}C^6_{\varphi G} + \frac{3v^4}{\Lambda^4}C^8_{\varphi G}\right) \tag{5.319}$$

Let us turn back to our phenomenological analysis. We provide contour plots for various combinations of anomalous couplings in Figure 8. The global minima of the decay rates as functions of the anomalous couplings lie far off from their SM central value hinting towards the potential sensitivity of the SM decay rate to small deviations and hence new physics. Note that we have to be cautious close to the parametric-suppression region $c_{ggh} \approx -2c_t/3$, since here the artificial fix (5.310) is essentially our LO and only physical result and we do not know the exact behavior at higher orders. The overall qualitative picture of the contour plots does not change when going from LO to NLO.
It is therefore easier to study the behavior of the decay rate when only one parameter is changed from its SM value. This is done in Figure 9, where we considered a rescaled result (by c_t^{-2}) and plotted its dependence on the ratio c_{ggh}/c_t with $c_b = c_t$. The non-overlap of the scale error bands for LO and NLO hint towards the potential necessity of even higher-order QCD calculations for this process[66]. Near the minimum, again, we can not really trust our numbers due to the fix. Chosen QCD K-factors, i.e. ratios between the NLO and LO decay rates, are finally shown in Figure 10. Of course, the "LO K-factors" are centered at a value of 1. While we do not observe any obscurities for c_{ggh} set to its SM value 0, we observe a highly non-trivial behaviour for negative values. As before, however, this can be traced back to the parameter space singularity and should not be overinterpreted. The bending of the NLO K-factor for fixed c_{ggh} and c_b for very small c_t can be traced back to the destructively interfering bottom loop that gets relatively enhanced. See also [150] for a similar plot concerning varying c_b which shows a nearly constant NLO enhancement of about 70%.
Our results may contribute to a possible extension of existing LO QCD global data fits [116, 227] into the full NLO QCD regime. So far, the available LHC data suggests deviations of the SM couplings of at most 10%. This includes the anomalous Higgs-gluon-gluon coupling, which is constrained by $c_{ggh} = -0.01 \pm 0.08$. In the light of these numbers, the necessity to push the theoretic, as well as experimental accuracy by at least an order of magnitude in future works and colliders seems unavoidable for an eventual detection of potential signals from highly hypothetical physics beyond the SM.

[66] Although the error bands become smaller when transiting to higher orders in QCD, we eventually expect them to overlap for a sufficiently converging perturbative series, since the hypothetical all-order result is scale independent by construction [225, 226].

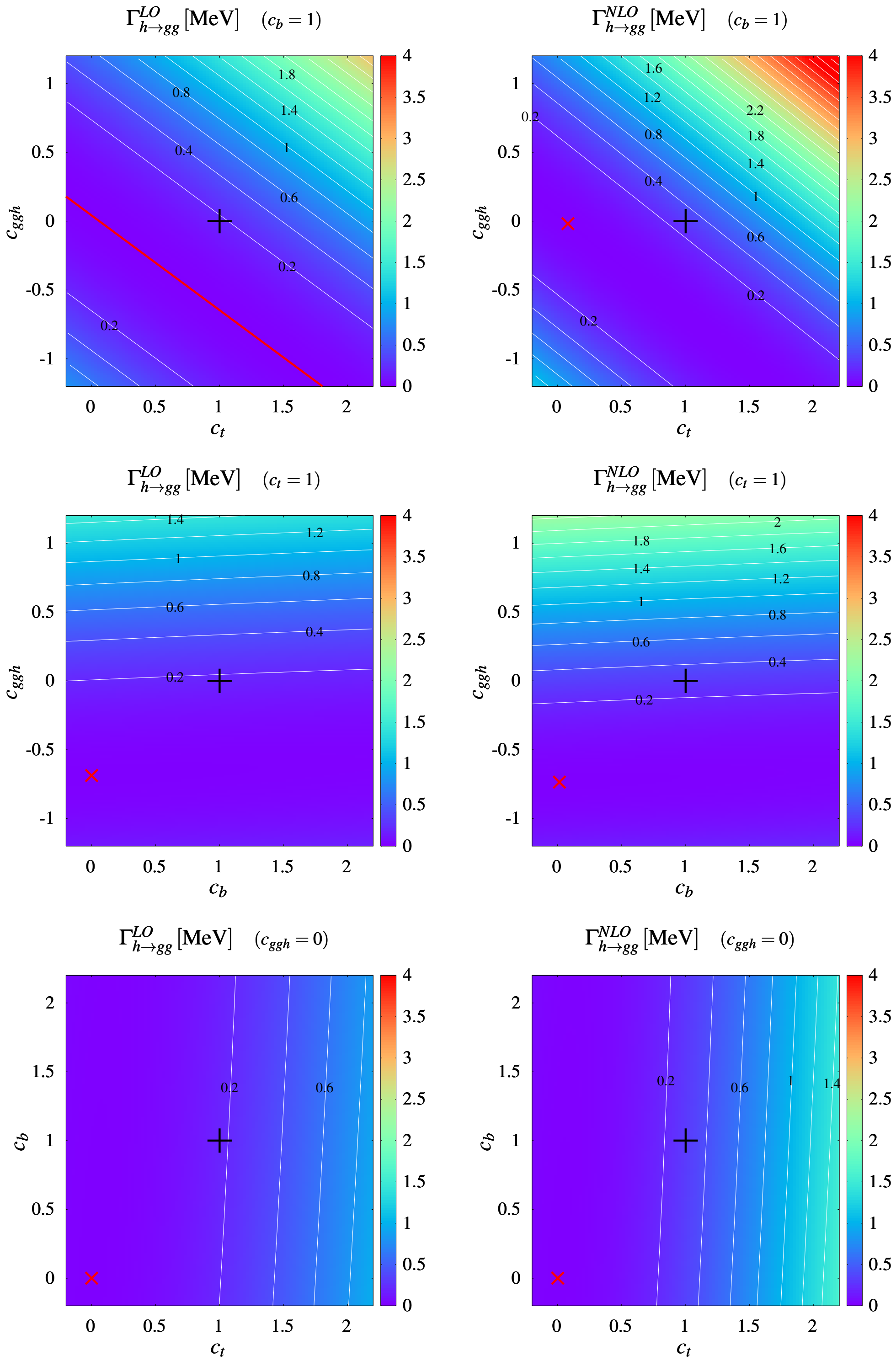

Figure 8: LO and NLO contour plots for the $h \to gg$ decay rates with varying effective couplings. A black cross indicates the SM configuration. The global minimum is highlighted with a red cross or line, see also [150].

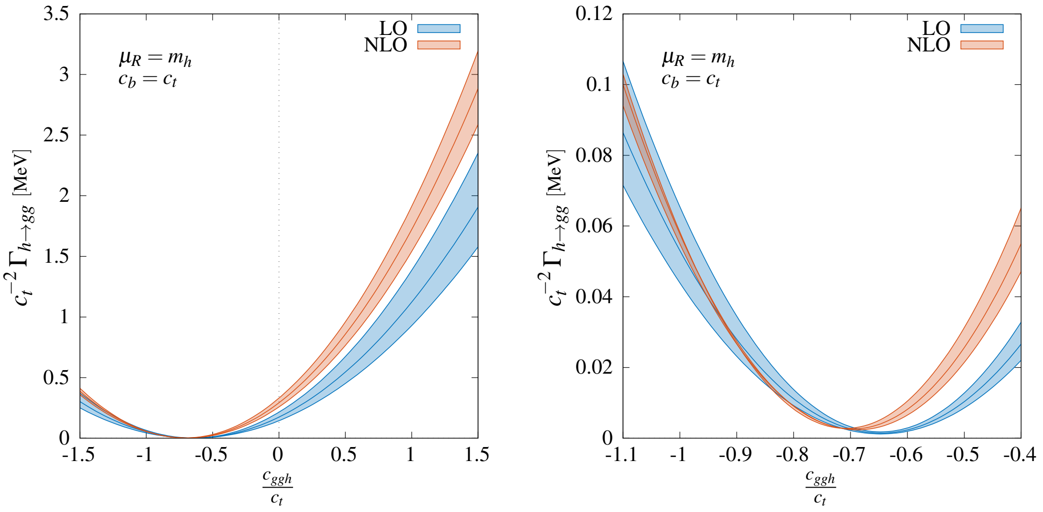

Figure 9: Rescaled LO (blue) and NLO (red) decay rate depending on the ratio c_{ggh}/c_t. The right plot is a zoomed-in version of the left one showing the well-behavior of the NLO decay rate by virtue of the fix (5.310) - without it, the NLO rate would "dip" below 0 by a small amount, which would be even worse than the fix. The error bands refer to scale variation ($m_h/2 < \mu_R < 2m_h$) and the dashed line indicates the SM result.

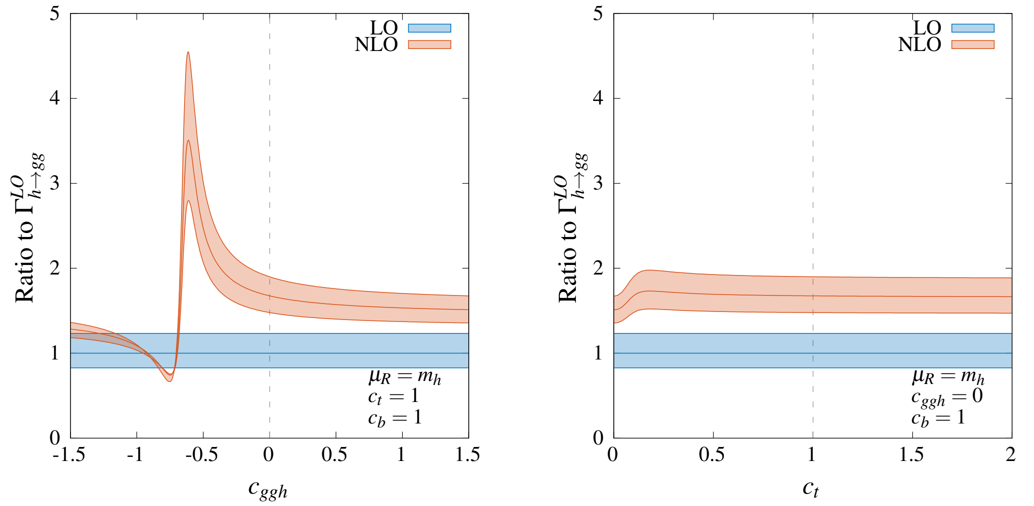

Figure 10: QCD K-factors, i.e. the ratio between the running LO or NLO decay rate to the LO result fixed at $\mu_R = m_h$. The colour code is the same as in Figure 9. Without the fix (5.310), the NLO K-factor of the left curve would be "stretched" yielding a true divergence around $c_{ggh} \approx -2/3$, again worse than the fix.

6. Conclusions and outlook

In this work, we have demonstrated how a power-counting scheme for SMEFT relying solely on canonical dimensions can result in inconsistencies within the perturbative expansion of the underlying QFT at high energies. To be more precise, without further assumptions about the UV sector, the relevant power-counting information is incomplete and therefore not suited as a consistent realistic EFT for the SM degrees of freedom. One possible minimal assumption about the full theory is that it can be defined as a renormalizable perturbative QFT with weak couplings. In fact, if this were not the case, other EFT frameworks such as the EWChL might prove to be better suited as a starting point for low-energy studies than SMEFT.

Based on specific examples and general setups, we have developed a systematic treatment for operators of canonical dimension six by introducing the notion of chiral dimensions to SMEFT. The latter act as a book-keeping device for counting loop orders equally to the expansion in the high energy scale. Our results confirm the observation that operators involving field strength tensors come with extra suppression factors on a quantitative level.

While variations of the power-counting scheme we propose and hence the hierarchy between operators are, of course, always possible, the approximations, assumptions and power-counting rules for the EFT should always be explicitly specified.

Our analysis concerns mainly operators of canonical dimension six. An extrapolation to higher dimensions is not straightforward, as field redefinitions and the application of the field equations of motion may spoil the classification of operators into field-strength operators and non-field-strength operators in a non-trivial way. Despite being of subleading phenomenological importance, it seems, however, plausible that a conceptually related analysis can also be performed for these higher-order effects in future works.

A first example for the importance of our power-counting rules for the LHC was given by our computation of the leading new-physics corrections (assumed to be in the third particle generation only) to the differential cross section for top-quark pair production via gluon fusion in SMEFT at LO QCD. A superficial numerical discussion serves as an illustration of how the overall SMEFT impact is relatively minor, as all effects are actually loop-suppressed within our power-counting framework. Given the expected significance of NLO QCD corrections for the process under study, a more comprehensive analysis should incorporate them as well, as there could indeed be enhancements of the impact of certain operators. We defer a general phenomenological study for hadron colliders including the initial-quark-anti-quark channel, PDFs and a more thorough analysis of the Warsaw-basis coefficients' parameter space to future works.

As a second example, we have conducted a comprehensive investigation of the Higgs-boson decay rates of $h \to gg$ and $h \to \gamma\gamma$ at NLO QCD, taking into account possible anomalous Higgs couplings arising from new-physics effects. In this case, there is no distinction between the predictions of SMEFT and the EWChL. The EFT follows a power counting in loop orders, which can be systematically integrated within QCD perturbation theory. Indeed, the extension of the QCD calculation from LO to NLO does not generate any further EFT parameters.

While having lesser importance for $h \to \gamma\gamma$, the phenomenological impact of QCD on the $h \to gg$ rate is substantial. It gives rise to a K-factor of about 1.7 and halves the scale uncertainty.
Our results may provide the basic ingredients for a global fit analysis of the SMEFT or EWChL parameters including NLO QCD effects. However, as even higher-order effects in QCD will eventually turn out to be significant, such an NLO QCD treatment of the anomalous couplings for $h \to gg$ will have to be extended to higher loop orders for more sensible predictions and hence potential constraints on new-physics signatures in experimental data in future works.

A. Input parameters

Throughout this work, we use the following numerical values as SM input parameters [61]:

m_h	125.25 ± 0.17 GeV
m_t (OS)	172.69 ± 0.30 GeV
m_b ($\overline{\text{MS}}$ at $\mu_b = m_b$)	$4.18^{+0.03}_{-0.02}$ GeV
m_b (OS)	4.78 ± 0.6 GeV
m_c ($\overline{\text{MS}}$ at $\mu_c = m_c$)	1.27 ± 0.02 GeV
m_c (OS)	1.67 ± 0.07 GeV
m_τ (OS)	1.77686 ± 0.00012 GeV
m_Z (OS)	91.1876 ± 0.0021 GeV
m_W (OS)	80.377 ± 0.012 GeV
$\alpha_s(m_Z)$	0.1179 ± 0.0009
G_F	$1.1663788 \cdot 10^{-5} \pm 6 \cdot 10^{-12}$ GeV^{-2}
$\alpha(0)$	$(7.2973525693 \pm 1.1 \cdot 10^{-9}) \cdot 10^{-3}$

With $g_s = 2\sqrt{\pi\alpha_s}$, $v = 1/\sqrt{\sqrt{2}G_F}$ and $e = 2\sqrt{\pi\alpha}$, we can alternatively use

$g_s(m_Z)$	1.217 ± 0.005
v	$246.21964 \pm 6 \cdot 10^{-5}$ GeV
$e(0)$	$0.302822120872 \pm 2.3 \cdot 10^{-11}$

B. Spinor helicity formalism

When working with polarization vectors, we have often suppressed the actual polarization, which can take one of two values ($\pm$). One can deal with polarizations after squaring the amplitude in terms of a polarization sum, e.g. (5.18). It is, however, advantageous to consider fixed polarization amplitudes from the start. The spinor helicity formalism then provides a useful tool helping to avoid lengthy expressions involving polarization vectors. This section contains a summary of how the different notation schemes are related to each other.

In the following, all external particles are assumed to be massless. In general, we apply the conventions of [228] and the corresponding textbook (the metric tensor, however, is chosen to be mostly minus; this causes actually some trouble and needs extra adjustments, see also [8]). Good reviews with an emphasis on the cases we are interested in can be found in [229–236]. The following table features the relevant physical quantities within the respective notation schemes:

Vector notation	Spinor helicity formalism
$\bar{u}_+(k_i) = \bar{v}_-(k_i)$	$[i\vert$
$\bar{u}_-(k_i) = \bar{v}_+(k_i)$	$\langle i\vert$
$v_+(k_i) = u_-(k_i)$	$\vert i]$
$v_-(k_i) = u_+(k_i)$	$\vert i\rangle$
$\epsilon_+^\mu(k_i) = \epsilon_-^{*\mu}(k_i)$	$\frac{1}{\sqrt{2}}\frac{[i\vert\gamma^\mu\vert n\rangle}{\langle ni\rangle}$
$\epsilon_-^\mu(k_i) = \epsilon_+^{*\mu}(k_i)$	$-\frac{1}{\sqrt{2}}\frac{\langle i\vert\gamma^\mu\vert n]}{[ni]}$

As dealing with explicit polarizations using the spinor helicity formalism bypasses complicated spin sums, when avoiding the latter, the dependence on the reference momentum $n \neq i$ (or $k_n \neq k_i$) for gauge bosons has to enter directly as indicated. In fact, a lot of simplification usually happens already on the amplitude level upon choosing smart combinations for the reference momenta, see for example (B.15) below.

Working with bra-kets is only powerful in combination with a bunch of identities. Some of them are given here (k_g, k_h, k_i, k_j are assumed to be massless four-vectors):

$$\not{k}_i = |i\rangle[i| + |i]\langle i| \tag{B.1}$$

$$\langle ij] = [ij\rangle = 0 \tag{B.2}$$

$$\langle ij\rangle = -\langle ji\rangle \tag{B.3}$$

$$[ij] = -[ji] \tag{B.4}$$

$$\langle ij\rangle^* = [ji] \tag{B.5}$$

$$2k_i \cdot k_j = \langle ij\rangle[ji] \tag{B.6}$$
$$\langle i|\gamma^\mu|j\rangle = [i|\gamma^\mu|j] = 0 \tag{B.7}$$
$$[i|\gamma^\mu|j\rangle = \langle j|\gamma^\mu|i] \tag{B.8}$$
$$[i|\gamma^\mu|j\rangle^* = [j|\gamma^\mu|i\rangle \tag{B.9}$$
$$\langle i|\not{k}_h|j] = \langle ih\rangle[hj] \tag{B.10}$$
$$\langle i|\gamma^\mu|j]\gamma_\mu = 2(|i\rangle[j| + |j]\langle i|) \tag{B.11}$$
$$[i|\gamma^\mu|j\rangle\gamma_\mu = 2(|i]\langle j| + |j\rangle[i|) \tag{B.12}$$
$$\langle g|\gamma^\mu|h]\langle i|\gamma_\mu|j] = 2\langle gi\rangle[jh] \quad \text{(Fierz identity)} \tag{B.13}$$
$$\langle ij\rangle\langle gh\rangle + \langle ig\rangle\langle hj\rangle + \langle ih\rangle\langle jg\rangle = 0 \quad \text{(Schouten identity)} \tag{B.14}$$

Let us carry out two examples. First, consider the polarization structure found in (5.16). Choosing both helicities explicitly, we find

$$\begin{aligned}
&\epsilon^*_{\mu+}(k_1)\epsilon^*_{\nu+}(k_2)(k_1^\nu k_2^\mu - k_1\cdot k_2 g^{\mu\nu}) = \epsilon_{\mu-}(k_1)\epsilon_{\nu-}(k_2)(k_1^\nu k_2^\mu - k_1\cdot k_2 g^{\mu\nu}) = \\
&= \frac{1}{2}\frac{\langle 1|\gamma_\mu|n]\langle 2|\gamma_\nu|m]}{[n1][m2]}(k_1^\nu k_2^\mu - k_1\cdot k_2 g^{\mu\nu}) = \\
&\overset{(B.6)}{=} \frac{1}{2[n1][m2]}\left(\langle 1|\not{k}_2|n]\langle 2|\not{k}_1|m] - \frac{1}{2}\langle 12\rangle[21]\langle 1|\gamma^\mu|n]\langle 2|\gamma_\mu|m]\right) = \\
&\overset{(B.10),(B.13)}{=} \frac{1}{2[n1][m2]}\left(\langle 12\rangle[2n]\langle 21\rangle[1m] - \langle 12\rangle[21]\langle 12\rangle[mn]\right) = \\
&\overset{n=2,m=1}{\longrightarrow} \frac{1}{2[21][12]}\left(0 - \langle 12\rangle[21]\langle 12\rangle[12]\right) = -\frac{1}{2}\langle 12\rangle^2
\end{aligned} \tag{B.15}$$

Second, for one specific case of the polarization structure found in (5.126), we obtain

$$\begin{aligned}
&\epsilon^*_{\mu+}(k_1)\bar{u}_-(k_q)\big((m_h^2 - s_{q\bar{q}})\gamma^\mu - 2\not{k}_1(k_q^\mu + k_{\bar{q}}^\mu)\big)v_+(k_{\bar{q}}) = \\
&= \epsilon_{\mu-}(k_1)\bar{u}_-(k_q)\big((m_h^2 - s_{q\bar{q}})\gamma^\mu - 2\not{k}_1(k_q^\mu + k_{\bar{q}}^\mu)\big)v_+(k_{\bar{q}}) = \\
&= -\frac{\langle 1|\gamma^\mu|n]}{\sqrt{2}[n1]}\langle q|\big((m_h^2 - s_{q\bar{q}})\gamma^\mu - 2\not{k}_1(k_q^\mu + k_{\bar{q}}^\mu)\big)|\bar{q}] = \\
&= -\frac{1}{\sqrt{2}[n1]}\big((m_h^2 - s_{q\bar{q}})\langle 1|\gamma^\mu|n]\langle q|\gamma^\mu|\bar{q}] - 2\langle 1|(\not{k}_q + \not{k}_{\bar{q}})|n]\langle q|\not{k}_1|\bar{q}]\big) = \\
&\overset{(B.10),(B.13)}{=} -\frac{1}{\sqrt{2}[n1]}\big(2(m_h^2 - s_{q\bar{q}})\langle 1q\rangle[\bar{q}n] - 2(\langle 1q\rangle[qn] + \langle 1\bar{q}\rangle[\bar{q}n])\langle q1\rangle[1\bar{q}]\big) = \\
&\overset{n=q+\bar{q}}{\longrightarrow} -\frac{\sqrt{2}}{[q1]+[\bar{q}1]}\big((\langle 1q\rangle[q1] + \langle 1\bar{q}\rangle[\bar{q}1])\langle 1q\rangle[\bar{q}q] - (\langle 1q\rangle[q\bar{q}] + \langle 1\bar{q}\rangle[\bar{q}q])\langle q1\rangle[1\bar{q}]\big) = \\
&\overset{(B.6)}{=} -\frac{\sqrt{2}s_{q\bar{q}}\langle 1q\rangle^2}{\langle q\bar{q}\rangle}
\end{aligned} \tag{B.16}$$

The following table summarizes some relevant equations (we include the respective reference vector as a second argument of the polarization vectors):

Vector notation	Spinor helicity formalism
$\epsilon_+^*(k_i,k_n)\cdot\epsilon_+^*(k_j,k_m)$	$\frac{\langle ij\rangle[mn]}{[ni][mj]}$
$\epsilon_-^*(k_i,k_n)\cdot\epsilon_-^*(k_j,k_m)$	$\frac{[ij]\langle mn\rangle}{\langle ni\rangle\langle mj\rangle}$
$\epsilon_+^*(k_i,k_n)\cdot\epsilon_-^*(k_j,k_m)$	$-\frac{[nj]\langle mi\rangle}{[ni]\langle mj\rangle}$
$\epsilon_+^*(k_i,k_n)\cdot k_j$	$-\frac{\langle ij\rangle[jn]}{\sqrt{2}[ni]}$
$\epsilon_-^*(k_i,k_n)\cdot k_j$	$\frac{[ij]\langle jn\rangle}{\sqrt{2}\langle ni\rangle}$
$\epsilon_{\mu+}^*(k_1,k_n)\epsilon_{\nu+}^*(k_2,k_m)(k_1^\nu k_2^\mu - k_1\cdot k_2 g^{\mu\nu})$	$\frac{\langle 12\rangle[2n]\langle 21\rangle[1m]-\langle 12\rangle[21]\langle 12\rangle[mn]}{2[n1][m2]}$
$\epsilon_{\mu-}^*(k_1,k_n)\epsilon_{\nu-}^*(k_2,k_m)(k_1^\nu k_2^\mu - k_1\cdot k_2 g^{\mu\nu})$	$\frac{[12]\langle 2n\rangle[21]\langle 1m\rangle-[12]\langle 21\rangle[12]\langle mn\rangle}{2\langle n1\rangle\langle m2\rangle}$
$\epsilon_{\mu+}^*(k_1,k_n)\epsilon_{\nu-}^*(k_2,k_m)(k_1^\nu k_2^\mu - k_1\cdot k_2 g^{\mu\nu})$	$\frac{\langle n2\rangle[21]\langle 21\rangle[1m]-\langle 12\rangle[21]\langle n2\rangle[m1]}{2\langle n1\rangle[m2]}$
$\epsilon_{\mu-}^*(k_1,k_n)\epsilon_{\nu+}^*(k_2,k_m)(k_1^\nu k_2^\mu - k_1\cdot k_2 g^{\mu\nu})$	$\frac{[n2]\langle 21\rangle[21]\langle 1m\rangle-[12]\langle 21\rangle[n2]\langle m1\rangle}{2[n1]\langle m2\rangle}$
$\epsilon_{\mu+}^*(k_1,k_n)\bar{u}_-(k_q)\big((m_h^2-s_{q\bar{q}})\gamma^\mu-2\not{k}_1(k_q^\mu+k_{\bar{q}}^\mu)\big)v_+(k_{\bar{q}})$	$-\frac{\sqrt{2}}{[n1]}\big((m_h^2 - s_{q\bar{q}})\langle 1q\rangle[\bar{q}n] - (\langle 1q\rangle[qn] + \langle 1\bar{q}\rangle[\bar{q}n])\langle q1\rangle[1\bar{q}]\big)$
$\epsilon_{\mu+}^*(k_1,k_n)\bar{u}_+(k_q)\big((m_h^2-s_{q\bar{q}})\gamma^\mu-2\not{k}_1(k_q^\mu+k_{\bar{q}}^\mu)\big)v_-(k_{\bar{q}})$	$-\frac{\sqrt{2}}{[n1]}\big((m_h^2 - s_{\bar{q}q})\langle 1\bar{q}\rangle[qn] - (\langle 1\bar{q}\rangle[\bar{q}n] + \langle 1q\rangle[qn])\langle\bar{q}1\rangle[1q]\big)$
$\epsilon_{\mu-}^*(k_1,k_n)\bar{u}_-(k_q)\big((m_h^2-s_{q\bar{q}})\gamma^\mu-2\not{k}_1(k_q^\mu+k_{\bar{q}}^\mu)\big)v_+(k_{\bar{q}})$	$\frac{\sqrt{2}}{\langle n1\rangle}\big((m_h^2 - s_{\bar{q}q})[1\bar{q}]\langle qn\rangle - ([1\bar{q}]\langle\bar{q}n\rangle + [1q]\langle qn\rangle)[\bar{q}1]\langle 1q\rangle\big)$
$\epsilon_{\mu-}^*(k_1,k_n)\bar{u}_+(k_q)\big((m_h^2-s_{q\bar{q}})\gamma^\mu-2\not{k}_1(k_q^\mu+k_{\bar{q}}^\mu)\big)v_-(k_{\bar{q}})$	$\frac{\sqrt{2}}{\langle n1\rangle}\big((m_h^2 - s_{\bar{q}q})[1q]\langle\bar{q}n\rangle - ([1q]\langle qn\rangle + [1\bar{q}]\langle\bar{q}n\rangle)[q1]\langle 1\bar{q}\rangle\big)$

C. Feynman rules for the SM

A generic SM amplitude $i\mathcal{M}$ can be obtained by applying the set of Feynman rules we list in this appendix [66, 237]. Only the Feynman rules that are explicitly used within this work are shown. Our conventions are as follows. We denote external field points by empty dots and interactions by black dots. Higgs, photon, gluon, fermion and W-boson lines are symbolized by dashed lines, curvy lines, spring-like lines, straight lines with arrows and edgy curvy lines with arrows, respectively. The usual spacetime indices read μ, ν, etc. and ϵ, u (or v) denote the polarization vectors and particle (or anti-particle) spinors. Fundamental and adjoint colours are given by c_i and A, etc., and flavours by f_i. The rest of our notational conventions should be self-explaining.

$$\equiv 1 \tag{C.1}$$

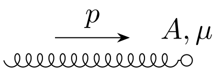

$$\equiv \begin{cases} \epsilon^A_\mu(p) & \text{for incoming} \\ \epsilon^{*A}_\mu(p) & \text{for outgoing} \end{cases} \tag{C.2}$$

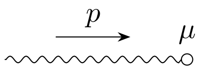

$$\equiv \begin{cases} \epsilon_\mu(p) & \text{for incoming} \\ \epsilon^{*}_\mu(p) & \text{for outgoing} \end{cases} \tag{C.3}$$

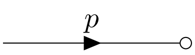

$$\equiv \begin{cases} u(p) & \text{for incoming} \\ \bar{u}(p) & \text{for outgoing} \end{cases} \tag{C.4}$$

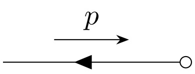

$$\equiv \begin{cases} \bar{v}(p) & \text{for incoming} \\ v(p) & \text{for outgoing} \end{cases} \tag{C.5}$$

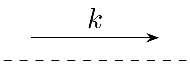

$$\equiv \frac{i}{k^2 - m^2} \tag{C.6}$$

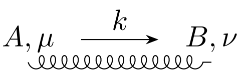

$$\equiv \frac{-ig_{\mu\nu}\delta^{AB}}{k^2} \text{ (Feynman gauge)} \tag{C.7}$$

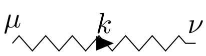

$$\equiv \frac{-i(m_W^2 g_{\mu\nu} - k_\mu k_\nu)}{m_W^2(k^2 - m_W^2)} \text{ (unitary gauge)} \tag{C.8}$$

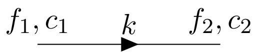

$$\equiv i\delta_{f_1 f_2}\delta_{c_1 c_2}\frac{\not{k}+m}{k^2-m^2} \tag{C.9}$$

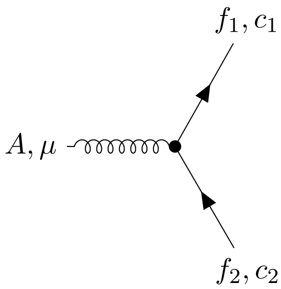

$$\equiv -ig_s\delta_{f_1 f_2}T^A_{c_1 c_2}\gamma^\mu \tag{C.10}$$

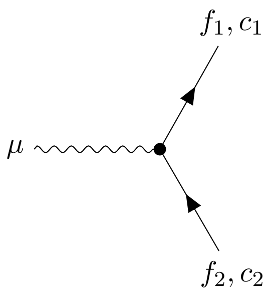

$$\equiv -ieQ_{f_{1/2}}\delta_{f_1 f_2}\delta_{c_1 c_2}\gamma^\mu \tag{C.11}$$

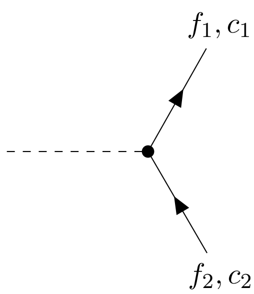

$$\equiv -i\frac{y_{f_{1/2}}}{\sqrt{2}}\delta_{f_1 f_2}\delta_{c_1 c_2} \tag{C.12}$$

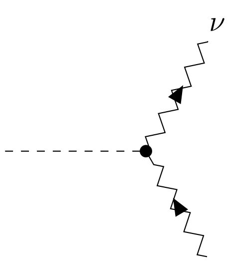

$$\equiv \frac{i}{2}g^2 v g^{\mu\nu} \tag{C.13}$$

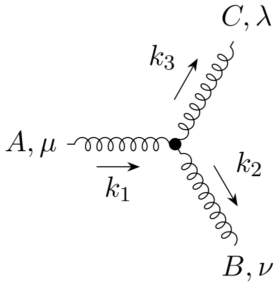

$$\equiv -ig_s V^{ABC}_{\mu\nu\lambda}(k_1, k_2, k_3) = -g_s f^{ABC}\big(g_{\mu\nu}(k_1 + k_2)_\lambda + - g_{\mu\lambda}(k_1 + k_3)_\nu + g_{\nu\lambda}(k_3 - k_2)_\mu\big) \tag{C.14}$$

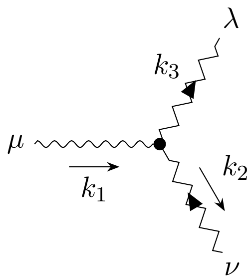

$$\equiv ie\big(g_{\mu\nu}(k_1 + k_2)_\lambda - g_{\mu\lambda}(k_1 + k_3)_\nu + g_{\nu\lambda}(k_3 - k_2)_\mu\big) \tag{C.15}$$

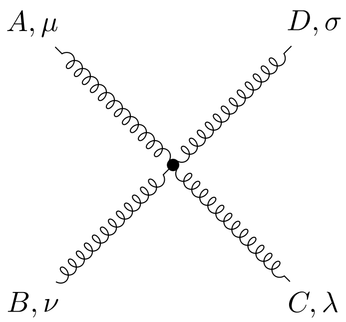

$$\equiv -ig_s^2 W^{ABCD}_{\mu\nu\lambda\sigma} = -ig_s^2\big(f^{ABE}f^{CDE}(g_{\mu\lambda}g_{\nu\sigma} - g_{\mu\sigma}g_{\nu\lambda}) + + f^{ACE}f^{BDE}(g_{\mu\nu}g_{\lambda\sigma} - g_{\mu\sigma}g_{\nu\lambda}) + + f^{ADE}f^{BCE}(g_{\mu\nu}g_{\lambda\sigma} - g_{\mu\lambda}g_{\nu\sigma})\big) \tag{C.16}$$

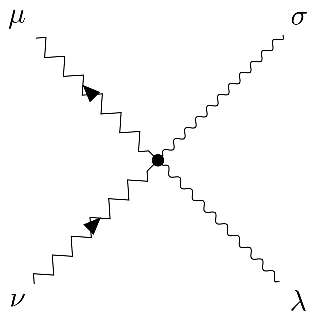

$$\equiv = ie^2(g^{\sigma\mu}g^{\lambda\nu} + g^{\sigma\nu}g^{\lambda\mu} - 2g^{\sigma\lambda}g^{\mu\nu}) \tag{C.17}$$

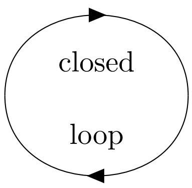

$$\equiv -1 \tag{C.18}$$

D. Momentum integrals

Evaluating loop integrals requires a good deal of calculational machinery. This appendix highlights some equations related to integration techniques that we apply quite frequently in this work.
One of the most relevant formulas for practical calculations in QFT is the d-dimensional momentum integral

$$\mu^{4-d}\int\frac{d^dk}{(2\pi)^d}\frac{k^{2a}}{(k^2-\Delta)^b}=i(-1)^{a-b}\frac{\left(\mu^2\right)^{2-\frac{d}{2}}}{(4\pi)^{\frac{d}{2}}}\frac{\Gamma\left(a+\frac{d}{2}\right)\Gamma\left(b-a-\frac{d}{2}\right)}{\Gamma(b)\Gamma\left(\frac{d}{2}\right)}\Delta^{a-b+\frac{d}{2}} \tag{D.1}$$

which can be found in any QFT book [5–8]. The Gamma function fulfills the properties [7]

$$\Gamma(n)=(n-1)\Gamma(n-1) \tag{D.2}$$

$$\Gamma(n+1)=n! \tag{D.3}$$

$$\Gamma\left(n+\frac{1}{2}\right)=\frac{\sqrt{\pi}(2n)!}{2^{2n}n!} \tag{D.4}$$

$$\Gamma(-n+x)=\frac{(-1)^n}{n!}\left(\frac{1}{x}-\gamma+\sum_{k=1}^{n}\frac{1}{k}\right)+\mathcal{O}(x) \tag{D.5}$$

where the Euler-Mascheroni constant is defined via

$$\gamma=\lim_{n\to\infty}\left(\sum_{k=1}^{n}\frac{1}{k}-\int_1^n\frac{dk}{k}\right)\approx 0.5772 \tag{D.6}$$

Special cases of (D.5) are given by

$$\Gamma(-1+x)=-\frac{1}{x}+\gamma-1+\mathcal{O}(x) \tag{D.7}$$

$$\Gamma(x)=\frac{1}{x}-\gamma+\mathcal{O}(x) \tag{D.8}$$

$$\Gamma(1+x)=1-x\gamma+\mathcal{O}(x^2) \tag{D.9}$$

It is also worth noting that one can always replace the loop-momenta in the numerator of (D.1) by the corresponding tensor structures via [5]

$$k^\mu k^\nu\longleftrightarrow\frac{k^2}{d}g^{\mu\nu} \tag{D.10}$$

$$k^\mu k^\nu k^\alpha k^\beta\longleftrightarrow\frac{k^4}{d(d+2)}(g^{\mu\nu}g^{\alpha\beta}+g^{\mu\alpha}g^{\nu\beta}+g^{\mu\beta}g^{\nu\alpha}) \tag{D.11}$$

$$\begin{aligned}k^\mu k^\nu k^\alpha k^\beta k^\gamma k^\delta\longleftrightarrow\frac{k^6}{d(d+2)(d+4)}&(g^{\mu\nu}g^{\alpha\beta}g^{\gamma\delta}+g^{\mu\alpha}g^{\nu\beta}g^{\gamma\delta}+g^{\mu\beta}g^{\nu\alpha}g^{\gamma\delta}+\\&+g^{\delta\nu}g^{\alpha\beta}g^{\gamma\mu}+g^{\delta\alpha}g^{\nu\beta}g^{\gamma\mu}+g^{\delta\beta}g^{\nu\alpha}g^{\gamma\mu}+\end{aligned}$$

$$+ g^{\mu\delta}g^{\alpha\beta}g^{\gamma\nu} + g^{\mu\alpha}g^{\delta\beta}g^{\gamma\nu} + g^{\mu\beta}g^{\delta\alpha}g^{\gamma\nu} +$$
$$+ g^{\mu\nu}g^{\delta\beta}g^{\gamma\alpha} + g^{\mu\delta}g^{\nu\beta}g^{\gamma\alpha} + g^{\mu\beta}g^{\nu\delta}g^{\gamma\alpha} +$$
$$+ g^{\mu\nu}g^{\alpha\delta}g^{\gamma\beta} + g^{\mu\alpha}g^{\nu\delta}g^{\gamma\beta} + g^{\mu\delta}g^{\nu\alpha}g^{\gamma\beta}) \tag{D.12}$$

For $a = 0, 1, 2$ in (D.1), we find

$$\mu^{4-d}\int\frac{d^dk}{(2\pi)^d}\frac{1}{(k^2-\Delta)^b} = i(-1)^b\frac{\left(\mu^2\right)^{2-\frac{d}{2}}}{(4\pi)^{\frac{d}{2}}}\frac{\Gamma\left(b-\frac{d}{2}\right)}{\Gamma(b)}\Delta^{-b+\frac{d}{2}} \tag{D.13}$$

$$\mu^{4-d}\int\frac{d^dk}{(2\pi)^d}\frac{k^\alpha k^\beta}{(k^2-\Delta)^b} = -i(-1)^b\frac{\left(\mu^2\right)^{2-\frac{d}{2}}}{(4\pi)^{\frac{d}{2}}}\frac{g^{\alpha\beta}}{2}\frac{\Gamma\left(b-1-\frac{d}{2}\right)}{\Gamma(b)}\Delta^{1-b+\frac{d}{2}} \tag{D.14}$$

$$\mu^{4-d}\int\frac{d^dk}{(2\pi)^d}\frac{k^\mu k^\nu k^\alpha k^\beta}{(k^2-\Delta)^b} = i(-1)^b\frac{\left(\mu^2\right)^{2-\frac{d}{2}}}{(4\pi)^{\frac{d}{2}}}\frac{g^{\mu\nu}g^{\alpha\beta}+g^{\mu\alpha}g^{\nu\beta}+g^{\mu\beta}g^{\nu\alpha}}{4}\frac{\Gamma\left(b-2-\frac{d}{2}\right)}{\Gamma(b)}\Delta^{2-b+\frac{d}{2}} \tag{D.15}$$

An expansion around $d = 4$ is now straightforward. The following list of integrals is valid for $\Delta \neq 0$ with $d = 4 - 2\epsilon$ up to $\mathcal{O}(\epsilon^0)$:

$$\mu^{2\epsilon}\int\frac{d^dk}{(2\pi)^d}\frac{1}{k^2-\Delta} = \frac{i}{16\pi^2}\Delta\left(\frac{1}{\epsilon}+\ln\frac{4\pi}{e^\gamma}+\ln\frac{\mu^2}{\Delta}+1\right) \tag{D.16}$$

$$\mu^{2\epsilon}\int\frac{d^dk}{(2\pi)^d}\frac{1}{(k^2-\Delta)^2} = \frac{i}{16\pi^2}\left(\frac{1}{\epsilon}+\ln\frac{4\pi}{e^\gamma}+\ln\frac{\mu^2}{\Delta}\right) \tag{D.17}$$

$$\mu^{2\epsilon}\int\frac{d^dk}{(2\pi)^d}\frac{k^\alpha k^\beta}{(k^2-\Delta)^2} = \frac{i}{16\pi^2}\frac{\Delta g^{\alpha\beta}}{2}\left(\frac{1}{\epsilon}+\ln\frac{4\pi}{e^\gamma}+\ln\frac{\mu^2}{\Delta}+1\right) \tag{D.18}$$

$$\mu^{2\epsilon}\int\frac{d^dk}{(2\pi)^d}\frac{1}{(k^2-\Delta)^3} = -\frac{i}{16\pi^2}\frac{1}{2\Delta} \tag{D.19}$$

$$\mu^{2\epsilon}\int\frac{d^dk}{(2\pi)^d}\frac{k^\alpha k^\beta}{(k^2-\Delta)^3} = \frac{i}{16\pi^2}\frac{g^{\alpha\beta}}{4}\left(\frac{1}{\epsilon}+\ln\frac{4\pi}{e^\gamma}+\ln\frac{\mu^2}{\Delta}\right) \tag{D.20}$$

$$\mu^{2\epsilon}\int\frac{d^dk}{(2\pi)^d}\frac{1}{(k^2-\Delta)^4} = \frac{i}{16\pi^2}\frac{1}{6\Delta^2} \tag{D.21}$$

$$\mu^{2\epsilon}\int\frac{d^dk}{(2\pi)^d}\frac{k^\alpha k^\beta}{(k^2-\Delta)^4} = -\frac{i}{16\pi^2}\frac{g^{\alpha\beta}}{12\Delta} \tag{D.22}$$

When dealing with infrared divergences, the finite expressions (D.19), (D.21) and (D.22) will lead to divergent Feynman parameter integrals. It is therefore better to work with general $d \neq 4$, i.e. (D.13)-(D.15) in these cases.
The class of momentum integrals with $\Delta = 0$ can be written as

$$\mu^{4-d}\int\frac{d^dk}{(2\pi)^d}\frac{1}{k^{2c}} \tag{D.23}$$

for fixed $c = b - a$ (in the notation of (D.1)) and is referred to as scaleless [238]. Substituting $k = \lambda k'$ (which corresponds to a simple momentum rescaling by λ) yields

$$\mu^{4-d} \lambda^{d-2c} \int \frac{d^d k'}{(2\pi)^d} \frac{1}{k'^{2c}} \tag{D.24}$$

The two expressions (D.23) and (D.24) hold for arbitrary choices of d and λ and can therefore only be equal if they are set to zero in dimensional regularization.

E. Tensor integral reduction for triangle graphs with two external gluons

As stated in the main text, tensor integral reduction methods are among the most common tools for computing loop corrections in a systematic manner [89–91]. For simple cases like fermion triangle graphs with massless external gluons, it can be done by hand. We have made use of the results presented in this appendix on several occasions in this work.

In the following discussion, we consider a process with two external gluons associated with a fermion triangle loop and evaluate the relevant one-loop tensor integrals by reducing them to an appropriate basis of scalar integrals.

Throughout this section, we set the gluon momenta on-shell by imposing $k_1^2 = k_2^2 = 0$ and define the incoming Higgs-momentum by $q = k_1 + k_2$ with $q^2 = m_h^2$. The mass of the loop particle is denoted by m and, for the sake of notation, we drop the $-i\eta$ parts associated with propagators. As usual, sending m^2 to $m^2 - i\eta$ in the end restores the correct prescription, which becomes important for figuring out the correct analytic behavior of the explicit loop functions in the complex plane.

For simplicity, we focus on the diagram

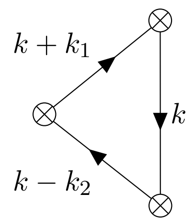

(E.1)

where features other than the triangle loop were left implicit. Applying dimensional regularization with $d = 4 - 2\epsilon$ and dropping terms of $\mathcal{O}(\epsilon)$ or higher, the relevant basic scalar integrals are given by

$$\begin{aligned} A \equiv& \mu^{2\epsilon} \int \frac{d^dk}{(2\pi)^d} \frac{1}{(k^2 - m^2)} = \mu^{2\epsilon} \int \frac{d^dk}{(2\pi)^d} \frac{1}{\big((k+k_1)^2 - m^2\big)} = \\ =& \mu^{2\epsilon} \int \frac{d^dk}{(2\pi)^d} \frac{1}{\big((k-k_2)^2 - m^2\big)} = \frac{i}{16\pi^2} m^2 \left(\frac{1}{\epsilon} + \ln \frac{4\pi}{e^\gamma} + \ln \frac{\mu^2}{m^2} + 1 \right) \end{aligned} \tag{E.2}$$

$$\begin{aligned} B \equiv& \mu^{2\epsilon} \int \frac{d^dk}{(2\pi)^d} \frac{1}{(k^2 - m^2)\big((k+k_1)^2 - m^2\big)} = \\ =& \mu^{2\epsilon} \int \frac{d^dk}{(2\pi)^d} \frac{1}{(k^2 - m^2)\big((k-k_2)^2 - m^2\big)} = \\ =& \frac{i}{16\pi^2} \left(\frac{1}{\epsilon} + \ln \frac{4\pi}{e^\gamma} + \ln \frac{\mu^2}{m^2} \right) = \frac{d-2}{2m^2} A \end{aligned} \tag{E.3}$$

$$
\begin{aligned}
\widetilde{B} \equiv& \mu^{2\epsilon} \int \frac{d^d k}{(2\pi)^d} \frac{1}{(k^2 - m^2)\big((k+q)^2 - m^2\big)} = \\
=& \mu^{2\epsilon} \int \frac{d^d k}{(2\pi)^d} \frac{1}{\big((k+k_1)^2 - m^2\big)\big((k-k_2)^2 - m^2\big)} = \\
=& B - \frac{i}{16\pi^2} \int_0^1 dx \ln\left(1 - x(1-x)\frac{q^2}{m^2}\right)
\end{aligned} \tag{E.4}
$$

$$
\begin{aligned}
C \equiv& \mu^{2\epsilon} \int \frac{d^d k}{(2\pi)^d} \frac{1}{(k^2 - m^2)\big((k+k_1)^2 - m^2\big)\big((k-k_2)^2 - m^2\big)} = \\
=& -\frac{i}{16\pi^2} \int_0^1 dz \int_0^{1-z} dy \frac{1}{m^2 - yzq^2}
\end{aligned} \tag{E.5}
$$

Feynman parameters have been introduced for C and the combination $B - \widetilde{B}$ which can be recognized as being finite. Evaluating the parameter integrals and defining $\tau \equiv q^2/4m^2$ yields

$$
B - \widetilde{B} = \frac{i}{16\pi^2}\left(2\sqrt{\frac{1}{\tau} - 1}\arctan\left(\sqrt{\frac{1}{\frac{1}{\tau} - 1}}\right) - 2\right) \tag{E.6}
$$

$$
\begin{aligned}
C =& -\frac{i}{16\pi^2 m_h^2}\left(\mathrm{Li}_2\left(\frac{2}{1 + \sqrt{1 - \frac{1}{\tau}}}\right) + \mathrm{Li}_2\left(\frac{2}{1 - \sqrt{1 - \frac{1}{\tau}}}\right)\right) = \\
=& \frac{i}{32\pi^2 m_h^2} \ln^2\left(1 - 2\tau\left(1 - \sqrt{1 - \frac{1}{\tau}}\right)\right)
\end{aligned} \tag{E.7}
$$

where $\mathrm{Li}_2(1-x) + \mathrm{Li}_2(1 - 1/x) = -\frac{1}{2}\ln^2 x$ has been used.
We now have to distinguish between the cases $0 < \tau < 1$ and $1 \leq \tau < \infty$. It is now time to reinsert the $i\eta$-terms as they provide clear prescriptions concerning the branch cuts of the logarithms and square roots.
For $0 < \tau < 1$, we find

$$
B - \widetilde{B} = \frac{i}{16\pi^2}\left(2\sqrt{\frac{1}{\tau} - 1}\arctan\left(\sqrt{\frac{1}{\frac{1}{\tau} - 1}}\right) - 2\right) \tag{E.8}
$$

$$
\begin{aligned}
C =& \frac{i}{32\pi^2 m_h^2} \ln^2\left(1 - 2\tau\left(1 - \sqrt{1 - \frac{1}{\tau} + i\eta}\right)\right) = \\
=& \frac{i}{32\pi^2 m_h^2} \ln^2\left(1 - 2\tau\left(1 - i\sqrt{\frac{1}{\tau} - 1}\right)\right) =
\end{aligned}
$$

$$
\begin{aligned}
&= \frac{i}{32\pi^2 m_h^2} \ln^2\left(\left(i\sqrt{\tau}+\sqrt{1-\tau}\right)^2\right) = \frac{i}{8\pi^2 m_h^2} \ln^2\left(i\sqrt{\tau}+\sqrt{1-\tau}\right) = \\
&= -\frac{i}{8\pi^2 m_h^2}\left(\frac{1}{i}\ln\left(i\sqrt{\tau}+\sqrt{1-\tau}\right)\right)^2 = -\frac{i}{8\pi^2 m_h^2}\arcsin^2\sqrt{\tau}
\end{aligned} \tag{E.9}
$$

whereas for $1 \leq \tau < \infty$, we get

$$
\begin{aligned}
B - \widetilde{B} &= \frac{i}{16\pi^2}\left(-i\sqrt{\frac{1}{\tau}-1}\ln\left(\frac{\sqrt{\frac{1}{\tau}-1}+i}{\sqrt{\frac{1}{\tau}-1}-i}\right)-2\right) = \\
&= \frac{i}{16\pi^2}\left(-i\sqrt{\frac{1}{\tau}-1-i\eta}\ln\left(\frac{\sqrt{\frac{1}{\tau}-1-i\eta}+i}{\sqrt{\frac{1}{\tau}-1-i\eta}-i}\right)-2\right) = \\
&= \frac{i}{16\pi^2}\left(-\sqrt{1-\frac{1}{\tau}}\ln\left(\frac{\sqrt{1-\frac{1}{\tau}}-1}{\sqrt{1-\frac{1}{\tau}}+1}+i\eta\right)-2\right) = \\
&= -\frac{i}{16\pi^2}\left(\sqrt{1-\frac{1}{\tau}}\left(\ln\left(\frac{1-\sqrt{1-\frac{1}{\tau}}}{1+\sqrt{1-\frac{1}{\tau}}}\right)+i\pi\right)+2\right)
\end{aligned} \tag{E.10}
$$

$$
\begin{aligned}
C &= \frac{i}{32\pi^2 m_h^2}\ln^2\left(\frac{1+\sqrt{1-\frac{1}{\tau}}}{1-\sqrt{1-\frac{1}{\tau}}}+2-4\tau\right) = \frac{i}{32\pi^2 m_h^2}\ln^2\left(-\frac{1-\sqrt{1-\frac{1}{\tau}}}{1+\sqrt{1-\frac{1}{\tau}}}\right) = \\
&= \frac{i}{32\pi^2 m_h^2}\ln^2\left(-\frac{1-\sqrt{1-\frac{1}{\tau}}}{1+\sqrt{1-\frac{1}{\tau}}}+i\eta\right) = \frac{i}{32\pi^2 m_h^2}\left(\ln\left(\frac{1-\sqrt{1-\frac{1}{\tau}}}{1+\sqrt{1-\frac{1}{\tau}}}\right)+i\pi\right)^2
\end{aligned} \tag{E.11}
$$

where we have employed the relations $\arcsin(x) = -i\ln\left(ix+\sqrt{1-x^2}\right)$ and $\arctan(x) = (-i/2)\ln\big((1+ix)/(1-ix)\big)$. The scalar integrals A, B, $\widetilde{B}$ and C are the building blocks for the more elaborate tensor integrals. Their reduction to scalar integrals neglecting terms of $\mathcal{O}(\epsilon)$ and higher is a straightforward computation that consists of expanding the tensor integral in terms of all allowed Lorentz structures with unknown coefficients and projecting out one coefficient at a time. This leads to a set of algebraic equations for the unknown coefficients in terms of tensor integrals of lower rank, which can be inverted by hand. The following list provides the final results.

$$
B^\mu(0,1) \equiv \mu^{2\epsilon}\int\frac{d^dk}{(2\pi)^d}\frac{k^\mu}{(k^2-m^2)\left((k+k_1)^2-m^2\right)} = -\frac{1}{2}k_1^\mu B \tag{E.12}
$$

$$B^{\mu}(0,2) \equiv \mu^{2\epsilon} \int \frac{d^dk}{(2\pi)^d} \frac{k^\mu}{(k^2-m^2)\Big((k-k_2)^2-m^2\Big)} = \frac{1}{2} k_2^\mu B \tag{E.13}$$

$$B^{\mu}(0,3) \equiv \mu^{2\epsilon} \int \frac{d^dk}{(2\pi)^d} \frac{k^\mu}{(k^2-m^2)\Big((k+q)^2-m^2\Big)} = -\frac{1}{2}\left(k_1^\mu + k_2^\mu\right) \widetilde{B} \tag{E.14}$$

$$B^{\mu}(1,2) \equiv \mu^{2\epsilon} \int \frac{d^dk}{(2\pi)^d} \frac{k^\mu}{\Big((k+k_1)^2-m^2\Big)\Big((k-k_2)^2-m^2\Big)} = -\frac{1}{2}\left(k_1^\mu - k_2^\mu\right) \widetilde{B} \tag{E.15}$$

$$\begin{aligned} B^{\mu\nu}(0,1) \equiv& \mu^{2\epsilon} \int \frac{d^dk}{(2\pi)^d} \frac{k^\mu k^\nu}{(k^2-m^2)\Big((k+k_1)^2-m^2\Big)} = \\ =& \frac{1}{d-1} g^{\mu\nu} \left(m^2 B + \frac{1}{2} A\right) + \frac{1}{3} k_1^\mu k_1^\nu B \end{aligned} \tag{E.16}$$

$$\begin{aligned} B^{\mu\nu}(0,2) \equiv& \mu^{2\epsilon} \int \frac{d^dk}{(2\pi)^d} \frac{k^\mu k^\nu}{(k^2-m^2)\Big((k-k_2)^2-m^2\Big)} = \\ =& \frac{1}{d-1} g^{\mu\nu} \left(m^2 B + \frac{1}{2} A\right) + \frac{1}{3} k_2^\mu k_2^\nu B \end{aligned} \tag{E.17}$$

$$\begin{aligned} B^{\mu\nu}(0,3) \equiv& \mu^{2\epsilon} \int \frac{d^dk}{(2\pi)^d} \frac{k^\mu k^\nu}{(k^2-m^2)\Big((k+q)^2-m^2\Big)} = \\ =& \frac{1}{4(d-1)(k_1\cdot k_2)} \Big(g^{\mu\nu}\big(2k_1\cdot k_2(2m^2 - k_1\cdot k_2)\widetilde{B} + 2k_1\cdot k_2 A\big) + \\ &+ \big(k_1^\mu k_1^\nu + k_1^\mu k_2^\nu + k_2^\mu k_1^\nu + k_2^\mu k_2^\nu\big)\big((-2m^2 + d k_1\cdot k_2)\widetilde{B} + (d-2)A\big)\Big) \end{aligned} \tag{E.18}$$

$$\begin{aligned} B^{\mu\nu}(1,2) \equiv& \mu^{2\epsilon} \int \frac{d^dk}{(2\pi)^d} \frac{k^\mu k^\nu}{\Big((k+k_1)^2-m^2\Big)\Big((k-k_2)^2-m^2\Big)} = \\ =& \frac{1}{4(d-1)(k_1\cdot k_2)} \Big(g^{\mu\nu}\big(2k_1\cdot k_2(2m^2 - k_1\cdot k_2)\widetilde{B} + 2k_1\cdot k_2 A\big) + \\ &+ \big(k_1^\mu k_1^\nu + k_2^\mu k_2^\nu\big)\big((-2m^2 + d k_1\cdot k_2)\widetilde{B} + (d-2)A\big) + \\ &+ \big(k_1^\mu k_2^\nu + k_2^\mu k_1^\nu\big)\big((-2m^2 - (d-2) k_1\cdot k_2)\widetilde{B} + (d-2)A\big)\Big) \end{aligned} \tag{E.19}$$

$$
\begin{aligned}
C^{\mu} \equiv& \mu^{2\epsilon} \int \frac{d^d k}{(2\pi)^d} \frac{k^{\mu}}{(k^2-m^2)\big((k+k_1)^2-m^2\big)\big((k-k_2)^2-m^2\big)} = \\
=& \frac{1}{2k_1\cdot k_2}\left(k_1^{\mu}-k_2^{\mu}\right)\left(\widetilde{B}-B\right)
\end{aligned}
\tag{E.20}
$$

$$
\begin{aligned}
C^{\mu\nu} \equiv& \mu^{2\epsilon} \int \frac{d^d k}{(2\pi)^d} \frac{k^{\mu}k^{\nu}}{(k^2-m^2)\big((k+k_1)^2-m^2\big)\big((k-k_2)^2-m^2\big)} = \\
=& \frac{1}{4k_1\cdot k_2}\left(k_1^{\mu}k_1^{\nu}+k_2^{\mu}k_2^{\nu}\right)\left(B-\widetilde{B}\right)+ \\
&+\frac{1}{k_1\cdot k_2}\left(k_1^{\mu}k_2^{\nu}+k_2^{\mu}k_1^{\nu}\right)\left(\frac{d-4}{4(d-2)}\widetilde{B}-\frac{m^2}{d-2}C\right)+ \\
&+\frac{1}{d-2}g^{\mu\nu}\left(\frac{1}{2}\widetilde{B}+m^2C\right)
\end{aligned}
\tag{E.21}
$$

$$
\begin{aligned}
C^{\mu\nu\lambda} \equiv& \mu^{2\epsilon} \int \frac{d^d k}{(2\pi)^d} \frac{k^{\mu}k^{\nu}k^{\lambda}}{(k^2-m^2)\big((k+k_1)^2-m^2\big)\big((k-k_2)^2-m^2\big)} = \\
=& \frac{1}{24(k_1\cdot k_2)^2}\Bigg(\left(k_1^{\mu}k_1^{\nu}k_1^{\lambda}-k_2^{\mu}k_2^{\nu}k_2^{\lambda}\right)\Big(-4k_1\cdot k_2B+ \\
&+\frac{3}{d-1}(dk_1\cdot k_2-2m^2)\widetilde{B}+\frac{3(d-2)}{d-1}A\Big)+ \\
&+\Big(k_1^{\mu}k_1^{\nu}k_2^{\lambda}+k_1^{\mu}k_2^{\nu}k_1^{\lambda}+k_2^{\mu}k_1^{\nu}k_1^{\lambda}-k_1^{\mu}k_2^{\nu}k_2^{\lambda}-k_2^{\mu}k_2^{\nu}k_1^{\lambda}-k_2^{\mu}k_1^{\nu}k_2^{\lambda}\Big)\Big(\frac{24m^2}{d-2}B+ \\
&-\frac{3}{d-1}(6m^2+(d-4)k_1\cdot k_2)\widetilde{B}-\frac{3(d+2)}{d-1}A\Big)+ \\
&+\Big(g^{\mu\nu}k_1^{\lambda}+g^{\lambda\nu}k_1^{\mu}+g^{\mu\lambda}k_1^{\nu}-g^{\mu\nu}k_2^{\lambda}-g^{\lambda\nu}k_2^{\mu}-g^{\mu\lambda}k_2^{\nu}\Big)\Big(-\frac{12m^2}{d-2}k_1\cdot k_2B+ \\
&+\frac{6}{d-1}(2m^2-k_1\cdot k_2)k_1\cdot k_2\widetilde{B}+\frac{6}{d-1}k_1\cdot k_2A\Big)\Bigg)
\end{aligned}
\tag{E.22}
$$

The last expression $C^{\mu\nu\lambda}$ differs from the actual result for *arbitrary* $d=4-2\epsilon$ by terms of $\mathcal{O}(\epsilon^2)$. All other formulas are exact.

F. Example calculation with γ_5 in $d \neq 4$ dimensions

In Section 4, we encounter left- and right-handed projectors inside divergent loop integrals. As the former feature the strictly four-dimensional object γ_5, we have to be careful when applying dimensional regularization. For such calculations, gauge invariance plays a crucial role for obtaining physically meaningful results. In this appendix, we show a sample calculation which demonstrates how imposing the Ward identity leads to unambiguous final results. For this, consider the integral

$$I \equiv I_1 + I_2 = \int \frac{d^4k}{(2\pi)^4} \frac{Tr\big((\not{k} + \not{k}_1 + m)\gamma^\mu(\not{k} + m)\gamma^\nu(\not{k} - \not{k}_2 + m)\gamma^\lambda\gamma^5\big)}{(k^2 - m^2)\big((k + k_1)^2 - m^2\big)\big((k - k_2)^2 - m^2\big)} + \\ + (\mu \leftrightarrow \nu, k_1 \leftrightarrow k_2) \tag{F.1}$$

where I_1 and I_2 refer to the two distinct loop momentum directions within a triangle diagram like in (E.1) involving two vector currents associated with the incoming momenta k_1 and k_2 and one axial-vector current associated with the outgoing momentum $q = k_1 + k_2$, respectively. The incoming external legs are considered as massless and transversal, so $k_1^2 = k_2^2 = 0$ and $q^2 = 2k_1 \cdot k_2$ and terms proportional to k_1^μ and k_2^ν are neglected. We also apply the formula $g^{\delta\lambda}\epsilon^{\mu\nu\alpha\sigma} = g^{\delta\mu}\epsilon^{\lambda\nu\alpha\sigma} - g^{\delta\nu}\epsilon^{\mu\lambda\alpha\sigma} + g^{\delta\alpha}\epsilon^{\lambda\mu\nu\sigma} - g^{\delta\sigma}\epsilon^{\lambda\mu\nu\alpha}$ to eliminate terms proportional to k_1^λ or k_2^λ during the calculation. Symmetry arguments reveal that $I_1 = I_2$. We now evaluate the diagram using two different methods, namely a direct computation using Feynman parameters, as well as employing tensor integral reduction methods.

Feynman parameters

Introducing Feynman parameters gives

$$I_1 = 2\int_0^1 dz \int_0^{1-z} dy \int \frac{d^4k}{(2\pi)^4} \frac{N}{(k^2 - m^2 + yzq^2)^3} \tag{F.2}$$

where the numerator is given by

$$\begin{aligned} N =& Tr\big((\not{k} + (1-y)\not{k}_1 + z\not{k}_2 + m)\gamma^\mu(\not{k} - y\not{k}_1 + z\not{k}_2 + m)\cdot \\ &\cdot \gamma^\nu(\not{k} - y\not{k}_1 - (1-z)\not{k}_2 + m)\gamma^\lambda\gamma^5\big) = \\ =& -4ik_\alpha k_\beta\Big(-2\epsilon^{\lambda\nu\alpha\sigma}k_{2\sigma}g^{\mu\beta} - 2\epsilon^{\lambda\mu\alpha\sigma}k_{1\sigma}g^{\nu\beta} + \\ &+ \epsilon^{\lambda\mu\nu\sigma}g^{\alpha\beta}\big((1-y)k_{1\sigma} - (1-z)k_{2\sigma}\big) + 2\epsilon^{\lambda\mu\nu\alpha}(zk_2^\beta - yk_1^\beta)\Big) + \\ &- 4i\Big(\epsilon^{\lambda\mu\nu\sigma}\big((y-1)k_{1\sigma} - (z-1)k_{2\sigma}\big)(m^2 + yzq^2) + 2yz(\epsilon^{\lambda\nu\sigma\delta}k_2^\mu - \epsilon^{\lambda\mu\sigma\delta}k_1^\nu)k_{1\sigma}k_{2\delta}\Big) \end{aligned} \tag{F.3}$$

where we dropped terms proportional to $\mathcal{O}(k^3)$ and $\mathcal{O}(k^1)$. We now continue to $d = 4-2\epsilon$ dimensions and use the formulas (D.19) and (D.20) with $\Delta = m^2 - yzq^2$. This gives

$$I_1 = \frac{1}{4\pi^2}\int_0^1 dz \int_0^{1-z} dy\ \epsilon^{\lambda\mu\nu\sigma}\Bigg((y-1)k_{1\sigma} - (z-1)k_{2\sigma} +$$

$$- \Big((1-3y)k_{1\sigma} - (1-3z)k_{2\sigma}\Big) \ln\left(1 - yz\frac{q^2}{m^2}\right)\Bigg) +$$
$$+ \frac{1}{4\pi^2}\int_0^1 dz \int_0^{1-z} dy\ \epsilon^{\lambda\mu\nu\sigma} \frac{yzq^2+m^2}{yzq^2-m^2}\big((y-1)k_{1\sigma} - (z-1)k_{2\sigma}\big) +$$
$$+ \frac{2yz}{m^2 - yzq^2}(\epsilon^{\lambda\mu\sigma\delta}k_1^\nu - \epsilon^{\lambda\nu\sigma\delta}k_2^\mu)k_{1\sigma}k_{2\delta} \tag{F.4}$$

where the first integral came from the $\mathcal{O}(k^2)$-term and the second one from the $\mathcal{O}(k^0)$-term. All but the last line are nothing else than the boundary terms of I_1 as can be seen by direct computation: We define

$$Tr\big((\not{k} + \not{k}_1 + m)\gamma^\mu(\not{k} + m)\gamma^\nu(\not{k} - \not{k}_2 + m)\gamma^\lambda\gamma^5\big)$$
$$\sim Tr\big(\not{k}\gamma^\mu\not{k}\gamma^\nu\not{k}\gamma^\lambda\gamma^5\big) = -4ig^{\alpha\beta}\epsilon^{\lambda\mu\nu\gamma}k_\alpha k_\beta k_\gamma \equiv f^{\mu\nu\lambda}(k) \tag{F.5}$$

where we have extracted the $\mathcal{O}(k^3)$-term. Shifting the loop momentum by a four-momentum a results in

$$\int \frac{d^4k}{(2\pi)^4} f^{\mu\nu\lambda}(k+a) = \int \frac{d^4k}{(2\pi)^4} f^{\mu\nu\lambda}(k) + a^\delta \int \frac{d^4k}{(2\pi)^4}\frac{\partial}{\partial k^\delta} f^{\mu\nu\lambda}(k) \tag{F.6}$$

where the boundary term is given by

$$a^\delta \int \frac{d^4k}{(2\pi)^4}\frac{\partial}{\partial k^\delta} f^{\mu\nu\lambda}(k) = ia^\delta \lim_{k_E\to\infty}\int \frac{k_E^2 k_{E\delta} d\Omega_4}{(2\pi)^4} f^{\mu\nu\lambda}(k_E) =$$
$$= a^\delta \lim_{k_E\to\infty}\int \frac{d\Omega_4}{(2\pi)^4}\frac{4g^{\alpha\beta}\epsilon^{\lambda\mu\nu\gamma}k_E^2 k_{E\delta}k_{E\alpha}k_{E\beta}k_{E\gamma}}{k_E^6} =$$
$$= \frac{\epsilon^{\lambda\mu\nu\sigma}a_\sigma}{8\pi^2} \tag{F.7}$$

The boundary term can be adjusted such that the final result obeys the Ward identity. Here, this is, however, not the case (see below). Numerically evaluating the parameter integrals of the boundary terms suggests that

$$\int_0^1 dz \int_0^{1-z} dy \left((y-1) - (1-3y)\ln\left(1 - yz\frac{q^2}{m^2}\right) + \frac{yzq^2+m^2}{yzq^2-m^2}(y-1)\right) =$$
$$= \int_0^1 dz \int_0^{1-z} dy \left((z-1) - (1-3z)\ln\left(1 - yz\frac{q^2}{m^2}\right) + \frac{yzq^2+m^2}{yzq^2-m^2}(z-1)\right) =$$
$$= \int_0^1 dz \int_0^{1-z} dy \frac{yzq^2}{m^2 - yzq^2} \tag{F.8}$$

Finally, we arrive at

$$I = 2I_1 = \frac{1}{2\pi^2}\Big(q^2\epsilon^{\lambda\mu\nu\sigma}(k_{1\sigma} - k_{2\sigma}) + 2(\epsilon^{\lambda\mu\sigma\delta}k_1^\nu - \epsilon^{\lambda\nu\sigma\delta}k_2^\mu)k_{1\sigma}k_{2\delta}\Big)\int_0^1 dz \int_0^{1-z} dy \frac{yz}{m^2 - yzq^2} \tag{F.9}$$

Multiplying with $k_{1\mu}$ or $k_{2\nu}$ yields 0 as it should, i.e. no boundary-term adjustment is in fact needed. The Ward identity is thus fulfilled.
Let us now examine the anomaly. For $m^2 = 0$, contracting (F.9) with q_λ, we obtain

$$\frac{1}{2\pi^2}\epsilon^{\lambda\sigma\mu\nu}k_{1\lambda}k_{2\sigma} \tag{F.10}$$

hinting towards the non-conservation of the axial current as expected.

Integral reduction
We write the integral as

$$I_1 = \mu^{2\epsilon}\int\frac{d^dk}{(2\pi)^d}\frac{\tilde{N}}{(k^2-m^2)\big((k+k_1)^2-m^2\big)\big((k-k_2)^2-m^2\big)} \tag{F.11}$$

where

$$\begin{aligned}\tilde{N} =& Tr\big((\not{k}+\not{k}_1+m)\gamma^\mu(\not{k}+m)\gamma^\nu(\not{k}-\not{k}_2+m)\gamma^\lambda\gamma^5\big) = \\ =& -4ig^{\alpha\beta}\epsilon^{\lambda\mu\nu\gamma}k_\alpha k_\beta k_\gamma + 4i\big(2g^{\nu\beta}\epsilon^{\lambda\mu\alpha\sigma}k_{1\sigma} + 2g^{\mu\beta}\epsilon^{\lambda\nu\alpha\sigma}k_{2\sigma} - g^{\alpha\beta}\epsilon^{\lambda\mu\nu\sigma}(k_{1\sigma}-k_{2\sigma})\big)k_\alpha k_\beta + \\ &+ 4i\big(g^{\lambda\nu}\epsilon^{\mu\alpha\sigma\delta}k_{1\delta}k_{2\sigma} - g^{\lambda\mu}\epsilon^{\nu\alpha\sigma\delta}k_{1\sigma}k_{2\delta} + g^{\mu\nu}\epsilon^{\lambda\alpha\delta\sigma}k_{1\delta}k_{2\sigma} - k_1^\nu\epsilon^{\lambda\mu\alpha\sigma}k_{2\sigma} + \\ &+ k_1^\alpha\epsilon^{\lambda\mu\nu\sigma}k_{2\sigma} + k_2^\alpha\epsilon^{\lambda\mu\nu\sigma}k_{1\sigma} + (m^2 - k_1\cdot k_2)\epsilon^{\lambda\mu\nu\alpha}\big)k_\alpha + 4im^2\epsilon^{\lambda\mu\nu\sigma}(k_{1\sigma}-k_{2\sigma})\end{aligned} \tag{F.12}$$

Applying the d-dimensional reduction formulas from Appendix E yields

$$\begin{aligned}I_1 =& -\frac{4i}{q^2}\epsilon^{\lambda\mu\nu\gamma}(k_{1\gamma}-k_{2\gamma})\left(m^2(\widetilde{B}-B) - \frac{q^2}{2}\widetilde{B}\right) + \\ &- 4i\epsilon^{\lambda\mu\nu\sigma}(k_{1\sigma}-k_{2\sigma})\left(\frac{d-3}{d-2}\widetilde{B} + \frac{d-4}{d-2}m^2C\right) + \\ &+ \frac{4i}{q^2}(\epsilon^{\lambda\mu\alpha\sigma}k_1^\nu - \epsilon^{\lambda\nu\alpha\sigma}k_2^\mu)k_{1\sigma}k_{2\alpha}\left(\frac{d-4}{d-2}\widetilde{B} - \frac{4}{d-2}m^2C\right) + \\ &+ 4i\frac{m^2}{q^2}\epsilon^{\lambda\mu\nu\alpha}(k_{1\alpha}-k_{2\alpha})(\widetilde{B}-B) + \\ &+ 4im^2\epsilon^{\lambda\mu\nu\sigma}(k_{1\sigma}-k_{2\sigma})C\end{aligned} \tag{F.13}$$

where the first line comes from the $\mathcal{O}(k^3)$-term, the second and third line from the $\mathcal{O}(k^2)$-term, the fourth line from the $\mathcal{O}(k^1)$-term and the last line to from $\mathcal{O}(k^0)$-term. When the dust settles, we arrive at

$$I_1 = \left(2i\epsilon^{\lambda\mu\nu\sigma}(k_{1\sigma}-k_{2\sigma}) - \frac{4i}{q^2}(\epsilon^{\lambda\mu\alpha\sigma}k_1^\nu - \epsilon^{\lambda\nu\alpha\sigma}k_2^\mu)k_{1\sigma}k_{2\alpha}\right)\left(\frac{4}{d-2}m^2C - \frac{d-4}{d-2}\widetilde{B}\right) \tag{F.14}$$

Note that

$$\frac{4}{d-2}m^2C - \frac{d-4}{d-2}\widetilde{B} = -\frac{i}{8\pi^2}\int_0^1 dz \int_0^{1-z} dy \frac{yzq^2}{m^2 - yzq^2} \tag{F.15}$$

This is the same result we obtained before, i.e. (F.9), hinting towards the consistency of our approach.
We remark that it is also possible to not touch the divergent structure of the loop integral - and hence the subtile part - at all [6]. For instance, one can expand I in terms of unknown structure functions using Lorentz invariance and identify the superficially divergent ones (the first terms in (F.9)) by counting the power of external contracted momenta. Their explicit form is then unambiguously dictated by the convergent structure functions (the second terms in (F.9)) upon imposing the Ward identity and Bose statistics. This approach is, of course, related to a manual adjustment of the boundary term $\sim \epsilon^{\lambda\mu\nu\sigma}a_\sigma$ by enforcing the Ward identity by hand. Strictly speaking, this is the procedure of choice. In fact, all but the last line in (F.4) is initially - at best - questionable and should hence be left open until the Ward identity fixes the final values. Here, however, it turns out that these suspicious terms are already the correct ones.

G. "Real-world" example: 2HDM and SMEFT

The QED toy model highlighted in Section 3.1 can easily be generalized to a more "realistic" situation in the context of the full SM. To be more specific, in this appendix, we consider the 2HDM in the decoupling limit and integrate out all non-SM fields for the process $u\bar{u} \to t\bar{t}$.
From the SM, the 2HDM differs by an extra $SU(2)$ doublet adding four degrees of freedom to the SM Higgs particle sector. However, it is advantageous to first consider two independent doublets ϕ_1 and ϕ_2 and identify the SM doublet on the go. Allowing both doublets to develop a vacuum expectation value, we can write them as

$$\phi_a = \begin{pmatrix} \varphi_a^+ \\ \frac{1}{\sqrt{2}}(v_a + \rho_a + i\eta_a) \end{pmatrix}, \text{where } a = 1, 2 \tag{G.1}$$

and define the vacuum expectation value as

$$\langle \phi_a \rangle \equiv \begin{pmatrix} 0 \\ \frac{v_a}{\sqrt{2}} \end{pmatrix} \tag{G.2}$$

A Lagrangian for the two doublets is then given by [239–243]

$$\mathcal{L}_{2HDM} = \mathcal{L}_{SM,\bar{H}\bar{Y}} + (D_\mu \phi_a)^\dagger D^\mu \phi_a - V(\phi_1, \phi_2) + \mathcal{L}_Y \tag{G.3}$$

where $\mathcal{L}_{SM,\bar{H}\bar{Y}}$ is the SM Lagrangian (2.11) without the Higgs and Yukawa sectors. We will deal with the latter - denoted by $\mathcal{L}_Y$ - below and focus on the Higgs sector first. The potential reads

$$\begin{aligned} V(\phi_1, \phi_2) = &- \mu_1^2 \phi_1^\dagger \phi_1 - \mu_2^2 \phi_2^\dagger \phi_2 - m^2(\phi_1^\dagger \phi_2 + \phi_2^\dagger \phi_1) + \lambda_1 (\phi_1^\dagger \phi_1)^2 + \lambda_2 (\phi_2^\dagger \phi_2)^2 + \\ &- \lambda_3 (\phi_1^\dagger \phi_1)(\phi_2^\dagger \phi_2) - \lambda_4 (\phi_1^\dagger \phi_2)(\phi_2^\dagger \phi_1) - \lambda_5 \big((\phi_1^\dagger \phi_2)^2 + (\phi_2^\dagger \phi_1)^2\big) \end{aligned} \tag{G.4}$$

where we have imposed CP-invariance and dropped uneven terms like $\phi_1^\dagger \phi_1 \phi_1^\dagger \phi_2$, etc. for simplicity. The covariant derivative reads

$$D_\mu \phi_a = \left(\partial_\mu + igW_\mu^\alpha \tau^\alpha + \frac{i}{2} g' B_\mu \right) \phi_a \tag{G.5}$$

The electroweak symmetry-breaking sector works as in the SM. Indeed, from the kinetic terms of the Higgs doublets, we find

$$(D_\mu \langle \phi_a \rangle)^\dagger D^\mu \langle \phi_a \rangle = \frac{1}{2} \begin{pmatrix} 0 & v_a \end{pmatrix} \left(gW_\mu^\alpha \tau^\alpha + \frac{1}{2} g' B_\mu \right) (gW^{\mu J} \tau^J + \frac{1}{2} g' B^\mu) \begin{pmatrix} 0 \\ v_a \end{pmatrix} =$$

$$=\frac{1}{2}\frac{v_a v_a}{4}\left(g^2(W_\mu^1)^2+g^2(W_\mu^2)^2+(g'B_\mu-gW_\mu^3)^2\right)=$$
$$=\frac{1}{2}\frac{v_a v_a}{4}\left(2g^2W_\mu^+W^{\mu-}+(g^2+g'^2)Z_\mu Z^\mu\right) \tag{G.6}$$

with $W_\mu^\pm=(W_\mu^1\mp iW_\mu^2)/\sqrt{2}$ and $Z_\mu=(gW_\mu^3-g'B_\mu)/\sqrt{g^2+g'^2}$. The gauge boson masses are therefore given by $m_W=gv_av_a/2$ and $m_Z=\sqrt{g^2+g'^2}v_av_a/2$. They are thus generated by an interplay between the vacuum expectation values of both doublets making it impossible to identify one of them with the SM Higgs doublet. Instead, we have to identify the propagating degrees of freedom first.

The vacuum expectation values v_1 and v_2 are, of course, linked to the Lagrangian parameters. The explicit relation is given by

$$\mu_1^2=v_1^2\lambda_1-\frac{1}{2}v_2^2\lambda_3-\frac{1}{2}v_2^2\lambda_4-v_2^2\lambda_5-\frac{v_2}{v_1}m^2 \tag{G.7}$$
$$\mu_2^2=v_2^2\lambda_2-\frac{1}{2}v_1^2\lambda_3-\frac{1}{2}v_1^2\lambda_4-v_1^2\lambda_5-\frac{v_1}{v_2}m^2 \tag{G.8}$$

and can be found by setting the linear terms in ρ_1 and ρ_2 to zero in the vicinity of the minimum of the potential[67]. The mass terms are obtained by keeping only the quadratic terms. We find

$$\mathcal{L}_{mass}=-\begin{pmatrix}\varphi_1^- & \varphi_2^-\end{pmatrix}M_1\begin{pmatrix}\varphi_1^+\\ \varphi_2^+\end{pmatrix}-\frac{1}{2}\begin{pmatrix}\rho_1 & \rho_2\end{pmatrix}M_2\begin{pmatrix}\rho_1\\ \rho_2\end{pmatrix}-\frac{1}{2}\begin{pmatrix}\eta_1 & \eta_2\end{pmatrix}M_3\begin{pmatrix}\eta_1\\ \eta_2\end{pmatrix}$$

where

$$M_1=\begin{pmatrix}v_1^2\lambda_1-\frac{1}{2}v_2^2\lambda_3-\mu_1^2 & -\left(m^2+\frac{1}{2}v_1v_2\lambda_4+v_1v_2\lambda_5\right)\\ -\left(m^2+\frac{1}{2}v_1v_2\lambda_4+v_1v_2\lambda_5\right) & v_2^2\lambda_2-\frac{1}{2}v_1^2\lambda_3-\mu_2^2\end{pmatrix}$$

$$M_2=\begin{pmatrix}3v_1^2\lambda_1-\frac{1}{2}v_2^2\lambda_3-\frac{1}{2}v_2^2\lambda_4-v_2^2\lambda_5-\mu_1^2 & -\left(m^2+v_1v_2\lambda_3+v_1v_2\lambda_4+2v_1v_2\lambda_5\right)\\ -\left(m^2+v_1v_2\lambda_3+v_1v_2\lambda_4+2v_1v_2\lambda_5\right) & 3v_2^2\lambda_2-\frac{1}{2}v_1^2\lambda_3-\frac{1}{2}v_1^2\lambda_4-v_1^2\lambda_5-\mu_2^2\end{pmatrix}$$

[67]The linear terms are given by

$$\phi_1^\dagger\phi_1\supset v_1\rho_1,\quad \phi_2^\dagger\phi_2\supset v_2\rho_2,\quad \phi_1^\dagger\phi_2+\phi_2^\dagger\phi_1\supset v_1\rho_2+v_2\rho_1,\quad (\phi_1^\dagger\phi_1)^2\supset v_1^3\rho_1,$$
$$(\phi_2^\dagger\phi_2)^2\supset v_2^3\rho_2,\quad (\phi_1^\dagger\phi_1)(\phi_2^\dagger\phi_2)\supset \frac{1}{2}v_1v_2^2\rho_1+\frac{1}{2}v_1^2v_2\rho_2,$$
$$(\phi_1^\dagger\phi_2)(\phi_2^\dagger\phi_1)\supset\frac{1}{2}v_1v_2^2\rho_1+\frac{1}{2}v_1^2v_2\rho_2,\quad (\phi_1^\dagger\phi_2)^2+(\phi_2^\dagger\phi_1)^2\supset v_1v_2^2\rho_1+v_1^2v_2\rho_2 \tag{G.9}$$

$$M_3 = \begin{pmatrix} v_1^2\lambda_1 - \frac{1}{2}v_2^2\lambda_3 - \frac{1}{2}v_2^2\lambda_4 + v_2^2\lambda_5 - \mu_1^2 & -\left(m^2 + 2v_1v_2\lambda_5\right) \\ -\left(m^2 + 2v_1v_2\lambda_5\right) & v_2^2\lambda_2 - \frac{1}{2}v_1^2\lambda_3 - \frac{1}{2}v_1^2\lambda_4 + v_1^2\lambda_5 - \mu_2^2 \end{pmatrix} \tag{G.10}$$

Eliminating μ_1 and μ_2 with (G.7) and (G.8), these matrices can be cast in the form

$$M_1 = \left(m^2 + \frac{1}{2}v_1v_2\lambda_4 + v_1v_2\lambda_5\right)\begin{pmatrix} \frac{v_2}{v_1} & -1 \\ -1 & \frac{v_1}{v_2} \end{pmatrix}$$

$$M_2 = v_1v_2\begin{pmatrix} 2\frac{v_1}{v_2}\lambda_1 + \frac{m^2}{v_1^2} & -\left(\frac{m^2}{v_1v_2} + \lambda_3 + \lambda_4 + 2\lambda_5\right) \\ -\left(\frac{m^2}{v_1v_2} + \lambda_3 + \lambda_4 + 2\lambda_5\right) & 2\frac{v_2}{v_1}\lambda_2 + \frac{m^2}{v_2^2} \end{pmatrix}$$

$$M_3 = (m^2 + 2v_1v_2\lambda_5)\begin{pmatrix} \frac{v_2}{v_1} & -1 \\ -1 & \frac{v_1}{v_2} \end{pmatrix} \tag{G.11}$$

Upon defining $v^2 \equiv v_1^2 + v_2^2$ and $\lambda \equiv \lambda_3 + \lambda_4 + 2\lambda_5$, we can find compact expressions for the rotated fields and their corresponding masses. The results are then given by

$$\mathcal{L}_{mass} = -\begin{pmatrix} \tilde{\varphi}_1^- & \tilde{\varphi}_2^- \end{pmatrix}\begin{pmatrix} M_{\pm 1}^2 & 0 \\ 0 & M_{\pm 2}^2 \end{pmatrix}\begin{pmatrix} \tilde{\varphi}_1^+ \\ \tilde{\varphi}_2^+ \end{pmatrix} - \frac{1}{2}\begin{pmatrix} \tilde{\rho}_1 & \tilde{\rho}_2 \end{pmatrix}\begin{pmatrix} M_{\rho 1}^2 & 0 \\ 0 & M_{\rho 2}^2 \end{pmatrix}\begin{pmatrix} \tilde{\rho}_1 \\ \tilde{\rho}_2 \end{pmatrix} + \\ -\frac{1}{2}\begin{pmatrix} \tilde{\eta}_1 & \tilde{\eta}_2 \end{pmatrix}\begin{pmatrix} M_{\eta 1}^2 & 0 \\ 0 & M_{\eta 2}^2 \end{pmatrix}\begin{pmatrix} \tilde{\eta}_1 \\ \tilde{\eta}_2 \end{pmatrix} \tag{G.12}$$

where

$$\begin{pmatrix} \tilde{\varphi}_1^+ \\ \tilde{\varphi}_2^+ \end{pmatrix} = \begin{pmatrix} \cos\beta & \sin\beta \\ -\sin\beta & \cos\beta \end{pmatrix}\begin{pmatrix} \varphi_1^+ \\ \varphi_2^+ \end{pmatrix}$$

$$\begin{pmatrix} \tilde{\rho}_1 \\ \tilde{\rho}_2 \end{pmatrix} = \begin{pmatrix} \cos\alpha & \sin\alpha \\ -\sin\alpha & \cos\alpha \end{pmatrix}\begin{pmatrix} \rho_1 \\ \rho_2 \end{pmatrix}$$

$$\begin{pmatrix} \tilde{\eta}_1 \\ \tilde{\eta}_2 \end{pmatrix} = \begin{pmatrix} \cos\beta & \sin\beta \\ -\sin\beta & \cos\beta \end{pmatrix} \begin{pmatrix} \eta_1 \\ \eta_2 \end{pmatrix}$$

with

$$\begin{aligned}
\sin^2\beta &= \frac{v_2^2}{v^2} \\
\cos^2\beta &= \frac{v_1^2}{v^2} \\
\sin^2\alpha &= \frac{m^2 M_{\rho 2}^2 v_2^2 - m^2 M_{\rho 1}^2 v_1^2 + 2\lambda_1 M_{\rho 2}^2 v_1^3 v_2 - 2\lambda_2 M_{\rho 1}^2 v_1 v_2^3}{v_1 v_2 (M_{\rho 2}^4 - M_{\rho 1}^4)} \\
\cos^2\alpha &= \frac{m^2 M_{\rho 2}^2 v_1^2 - m^2 M_{\rho 1}^2 v_2^2 + 2\lambda_2 M_{\rho 2}^2 v_1 v_2^3 - 2\lambda_1 M_{\rho 1}^2 v_1^3 v_2}{v_1 v_2 (M_{\rho 2}^4 - M_{\rho 1}^4)}
\end{aligned} \tag{G.13}$$

The masses are given by[68]

$$\begin{aligned}
&M_{\pm 1}^2 = 0,\ M_{\pm 2}^2 = \frac{v^2}{v_1 v_2}(m^2 + \frac{1}{2} v_1 v_2 \lambda_4 + v_1 v_2 \lambda_5) = M_{\eta 2}^2 + \frac{v^2}{2}(\lambda_4 - 2\lambda_5) \\
&M_{\eta 1}^2 = 0,\ M_{\eta 2}^2 = \frac{v^2}{v_1 v_2}(m^2 + 2 v_1 v_2 \lambda_5) \\
&M_{\rho 1,2}^2 = \frac{m^2 v_1^2}{2 v_1 v_2} + \frac{m^2 v_2 + 2\lambda_1 v_1^3 + 2\lambda_2 v_1 v_2^2}{2 v_1} + \\
&\pm \frac{\sqrt{\left(m^2(v_1^2 + v_2^2) + 2 v_1 v_2 (\lambda_1 v_1^2 + \lambda_2 v_2^2)\right)^2 - 8 m^2 \left(\lambda_1 v_1^5 v_2 - \lambda v_1^3 v_2^3 + \lambda_2 v_1 v_2^5\right) + \iota}}{2 v_1 v_2}
\end{aligned} \tag{G.15}$$

where $\iota \equiv 4 v_1^4 v_2^4 \left(\lambda^2 - 4\lambda_1\lambda_2\right)$. The link to the SM Higgs doublet can be established by rotating

$$\begin{pmatrix} H_1 \\ H_2 \end{pmatrix} = \begin{pmatrix} \cos\beta & \sin\beta \\ -\sin\beta & \cos\beta \end{pmatrix} \begin{pmatrix} \phi_1 \\ \phi_2 \end{pmatrix} \tag{G.16}$$

[68] For $m^2 = 0$, these formulas reduce to the particularly simple form

$$\begin{aligned}
&M_{\pm 1}^2 = 0,\ M_{\pm 2}^2 = \frac{1}{2} v^2 (\lambda_4 + 2\lambda_5), \\
&M_{\eta 1}^2 = 0,\ M_{\eta 2}^2 = 2 v^2 \lambda_5, \\
&M_{\rho 1,2}^2 = v_1^2 \lambda_1 + v_2^2 \lambda_2 \pm \sqrt{(v_1^2 \lambda_1 - v_2^2 \lambda_2)^2 + v_1^2 v_2^2 \lambda^2}
\end{aligned} \tag{G.14}$$

Note that this will change the potential in a non-trivial way. The new doublets are given by

$$H_a = \begin{pmatrix} \tilde{\varphi}_a^+ \\ \frac{1}{\sqrt{2}}(V_a + h_a^\rho + i\tilde{\eta}_a) \end{pmatrix} \tag{G.17}$$

with

$$\begin{pmatrix} h_1^\rho \\ h_2^\rho \end{pmatrix} = \begin{pmatrix} \cos\beta & \sin\beta \\ -\sin\beta & \cos\beta \end{pmatrix} \begin{pmatrix} \rho_1 \\ \rho_2 \end{pmatrix} = \begin{pmatrix} \cos(\alpha-\beta) & -\sin(\alpha-\beta) \\ \sin(\alpha-\beta) & \cos(\alpha-\beta) \end{pmatrix} \begin{pmatrix} \tilde{\rho}_1 \\ \tilde{\rho}_2 \end{pmatrix} \tag{G.18}$$

and $V_1 = v$ and $V_2 = 0$. All effects related to electroweak symmetry breaking are therefore incorporated in H_1. We can go to unitary gauge by imposing

$$H_1 = \begin{pmatrix} 0 \\ \frac{1}{\sqrt{2}}(V_1 + h_1^\rho) \end{pmatrix}, \qquad H_2 = \begin{pmatrix} \tilde{\varphi}_2^+ \\ \frac{1}{\sqrt{2}}(h_2^\rho + i\tilde{\eta}_2) \end{pmatrix} \tag{G.19}$$

It is now possible to interpret H_1 as the SM Higgs doublet, which is, inconveniently, not a physical object (h_1^ρ is not a propagating degree of freedom). In the limit $\sin(\alpha-\beta) \to -1$ and $\cos(\alpha-\beta) \to 0$, however, this situation changes as $h_1^\rho \to \tilde{\rho}_2$ and $h_2^\rho \to \tilde{\rho}_1$. The heavier scalar ρ_1 then decouples from the electroweak gauge bosons and we expect the possibility of choosing the Lagrangian parameters such that

$$m_h^2 \equiv M_{\rho 2}^2 \ll M_{\pm 2}^2, M_{\rho 1}^2, M_{\eta 2}^2 \equiv m_s^2 \tag{G.20}$$

where we assumed no hierarchy pattern between the heavy states by formally introducing the mass scale m_s.
Before integrating out the heavy states, we have to specify the Yukawa couplings. Assuming only the top-quark to be massive, out of many possibilities to combine the quarks and the doublets, let us choose

$$\mathcal{L}_Y = -Y_t' \bar{q}_L \tilde{\phi}_2 t_R + h.c. \tag{G.21}$$

for our analysis (q_L and t_R are the third generation left-handed quark doublet and right-handed top-quark, respectively). The SM Yukawa coupling $y_t = \sqrt{2} m_t / v$ is related to Y_t' via $y_t = Y_t' \cos\beta$, since $\phi_2 = H_1 \cos\beta + ...$. As usual, we have employed the notation $\tilde{\phi}_2 = i\sigma_2 \phi_2^*$ to project out the top-quark component of $\bar{q}_L$ in a symmetry-preserving way. Collecting all non-Yukawa scalar interactions in an object $\mathcal{L}_{H,int}$, the full Lagrangian is then given by

$$\mathcal{L}_{2HDM} = \mathcal{L}_{SM} + \mathcal{L}_{H,int} - H_2^\dagger \Box H_2 - m_s^2 H_2^\dagger H_2 - y_t \cot\beta \bar{q}_L \tilde{H}_2 t_R + h.c. \tag{G.22}$$

Let us first integrate out the heavy fields at tree level. The equations of motion are given by

$$(\Box + m_s^2) H_2^j = -y_t \cot\beta \bar{q}_L^i \epsilon^{ij} t_R \tag{G.23}$$

$$(\Box + m_s^2) H_2^{\dagger j} = y_t \cot\beta \bar{t}_R \epsilon^{ji} q_L^i \tag{G.24}$$

Reinserting these expressions into the Lagrangian and using $\epsilon^{ij}\epsilon^{jk} = -\delta^{ik}$, we arrive at the effective Lagrangian

$$\mathcal{L}_{eff,tree} = \frac{y_t^2 \cot^2\beta}{m_s^2} \bar{t}_R q_L^i \bar{q}_L^i t_R = \frac{m_t^2 \cot^2\beta}{v^2 m_s^2} \left(\frac{1}{2}\bar{t}t\bar{t}t + \frac{1}{2}\bar{t}i\gamma_5 t\bar{t}i\gamma_5 t + 2\bar{t}P_L b\bar{b}P_R t \right) \tag{G.25}$$

where the $SU(2)$ indices have been made explicit in the first step. Tree-level matching thus generates four-fermion operators only.
Our next task is the full one-loop computation for $u\bar{u} \to t\bar{t}$. We first massage the Lagrangian in a suitable form. Writing out all relevant kinetic and interaction terms, we find

$$\mathcal{L}_{rel} = \frac{1}{2}\partial_\mu\tilde{\rho}_1\partial^\mu\tilde{\rho}_1 - \frac{1}{2}m_s^2\tilde{\rho}_1^2 + \frac{1}{2}\partial_\mu\tilde{\eta}_2\partial^\mu\tilde{\eta}_2 - \frac{1}{2}m_s^2\tilde{\eta}_2^2 + \partial_\mu\tilde{\varphi}_2^+\partial^\mu\tilde{\varphi}_2^- - m_s^2\tilde{\varphi}_2^+\tilde{\varphi}_2^- + \tag{G.26}$$

$$-\frac{m_t}{v}\cot\beta\bar{t}t\tilde{\rho}_1 + \frac{m_t}{v}\cot\beta\bar{t}i\gamma_5 t\tilde{\eta}_2 + \frac{\sqrt{2}}{v}m_t\cot\beta\bar{t}P_L b\tilde{\varphi}_2^+ + \frac{\sqrt{2}}{v}m_t\cot\beta\bar{b}P_R t\tilde{\varphi}_2^- \tag{G.27}$$

The computation of the vertex correction is lengthy but in principle only marginally different from the one highlighted in the appendix to Section 3. To $\mathcal{O}(1/m_s^2)$, employing the usual notation, it is given by[69]

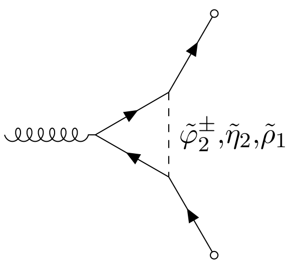

$$\equiv -ig_s T^A \delta\Gamma^\mu = -ig_s T^A \frac{m_t^2\cot^2\beta}{16\pi^2 v^2 m_s^2}\Bigg(m_t i\sigma^{\mu\nu}q_\nu +$$

$$+\frac{2}{3}\left(\frac{1}{3} - \ln\frac{q^2}{m_s^2} + i\pi\right)\left(q^2\gamma^\mu P_R - m_t q^\mu\gamma_5\right) - 2\left(\frac{1}{3}\ln\frac{m_t^2}{m_s^2} + \frac{4}{9} + h_1(z)\right)q^2\gamma^\mu\Bigg) \tag{G.28}$$

where $h_1(z)$ was defined in (3.10) with $z = q^2/m_t^2$ and the imaginary part arises due to the vanishing bottom mass. Being a gauge relict, the term $\sim q^\mu$ may be dropped, as it is annihilated when contracted with the up-quark current on the left (not displayed). The corresponding loop-level Lagrangian reads

$$\mathcal{L}_{eff,loop} = -\frac{g_s m_t^2\cot^2\beta}{16\pi^2 v^2 m_s^2}\frac{2}{3}\left(\ln\frac{\mu^2}{m_s^2} + \frac{4}{3}\right)\left(D^\mu G_{\mu\nu}^A \bar{t}_R T^A\gamma^\nu t_R + D^\mu G_{\mu\nu}^A \bar{t}T^A\gamma^\nu t\right) +$$

[69]We have evaluated this diagram both by direct computation and by applying the strategy of regions.

$$-\frac{g_s m_t^2 \cot^2\beta}{16\pi^2 v^2 m_s^2}\frac{1}{2} m_t G^A_{\mu\nu}\bar{t}T^A\sigma^{\mu\nu}t \tag{G.29}$$

Using (G.25) and (G.29) for loop- and tree-topology-diagrams, respectively, yields

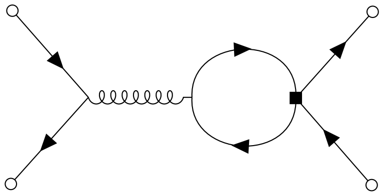

$$= i\frac{g_s^2}{q^2}\bar{v}(k_2)T^A\gamma_\mu u(k_1)\cdot$$

$$\cdot\,\bar{u}(p_1)T^A\frac{m_t^2\cot^2\beta}{16\pi^2 v^2 m_s^2}\left(\frac{2}{3}\left(\frac{5}{3}-\ln\frac{q^2}{\mu^2}+i\pi\right)q^2\gamma^\mu P_R-\frac{2}{3}\left(\ln\frac{m_t^2}{\mu^2}+3h_1(z)\right)q^2\gamma^\mu\right)v(p_2) \tag{G.30}$$

and

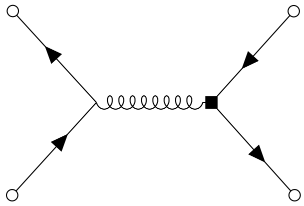

$$= i\frac{g_s}{q^2}\bar{v}(k_2)T^A\gamma_\mu u(k_1)\cdot$$

$$\cdot\,\bar{u}(p_1)T^A\frac{g_s m_t^2\cot^2\beta}{16\pi^2 v^2 m_s^2}\left(-\frac{2}{3}\left(\ln\frac{\mu^2}{m_s^2}+\frac{4}{3}\right)\left(q^2\gamma^\mu P_R+q^2\gamma^\mu\right)+m_t i\sigma^{\mu\nu}q_\nu\right)v(p_2) \tag{G.31}$$

Combining (G.31) and (G.30) restores the full result (G.28). When comparing to the Warsaw basis, as we will do next, we have to reinterpret terms $\sim q^2\gamma^\mu$ in favor of four-fermion operators. Instead of (G.31), we should therefore use

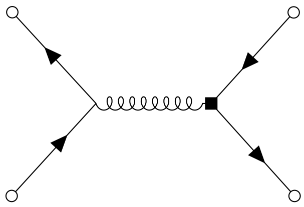

$$= i\frac{g_s}{q^2}\bar{v}(k_2)T^A\gamma_\mu u(k_1)\bar{u}(p_1)T^A\frac{g_s m_t^2\cot^2\beta}{16\pi^2 v^2 m_s^2}m_t i\sigma^{\mu\nu}q_\nu v(p_2) \tag{G.32}$$

and

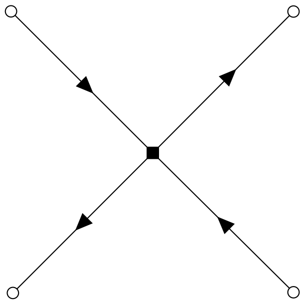

$$= -i\bar{v}(k_2)T^A\gamma_\mu u(k_1)\bar{u}(p_1)T^A \frac{g_s^2 m_t^2 \cot^2\beta}{16\pi^2 v^2 m_s^2}\cdot$$

$$\cdot \frac{2}{3}\left(\ln\frac{\mu^2}{m_s^2}+\frac{4}{3}\right)\left(\gamma^\mu P_R+\gamma^\mu\right)v(p_2) \qquad \text{(G.33)}$$

This can be justified by converting the corresponding field strength operators into four-fermion ones via the equation of motion for the gluon field

$$\begin{aligned} D^\nu G^A_{\nu\mu} = g_s(&\bar{q}_{L,1}\gamma_\mu T^A q_{L,1} + \bar{q}_{L,3}\gamma_\mu T^A q_{L,3} + \bar{u}_R\gamma_\mu T^A u_R + \\ &+ \bar{t}_R\gamma_\mu T^A t_R + \bar{d}_R\gamma_\mu T^A d_R + \bar{b}_R\gamma_\mu T^A b_R) \end{aligned} \qquad \text{(G.34)}$$

where we have introduced generation indices on the left-handed quark fields (we neglect the second particle generation here); the rest of the notation should be self-explaining. In addition, one can use Fierz identities[70] and related tricks to match the operator structure we found to the Warsaw basis. Without showing the calculational details, we arrive at

$$\bar{t}_R q_L^i \bar{q}_L^i t_R = -\left(Q_{qu}^{(8)3333}+\frac{1}{6}Q_{qu}^{(1)3333}\right) \qquad \text{(G.36)}$$

$$D^\mu G^A_{\mu\nu}\bar{t}_R T^A\gamma^\nu t_R = g_s\left(Q_{qu}^{(8)1133}+\frac{1}{4}Q_{uu}^{1331}+\frac{1}{4}Q_{uu}^{3113}-\frac{1}{12}Q_{uu}^{1133}-\frac{1}{12}Q_{uu}^{3311}\right) \qquad \text{(G.37)}$$

$$\begin{aligned} D^\mu G^A_{\mu\nu}\bar{t}T^A\gamma^\nu t = g_s\Big(&Q_{qu}^{(8)3311}+Q_{qu}^{(8)1133}+\frac{1}{4}Q_{uu}^{1331}+\frac{1}{4}Q_{uu}^{3113}-\frac{1}{12}Q_{uu}^{1133}-\frac{1}{12}Q_{uu}^{3311}+ \\ &+\frac{1}{8}Q_{qq}^{(1)1331}+\frac{1}{8}Q_{qq}^{(1)3113}+\frac{1}{8}Q_{qq}^{(3)1331}+\frac{1}{8}Q_{qq}^{(3)3113}-\frac{1}{12}Q_{qq}^{(1)1133}-\frac{1}{12}Q_{qq}^{(1)3311}\Big) \end{aligned} \qquad \text{(G.38)}$$

$$m_t G^A_{\mu\nu}\bar{t}T^A\sigma^{\mu\nu}t = \frac{\sqrt{2}m_t}{v}\left(Q_{uG}^{33}+Q_{uG}^{*33}\right) \qquad \text{(G.39)}$$

We have only included four-fermion operators that contribute to the process at hand and symmetrized the generation index as far as possible. These formulas provide the

[70] For example, in colour space we have

$$\delta^{\alpha\beta}\delta^{\gamma\delta}\bar{t}_R^\alpha q_L^{i,\beta}\bar{q}_L^{i,\gamma}t_R^\delta = -\frac{1}{2}\delta^{\alpha\beta}\delta^{\gamma\delta}\bar{q}_L^{i,\gamma}\gamma^\mu q_L^{i,\beta}\bar{t}_R^\alpha\gamma_\mu t_R^\delta = -C_{qu}^{(8)3333}-\frac{1}{6}C_{qu}^{(1)3333} \qquad \text{(G.35)}$$

where the $SU(3)$ relation $2T^{A,\alpha\beta}T^{A,\gamma\delta} = \delta^{\alpha\delta}\delta^{\gamma\beta}-\delta^{\alpha\beta}\delta^{\gamma\delta}/3$ has been used.

building blocks for a proper matching to SMEFT. The Wilson coefficients are then given by

$$C_{qu}^{(8)3333} = 6C_{qu}^{(1)3333} = -\frac{2m_t^2 \cot^2\beta}{v^2} \tag{G.40}$$

$$\begin{aligned} 2C_{uu}^{1331} &= 2C_{uu}^{3113} = -6C_{uu}^{1133} = -6C_{uu}^{3311} = C_{qu}^{(8)3311} = \frac{1}{2}C_{qu}^{(8)1133} \\ &= 8C_{qq}^{(3)1331} = 8C_{qq}^{(3)3113} = -12C_{qq}^{(1)1133} = -12C_{qq}^{(1)3311} = 8C_{qq}^{(1)1331} = 8C_{qq}^{(1)3113} \\ &= -\frac{g_s^2 m_t^2 \cot^2\beta}{16\pi^2 v^2}\left(\frac{2}{3}\ln\frac{\mu^2}{m_s^2} + \frac{8}{9}\right) \end{aligned} \tag{G.41}$$

$$C_{uG}^{33} = C_{uG}^{*33} = -\frac{g_s m_t^3 \cot^2\beta}{16\pi^2 v^3}\frac{1}{\sqrt{2}} \tag{G.42}$$

If we had instead proceeded in a bottom-up approach using the Warsaw basis, we would have again included the diagrams (G.30), (G.32) and (G.33) - denote their contributions by $\delta\Gamma_1^\mu$, $\delta\Gamma_2^\mu$ and $\delta\Gamma_3^\mu$, respectively, this time with unknown coefficients and cut-off scale Λ, and would have found[71]

$$\begin{aligned} \delta\Gamma_1^\mu = -\frac{1}{16\pi^2\Lambda^2}\Bigg[& q^2\gamma^\mu\Bigg(\left(\frac{5}{9} - \frac{1}{3}\ln\frac{q^2}{\mu^2} + i\frac{\pi}{3}\right)\cdot \\ & \cdot\left(\left(C_{ud}^{(8)3333} + C_{qu}^{(8)3333}\right)P_R + \left(C_{qd}^{(8)3333} + 8C_{qq}^{(3)3333}\right)P_L\right) + \\ & -\left(\frac{1}{3}\ln\frac{m_t^2}{\mu^2} + h_1(z)\right)\left(C_{qu}^{(8)3333} + 4(C_{qq}^{(1)3333} + C_{qq}^{(3)3333})P_L + 4C_{uu}^{3333}P_R\right) \\ & -\frac{4}{3}\left((C_{qq}^{(1)3333} + 3C_{qq}^{(3)3333})P_L + C_{uu}^{3333}P_R\right)\Bigg) + 2m_t i\sigma^{\mu\nu}q_\nu\left(C_{qu}^{(1)3333} - \frac{1}{6}C_{qu}^{(8)3333}\right)\Bigg] \end{aligned} \tag{G.43}$$

for the closed fermion loop,

$$\delta\Gamma_2^\mu = -\frac{\sqrt{2}v}{g_s\Lambda^2} i\sigma^{\mu\nu}q_\nu\left(C_{uG}^{*33}P_L + C_{uG}^{33}P_R\right) \tag{G.44}$$

for the chromomagnetic tree-level contribution, and finally the plain four-fermion vertex

$$\begin{aligned} & ig_s^2\bar{v}(k_2)T^A\gamma_\mu u(k_1)\bar{u}(p_1)T^A\delta\Gamma_3^\mu v(p_2) \equiv \\ & \equiv \frac{i}{\Lambda^2}\Bigg(2\left(C_{qq}^{(1)1133} + C_{qq}^{(3)1133}\right)\bar{v}(k_2)\gamma_\mu P_L u(k_1)\bar{u}(p_1)\gamma^\mu P_L v(p_2) + \\ & \quad -2\left(C_{qq}^{(1)1331} + C_{qq}^{(3)1331}\right)\bar{v}(k_2)\gamma_\mu P_L v(p_2)\bar{u}(p_1)\gamma^\mu P_L u(k_1) + \\ & \quad +2C_{uu}^{(1)1133}\bar{v}(k_2)\gamma_\mu P_R u(k_1)\bar{u}(p_1)\gamma^\mu P_R v(p_2) + \end{aligned}$$

[71] For simplicity, we assume the new physics to couple only to the third particle generation. This, however, does not affect $\delta\Gamma_3^\mu$.

$$
\begin{aligned}
&-2C_{uu}^{(1)1331}\bar{v}(k_2)\gamma_\mu P_R v(p_2)\bar{u}(p_1)\gamma^\mu P_R u(k_1)+\\
&+C_{qu}^{(1)1133}\bar{v}(k_2)\gamma_\mu P_L u(k_1)\bar{u}(p_1)\gamma^\mu P_R v(p_2)+\\
&+C_{qu}^{(1)3311}\bar{v}(k_2)\gamma_\mu P_R u(k_1)\bar{u}(p_1)\gamma^\mu P_L v(p_2)+\\
&-C_{qu}^{(1)1331}\bar{v}(k_2)\gamma_\mu P_L v(p_2)\bar{u}(p_1)\gamma^\mu P_R u(k_1)+\\
&-C_{qu}^{(1)3113}\bar{v}(k_2)\gamma_\mu P_R v(p_2)\bar{u}(p_1)\gamma^\mu P_L u(k_1)+\\
&+C_{qu}^{(8)1133}\bar{v}(k_2)T^A\gamma_\mu P_L u(k_1)\bar{u}(p_1)T^A\gamma^\mu P_R v(p_2)+\\
&+C_{qu}^{(8)3311}\bar{v}(k_2)T^A\gamma_\mu P_R u(k_1)\bar{u}(p_1)T^A\gamma^\mu P_L v(p_2)+\\
&-C_{qu}^{(8)1331}\bar{v}(k_2)T^A\gamma_\mu P_L v(p_2)\bar{u}(p_1)T^A\gamma^\mu P_R u(k_1)+\\
&-C_{qu}^{(8)3113}\bar{v}(k_2)T^A\gamma_\mu P_R v(p_2)\bar{u}(p_1)T^A\gamma^\mu P_L u(k_1)\Bigg)
\end{aligned}
\tag{G.45}
$$

For a proper comparison, the last expression has to be converted to the form of (G.33) using Fierz identities[72]. Comparing to (G.40)-(G.42) with the identification $\Lambda \leftrightarrow m_s$ reveals that most of the four-fermion operators in $\delta\Gamma_1^\mu$ are in fact not generated in this model. The loop contribution is, however, important in order to fulfill the SMEFT renormalization group equations [104–107] for $\delta\Gamma_2^\mu$.

Our analysis in this appendix demonstrates how the basic ideas of the toy model from Section 3 can be taken over to the full SM. While the 2HDM is, at the end of the day, an arbitrary choice of UV physics, its implications for the hierarchy of operator structures in SMEFT are actually quite universal. Indeed, there exists no mechanism that could enhance the expected numerical values for the Wilson coefficients of field-strength operators, as long as the (renormalizable) UV theory is considered weakly coupled, which is in fact the basic assumption SMEFT relies on.

[72] In particular, we use $\bar{v}(k_2)\gamma_\mu P_L v(p_2)\bar{u}(p_1)\gamma^\mu P_L u(k_1)$ together with the appropriate manipulations in colour space.

References

[1] Steven Weinberg. *The Quantum theory of fields. Vol. 1: Foundations*. Cambridge University Press, June 2005. ISBN: 978-0-521-67053-1, 978-0-511-25204-4.

[2] Steven Weinberg. “What is quantum field theory, and what did we think it is?” In: *Conference on Historical Examination and Philosophical Reflections on the Foundations of Quantum Field Theory*. Mar. 1996, pp. 241–251. arXiv: hep-th/9702027.

[3] David B. Malament. “In Defense of Dogma: Why There Cannot be a Relativistic Quantum Mechanics of (Localizable) Particles”. In: *Perspectives on Quantum Reality: Non-Relativistic, Relativistic, and Field-Theoretic*. Ed. by Rob Clifton. Dordrecht: Springer Netherlands, 1996, pp. 1–10. ISBN: 978-94-015-8656-6. DOI: 10.1007/978-94-015-8656-6_1. URL: https://doi.org/10.1007/978-94-015-8656-6_1.

[4] Art Hobson. “There are no particles, there are only fields”. In: *Am. J. Phys.* 81 (2013), pp. 211–223. DOI: 10.1119/1.4789885. arXiv: 1204.4616 [physics.hist-ph].

[5] Michael E. Peskin and Daniel V. Schroeder. *An Introduction to quantum field theory*. Reading, USA: Addison-Wesley, 1995. ISBN: 978-0-201-50397-5.

[6] A. Zee. *Quantum Field Theory in a Nutshell, 2nd revised edition*. Princeton University Press, 2010.

[7] M. Srednicki. *Quantum field theory*. Cambridge University Press, Jan. 2007. ISBN: 978-0-521-86449-7, 978-0-511-26720-8.

[8] Matthew D. Schwartz. *Quantum Field Theory and the Standard Model*. Cambridge University Press, Mar. 2014. ISBN: 978-1-107-03473-0.

[9] S. Tomonaga. “On a relativistically invariant formulation of the quantum theory of wave fields”. In: *Prog. Theor. Phys.* 1 (1946), pp. 27–42. DOI: 10.1143/PTP.1.27.

[10] Julian S. Schwinger. “On Quantum electrodynamics and the magnetic moment of the electron”. In: *Phys. Rev.* 73 (1948), pp. 416–417. DOI: 10.1103/PhysRev.73.416.

[11] R. P. Feynman. “Space - time approach to quantum electrodynamics”. In: *Phys. Rev.* 76 (1949). Ed. by L. M. Brown, pp. 769–789. DOI: 10.1103/PhysRev.76.769.

[12] Chen-Ning Yang and Robert L. Mills. “Conservation of Isotopic Spin and Isotopic Gauge Invariance”. In: *Phys. Rev.* 96 (1954). Ed. by Jong-Ping Hsu and D. Fine, pp. 191–195. DOI: 10.1103/PhysRev.96.191.

[13] H. Fritzsch, Murray Gell-Mann, and H. Leutwyler. “Advantages of the Color Octet Gluon Picture”. In: *Phys. Lett. B* 47 (1973), pp. 365–368. DOI: 10.1016/0370-2693(73)90625-4.

[14] Gerard ’t Hooft and M. J. G. Veltman. “Regularization and Renormalization of Gauge Fields”. In: *Nucl. Phys. B* 44 (1972), pp. 189–213. DOI: 10.1016/0550-3213(72)90279-9.

[15] S. L. Glashow. “Partial Symmetries of Weak Interactions”. In: *Nucl. Phys.* 22 (1961), pp. 579–588. DOI: 10.1016/0029-5582(61)90469-2.

[16] Steven Weinberg. “A Model of Leptons”. In: *Phys. Rev. Lett.* 19 (1967), pp. 1264–1266. DOI: 10.1103/PhysRevLett.19.1264.
[17] Abdus Salam. “Weak and Electromagnetic Interactions”. In: *Conf. Proc. C* 680519 (1968), pp. 367–377. DOI: 10.1142/9789812795915_0034.
[18] R. P. Feynman. “Quantum theory of gravitation”. In: *Acta Phys. Polon.* 24 (1963). Ed. by Jong-Ping Hsu and D. Fine, pp. 697–722.
[19] Gerard ’t Hooft and M. J. G. Veltman. “One loop divergencies in the theory of gravitation”. In: *Ann. Inst. H. Poincare Phys. Theor. A* 20 (1974), pp. 69–94.
[20] John F. Donoghue. “Leading quantum correction to the Newtonian potential”. In: *Phys. Rev. Lett.* 72 (1994), pp. 2996–2999. DOI: 10.1103/PhysRevLett.72.2996. arXiv: gr-qc/9310024.
[21] Barry R. Holstein and John F. Donoghue. “Classical physics and quantum loops”. In: *Phys. Rev. Lett.* 93 (2004), p. 201602. DOI: 10.1103/PhysRevLett.93.201602. arXiv: hep-th/0405239.
[22] John F. Donoghue. “Quantum General Relativity and Effective Field Theory”. In: (Nov. 2022). arXiv: 2211.09902 [hep-th].
[23] Steven Weinberg. “Phenomenological Lagrangians”. In: *Physica A* 96.1-2 (1979). Ed. by S. Deser, pp. 327–340. DOI: 10.1016/0378-4371(79)90223-1.
[24] Enrico Fermi. “Tentativo di una teoria dell’emissione dei raggi beta”. In: *Ric. Sci.* 4 (1933), pp. 491–495.
[25] Aneesh V. Manohar. “Introduction to Effective Field Theories”. In: (Apr. 2018). Ed. by Sacha Davidson et al. DOI: 10.1093/oso/9780198855743.003.0002. arXiv: 1804.05863 [hep-ph].
[26] J. Gasser and H. Leutwyler. “Chiral Perturbation Theory to One Loop”. In: *Annals Phys.* 158 (1984), p. 142. DOI: 10.1016/0003-4916(84)90242-2.
[27] A. Pich. “Chiral perturbation theory”. In: *Rept. Prog. Phys.* 58 (1995), pp. 563–610. DOI: 10.1088/0034-4885/58/6/001. arXiv: hep-ph/9502366.
[28] John F. Donoghue. “Introduction to the effective field theory description of gravity”. In: *Advanced School on Effective Theories*. June 1995. arXiv: gr-qc/9512024.
[29] R. P. Feynman. *Feynman lectures on gravitation*. Ed. by F. B. Morinigo, W. G. Wagner, and B. Hatfield. 1996.
[30] W. Buchmuller and D. Wyler. “Effective Lagrangian Analysis of New Interactions and Flavor Conservation”. In: *Nucl. Phys. B* 268 (1986), pp. 621–653. DOI: 10.1016/0550-3213(86)90262-2.
[31] B. Grzadkowski et al. “Dimension-Six Terms in the Standard Model Lagrangian”. In: *JHEP* 10 (2010), p. 085. DOI: 10.1007/JHEP10(2010)085. arXiv: 1008.4884 [hep-ph].
[32] Scott Willenbrock and Cen Zhang. “Effective Field Theory Beyond the Standard Model”. In: *Ann. Rev. Nucl. Part. Sci.* 64 (2014), pp. 83–100. DOI: 10.1146/annurev-nucl-102313-025623. arXiv: 1401.0470 [hep-ph].
[33] André David and Giampiero Passarino. “Through precision straits to next standard model heights”. In: *Rev. Phys.* 1 (2016), pp. 13–28. DOI: 10.1016/j.revip.2016.01.001. arXiv: 1510.00414 [hep-ph].

[34] Timothy Cohen et al. "Is SMEFT Enough?" In: *JHEP* 03 (2021), p. 237. DOI: 10.1007/JHEP03(2021)237. arXiv: 2008.08597 [hep-ph].

[35] Michael Trott. "Methodology for theory uncertainties in the standard model effective field theory". In: *Phys. Rev. D* 104.9 (2021), p. 095023. DOI: 10.1103/PhysRevD.104.095023. arXiv: 2106.13794 [hep-ph].

[36] F. Feruglio. "The Chiral approach to the electroweak interactions". In: *Int. J. Mod. Phys. A* 8 (1993), pp. 4937–4972. DOI: 10.1142/S0217751X93001946. arXiv: hep-ph/9301281.

[37] J. Bagger et al. "The Strongly interacting W W system: Gold plated modes". In: *Phys. Rev. D* 49 (1994), pp. 1246–1264. DOI: 10.1103/PhysRevD.49.1246. arXiv: hep-ph/9306256.

[38] Vassilis Koulovassilopoulos and R. Sekhar Chivukula. "The Phenomenology of a nonstandard Higgs boson in W(L) W(L) scattering". In: *Phys. Rev. D* 50 (1994), pp. 3218–3234. DOI: 10.1103/PhysRevD.50.3218. arXiv: hep-ph/9312317.

[39] C. P. Burgess, J. Matias, and M. Pospelov. "A Higgs or not a Higgs? What to do if you discover a new scalar particle". In: *Int. J. Mod. Phys. A* 17 (2002), pp. 1841–1918. DOI: 10.1142/S0217751X02009813. arXiv: hep-ph/9912459.

[40] Li-Ming Wang and Qing Wang. "Nonstandard Higgs in electroweak chiral Lagrangian". In: (May 2006). arXiv: hep-ph/0605104.

[41] Benjamin Grinstein and Michael Trott. "A Higgs-Higgs bound state due to new physics at a TeV". In: *Phys. Rev. D* 76 (2007), p. 073002. DOI: 10.1103/PhysRevD.76.073002. arXiv: 0704.1505 [hep-ph].

[42] Roberto Contino et al. "Strong Double Higgs Production at the LHC". In: *JHEP* 05 (2010), p. 089. DOI: 10.1007/JHEP05(2010)089. arXiv: 1002.1011 [hep-ph].

[43] Roberto Contino. "The Higgs as a Composite Nambu-Goldstone Boson". In: *Theoretical Advanced Study Institute in Elementary Particle Physics: Physics of the Large and the Small.* 2011, pp. 235–306. DOI: 10.1142/9789814327183_0005. arXiv: 1005.4269 [hep-ph].

[44] R. Alonso et al. "The Effective Chiral Lagrangian for a Light Dynamical "Higgs Particle"". In: *Phys. Lett. B* 722 (2013). [Erratum: Phys.Lett.B 726, 926 (2013)], pp. 330–335. DOI: 10.1016/j.physletb.2013.04.037. arXiv: 1212.3305 [hep-ph].

[45] R. Alonso et al. "Flavor with a light dynamical "Higgs particle"". In: *Phys. Rev. D* 87.5 (2013), p. 055019. DOI: 10.1103/PhysRevD.87.055019. arXiv: 1212.3307 [hep-ph].

[46] Gerhard Buchalla, Oscar Catà, and Claudius Krause. "Complete Electroweak Chiral Lagrangian with a Light Higgs at NLO". In: *Nucl. Phys. B* 880 (2014). [Erratum: Nucl.Phys.B 913, 475–478 (2016)], pp. 552–573. DOI: 10.1016/j.nuclphysb.2014.01.018. arXiv: 1307.5017 [hep-ph].

[47] Ilaria Brivio and Michael Trott. "The Standard Model as an Effective Field Theory". In: *Phys. Rept.* 793 (2019), pp. 1–98. DOI: 10.1016/j.physrep.2018.11.002. arXiv: 1706.08945 [hep-ph].

[48] C. G. Tully. *Elementary Particle Physics in a Nutshell.* Princeton University Press, 2011.

[49] G. Kane. *Modern Elementary Particle Physics, 2nd edition*. Cambridge University Press, 2017.
[50] M. Thomson. *Modern Particle Physics*. Cambridge University Press, 2013.
[51] D. Griffiths. *Introduction to Elementary Particles, 2nd edition*. Cambridge University Press, 2008.
[52] J. J. Sakurai and Jim Napolitano. *Modern Quantum Mechanics*. 2nd ed. Cambridge University Press, 2017. DOI: 10.1017/9781108499996.
[53] Georges Aad et al. "Observation of a new particle in the search for the Standard Model Higgs boson with the ATLAS detector at the LHC". In: *Phys. Lett. B* 716 (2012), pp. 1–29. DOI: 10.1016/j.physletb.2012.08.020. arXiv: 1207.7214 [hep-ex].
[54] F. Englert and R. Brout. "Broken Symmetry and the Mass of Gauge Vector Mesons". In: *Phys. Rev. Lett.* 13 (9 Aug. 1964), pp. 321–323. DOI: 10.1103/PhysRevLett.13.321. URL: https://link.aps.org/doi/10.1103/PhysRevLett.13.321.
[55] T. W. B. Kibble. "Symmetry Breaking in Non-Abelian Gauge Theories". In: *Phys. Rev.* 155 (5 Mar. 1967), pp. 1554–1561. DOI: 10.1103/PhysRev.155.1554. URL: https://link.aps.org/doi/10.1103/PhysRev.155.1554.
[56] Peter W. Higgs. "Spontaneous Symmetry Breakdown without Massless Bosons". In: *Phys. Rev.* 145 (4 May 1966), pp. 1156–1163. DOI: 10.1103/PhysRev.145.1156. URL: https://link.aps.org/doi/10.1103/PhysRev.145.1156.
[57] G. S. Guralnik, C. R. Hagen, and T. W. B. Kibble. "Global Conservation Laws and Massless Particles". In: *Phys. Rev. Lett.* 13 (20 Nov. 1964), pp. 585–587. DOI: 10.1103/PhysRevLett.13.585. URL: https://link.aps.org/doi/10.1103/PhysRevLett.13.585.
[58] Peter W. Higgs. "Broken Symmetries and the Masses of Gauge Bosons". In: *Phys. Rev. Lett.* 13 (16 Oct. 1964), pp. 508–509. DOI: 10.1103/PhysRevLett.13.508. URL: https://link.aps.org/doi/10.1103/PhysRevLett.13.508.
[59] P.W. Higgs. "Broken symmetries, massless particles and gauge fields". In: *Physics Letters* 12.2 (1964), pp. 132–133. ISSN: 0031-9163. DOI: https://doi.org/10.1016/0031-9163(64)91136-9. URL: https://www.sciencedirect.com/science/article/pii/0031916364911369.
[60] Steven Weinberg. "Baryon- and Lepton-Nonconserving Processes". In: *Phys. Rev. Lett.* 43 (21 Nov. 1979), pp. 1566–1570. DOI: 10.1103/PhysRevLett.43.1566. URL: https://link.aps.org/doi/10.1103/PhysRevLett.43.1566.
[61] R. L. Workman et al. "Review of Particle Physics". In: *PTEP* 2022 (2022), p. 083C01. DOI: 10.1093/ptep/ptac097.
[62] Susanne Mertens. "Direct Neutrino Mass Experiments". In: *J. Phys. Conf. Ser.* 718.2 (2016), p. 022013. DOI: 10.1088/1742-6596/718/2/022013. arXiv: 1605.01579 [nucl-ex].
[63] F. Capozzi et al. "Neutrino masses and mixings: Status of known and unknown 3ν parameters". In: *Nucl. Phys. B* 908 (2016), pp. 218–234. DOI: 10.1016/j.nuclphysb.2016.02.016. arXiv: 1601.07777 [hep-ph].

[64] M. Aker et al. “KATRIN: status and prospects for the neutrino mass and beyond”. In: *J. Phys. G* 49.10 (2022), p. 100501. DOI: 10.1088/1361-6471/ac834e. arXiv: 2203.08059 [nucl-ex].

[65] A.A. Petrov and A.E. Blechman. *Effective Field Theories*. World Scientific Publishing Company, 2015. ISBN: 9789814434942. URL: https://books.google.de/books?id=B3zFCwAAQBAJ.

[66] A. Dedes et al. “Feynman rules for the Standard Model Effective Field Theory in R -gauges”. In: *JHEP* 06 (2017), p. 143. DOI: 10.1007/JHEP06(2017)143. arXiv: 1704.03888 [hep-ph].

[67] Landon Lehman. “Extending the Standard Model Effective Field Theory with the Complete Set of Dimension-7 Operators”. In: *Phys. Rev. D* 90.12 (2014), p. 125023. DOI: 10.1103/PhysRevD.90.125023. arXiv: 1410.4193 [hep-ph].

[68] Yi Liao and Xiao-Dong Ma. “Renormalization Group Evolution of Dimension-seven Baryon- and Lepton-number-violating Operators”. In: *JHEP* 11 (2016), p. 043. DOI: 10.1007/JHEP11(2016)043. arXiv: 1607.07309 [hep-ph].

[69] Yi Liao and Xiao-Dong Ma. “Renormalization Group Evolution of Dimension-seven Operators in Standard Model Effective Field Theory and Relevant Phenomenology”. In: *JHEP* 03 (2019), p. 179. DOI: 10.1007/JHEP03(2019)179. arXiv: 1901.10302 [hep-ph].

[70] Christopher W. Murphy. “Dimension-8 operators in the Standard Model Eective Field Theory”. In: *JHEP* 10 (2020), p. 174. DOI: 10.1007/JHEP10(2020)174. arXiv: 2005.00059 [hep-ph].

[71] Hao-Lin Li et al. “Complete set of dimension-eight operators in the standard model effective field theory”. In: *Phys. Rev. D* 104.1 (2021), p. 015026. DOI: 10.1103/PhysRevD.104.015026. arXiv: 2005.00008 [hep-ph].

[72] Hao-Lin Li et al. “Complete set of dimension-nine operators in the standard model effective field theory”. In: *Phys. Rev. D* 104 (1 July 2021), p. 015025. DOI: 10.1103/PhysRevD.104.015025. URL: https://link.aps.org/doi/10.1103/PhysRevD.104.015025.

[73] Yi Liao and Xiao-Dong Ma. “An explicit construction of the dimension-9 operator basis in the standard model effective field theory”. In: *JHEP* 11 (2020), p. 152. DOI: 10.1007/JHEP11(2020)152. arXiv: 2007.08125 [hep-ph].

[74] Gerhard Buchalla Gudrun Heinrich, Christoph Müller-Salditt, and Florian Pandler. “Loop counting matters in SMEFT”. In: *SciPost, accepted for publication* (2023). arXiv: 2204.11808 [hep-ph].

[75] Christoph Englert, Peter Galler, and Chris D. White. “Effective field theory and scalar extensions of the top quark sector”. In: *Phys. Rev. D* 101.3 (2020), p. 035035. DOI: 10.1103/PhysRevD.101.035035. arXiv: 1908.05588 [hep-ph].

[76] Aneesh Manohar and Howard Georgi. “Chiral Quarks and the Nonrelativistic Quark Model”. In: *Nucl. Phys. B* 234 (1984), pp. 189–212. DOI: 10.1016/0550-3213(84)90231-1.

[77] Elizabeth E. Jenkins, Aneesh V. Manohar, and Michael Trott. “Naive Dimensional Analysis Counting of Gauge Theory Amplitudes and Anomalous Dimen-

sions". In: *Phys. Lett. B* 726 (2013), pp. 697–702. DOI: 10.1016/j.physletb.2013.09.020. arXiv: 1309.0819 [hep-ph].
[78] Aneesh V. Manohar. "An Exactly Solvable Model for Dimension Six Higgs Operators and $h \to \gamma\gamma$". In: *Phys. Lett. B* 726 (2013), pp. 347–351. DOI: 10.1016/j.physletb.2013.08.072. arXiv: 1305.3927 [hep-ph].
[79] Matthew McCullough. "Examining the Higgs". In: *unpublished*. Higgs Centre School (2021). URL: https://higgs.ph.ed.ac.uk/workshops/higgs-centre-school-2021/.
[80] N. E. J. Bjerrum-Bohr et al. "General Relativity from Scattering Amplitudes". In: *Phys. Rev. Lett.* 121.17 (2018), p. 171601. DOI: 10.1103/PhysRevLett.121.171601. arXiv: 1806.04920 [hep-th].
[81] David A. Kosower, Ben Maybee, and Donal O'Connell. "Amplitudes, Observables, and Classical Scattering". In: *JHEP* 02 (2019), p. 137. DOI: 10.1007/JHEP02(2019)137. arXiv: 1811.10950 [hep-th].
[82] C. Arzt, M. B. Einhorn, and J. Wudka. "Patterns of deviation from the standard model". In: *Nucl. Phys. B* 433 (1995), pp. 41–66. DOI: 10.1016/0550-3213(94)00336-D. arXiv: hep-ph/9405214.
[83] Nathaniel Craig et al. "Loops and Trees in Generic EFTs". In: *JHEP* 08 (2020), p. 086. DOI: 10.1007/JHEP08(2020)086. arXiv: 2001.00017 [hep-ph].
[84] Ran Huo. "Standard Model Effective Field Theory: Integrating out Vector-Like Fermions". In: *JHEP* 09 (2015), p. 037. DOI: 10.1007/JHEP09(2015)037. arXiv: 1506.00840 [hep-ph].
[85] Matthew J. Dolan et al. "Simplified Models for Higgs Physics: Singlet Scalar and Vector-like Quark Phenomenology". In: *JHEP* 07 (2016), p. 039. DOI: 10.1007/JHEP07(2016)039. arXiv: 1601.07208 [hep-ph].
[86] Gino Isidori, Felix Wilsch, and Daniel Wyler. "The Standard Model effective field theory at work". In: (Mar. 2023). arXiv: 2303.16922 [hep-ph].
[87] Vladimir A. Smirnov. "'Strategy of regions': Expansions of Feynman diagrams both in Euclidean and pseudo-Euclidean regimes". In: *5th International Symposium on Radiative Corrections: Applications of Quantum Field Theory to Phenomenology*. Jan. 2001. arXiv: hep-ph/0101152.
[88] Thomas Becher, Alessandro Broggio, and Andrea Ferroglia. *Introduction to Soft-Collinear Effective Theory*. Vol. 896. Springer, 2015. DOI: 10.1007/978-3-319-14848-9. arXiv: 1410.1892 [hep-ph].
[89] Gerard 't Hooft and M. J. G. Veltman. "Scalar One Loop Integrals". In: *Nucl. Phys. B* 153 (1979), pp. 365–401. DOI: 10.1016/0550-3213(79)90605-9.
[90] G. Passarino and M. J. G. Veltman. "One Loop Corrections for e+ e- Annihilation Into mu+ mu- in the Weinberg Model". In: *Nucl. Phys. B* 160 (1979), pp. 151–207. DOI: 10.1016/0550-3213(79)90234-7.
[91] Ansgar Denner and S. Dittmaier. "Reduction schemes for one-loop tensor integrals". In: *Nucl. Phys. B* 734 (2006), pp. 62–115. DOI: 10.1016/j.nuclphysb.2005.11.007. arXiv: hep-ph/0509141.

[92] Vladyslav Shtabovenko, Rolf Mertig, and Frederik Orellana. "FeynCalc 9.3: New features and improvements". In: *Comput. Phys. Commun.* 256 (2020), p. 107478. DOI: 10.1016/j.cpc.2020.107478. arXiv: 2001.04407 [hep-ph].

[93] Thomas Hahn, Sebastian Passehr, and Christian Schappacher. "FormCalc 9 and Extensions". In: *PoS* LL2016 (2016). Ed. by Luis Salinas and Claudio Torres, p. 068. DOI: 10.1088/1742-6596/762/1/012065. arXiv: 1604.04611 [hep-ph].

[94] Hiren H. Patel. "Package-X 2.0: A Mathematica package for the analytic calculation of one-loop integrals". In: *Comput. Phys. Commun.* 218 (2017), pp. 66–70. DOI: 10.1016/j.cpc.2017.04.015. arXiv: 1612.00009 [hep-ph].

[95] Davison E. Soper. "Parton distribution functions". In: *Nucl. Phys. B Proc. Suppl.* 53 (1997). Ed. by C. Bernard et al., pp. 69–80. DOI: 10.1016/S0920-5632(96)00600-7. arXiv: hep-lat/9609018.

[96] A. D. Martin et al. "Parton distributions for the LHC". In: *Eur. Phys. J. C* 63 (2009), pp. 189–285. DOI: 10.1140/epjc/s10052-009-1072-5. arXiv: 0901.0002 [hep-ph].

[97] Diogo Buarque Franzosi and Cen Zhang. "Probing the top-quark chromomagnetic dipole moment at next-to-leading order in QCD". In: *Phys. Rev. D* 91.11 (2015), p. 114010. DOI: 10.1103/PhysRevD.91.114010. arXiv: 1503.08841 [hep-ph].

[98] Nicolas Deutschmann et al. "Gluon-fusion Higgs production in the Standard Model Effective Field Theory". In: *JHEP* 12 (2017). [Erratum: JHEP 02, 159 (2018)], p. 063. DOI: 10.1007/JHEP12(2017)063. arXiv: 1708.00460 [hep-ph].

[99] Christoph Müller. "Top-pair production via gluon fusion in the Standard Model effective field theory". In: *Phys. Rev. D* 104.9 (2021), p. 095003. DOI: 10.1103/PhysRevD.104.095003. arXiv: 2102.05040 [hep-ph].

[100] P. Bärnreuther. "Top Quark Pair Production at the LHC". In: *Doctoral Thesis, RWTH Aachen University* (2012).

[101] P.A. Zyla et al. "Review of Particle Physics". In: *PTEP* 2020.8 (2020), p. 083C01. DOI: 10.1093/ptep/ptaa104.

[102] Cen Zhang and Scott Willenbrock. "Effective-Field-Theory Approach to Top-Quark Production and Decay". In: *Phys. Rev. D* 83 (2011), p. 034006. DOI: 10.1103/PhysRevD.83.034006. arXiv: 1008.3869 [hep-ph].

[103] Ilaria Brivio et al. "O new physics, where art thou? A global search in the top sector". In: *JHEP* 02 (2020), p. 131. DOI: 10.1007/JHEP02(2020)131. arXiv: 1910.03606 [hep-ph].

[104] Alejandro Celis et al. "DsixTools: The Standard Model Effective Field Theory Toolkit". In: *Eur. Phys. J. C* 77.6 (2017), p. 405. DOI: 10.1140/epjc/s10052-017-4967-6. arXiv: 1704.04504 [hep-ph].

[105] Elizabeth E. Jenkins, Aneesh V. Manohar, and Michael Trott. "Renormalization Group Evolution of the Standard Model Dimension Six Operators I: Formalism and lambda Dependence". In: *JHEP* 10 (2013), p. 087. DOI: 10.1007/JHEP10(2013)087. arXiv: 1308.2627 [hep-ph].

[106] Elizabeth E. Jenkins, Aneesh V. Manohar, and Michael Trott. "Renormalization Group Evolution of the Standard Model Dimension Six Operators II: Yukawa

Dependence". In: *JHEP* 01 (2014), p. 035. DOI: 10.1007/JHEP01(2014)035. arXiv: 1310.4838 [hep-ph].
[107] Rodrigo Alonso et al. "Renormalization Group Evolution of the Standard Model Dimension Six Operators III: Gauge Coupling Dependence and Phenomenology". In: *JHEP* 04 (2014), p. 159. DOI: 10.1007/JHEP04(2014)159. arXiv: 1312.2014 [hep-ph].
[108] C. Gnendiger et al. "To d, or not to d: recent developments and comparisons of regularization schemes". In: *Eur. Phys. J. C* 77.7 (2017), p. 471. DOI: 10.1140/epjc/s10052-017-5023-2. arXiv: 1705.01827 [hep-ph].
[109] W. Beenakker et al. "QCD Corrections to Heavy Quark Production in p anti-p Collisions". In: *Phys. Rev. D* 40 (1989), pp. 54–82. DOI: 10.1103/PhysRevD.40.54.
[110] P. Nason, S. Dawson, and R.Keith Ellis. "The Total Cross-Section for the Production of Heavy Quarks in Hadronic Collisions". In: *Nucl. Phys. B* 303 (1988), pp. 607–633. DOI: 10.1016/0550-3213(88)90422-1.
[111] Fabio Maltoni, Eleni Vryonidou, and Cen Zhang. "Higgs production in association with a top-antitop pair in the Standard Model Effective Field Theory at NLO in QCD". In: *JHEP* 10 (2016), p. 123. DOI: 10.1007/JHEP10(2016)123. arXiv: 1607.05330 [hep-ph].
[112] Fabio Maltoni, Manoj K. Mandal, and Xiaoran Zhao. "Top-quark effects in diphoton production through gluon fusion at next-to-leading order in QCD". In: *Phys. Rev. D* 100.7 (2019), p. 071501. DOI: 10.1103/PhysRevD.100.071501. arXiv: 1812.08703 [hep-ph].
[113] Giovanni Banelli et al. "The Present and Future of Four Tops". In: (Oct. 2020). arXiv: 2010.05915 [hep-ph].
[114] Morad Aaboud et al. "Search for four-top-quark production in the single-lepton and opposite-sign dilepton final states in pp collisions at $\sqrt{s} = 13$ TeV with the ATLAS detector". In: *Phys. Rev. D* 99.5 (2019), p. 052009. DOI: 10.1103/PhysRevD.99.052009. arXiv: 1811.02305 [hep-ex].
[115] J. Alison et al. "Higgs boson potential at colliders: Status and perspectives". In: *Rev. Phys.* 5 (2020). Ed. by Biagio Di Micco et al., p. 100045. DOI: 10.1016/j.revip.2020.100045. arXiv: 1910.00012 [hep-ph].
[116] Jorge de Blas, Otto Eberhardt, and Claudius Krause. "Current and Future Constraints on Higgs Couplings in the Nonlinear Effective Theory". In: *JHEP* 07 (2018), p. 048. DOI: 10.1007/JHEP07(2018)048. arXiv: 1803.00939 [hep-ph].
[117] Frank Krauss, Silvan Kuttimalai, and Tilman Plehn. "LHC multijet events as a probe for anomalous dimension-six gluon interactions". In: *Phys. Rev. D* 95.3 (2017), p. 035024. DOI: 10.1103/PhysRevD.95.035024. arXiv: 1611.00767 [hep-ph].
[118] Valentin Hirschi et al. "Constraining anomalous gluon self-interactions at the LHC: a reappraisal". In: *JHEP* 07 (2018), p. 093. DOI: 10.1007/JHEP07(2018)093. arXiv: 1806.04696 [hep-ph].

[119] Andy Buckley et al. "Constraining top quark effective theory in the LHC Run II era". In: *JHEP* 04 (2016), p. 015. DOI: 10.1007/JHEP04(2016)015. arXiv: 1512.03360 [hep-ph].

[120] D. Barducci et al. "Interpreting top-quark LHC measurements in the standard-model effective field theory". In: (Feb. 2018). Ed. by Juan Antonio Aguilar-Saavedra et al. arXiv: 1802.07237 [hep-ph].

[121] Nathan P. Hartland et al. "A Monte Carlo global analysis of the Standard Model Effective Field Theory: the top quark sector". In: *JHEP* 04 (2019), p. 100. DOI: 10.1007/JHEP04(2019)100. arXiv: 1901.05965 [hep-ph].

[122] Céline Degrande et al. "Automated one-loop computations in the SMEFT". In: (Aug. 2020). arXiv: 2008.11743 [hep-ph].

[123] J. Alwall et al. "The automated computation of tree-level and next-to-leading order differential cross sections, and their matching to parton shower simulations". In: *JHEP* 07 (2014), p. 079. DOI: 10.1007/JHEP07(2014)079. arXiv: 1405.0301 [hep-ph].

[124] R. Frederix et al. "The automation of next-to-leading order electroweak calculations". In: *JHEP* 07 (2018), p. 185. DOI: 10.1007/JHEP07(2018)185. arXiv: 1804.10017 [hep-ph].

[125] M. Paraskevas. "Dirac and Majorana Feynman Rules with four-fermions". In: (Feb. 2018). arXiv: 1802.02657 [hep-ph].

[126] F. Jegerlehner. "Facts of life with gamma(5)". In: *Eur. Phys. J. C* 18 (2001), pp. 673–679. DOI: 10.1007/s100520100573. arXiv: hep-th/0005255.

[127] E.V. Zhemchugov. "On $Z \to \gamma\gamma$ decay and cancellation of axial anomaly in $Z \to \gamma\gamma$ transition amplitude for massive fermions". In: *Phys. Atom. Nucl.* 77 (2014), p. 11. DOI: 10.1134/S1063778814100147. arXiv: 1402.1203 [hep-ph].

[128] Oscar Catà, Wolfgang Kilian, and Nils Kreher. "Gauge anomalies in the Standard-Model Effective Field Theory". In: (Nov. 2020). arXiv: 2011.09976 [hep-ph].

[129] Quentin Bonnefoy et al. "Comments on gauge anomalies at dimension-six in the Standard Model Effective Field Theory". In: (Dec. 2020). arXiv: 2012.07740 [hep-ph].

[130] Ferruccio Feruglio. "A Note on Gauge Anomaly Cancellation in Effective Field Theories". In: (Dec. 2020). arXiv: 2012.13989 [hep-ph].

[131] K.G. Chetyrkin and M.F. Zoller. "Three-loop beta-functions for top-Yukawa and the Higgs self-interaction in the Standard Model". In: *JHEP* 06 (2012), p. 033. DOI: 10.1007/JHEP06(2012)033. arXiv: 1205.2892 [hep-ph].

[132] A.V. Bednyakov, A.F. Pikelner, and V.N. Velizhanin. "Yukawa coupling beta-functions in the Standard Model at three loops". In: *Phys. Lett. B* 722 (2013), pp. 336–340. DOI: 10.1016/j.physletb.2013.04.038. arXiv: 1212.6829 [hep-ph].

[133] A.V. Bednyakov, A.F. Pikelner, and V.N. Velizhanin. "Three-loop beta-functions and anomalous dimensions in the Standard Model". In: *J. Phys. Conf. Ser.* 523 (2014). Ed. by Jianxiong Wang, p. 012045. DOI: 10.1088/1742-6596/523/1/012045. arXiv: 1309.1643 [hep-ph].

[134] Radja Boughezal et al. "Top quark decay at next-to-leading order in the Standard Model Effective Field Theory". In: *Phys. Rev. D* 100.5 (2019), p. 056023. DOI: 10.1103/PhysRevD.100.056023. arXiv: 1907.00997 [hep-ph].

[135] T. P. Cheng and L. F. Li. *Gauge theory of elementary particle physics*. Oxford, UK: Oxford University Press, 1984. ISBN: 978-0-19-851961-4, 978-0-19-851961-4.

[136] U. Baur and E.W.Nigel Glover. "Higgs Boson Production at Large Transverse Momentum in Hadronic Collisions". In: *Nucl. Phys. B* 339 (1990), pp. 38–66. DOI: 10.1016/0550-3213(90)90532-I.

[137] M. Spira et al. "Higgs boson production at the LHC". In: *Nucl. Phys. B* 453 (1995), pp. 17–82. DOI: 10.1016/0550-3213(95)00379-7. arXiv: hep-ph/9504378.

[138] W. Beenakker et al. "NLO QCD corrections to t anti-t H production in hadron collisions". In: *Nucl. Phys. B* 653 (2003), pp. 151–203. DOI: 10.1016/S0550-3213(03)00044-0. arXiv: hep-ph/0211352.

[139] Vittorio Del Duca, Alberto Frizzo, and Fabio Maltoni. "Higgs boson production in association with three jets". In: *JHEP* 05 (2004), p. 064. DOI: 10.1088/1126-6708/2004/05/064. arXiv: hep-ph/0404013.

[140] Robert Harlander and Philipp Kant. "Higgs production and decay: Analytic results at next-to-leading order QCD". In: *JHEP* 12 (2005), p. 015. DOI: 10.1088/1126-6708/2005/12/015. arXiv: hep-ph/0509189.

[141] Charalampos Anastasiou et al. "Two-loop amplitudes and master integrals for the production of a Higgs boson via a massive quark and a scalar-quark loop". In: *JHEP* 01 (2007), p. 082. DOI: 10.1088/1126-6708/2007/01/082. arXiv: hep-ph/0611236.

[142] U. Aglietti et al. "Analytic Results for Virtual QCD Corrections to Higgs Production and Decay". In: *JHEP* 01 (2007), p. 021. DOI: 10.1088/1126-6708/2007/01/021. arXiv: hep-ph/0611266.

[143] S. Borowka et al. "Full top quark mass dependence in Higgs boson pair production at NLO". In: *JHEP* 10 (2016), p. 107. DOI: 10.1007/JHEP10(2016)107. arXiv: 1608.04798 [hep-ph].

[144] Michael Spira. "Higgs Boson Production and Decay at Hadron Colliders". In: *Prog. Part. Nucl. Phys.* 95 (2017), pp. 98–159. DOI: 10.1016/j.ppnp.2017.04.001. arXiv: 1612.07651 [hep-ph].

[145] R. Keith Ellis and Satyajit Seth. "On Higgs boson plus gluon amplitudes at one loop". In: *JHEP* 11 (2018), p. 006. DOI: 10.1007/JHEP11(2018)006. arXiv: 1808.09292 [hep-ph].

[146] H. M. Georgi et al. "Higgs Bosons from Two Gluon Annihilation in Proton Proton Collisions". In: *Phys. Rev. Lett.* 40 (1978), p. 692. DOI: 10.1103/PhysRevLett.40.692.

[147] S. Dawson. "Radiative corrections to Higgs boson production". In: *Nucl. Phys. B* 359 (1991), pp. 283–300. DOI: 10.1016/0550-3213(91)90061-2.

[148] A. Djouadi, M. Spira, and P. M. Zerwas. "Production of Higgs bosons in proton colliders: QCD corrections". In: *Phys. Lett. B* 264 (1991), pp. 440–446. DOI: 10.1016/0370-2693(91)90375-Z.

[149] Aneesh V. Manohar and Mark B. Wise. “Modifications to the properties of the Higgs boson”. In: *Phys. Lett. B* 636 (2006), pp. 107–113. DOI: 10.1016/j.physletb.2006.03.030. arXiv: hep-ph/0601212.
[150] Gerhard Buchalla, Marius Höfer, and Christoph Müller-Salditt. “h→gg and h→$\gamma\gamma$ with anomalous couplings at next-to-leading order in QCD”. In: *Phys. Rev. D* 107.7 (2023), p. 076021. DOI: 10.1103/PhysRevD.107.076021. arXiv: 2212.08560 [hep-ph].
[151] Thomas Appelquist and Claude Bernard. “Strongly interacting Higgs bosons”. In: *Phys. Rev. D* 22 (1 July 1980), pp. 200–213. DOI: 10.1103/PhysRevD.22.200. URL: https://link.aps.org/doi/10.1103/PhysRevD.22.200.
[152] Anthony C. Longhitano. “Heavy Higgs bosons in the Weinberg-Salam model”. In: *Phys. Rev. D* 22 (5 Sept. 1980), pp. 1166–1175. DOI: 10.1103/PhysRevD.22.1166. URL: https://link.aps.org/doi/10.1103/PhysRevD.22.1166.
[153] Anthony C. Longhitano. “Low-Energy Impact of a Heavy Higgs Boson Sector”. In: *Nucl. Phys. B* 188 (1981), pp. 118–154. DOI: 10.1016/0550-3213(81)90109-7.
[154] Gerhard Buchalla and Oscar Cata. “Effective Theory of a Dynamically Broken Electroweak Standard Model at NLO”. In: *JHEP* 07 (2012), p. 101. DOI: 10.1007/JHEP07(2012)101. arXiv: 1203.6510 [hep-ph].
[155] Gerhard Buchalla, Oscar Catá, and Claudius Krause. “On the Power Counting in Effective Field Theories”. In: *Phys. Lett. B* 731 (2014), pp. 80–86. DOI: 10.1016/j.physletb.2014.02.015. arXiv: 1312.5624 [hep-ph].
[156] G. Buchalla et al. “Standard Model Extended by a Heavy Singlet: Linear vs. Nonlinear EFT”. In: *Nucl. Phys. B* 917 (2017), pp. 209–233. DOI: 10.1016/j.nuclphysb.2017.02.006. arXiv: 1608.03564 [hep-ph].
[157] G. Buchalla et al. “Comment on ”Analysis of General Power Counting Rules in Effective Field Theory””. In: (Mar. 2016). arXiv: 1603.03062 [hep-ph].
[158] G. Buchalla et al. “Complete One-Loop Renormalization of the Higgs-Electroweak Chiral Lagrangian”. In: *Nucl. Phys. B* 928 (2018), pp. 93–106. DOI: 10.1016/j.nuclphysb.2018.01.009. arXiv: 1710.06412 [hep-ph].
[159] Claudius Krause et al. “Complete One-Loop Renormalization of the Higgs-Electroweak Chiral Lagrangian”. In: *PoS* CD2018 (2019), p. 072. DOI: 10.22323/1.317.0072. arXiv: 1907.07605 [hep-ph].
[160] G. Buchalla et al. “Higgs-electroweak chiral Lagrangian: One-loop renormalization group equations”. In: *Phys. Rev. D* 104.7 (2021), p. 076005. DOI: 10.1103/PhysRevD.104.076005. arXiv: 2004.11348 [hep-ph].
[161] J. Gasser and H. Leutwyler. “Chiral Perturbation Theory: Expansions in the Mass of the Strange Quark”. In: *Nucl. Phys. B* 250 (1985), pp. 465–516. DOI: 10.1016/0550-3213(85)90492-4.
[162] R. J. Crewther and Lewis C. Tunstall. “Origin of $\Delta I = 1/2$ Rule for Kaon Decays: QCD Infrared Fixed Point”. In: (Mar. 2012). arXiv: 1203.1321 [hep-ph].
[163] R. J. Crewther and Lewis C. Tunstall. “Infrared Fixed Point in the Strong Running Coupling: Unraveling the $\Delta I = 1/2$ puzzle in K-Decays”. In: *Mod. Phys. Lett. A* 28 (2013), p. 1360010. DOI: 10.1142/S0217732313600109. arXiv: 1306.4445 [hep-ph].

[164] R. J. Crewther and Lewis C. Tunstall. “$\Delta I = 1/2$ rule for kaon decays derived from QCD infrared fixed point”. In: *Phys. Rev. D* 91.3 (2015), p. 034016. DOI: 10.1103/PhysRevD.91.034016. arXiv: 1312.3319 [hep-ph].
[165] R. J. Crewther and Lewis C. Tunstall. “Chiral-Scale Perturbation Theory About an Infrared Fixed Point”. In: *EPJ Web Conf.* 73 (2014). Ed. by Marco Battaglieri et al., p. 03006. DOI: 10.1051/epjconf/20147303006. arXiv: 1401.8238 [hep-ph].
[166] R. J. Crewther and Lewis C. Tunstall. “Status of Chiral-Scale Perturbation Theory”. In: *PoS* CD15 (2015), p. 132. DOI: 10.22323/1.253.0132. arXiv: 1510.01322 [hep-ph].
[167] Oscar Catà and Christoph Müller. “Chiral effective theories with a light scalar at one loop”. In: *Nucl. Phys. B* 952 (2020), p. 114938. DOI: 10.1016/j.nuclphysb.2020.114938. arXiv: 1906.01879 [hep-ph].
[168] G. Buchalla et al. “Note on Anomalous Higgs-Boson Couplings in Effective Field Theory”. In: *Phys. Lett. B* 750 (2015), pp. 298–301. DOI: 10.1016/j.physletb.2015.09.027. arXiv: 1504.01707 [hep-ph].
[169] Hao Sun, Ming-Lei Xiao, and Jiang-Hao Yu. “Complete NLO operators in the Higgs effective field theory”. In: *JHEP* 05 (2023), p. 043. DOI: 10.1007/JHEP05(2023)043. arXiv: 2206.07722 [hep-ph].
[170] Luká Gráf et al. “Hilbert series, the Higgs mechanism, and HEFT”. In: *JHEP* 02 (2023), p. 064. DOI: 10.1007/JHEP02(2023)064. arXiv: 2211.06275 [hep-ph].
[171] Gudrun Heinrich, Jannis Lang, and Ludovic Scyboz. “SMEFT predictions for $gg \to hh$ at full NLO QCD and truncation uncertainties”. In: (Apr. 2022). arXiv: 2204.13045 [hep-ph].
[172] Gudrun Heinrich, Jannis Lang, and Ludovic Scyboz. “Beyond dimension six in SM Effective Field Theory: a case study in Higgs pair production at NLO QCD”. In: *PoS* LL2022 (2022), p. 009. DOI: 10.22323/1.416.0009. arXiv: 2207.08790 [hep-ph].
[173] Gudrun Heinrich and Jannis Lang. “SMEFT truncation effects in Higgs boson pair production at NLO QCD”. In: *J. Phys. Conf. Ser.* 2438.1 (2023), p. 012153. DOI: 10.1088/1742-6596/2438/1/012153. arXiv: 2212.00711 [hep-ph].
[174] Andreas Helset, Adam Martin, and Michael Trott. “The Geometric Standard Model Effective Field Theory”. In: *JHEP* 03 (2020), p. 163. DOI: 10.1007/JHEP03(2020)163. arXiv: 2001.01453 [hep-ph].
[175] Tyler Corbett, Adam Martin, and Michael Trott. “Consistent higher order $\sigma(\mathcal{GG} \to h)$, $\Gamma(h \to \mathcal{GG})$ and $\Gamma(\mathrm{h} \to \gamma\gamma)$ in geoSMEFT”. In: *JHEP* 12 (2021), p. 147. DOI: 10.1007/JHEP12(2021)147. arXiv: 2107.07470 [hep-ph].
[176] Adam Martin and Michael Trott. “ggh variations”. In: *Phys. Rev. D* 105.7 (2022), p. 076004. DOI: 10.1103/PhysRevD.105.076004. arXiv: 2109.05595 [hep-ph].
[177] Michael Trott. “The geometric SMEFT”. In: *56th Rencontres de Moriond on Electroweak Interactions and Unified Theories*. June 2022. arXiv: 2206.01577 [hep-ph].

[178] D Maitre. "HPL, a mathematica implementation of the harmonic polylogarithms". In: *Comput. Phys. Commun.* 174 (2006), pp. 222–240. DOI: 10.1016/j.cpc.2005.10.008. arXiv: hep-ph/0507152.

[179] A. Gehrmann-De Ridder, T. Gehrmann, and G. Heinrich. "Four particle phase space integrals in massless QCD". In: *Nucl. Phys. B* 682 (2004), pp. 265–288. DOI: 10.1016/j.nuclphysb.2004.01.023. arXiv: hep-ph/0311276.

[180] Thomas Hahn. "Generating Feynman diagrams and amplitudes with FeynArts 3". In: *Comput. Phys. Commun.* 140 (2001), pp. 418–431. DOI: 10.1016/S0010-4655(01)00290-9. arXiv: hep-ph/0012260.

[181] T. Kinoshita. "Mass singularities of Feynman amplitudes". In: *J. Math. Phys.* 3 (1962), pp. 650–677. DOI: 10.1063/1.1724268.

[182] T. D. Lee and M. Nauenberg. "Degenerate Systems and Mass Singularities". In: *Phys. Rev.* 133 (1964). Ed. by G. Feinberg, B1549–B1562. DOI: 10.1103/PhysRev.133.B1549.

[183] Wolfram Research Inc. *Mathematica, Version 13.2*. Champaign, IL, 2022. URL: https://www.wolfram.com/mathematica.

[184] R.Keith Ellis et al. "Higgs Decay to tau+ tau-: A Possible Signature of Intermediate Mass Higgs Bosons at the SSC". In: *Nucl. Phys. B* 297 (1988), pp. 221–243. DOI: 10.1016/0550-3213(88)90019-3.

[185] James Currie, E. W. N. Glover, and Steven Wells. "Infrared Structure at NNLO Using Antenna Subtraction". In: *JHEP* 04 (2013), p. 066. DOI: 10.1007/JHEP04(2013)066. arXiv: 1301.4693 [hep-ph].

[186] A. Gehrmann-De Ridder, T. Gehrmann, and E. W. Nigel Glover. "Gluon-gluon antenna functions from Higgs boson decay". In: *Phys. Lett. B* 612 (2005), pp. 49–60. DOI: 10.1016/j.physletb.2005.03.003. arXiv: hep-ph/0502110.

[187] A. Gehrmann-De Ridder, T. Gehrmann, and E. W. Nigel Glover. "Antenna subtraction at NNLO". In: *JHEP* 09 (2005), p. 056. DOI: 10.1088/1126-6708/2005/09/056. arXiv: hep-ph/0505111.

[188] A. Daleo, T. Gehrmann, and D. Maitre. "Antenna subtraction with hadronic initial states". In: *JHEP* 04 (2007), p. 016. DOI: 10.1088/1126-6708/2007/04/016. arXiv: hep-ph/0612257.

[189] John M. Campbell, M. A. Cullen, and E. W. Nigel Glover. "Four jet event shapes in electron - positron annihilation". In: *Eur. Phys. J. C* 9 (1999), pp. 245–265. DOI: 10.1007/s100529900034. arXiv: hep-ph/9809429.

[190] S. Catani and M. H. Seymour. "A General algorithm for calculating jet cross-sections in NLO QCD". In: *Nucl. Phys. B* 485 (1997). [Erratum: Nucl.Phys.B 510, 503–504 (1998)], pp. 291–419. DOI: 10.1016/S0550-3213(96)00589-5. arXiv: hep-ph/9605323.

[191] Stefano Catani. "The Singular behavior of QCD amplitudes at two loop order". In: *Phys. Lett. B* 427 (1998), pp. 161–171. DOI: 10.1016/S0370-2693(98)00332-3. arXiv: hep-ph/9802439.

[192] A. Gehrmann-De Ridder, T. Gehrmann, and E. W. Nigel Glover. "Gluon-gluon antenna functions from Higgs boson decay". In: *Phys. Lett. B* 612 (2005), pp. 49–60. DOI: 10.1016/j.physletb.2005.03.003. arXiv: hep-ph/0502110.

[193] John R. Ellis, Mary K. Gaillard, and Dimitri V. Nanopoulos. "A Phenomenological Profile of the Higgs Boson". In: *Nucl. Phys. B* 106 (1976), p. 292. DOI: 10.1016/0550-3213(76)90382-5.

[194] Mikhail A. Shifman et al. "Low-Energy Theorems for Higgs Boson Couplings to Photons". In: *Sov. J. Nucl. Phys.* 30 (1979), pp. 711–716.

[195] Han- Qing Zheng and Dan- Di Wu. "First order QCD corrections to the decay of the Higgs boson into two photons". In: *Phys. Rev. D* 42 (1990), pp. 3760–3763. DOI: 10.1103/PhysRevD.42.3760.

[196] A. Djouadi et al. "QCD corrections to gamma gamma decays of Higgs particles in the intermediate mass range". In: *Phys. Lett. B* 257 (1991), pp. 187–190. DOI: 10.1016/0370-2693(91)90879-U.

[197] S. Dawson and R. P. Kauffman. "QCD corrections to H —> gamma gamma". In: *Phys. Rev. D* 47 (1993), pp. 1264–1267. DOI: 10.1103/PhysRevD.47.1264.

[198] A. Djouadi, M. Spira, and P. M. Zerwas. "Two photon decay widths of Higgs particles". In: *Phys. Lett. B* 311 (1993), pp. 255–260. DOI: 10.1016/0370-2693(93)90564-X. arXiv: hep-ph/9305335.

[199] K. Melnikov and Oleg I. Yakovlev. "Higgs —> two photon decay: QCD radiative correction". In: *Phys. Lett. B* 312 (1993), pp. 179–183. DOI: 10.1016/0370-2693(93)90507-E. arXiv: hep-ph/9302281.

[200] M. Inoue et al. "QCD corrections to two photon decay of the Higgs boson and its reverse process". In: *Mod. Phys. Lett. A* 9 (1994), pp. 1189–1194. DOI: 10.1142/S0217732394001003.

[201] J. Fleischer, O. V. Tarasov, and V. O. Tarasov. "Analytical result for the two loop QCD correction to the decay H —> 2 gamma". In: *Phys. Lett. B* 584 (2004), pp. 294–297. DOI: 10.1016/j.physletb.2004.01.063. arXiv: hep-ph/0401090.

[202] Christine Hartmann and Michael Trott. "On one-loop corrections in the standard model effective field theory; the $\Gamma(h \to \gamma\gamma)$ case". In: *JHEP* 07 (2015), p. 151. DOI: 10.1007/JHEP07(2015)151. arXiv: 1505.02646 [hep-ph].

[203] Christine Hartmann and Michael Trott. "Higgs Decay to Two Photons at One Loop in the Standard Model Effective Field Theory". In: *Phys. Rev. Lett.* 115.19 (2015), p. 191801. DOI: 10.1103/PhysRevLett.115.191801. arXiv: 1507.03568 [hep-ph].

[204] A. Dedes et al. "The decay $h \to \gamma\gamma$ in the Standard-Model Effective Field Theory". In: *JHEP* 08 (2018), p. 103. DOI: 10.1007/JHEP08(2018)103. arXiv: 1805.00302 [hep-ph].

[205] R. Gastmans, Sau Lan Wu, and Tai Tsun Wu. "Higgs Decay H –>\gamma\gamma\ through a W Loop: Difficulty with Dimensional Regularization". In: (Aug. 2011). arXiv: 1108.5322 [hep-ph].

[206] R. Gastmans, Sau Lan Wu, and Tai Tsun Wu. "Higgs Decay into Two Photons, Revisited". In: (Aug. 2011). arXiv: 1108.5872 [hep-ph].

[207] Stefan Weinzierl. "Review on loop integrals which need regularization but yield finite results". In: *Mod. Phys. Lett. A* 29.15 (2014), p. 1430015. DOI: 10.1142/S0217732314300158. arXiv: 1402.4407 [hep-ph].

[208] M. Shifman et al. “Higgs Decay into Two Photons through the W-boson Loop: No Decoupling in the m_W -> 0 Limit”. In: *Phys. Rev. D* 85 (2012), p. 013015. DOI: 10.1103/PhysRevD.85.013015. arXiv: 1109.1785 [hep-ph].
[209] Da Huang, Yong Tang, and Yue-Liang Wu. “Note on Higgs Decay into Two Photons $H \to \gamma\gamma$”. In: *Commun. Theor. Phys.* 57 (2012), pp. 427–434. DOI: 10.1088/0253-6102/57/3/14. arXiv: 1109.4846 [hep-ph].
[210] Roberto Contino et al. “Effective Lagrangian for a light Higgs-like scalar”. In: *JHEP* 07 (2013), p. 035. DOI: 10.1007/JHEP07(2013)035. arXiv: 1303.3876 [hep-ph].
[211] Roberto Contino et al. “eHDECAY: an Implementation of the Higgs Effective Lagrangian into HDECAY”. In: *Comput. Phys. Commun.* 185 (2014), pp. 3412–3423. DOI: 10.1016/j.cpc.2014.06.028. arXiv: 1403.3381 [hep-ph].
[212] K. G. Chetyrkin, Johann H. Kuhn, and M. Steinhauser. “RunDec: A Mathematica package for running and decoupling of the strong coupling and quark masses”. In: *Comput. Phys. Commun.* 133 (2000), pp. 43–65. DOI: 10.1016/S0010-4655(00)00155-7. arXiv: hep-ph/0004189.
[213] Barbara Schmidt and Matthias Steinhauser. “CRunDec: a C++ package for running and decoupling of the strong coupling and quark masses”. In: *Comput. Phys. Commun.* 183 (2012), pp. 1845–1848. DOI: 10.1016/j.cpc.2012.03.023. arXiv: 1201.6149 [hep-ph].
[214] Florian Herren and Matthias Steinhauser. “Version 3 of RunDec and CRunDec”. In: *Comput. Phys. Commun.* 224 (2018), pp. 333–345. DOI: 10.1016/j.cpc.2017.11.014. arXiv: 1703.03751 [hep-ph].
[215] T. Hahn. “CUBA: A Library for multidimensional numerical integration”. In: *Comput. Phys. Commun.* 168 (2005), pp. 78–95. DOI: 10.1016/j.cpc.2005.01.010. arXiv: hep-ph/0404043.
[216] G. Buchalla et al. “Higgs boson pair production in non-linear Effective Field Theory with full m_t-dependence at NLO QCD”. In: *JHEP* 09 (2018), p. 057. DOI: 10.1007/JHEP09(2018)057. arXiv: 1806.05162 [hep-ph].
[217] Adam Martin and Michael Trott. “More accurate $\sigma(\mathcal{G}\,\mathcal{G} \to h), \Gamma(h \to \mathcal{G}\,\mathcal{G}, \mathcal{A}\mathcal{A}, \bar{\Psi}\Psi)$ and Higgs width results via the geoSMEFT”. In: (May 2023). arXiv: 2305.05879 [hep-ph].
[218] Florian Goertz et al. “Higgs boson pair production in the D=6 extension of the SM”. In: *JHEP* 04 (2015), p. 167. DOI: 10.1007/JHEP04(2015)167. arXiv: 1410.3471 [hep-ph].
[219] Ramona Grober et al. “NLO QCD Corrections to Higgs Pair Production including Dimension-6 Operators”. In: *JHEP* 09 (2015), p. 092. DOI: 10.1007/JHEP09(2015)092. arXiv: 1504.06577 [hep-ph].
[220] R. Grober, M. Muhlleitner, and M. Spira. “Higgs Pair Production at NLO QCD for CP-violating Higgs Sectors”. In: *Nucl. Phys. B* 925 (2017), pp. 1–27. DOI: 10.1016/j.nuclphysb.2017.10.002. arXiv: 1705.05314 [hep-ph].
[221] Daniel de Florian, Ignacio Fabre, and Javier Mazzitelli. “Higgs boson pair production at NNLO in QCD including dimension 6 operators”. In: *JHEP* 10 (2017), p. 215. DOI: 10.1007/JHEP10(2017)215. arXiv: 1704.05700 [hep-ph].

[222] Matteo Capozi and Gudrun Heinrich. "Exploring anomalous couplings in Higgs boson pair production through shape analysis". In: *JHEP* 03 (2020), p. 091. DOI: 10.1007/JHEP03(2020)091. arXiv: 1908.08923 [hep-ph].

[223] Gudrun Heinrich et al. "A non-linear EFT description of $gg \to HH$ at NLO interfaced to POWHEG". In: *JHEP* 10 (2020), p. 021. DOI: 10.1007/JHEP10(2020)021. arXiv: 2006.16877 [hep-ph].

[224] Daniel de Florian et al. "Anomalous couplings in Higgs-boson pair production at approximate NNLO QCD". In: *JHEP* 09 (2021), p. 161. DOI: 10.1007/JHEP09(2021)161. arXiv: 2106.14050 [hep-ph].

[225] R. K. Ellis, W. J. Stirling, and B. R. Webber. *QCD and Collider Physics*. Cambridge Monographs on Particle Physics, Nuclear Physics and Cosmology. Cambridge University Press, 1996. DOI: 10.1017/CBO9780511628788.

[226] John Campbell, Joey Huston, and Frank Krauss. *The Black Book of Quantum Chromodynamics: A Primer for the LHC Era*. Oxford University Press, Dec. 2017. ISBN: 9780199652747. DOI: 10.1093/oso/9780199652747.001.0001. URL: https://doi.org/10.1093/oso/9780199652747.001.0001.

[227] G. Buchalla et al. "Fitting Higgs Data with Nonlinear Effective Theory". In: *Eur. Phys. J. C* 76.5 (2016), p. 233. DOI: 10.1140/epjc/s10052-016-4086-9. arXiv: 1511.00988 [hep-ph].

[228] Henriette Elvang and Yu-tin Huang. "Scattering Amplitudes". In: (Aug. 2013). arXiv: 1308.1697 [hep-th].

[229] P. De Causmaecker et al. "Multiple Bremsstrahlung in Gauge Theories at High-Energies. 1. General Formalism for Quantum Electrodynamics". In: *Nucl. Phys. B* 206 (1982), pp. 53–60. DOI: 10.1016/0550-3213(82)90488-6.

[230] R. Kleiss and W. James Stirling. "Spinor Techniques for Calculating p anti-p —> W+- / Z0 + Jets". In: *Nucl. Phys. B* 262 (1985), pp. 235–262. DOI: 10.1016/0550-3213(85)90285-8.

[231] Zhan Xu, Da-Hua Zhang, and Lee Chang. "Helicity Amplitudes for Multiple Bremsstrahlung in Massless Nonabelian Gauge Theories". In: *Nucl. Phys. B* 291 (1987), pp. 392–428. DOI: 10.1016/0550-3213(87)90479-2.

[232] J.S. Rozowsky. "Feynman diagrams and cutting rules". In: (Sept. 1997). arXiv: hep-ph/9709423.

[233] Lance J. Dixon, E.W.Nigel Glover, and Valentin V. Khoze. "MHV rules for Higgs plus multi-gluon amplitudes". In: *JHEP* 12 (2004), p. 015. DOI: 10.1088/1126-6708/2004/12/015. arXiv: hep-th/0411092.

[234] S.D. Badger, E.W.Nigel Glover, and Valentin V. Khoze. "MHV rules for Higgs plus multi-parton amplitudes". In: *JHEP* 03 (2005), p. 023. DOI: 10.1088/1126-6708/2005/03/023. arXiv: hep-th/0412275.

[235] Carola F. Berger, Vittorio Del Duca, and Lance J. Dixon. "Recursive Construction of Higgs-Plus-Multiparton Loop Amplitudes: The Last of the Phi-nite Loop Amplitudes". In: *Phys. Rev. D* 74 (2006). [Erratum: Phys.Rev.D 76, 099901 (2007)], p. 094021. DOI: 10.1103/PhysRevD.76.099901. arXiv: hep-ph/0608180.

[236] Lance J. Dixon. "A brief introduction to modern amplitude methods". In: *Theoretical Advanced Study Institute in Elementary Particle Physics: Particle Physics:*

The Higgs Boson and Beyond. 2014, pp. 31–67. DOI: 10.5170/CERN-2014-008.31. arXiv: 1310.5353 [hep-ph].

[237] Jorge C. Romao and Joao P. Silva. "A resource for signs and Feynman diagrams of the Standard Model". In: *Int. J. Mod. Phys. A* 27 (2012), p. 1230025. DOI: 10.1142/S0217751X12300256. arXiv: 1209.6213 [hep-ph].

[238] S. Scherer and M. R. Schindler. "A Primer for Chiral Perturbation Theory". In: *Lect. Notes Phys. (Springer)* 830 (2012), p. 127.

[239] G. C. Branco et al. "Theory and phenomenology of two-Higgs-doublet models". In: *Phys. Rept.* 516 (2012), pp. 1–102. DOI: 10.1016/j.physrep.2012.02.002. arXiv: 1106.0034 [hep-ph].

[240] John F. Gunion and Howard E. Haber. "The CP conserving two Higgs doublet model: The Approach to the decoupling limit". In: *Phys. Rev. D* 67 (2003), p. 075019. DOI: 10.1103/PhysRevD.67.075019. arXiv: hep-ph/0207010.

[241] Hermès Bélusca-Mato et al. "Higgs EFT for 2HDM and beyond". In: *Eur. Phys. J. C* 77.3 (2017), p. 176. DOI: 10.1140/epjc/s10052-017-4745-5. arXiv: 1611.01112 [hep-ph].

[242] Igor P. Ivanov. "Building and testing models with extended Higgs sectors". In: *Prog. Part. Nucl. Phys.* 95 (2017), pp. 160–208. DOI: 10.1016/j.ppnp.2017.03.001. arXiv: 1702.03776 [hep-ph].

[243] Sally Dawson et al. "Matching the 2HDM to the HEFT and the SMEFT: Decoupling and Perturbativity". In: (May 2023). arXiv: 2305.07689 [hep-ph].

Acknowledgements

I want to express my gratitude to all those who have supported me over the time of my PhD. Firstly, I extend my heartfelt appreciation to Gerhard Buchalla for his exceptional guidance and mentorship. Special thanks and appreciation also go to Oscar Catà, Gudrun Heinrich, Marius Höfer, Florian König and Florian Pandler for their phenomenal collaboration, outstanding contributions and teamwork. I couldn't have asked for a better office mate than you, Florian Pandler, who shares the same sense of humor as me and has made our time together so enjoyable. I also want to thank Stephan Brandt, Patrick Hager, Johannes Kainz, Martin Peev, Koushik Swaminathan and Maximilian Urban for their friendship and support. My sister in law, Clara Salditt, deserves special thanks for the loving treatment of her niece. So do Günter and Irmgard Klein for constantly providing the most professional catering during the past decade. Thank you also to my entire family, especially my parents and my brother Thomas Müller, for the love and encouragement I have been fortunate to receive since I was born. Words are clearly not enough here. A very big thank you goes to my wife Annalena together with our little daughter Annika for helping and supporting me in every aspect of life. You are the driving force behind everything for me.

This work was supported by the Deutsche Forschungsgemeinschaft (DFG, German Research Foundation) under grant BU 1391/2-2 (project number 261324988) and by the DFG under Germanys Excellence Strategy - EXC-2094 - 390783311 (Origins-Cluster). I was also supported in part by a fellowship of the Studienstiftung des deutschen Volkes (German Academic Scholarship Foundation), the Cusanuswerk and an International Max-Planck-Research-School (IMPRS) program at the Max-Planck-Institute for Physics in Munich.

Attempting to work without music is like trying to eat a sandwich without the filling. I am particularly grateful to Adams, d'Albert, Bartók, Berg, Britten, Busoni, Catalani, Debussy, Humperdinck, Janáček, Korngold, Leoncavallo, Mascagni, Menotti, Orff, Pfitzner, Poulenc, Puccini, Ravel, Reznicek, Schillings, Schmidt, Schoeck, Schönberg, Schostakowitsch, Schreker, Schulhoff, Stephan, Strauss, Wagner, Wolf Ferrari, Zandonai, Zemlinsky and Zimmermann for

*** Arabella, Ariadne auf Naxos, Daphne, Der Zwerg, Die Gezeichneten, Die tote Stadt, Flammen, Francesca da Rimini, Hänsel und Gretel, Herzog Blaubarts Burg, La rondine, L'enfant et les sortilèges, Madama Butterfly, Suor Angelica, The Consul, Tiefland, Tosca, Wozzeck

** Cavallerina rusticana, Das Schloss Dürande, Der ferne Klang, Der Golem, Der Mond, Der Ring des Polykrates, Der Rosenkavalier, Der Schmied von Gent, Der Schmuck der Madonna, Die ägyptische Helena, Die ersten Menschen, Die Frau ohne Schatten, Die Kathrin, Die Kluge, Die toten Augen, Elektra, Flammen, Irrelhohe, Königskinder, La Bohème, La fanciulla del West, La Wally, Le Villi, Lulu, Mona Lisa, Moses und Aron, Nixon in China, Notre Dame, Pagliacci, Palestrina, Peter Grimes, Ritter Blaubart, Salome, The Telephone or L'amour à trois, Turandot

* Arlecchino oder Die Fenster, Aus einem Totenhaus, Capriccio, Das schlaue Füchslein, Der Bärenhäuter, Der Kreidekreis, Der Schatzgräber, Des Esels Schatten, Dialogues des Carmélites, Die Abreise, Die Nase, Die Sache Makropulos, Die schweigsame Frau, Die Soldaten, Edgar, Feuersnot, Friedenstag, Gianni Schicchi, Il tabarro, Intermezzo, Lady Macbeth von Mzensk, L'heure espagnole, Manon Lescaut, Pelléas et Mélisande, The Medium, Turandot, Violanta